

FINAL REPORT

Integration of Suspended Particulate Matter
and Oil Transportation Study

(Contract No. 14-12-0001-30146)

September 15, 1987

Submitted to:

Minerals Management Service
Environmental Studies
949 East 36th Street
Anchorage, Alaska 99508

Submitted by:

J.R. Payne, B.E. Kirstein, J.R. Clayton, Jr., C. Clary,
R. Redding, D. McNabb, Jr., and G. Farmer

Science Applications International Corporation
10260 Campus Point Drive
San Diego, CA 92121

TABLE OF CONTENTS

<u>Section</u>	<u>Page</u>
1.0 INTRODUCTION.....	1-1
1.1 BACKGROUND AND RELEVANCE OF OIL/SUSPENDED-PARTICULATE-MATERIAL INTERACTIONS TO OCS OIL AND GAS DEVELOPMENT.....	1-2
1.2 MODELING APPROACH FOR OIL/SPM INTERACTIONS.....	1-12
1.2.1 Dispersion of Oil Droplets.....	1-16
1.2.2 Sediment Transport.....	1-21
1.2.3 Interaction of Crude Oil with Suspended Particulate Material.....	1-23
1.3 OIL/SPM INTERACTION MODEL DEVELOPMENT.....	1-26
1.3.1 Formal Description of Suspended Particulate Matter and Oil Interactions.....	1-28
1.3.2 Detailed Discussion of Oil-SPM Kinetics.....	1-32
2.0 EXPERIMENTAL MEASUREMENTS OF OIL-DROPLET AND SUSPENDED-PARTICULATE-MATTER KINETICS.....	2-1
2.1 BACKGROUND.....	2-1
2.2 EXPERIMENTAL TECHNIQUES AND RESULTS.....	2-5
2.3 IMPLICATIONS FOR MODEL DEVELOPMENT.....	2-30
2.3.1 Application of Oil-SPM Kinetic Equations.....	2-30
2.3.2 Kinetic Algorithm Use in an Ocean Circulation Model.....	2-34
2.4 RESULTS OF OIL/SPM INTERACTION KINETICS DETERMINATIONS USING A 28 LITER STIRRED CHAMBER.....	2-35
2.4.1 Background, Required Assumptions and Limitations of Experiments.....	2-35
2.4.2 Results and Discussion of Experiments with Fresh Prudhoe Bay Crude Oil, 2-Day Weathered Crude Oil, 12-Day Weathered Crude Oil and Jakolof Bay SPM.....	2-44
2.4.2.1 Oil/SPM Interaction Rate Constant with Fresh Prudhoe Bay Crude Oil.....	2-44
2.4.2.2 Oil/SPM Interaction Rate Constant with 2- and 12-Day Weathered Crude Oil.....	2-51

TABLE OF CONTENTS (continued)

<u>Section</u>	<u>Page</u>
3.0 CHEMICAL PARTITIONING AND PHYSICAL BEHAVIOR OF DISPERSED OIL DROPLETS AND OIL/SPM AGGLOMERATES.....	3-1
3.1 SEPARATION AND ANALYSIS OF SPM AND DISPERSED OIL FRACTIONS.....	3-1
3.1.1 Method Validation for Polyester Filter-Vacuum Filtration Procedure.....	3-2
3.2 UTILIZATION OF THE OIL SEPARATION TECHNIQUE IN OIL-SPM INTERACTION AND SEDIMENTATION RATE STUDIES.....	3-8
3.2.1 Oil-SPM Sedimentation Rate Studies.....	3-11
3.2.1.1 FID-GC Analyses of Oil Fractions in the Sedimentation Experiment.....	3-13
3.2.2 SPM Load and Hydrocarbon Information from Oil-SPM Interaction Studies with the 28 Liter Stirred Chamber System.....	3-18
3.2.2.1 Effect of Prior Weathering History of Prudhoe Bay Crude Oil on SPM Loads and Dispersion of Oil into the Water Column Over Time.....	3-19
3.2.2.2 Distribution of Oil Between Dispersed, Dissolved and SPM Phases in Experiments With Fresh, 2-day and 12-day Weathered Oil.....	3-22
3.2.2.3 FID-GC Analyses of Oil Fractions in the SPM and Dispersed Oil Phases of Experiments in the 28 Liter System.....	3-22
3.3 PARTITIONING OF DISSOLVED PETROLEUM HYDROCARBONS BETWEEN SEDIMENT AND WATER.....	3-28
4.0 MODELING OF PHYSICAL PROCESSES INVOLVED WITH THE INTERACTION OF OIL DROPLETS AND SPM IN THE WATER COLUMN.....	4-1
4.1 WATER COLUMN PROCESSES.....	4-1
4.2 BOUNDARY CONDITIONS.....	4-4
4.3 WATER COLUMN PROCESSES.....	4-6
4.4 COMPONENT MODELS OF OIL-SPM TRANSPORT AND FATE.....	4-8

TABLE OF CONTENTS (continued)

<u>Section</u>	<u>Page</u>
5.0 APPLICATION OF THE GRANT-MADSEN-GLENN BOUNDARY LAYER MODEL TO A MODEL OF SUSPENDED PARTICULATE TRANSPORT.....	5-1
5.1 INTRODUCTION.....	5-1
5.2 MODEL ELEMENTS.....	5-2
5.2.1 Boundary Layer Hydrodynamics.....	5-2
5.2.2 Initiation of Sediment Motion.....	5-6
5.2.3 Sediment Suspension.....	5-8
5.2.4 Reference Sediment Concentration.....	5-11
5.2.5 Suspended Sediment Stratification Effects.....	5-12
5.2.6 Bedload and Suspended Sediment Transport.....	5-13
5.2.7 Bottom Roughness.....	5-15
5.3 RUNNING THE GMG MODEL.....	5-18
5.4 APPLICATION TO A SUSPENDED PARTICULATE FLUX MODEL.....	5-24
5.4.1 Interfacing with a Wave Prediction Model.....	5-28
5.4.2 Problems.....	5-28
5.5 APPENDIX: FRICTION FACTOR, SHEAR STRESS AND SHEAR VELOCITY SOLUTIONS.....	5-29
6.0 EXECUTIVE SUMMARY.....	6-1
7.0 BIBLIOGRAPHY.....	7-1
APPENDIX A COMPOUND SPECIFIC HYDROCARBON CONCENTRATIONS FROM 28 LITER STIRRED CHAMBER EXPERIMENTS.....	A-1
APPENDIX B TABLE OF MATHEMATICAL EXPRESSIONS.....	B-1

LIST OF TABLES

<u>Table</u>		<u>Page</u>
1-1	Results of equilibrium partitioning oil/SPM interaction studies.....	1-5
1-2A	Total organic carbon (TOC) and microscopic composition of sediments.....	1-6
1-2B	Sediment mineralogy as determined by x-ray diffraction.....	1-7
1-3	Observed Energy Dissipation Rates.....	1-18
2-1	Thursday - November 6, 1986, 11:30 a.m. OIL-SPM, Half Field.....	2-11
2-2	Thursday - November 6, 1986, 3:00 p.m. OIL-SPM, Half Field.....	2-12
2-3	Thursday - November 7, 1986, 5:00 p.m. OIL-SPM, Full Field.....	2-13
2-4	Thursday - November 8, 1986, 10:45 a.m. OIL-SPM, Half Field/Full Field.....	2-14
2-5	Thursday - November 6, 1986, 10:50 a.m. OIL ONLY, Full Field.....	2-15
2-6	Friday - November 7, 1986, 8:00 a.m. OIL ONLY, Full Field.....	2-16
2-7	Saturday - November 8, 1986, 3:20 a.m. OIL ONLY, Full Field.....	2-17
2-8	Oil/SPM Interaction and Sedimentation Experiments.....	2-18
2-9	Oil/SPM Interaction and Sedimentation Experiments.....	2-19
2-10	Chemical and Physical Characteristics of Oil from Wave Tank #4 Oil/SPM Interaction Experiment.....	2-41
2-11	Values for m and k (equations 2-37 through 2-39) calculated from data plots in Figures 2-16 and 2-17.....	2-48
3-1	Polyester Filter vs. NOAA Status and Trends Sediment Extraction Comparison.....	3-7

LIST OF TABLES (continued)

3-2	Partitioning Experiment Results.....	3-30
5-1	Some results for neutral, near-bottom model run for a moderate storm wave on the continental shelf, as described in text.....	5-22
5-2	Some results for stratified near-bottom model run for a moderate storm wave, strong current, and a silt bed on the continental shelf.....	5-25

LIST OF FIGURES

<u>Figure</u>		<u>Page</u>
1-1	Flame ionization detector capillary gas chromatograms from KB-4 (Seldovia River Salt Marsh) oil/SPM interaction studies.....	1-8
1-2	Illustration of differential volume element used to derive momentum transport equation(s), or continuity equation.....	1-14
1-3	Illustrations of possible oil/SPM interactions showing transport and reaction paths.....	1-24
1-4	"Collision" Sphere of Radius a , which denotes the collision geometry for monodispersed spheres of diameter a	1-33
2-1	Experimental Hardware Used to Determine Oil-SPM Interaction Kinetics.....	2-6
2-2	Execution of 4-liter oil/SPM interaction experiment at the NOAA Kasitsna Bay field laboratory.....	2-7
2-3	Microscope Slide Arrangement for Viewing Oil Droplets and SPM.....	2-9
2-4	Oil/SPM Interactions Free Oil Count.....	2-20
2-5	Oil Interactions (Oil Only).....	2-21
2-6	Oil-SPM Interactions Total Free SPM.....	2-22
2-7	Experimental Hardware to Measure the Power Dissipated in a Stirred Vessel.....	2-25
2-8	Determination of weight required to achieve 400 rpm stirring turbulence in the 4-liter beaker experiments.....	2-26
2-9	Construction of the binary counting circuit board used to accurately measure rpm in the 4-liter beaker oil/SPM interaction experiments.....	2-27
2-10	Trigger mechanism attached to the stirrer shaft and binary counting circuit board (in the background adjacent to the battery power supply) for the experimental rpm determinations.....	2-28

LIST OF FIGURES (continued)

<u>Figure</u>		<u>Page</u>
2-11	Prototype tank design for evaporation/dissolution and oil/SPM interaction experiments.....	2-37
2-12	Twenty-eight liter oil/SPM interaction chamber equipped with directional air manifold and stirring motor for introduction of turbulence.....	2-38
2-13	Dispersed oil droplets and SPM in the 28 liter stirred reaction chamber using 12-day weathered Prudhoe Bay crude oil and <54 μm sieved Jakolof Bay SPM.....	2-39
2-14	Twenty-eight liter oil-SPM interaction chamber containing residual dispersed oil droplets and SPM two minutes after termination of stirring turbulence.....	2-40
2-15	Idealized time-series profiles of free oil (C_o), free SPM (C_s) and oiled SPM loads in 28 liter stirred chamber experiments.....	2-45
2-16	Dispersed oil concentrations (mg total resolved hydrocarbons/liter of seawater) over time (hours after the spill event) for experiments with fresh, 2-day weathered and 12-day weathered Prudhoe Bay crude oil.....	2-46
2-17	Natural logarithms of the ratios of SPM concentrations at time = "t" hours to that at time = 0 hours versus time in experiments with fresh, 2-day weathered and 12-day weathered Prudhoe Bay crude oil and no oil addition.....	2-47
2-18	Computer generated plots of product concentrations ($\mu\text{g oil}_{\text{SPM}}$ /liter seawater) versus time (hours after spill event) for values of Q ranging from 0.03 to 0.12.....	2-50
3-1a	Unweathered Prudhoe Bay crude oil used for experimental oil-SPM-water system.....	3-4
3-1b	"Dissolved phase" from experimental oil-SPM-water system.....	3-4
3-1c	"SPM phase" from experimental oil-SPM-water system.....	3-5
3-1d	Second methylene chloride rinse of filter from "SPM phase" in Figure 3-1c.....	3-5
3-2	Gravimetric concentrations of SPM in sedimentation experiments conducted with oiled and unoled Jakolof Bay sediments (sieved to $\leq 53 \mu\text{m}$).....	3-12

LIST OF FIGURES (continued)

<u>Figure</u>		<u>Page</u>
3-3(a)	Concentration ratios of n-alkanes to nC ₂₁ in oil samples from the parent oil-SPM kinetics rate experiment.....	3-14
3-3(b)	Comparable concentration ratio information for selected aromatic compounds.....	3-14
3-4(a)	Absolute concentrations of n-alkanes associated with "sedimented" and "residual suspended" SPM fractions after 110 minutes of settling in the oiled sedimentation experiment.....	3-16
3-4(b)	Comparable concentrations for aromatic hydrocarbons.....	3-16
3-5(a)	Concentration ratios of n-alkanes to nC ₂₁ in the initial blended oil (2 minutes after blending) and the final "sedimented" and "residual suspended" SPM after 110 minutes of settling in the oiled sedimentation experiment.....	3-17
3-5(b)	Comparable concentration ratio information for selected aromatic compounds (see Figure 3-4(b) for compound identification).....	3-17
3-6(a)	SPM loads over time in experiments with fresh, 2-day weathered and 12-day weathered Prudhoe Bay crude oil and with no oil addition in the 28 liter stirred chamber system.....	3-20
3-6(b)	Dispersed oil concentrations in the corresponding experiments with oil.....	3-20
3-7(a)	Concentrations of oil (i.e., total resolved hydrocarbons) over time in the dispersed oil, dissolved and SPM phases of whole water samples from the experiment with fresh Prudhoe Bay crude oil in the 28 liter stirred chamber system.....	3-23
3-7(b)	Comparable information from the experiment with 2-day weathered Prudhoe Bay crude oil.....	3-23
3-7(c)	Comparable information from the experiment with 12-day weathered Prudhoe Bay crude oil (cont.).....	3-24
3-8(a)	Absolute concentrations of n-alkanes associated with "sedimented" and "residual suspended" SPM fractions at the final sampling time in the 28 liter stirred chamber experiment with 2-day weathered Prudhoe Bay crude oil.....	3-26

LIST OF FIGURES (continued)

<u>Figure</u>		<u>Page</u>
3-8(b)	Comparable concentrations for selected aromatic compounds (naphth = naphthalene; see Figure 3-4(b) for other compound identification.....	3-26
3-9(a)	Concentration ratio information for n-alkanes to nC ₂₁ from the experiment in Figure 3-8.....	3-27
3-9(b)	Comparable information for aromatic compound ratios in Figure 3-8.....	3-27
4-1	Sketch of water column processes affecting the distribution of oil and SPM.....	4-3
4-2	Sketch of a plan view of oil-SPM transport processes.....	4-10
4-3	Component Models of a 3-D oil-SPM transport model.....	4-11
5-1	Extended Shields Curve.....	5-9
5-2	Flow chart tracing computational procedure for boundary layer model. Labels are referred to in text.....	5-19
5-3	Predicted neutral and stratified velocity and concentration profiles to a height $z = \delta_c/6$ for a moderate storm wave with a moderate storm wave with a reference current of 26 cm/sec.....	5-23
6-1	Plots of ln (oil droplet number density) vs time for experiments with fresh Prudhoe Bay crude oil and Grewingk Glacier till. The energy ₃ dissipation rate constant (ϵ) was approximately 260 ergs/cm sec in each experiment. (a) oil plus glacial till. (b) oil only.....	6-6
6-2	Photomicrograph of blended oil droplets on microscope slide.....	6-7
6-3	Photomicrograph of oil-SPM agglomerates on microscope slide.....	6-8

ACKNOWLEDGEMENTS

Various consultants have contributed greatly to this project over a period of many months. The late Dr. William Grant of Woods Hole Oceanographic Institution provided initial guidance and review on modeling bottom boundary layer conditions as influenced by wind and wave turbulence. With Dr. Grant's untimely passing, W.R. Geyer provided additional assistance with his review of bottom boundary layer modeling, and he was in essence responsible for the preparation of Section 5 of this report in its present form. Mr. Wilson Hom and Dr. Tom Fogg are acknowledged for their assistance and contributions in the mathematical derivations of the reaction rate constants measured in the 28 liter stirred chamber system. Gas chromatography/mass spectrometry analyses were completed by Mr. Gary Smith. The photographic prints presented in this report were prepared by Larry Haynes of Design Photographics. Lucy Kaelin, Mabel O'Byrne and Laurie Hughey are thanked for their tireless efforts on the word processor and for their assistance in the preparation of this report in its present form.

1.0 INTRODUCTION

The objective of this study was to characterize the nature of oil/suspended particulate material (SPM) interactions such that mathematical formulations could be derived and (ultimately) incorporated into an ocean oil-spill trajectory and circulation model. This report details the results and findings from experiments and derivations which have been completed to date and contains suggestions for areas of additional study.

The remainder of Section 1 contains a review of previous oil/SPM interaction studies, the derivations and assumptions necessary to model these interactions (including uncertainties on oil droplet dispersion, turbulence requirements, and oil/SPM kinetics). Section 2 presents the derivations and results from laboratory studies completed to measure the reaction rate constant for oil/SPM binding, and interestingly, similar results were obtained with two very different experimental systems. Section 3 contains the results of chemical characterizations of the selective partitioning behavior which occurs among the discrete phases of dispersed oil droplets, dissolved oil constituents, free (un-oiled) SPM, oiled-SPM agglomerates still in suspension and sedimented oil-SPM which has been removed from the water column. Section 4 presents an overview of the potential computer requirements (and limitations) for modeling oil/SPM interactions within the context of a full three-dimensional ocean circulation model. Section 5 presents an overview of the late Dr. William Grant's contribution to modeling the bottom boundary layer and sediment resuspension/transport as controlled by wave and current regimes. Section 6 contains an executive summary of major program elements, problems encountered in experimental and modeling efforts, and solutions derived and used to achieve the results presented. Finally, Section 7 is the bibliography of all cited literature, and the Appendix contains all of the reduced compound specific oil/SPM concentration data obtained from FID-GC and GC/MS analyses of samples collected. These data can ultimately be combined into boiling point ranges to allow comparison of oiled-SPM composition with Open-Ocean Oil Weathering Model predictions of oil composition by distillate cuts.

It is not insignificant that several important program elements (e.g., wave and current induced sediment resuspension and transport, breaking wave-induced oil droplet dispersion and turbulent energy dissipation rate predictions) are all areas of on-going Ph.D.-level research in universities, oceanographic institutions and private laboratories. As a result, there are still many gaps in our knowledge. At this time it would be premature to believe that a fully operational three-dimensional ocean circulation model that incorporates all of the desired interaction terms (oil droplet dispersion, sediment resuspension for all size classes of SPM, oil/SPM collisions as a function of oil and SPM loadings and turbulence, etc.) is possible in the very near future. As discussed in Section 4, there are several possible approaches including finite element circulation models based on conservation of mass and energy as well as probability distribution functions (PDFs) which might be used to approximate the problem. In any case, extensive computer capabilities and resources may be required to ultimately develop predictive models that incorporate all of the variables and stochastic processes involved.

1.1 BACKGROUND AND RELEVANCE OF OIL/SUSPENDED-PARTICULATE-MATERIAL INTERACTIONS TO OCS OIL AND GAS DEVELOPMENT

The fate of hydrocarbon contaminants released into the outer continental shelf waters of Alaska will be controlled by simultaneous physical (e.g. circulation, sediment transport and deposition), chemical (oil weathering and oil/suspended particulate material interactions), and biological (microbial) processes (Payne et al., 1984; Atlas et al., 1983). Interactions between spilled oil and suspended particulate material (SPM) represent a major potential pathway for the dispersal and deposition of petroleum hydrocarbons in coastal environments, particularly in areas characterized by naturally high concentrations of river-derived and bottom-resuspended SPM.

The ability to predict the water column residence times and eventual sinks for hypothetical oil spills facilitates predictions of effects to potentially impacted benthic ecosystems. Such predictions require a method for synthesizing and integrating representative data for dispersed oil and suspended

sediment concentrations, transport, deposition, and resuspension rates, as well as sediment/oil partition coefficients under a variety of possible spill scenarios.

Oil and SPM interactions occur through two primary mechanisms: (1) oil droplets colliding with suspended particulate material and (2) molecular sorption of dissolved species. The parameters and/or conditions that might influence the rate of "reaction" between dispersed oil droplets and SPM are numerous; the concentrations of dispersed oil and SPM, size distribution of the oil droplets and SPM, composition of the oil and SPM, and the density of the oil and SPM will all have some effect on the rate of oil droplet/SPM associations and ultimate sedimentation. The solubility of individual hydrocarbon components in seawater also influences rates of molecular sorption of dissolved species onto SPM (Quinn, in press; Boehm 1987). However, data from field and laboratory studies suggest that sorption of truly dissolved components is not important to the overall mass balance of an oil spill (Payne et al., 1987). Such adsorption may be important, however, for biological considerations as described below.

Sorption of oil onto suspended particles depends on the solubility behavior of hydrocarbons and the nature of the particles. In general, a greater water solubility of a particular hydrocarbon component accompanies a reduced tendency to associate with particulate matter (Gearing et al., 1980). Differences in solubility and adsorption behavior subsequently may result in a fractionation of the oil, with soluble lower molecular weight aromatic hydrocarbons enriched in the water phase, and relatively insoluble higher molecular weight components associated with the suspended particulate phase. However, changes in salinity, pH, turbulence, temperature, concentrations of oil, and presence of natural surfactants (dissolved organic matter) will also influence the partitioning of oil onto SPM (Quinn, in press). The affinity of a particular hydrocarbon component for particulate adsorption is described by the partition coefficient (or adsorption efficiencies) (K_p) such that $K_p = C_p/C_w$, where C_p is the concentration of the hydrocarbon on a given weight of particles and C_w is the concentration of the hydrocarbon in an equal weight of water.

As part of an Open Ocean Oil Weathering Program, SAIC measured compound-specific partition coefficients between fresh Prudhoe Bay crude oil and four representative sediment types characteristic of suspended particulate material encountered in Alaskan Outer Continental Shelf waters (Payne et al. 1984). Table 1-1 presents the SPM/water phase concentrations obtained on specific aromatic compounds from those measurements. Tables 1-2A and 1-2B present information regarding the chemical and visual (i.e., microscopic) composition of the sediment types. Figure 1-1 presents representative chromatograms showing the preferential partitioning of lower molecular weight aromatics (i.e., shorter retention times in Figure 1-1G) into the water column and intermediate and higher molecular weight aromatic and aliphatic hydrocarbons (i.e., longer retention times in Figures 1-1A and D) partitioning onto the suspended particulate material.

Gearing et al. (1979) also reported the fractionation or partitioning of lower molecular weight aromatic compounds (including up to 3-ring aromatics) into the dissolved phase before adsorption of the oil onto suspended particulate material and subsequent sinking. In test tank studies completed at the Marine Ecosystem Research Laboratory at the University of Rhode Island, the aromatic/aliphatic ratio in the sediment was much lower than that in the parent oil suggesting that preferential dissolution of lower molecular weight aromatic compounds may be occurring. Specifically, 2-35% of the higher molecular weight aliphatic, acyclic and greater than 3-ring hydrocarbons were adsorbed onto the suspended particulates and sediments in contrast to 0.1% of the more water soluble naphthalene and methylnaphthalene components which were the predominant aromatic materials in the No. 2 fuel oils used in their studies.

Winters (1978) observed similar partitioning in two simulated oil spills and one mixture of aromatic compounds added to a test tank. The petroleum-derived alkanes were approximately 10 times greater in the particulate fraction, and the lower molecular weight aromatics were at least 5 times more concentrated in the dissolved phase.

In samples of suspended particulate material collected along transects perpendicular to the South Texas OCS near Corpus Christi, Parker and Macko

Table 1-1. Results of equilibrium partitioning oil/SPM interaction studies
(From Payne et al., 1984)

Sample*	ALIPHATIC FRACTION**				AROMATIC FRACTION***											
	Total Res	Total UCM	n-alk	In-alk Branched	Total Res	Total UCM	Benzenes			Naphthalenes					Phenanthrenes	
							1,4,6,1,3-dimethyl (884)	ethyl (874)	naphthalene (1196)	2-methyl (1305)	1-methyl (1322)	2-ethyl (1404)	2,3-dimethyl (1430)	1,6,7-trimethyl (1542)	phenanthrene (1788)	2-methyl (1904)
K. Bay-1 Sediment	340,000	73,000	26,000	0.08	46,000	42,000	15	62	40	630	400	103	440	290	570	390
Aqueous Phase	4,760	0	33	0.007	601	75	2.9	0.56	1.3	7.4	7.4	9.8	3.1	1.0	0.23	-
K. Bay-2A Sediment	795,000	18,000	16,000	0.02	385,000	7,100	46	270	90	550	310	96	240	143	200	83
Aqueous Phase	3,380	0	11	0.003	1,907	0	3.4	1.4	3.3	7.2	6.8	0.7	2.2	1.0	-	-
K. Bay-2B Sediment	647,000	51,000	14,000	0.02	9,600	22,000										
Aqueous Phase	170	0	17	0.1	2,720	0										
K. Bay-3 Sediment	85,000	10,000	5,000	0.06	12,000	10,000	33	130	4	91	83	25	89	35	44	-
Aqueous Phase	5,840	0	8	0.001	512	0	2.0	0.74	-	0.63	4.4	0.28	2.3	0.28	0.53	-
K. Bay-4 Sediment	253,000	262,000	60,000	0.3	44,000	75,000	12	200	29	48	370	125	337	210	71	-
Aqueous Phase	Not reduced very low				2,180	0	2.9	0.46	0.16	0.49	1.3	0.12	2.2	0.34	-	-

- *K. Bay-1--Growingh Glacier Till
- K. Bay-2A-China Poot Bay surface 1 cm
- K. Bay-2B-China Poot Bay depth 1-8 cm
- K. Bay-3--Kasitsna Bay consolidated sediment
- K. Bay-4--Seldovia River salt marsh

**Sediment concentration in µg/kg, water concentration in µg/l

***Sediment concentration in µg/kg, water concentration in µg/l; numbers in parentheses are compound Kovat indices.

TABLE 1-2A. Total Organic Carbon (TOC) and Microscopic Composition of Sediments

<u>ID</u>	<u>TOTAL ORGANIC CARBON (mg/g)</u>	<u>MICRO- SCOPE SIZE</u>	<u>GENERAL COMPOSITION</u>
Grewingk Glacial till	1.20	Approx. 1-10 μ m	almost entirely clay fragments
China Poot Bay-0-1 cm	NA	most<5 μ m	diatoms, terrestrial plant material, clay fragments
China Poot Bay-1-8 cm	NA	most<5 μ m	mostly clay fragments, some diatoms and terrestrial plant material
Kasitsna Bay	6.05	90% diatoms>5 μ m some terrestrial <5 μ m	mostly diatoms, some clay fragments
Seldovia River salt marsh	NA	NA	mostly organic debris and fecal pellets, a few diatoms, very few clay fragments
Jakolof Bay	26.52	Approx 1-50 μ m	organic debris and clay fragments

NA = not available

TABLE 1-2B. Sediment Mineralogy as Determined by X-Ray Diffraction^a

SEDIMENT SOURCE	COMPOSITION (%)						
	Quartz	Kaolinite	Feldspar	Calcite	Mica	Sodium Chloride	Other
KB-1 (Grewingk Glacier till)	>50	20-40	20-40	None	<2	None	—
KB-3 (Kasitsna Bay)	>50	5-10	20-40	None	None	2-5	Gypsum <2
KB-4 (Seldovia salt marsh)	>50	5-10	20-40	None	None	2-5	—
KB-5 (Jakolof Bay)	>50	10-20	20-40	<2	None	2-5	—

^a - Analyses completed by Technology of Minerals - 2030 Alameda Padre Serra, Santa Barbara, CA 93103

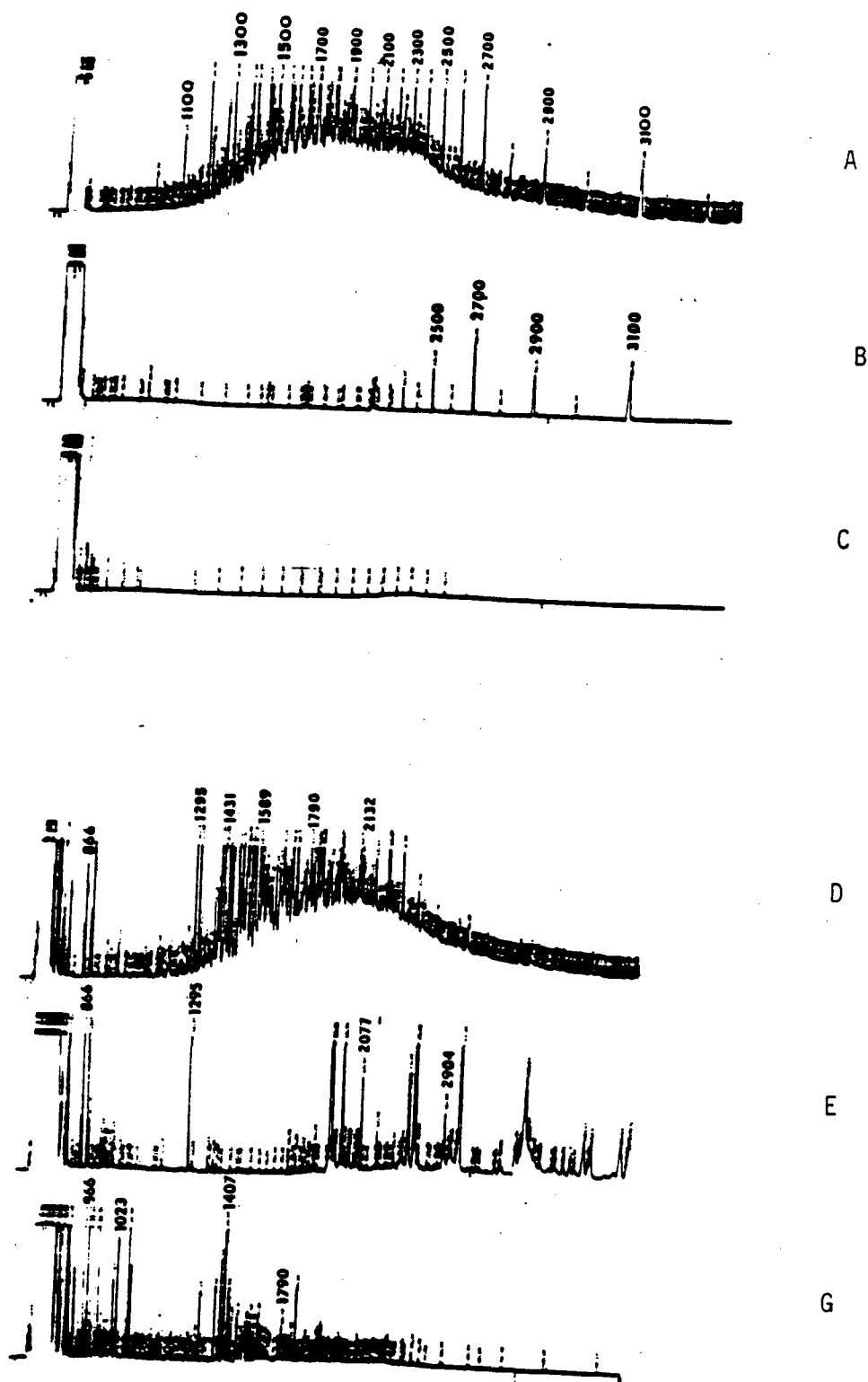


Figure 1-1. Flame ionization detector capillary gas chromatograms from KB-4 (Seldovia River Salt Marsh) oil/SPM interaction studies: (A) Aliphatic hydrocarbons in the oil exposed sediments; (B) Background level aliphatic hydrocarbons measured in unexposed sediment; (C) Aliphatic hydrocarbons in the water column extract; (D) Aromatic hydrocarbons in the oil exposed sediments; (E) Background level aromatic hydrocarbon components measured in the unexposed sample; and (G) Aromatic hydrocarbons in the water column extract. (From Payne et al., 1984)

(1978) noted that the concentrations of higher molecular weight (nC-28 through nC-30) compounds remained relatively constant with distance from the shore, whereas the total particulate hydrocarbon burdens decreased with increasing distance. These authors attributed this to the introduction and sorption of the hydrocarbons near the shore with subsequent movement of particulate-bound oil and preferential retention of the higher molecular weight compounds during weathering. Several higher molecular weight polynuclear aromatic hydrocarbons were also identified on the particulate material, including alkyl-substituted naphthalenes, phenanthrenes, dibenzothiophenes, fluoranthene and pyrene. Concentrations of these materials were too low for quantitation; however, they could be detected by selected ion monitoring GC/MS.

Selective partitioning of lower and higher molecular weight compounds has also been observed by deLappe et al. (1979) in a study designed to measure the partitioning of petroleum hydrocarbons among seawater, particulates, and the filter feeding mussel, Mytilus californianus. Payne et al. (1980) and Boehm and Fiest (1980) also observed a similar partitioning between lower and higher molecular weight compounds in the dissolved phase and suspended particulate material samples removed by filtration of large volume water samples obtained in the vicinity of the IXTOC-1 blowout in the Gulf of Mexico.

In a laboratory study, Meyers and Quinn (1973) found that the hydrocarbon adsorption efficiency (for the less than 44 μm particle sized fractions) decreased in the order of bentonite > kaolinite > illite > montmorillonite. When Meyers and Quinn treated sediment samples from Narragansett Bay with 30% peroxide to remove indigenous organic material, an increase in adsorption potential was noted. The organic material (which was presumably humic substances) was believed to mask the sorption sites on the sediment, thereby reducing the available surface area for adsorption of the organic compounds. Seuss (1968), on the other hand, suggested that a 3 to 4% organic material coating on clay will enhance sorption processes by providing, in effect, a lipophilic layer to enhance non-polar hydrophobic binding. These findings would be more in line with the results of Payne et al. (1984) in comparing the

adsorption potential of the organic-rich materials from the Seldovia River estuary to the composite diatom rich sediment samples from Kasitsna Bay (Table 1-1).

In a laboratory study, Zurcher and Thuer (1978) considered the dissolution, suspension, agglomeration and adsorption of fuel oil onto pure kaolinite. In their studies, the dissolved water column samples showed significant levels of lower molecular aromatics in the benzene to methylnaphthalene range, and the adsorbed fraction contained n-alkanes and aromatics from Kovat indices 1400 through 3200 (Kovats, 1958). The clay minerals in this experiment adsorbed about 200 mg of hydrocarbons per kilogram of dry material. Meyers and Quinn (1973) reported a similar value of 162 mg/kilogram for dry kaolinite. Payne et al. (1984) reported values from a low of 122 mg/kilogram (total resolved and UCM from both the aliphatic and aromatic fractions) from the SPM samples from Kasitsna Bay to a high of 1.2 g/kilogram for the 0 to 1-cm subsamples from the tidal mud flats from China Poot Bay.

While the results of these more recent oil/SPM interaction studies using representative samples from lower Cook Inlet parallel the findings reported by previous investigators, they are somewhat contradictory to results reported by Malinky and Shaw (1979). These authors examined the association of two lower molecular weight petroleum components and suspended sediments (primarily glacially-derived sediments from the south central Alaska region) and concluded that sedimentation of oil by the adsorption to suspended mineral particles may not be a major pathway for the dispersion of petroleum in the marine environment. In that study, however, they used ^{14}C -labelled decane and biphenyl at near saturation levels (i.e., the ppm range, although exact concentrations were not specified by the authors). In their experiments, the concentrations of the two hydrocarbons associated with the sediments was approximately 30% of the original aqueous concentration in parts per million. From loadings of permitted discharges in Port Valdez and measured sediment loads, the authors calculated that less than 3% of the oil released into the harbor could be associated with the sediment. Thus, the authors concluded that adsorption of hydrocarbons to suspended particulate material was not that significant, and that the role of suspended mineral particulate material may be

far less significant in adsorption of polynuclear aromatic hydrocarbons in natural waters than is the role of total suspended matter. The applicability of their findings to real oil spill situations in natural environments may be limited, however, in light of the fact that they did not use a natural oil or even a water accommodated fraction of a natural oil, and by the fact that the compounds which were utilized have significantly higher water solubilities than the higher molecular weight polynuclear aromatic hydrocarbons of interest. Clearly, the results of Payne et al. (1984) on glacially-derived till from the Grewingk Glacier (Table 1-1) show that the particulate material does have a high affinity for polynuclear aromatic hydrocarbons (inspite of its low TOC; see Table 1-2A) and that the high surface area of the glacial till can provide an active site for oil adsorption and ultimate sedimentation.

From the aforementioned equilibrium studies, it is clear that interactions between spilled oil and suspended particulates represent an important mechanism for the dispersal and removal of oil from surface waters. Rates for oil/SPM interactions and dispersal are, in turn, related to concentrations of suspended materials and fluxes of SPM into and out of an impacted area. In particular, oil spills in nearshore waters with high suspended particulate loads experience rapid dispersal and removal of the oil due to sorption onto SPM along frontal zones (e.g., Forrester, 1971; Kolpack, 1971). Boehm (1987) characterized the SPM concentration dependence on oil/SPM fluxes as follows: at SPM concentrations from 1-10 mg/liter, no appreciable transport of particle-associated oil to the benthos occurs; at SPM loads from 10-100 mg/liter, considerable oil/SPM interaction, with subsequent transport and deposition is possible in the presence of sufficient turbulent mixing; and at SPM concentrations > 100 mg/liter massive oil transport may occur with potentials for significant adverse impacts to the benthos.

Consideration of dispersed oil droplets and SPM interactions are particularly germane to predicting oil spill behavior in areas of high SPM loads such as Norton Sound where high SPM levels in nearshore waters are affected by the Yukon River discharge. In this case, adsorption of dispersed oil onto suspended particulates may provide a relatively efficient mechanism for sedimenting significant fractions of the oil mass. For example, following the TSESIS

oil spill in the Baltic Sea, approximately 10-15% of the 300 tons of spilled oil were removed by sedimentation of SPM-adsorbed oil. The high oil flux was due to the large SPM concentrations resulting from turbulent resuspension of bottom sediments (Johansson et al., 1980).

1.2 MODELING APPROACH FOR OIL/SPM INTERACTIONS

In this program we have utilized previously existing information (to the greatest extent possible) and generated new data to develop a mathematical model to quantify the interaction of oil with suspended particulate matter. The interaction kinetics of oil droplets and suspended particulate matter can be used in a variety of "models." The original intent for the use of the kinetics was in conjunction with an existing ocean-circulation model which could add on a material balance calculation. However, since such an ocean-circulation model is not easily accessible, work is now in progress that will illustrate how the kinetics (model) can be used. The models that are being considered are one-dimensional and will be accessible to other researchers by way of a personal computer. These models are intended to provide "bounded" calculations and illustrate other concepts that must also be addressed by an ocean-circulation model implementing the oil-spm kinetics.

It is important to note that the oil-spm interaction model that is being developed is intended to be an "add on" calculation for a general circulation model that addresses both vertical and horizontal transport. Since a general circulation model must be used, it is necessary to describe how a suspended-particulate matter and oil-interaction description will "fit" into a circulation model. Circulation models are always finite-element numerical integration codes, and as such, they require considerable effort in development and use. It must also be recognized that the description of the transport of trace constituents in circulation models is usually an "add-on" calculation. For example, the transport of dissolved oil or small oil droplets in the water column is an "add-on" because these constituents do not affect the momentum transport calculations (i.e., circulation) in any measurable way.

All circulation models are essentially solutions to momentum transport equations. For modeling purposes, sediment transport depends on ocean circulation. Consequently horizontal (x and y) and vertical (z) transport and time dimensions must be considered. Also included with the momentum transport equation is the continuity equation in 3 dimensions. When these equations are applied to specific boundary conditions, such as bottom topography, shoreline, and weather, a specific 3-D circulation model is obtained. These models are "huge" because the large number of equations and the form of the boundary conditions make it impossible to "simplify" the mathematics. In essence, every differential element of the model affects every other differential element.

Weather is an important "driver" of circulation in these types of models. In particular, wind energy transports momentum to the water column. This transferred momentum manifests "itself" in water velocity profiles which in turn transfer momentum from the water column to the bottom, thus affecting sediment resuspension and deposition. These factors are considered in greater detail in Sections 4 and 5.

Figure 1-2 illustrates a differential volume element used to derive the momentum transport equation(s). The arrows indicate inputs and outputs (momentum flux) to the volume. Arrows for inputs and outputs of sediment, oil droplets (as dispersed oil), and dissolved oil are also to be added to this figure.

Interactions of oil and sediment are described (mathematically) as occurring inside the volume element illustrated in Figure 1-2. Thus, for the sorption of dissolved oil onto sediment, partition coefficients (also called sorption efficiencies) relating dissolved oil and sorbed oil (on the solid surface) are required. Taking the limit as $\Delta X, \Delta Y, \Delta Z, \rightarrow 0$ yields the general momentum balance equations along with the appropriate equations of continuity (conservation of mass for water, oil species, and sediment).

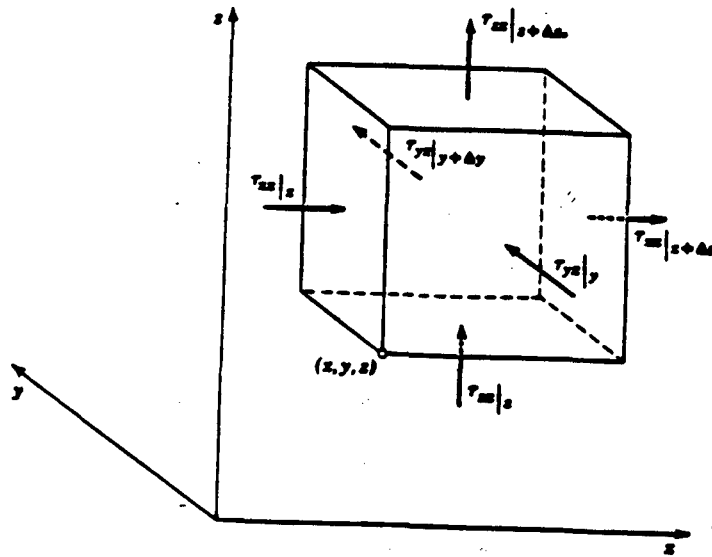


Figure 1-2. Illustration of differential volume element used to derive momentum transport equation(s), or continuity equation (τ is momentum flux, usually $\tau_{xz} = \mu \frac{d\bar{v}_z}{dx}$)

Two things of importance occur at the air-sea interface: (1) momentum is transferred to the water column from the "weather", and (2) oil is "injected" into the water column. The weather input at this boundary should be generated by a stochastic weather model. Thus, when a request for oil trajectories is made, it is not correct to run just one trajectory because of the stochastic (probabilistic) nature of the weather. It is necessary to run many trajectory cases and then examine all of the trajectories to see the range of coverage and probable land hits. By including weather, and this weather must be an image of the past meteorological records, the specific site is truly considered. Oil is also put into the differential volume element at the air-sea boundary.

When the differential volume element is on the ocean bottom or shoreline, boundaries exist where sediment is input into and taken out of the water column, along with oil either as oil droplets, oil SPM-particle agglomerates, or dissolved oil. The sediment in the water column is described as a concentration. Since weather generates the shear stresses necessary for suspension (or deposition), a site-specific weather model must again be used.

Integrating an existing circulation model with the inputs of oil at the air-sea interface and sediment from the bottom and shoreline will yield a description of oil and SPM transport, and the interaction of these two additional "species". These species will not affect the general circulation in any way because their presence does not significantly affect momentum transport. Thus, the fate of oil and SPM depends on circulation (and weather) but circulation does not depend on oil and SPM. The defining equations for oil and SPM are thus decoupled and essentially "ride along" as the momentum equations are solved.

The output, or predictions of such a model integration will be a sediment material balance yielding water column concentrations of "oil" and SPM, and bottom concentrations of sediment (size and quantity) and oil in the sediment. Therefore, the initial (time = 0) condition for sediment on the bottom

and in the water column must also be specified. This requires that a sediment-inventory map of the entire bottom be available which includes particle size distribution.

The output predictions of the oil-SPM interaction(s) and deposition model will ultimately need to be coupled to a set of oil slick trajectories. The result of these interactions is a "footprint" of oiled sediment on the ocean bottom. This "footprint" will be characterized by concentration contours (gms oil/gms sediment) and depth of oil accumulation.

In summary, a specific ocean circulation model must (ultimately) be used to describe oil-SPM interactions and fates because of the following:

- o Both vertical and horizontal transport are to be considered
- o Specific weather must be used because weather determines or drives circulation for specific sites and weather determines some of the environmental parameters.
- o Circulation is the determining variable for transport and resuspension, position of oil inputs, and is essentially the INTEGRATOR that brings the model together.

1.2.1 Dispersion of Oil Droplets

The dispersion of oil droplets into the water column is not a well-understood process. Yet, to predict the collision and result of a collision between oil droplets and suspended particulates, the rate of input (i.e., dispersion rate) of oil droplets into the water must be known along with the droplet number concentration (not just oil concentration in mg/l). To date, prediction of the dispersion rate is based (mostly) on empirical models which are lumped-parameter models. No model based on a "statistical-mechanical approach" for dispersion-rate prediction has ever been presented which is usable. Therefore, the prediction of oil droplet and suspended particulate interactions must begin with a review of the prediction of the source of one of the reacting components, i.e., oil droplets. The dispersion of oil droplets forms an

oil-in-water emulsion, the properties of which are fairly well known. In order to provide a source of oil droplets for the oil-SPM collision process, this emulsion must be relatively stable.

As discussed in the following sections, turbulence alone cannot account for the observed oil droplet sizes. The thermodynamics of the oil-in-water interaction may be the chief driving force for the production of the majority of droplets, with turbulence and the presence of suspended particulate material affecting oil-SPM interaction rates.

Turbulence

Turbulence must be considered for an oil-spm kinetics model for two reasons: the turbulent energy dissipation rate appears as a coefficient in the particle-particle collision expression, and turbulence is suspected as determining (in part) the oil-droplet-size distribution. "Turbulence" as a topic in itself is an on-going research topic. It is the intent of the following discussion to summarize information on "turbulence" with sufficient reference to what is known and can be used in an oil-spm kinetic expression.

The most common models of oil dispersion are based on the turbulent breakup of the oil where the turbulent energy is supplied by breaking waves (Raj, 1977; Milgram, 1978; Shonting, 1979). The breaking waves "beat" the oil into the water column where a fraction of the "injected" oil remains as dispersed droplets and the rest returns to the surface slick. These models have been developed relating turbulent energy dissipation rates (ϵ) to sea state, especially wind speed. Sea state is a parameter also used to calculate the oil concentration in the water column. Difficulties encountered with this method of modeling oil droplet size and production rate using turbulence alone include the lack of data on observed energy dissipation rates and the lack of correlation of theoretical oil concentrations and droplet sizes with observed values.

Table 1-3 lists energy dissipation rates measured in the ocean. Emphasis has primarily been on deep ocean measurements and not at the surface (0-2 m) or ocean floor. The ocean surface has been estimated to have turbulent energy

Table 1-3. Observed Energy Dissipation Rates

Depth (m)	ϵ (ergs/cm ³ /sec)	References
1	6.4 E-2	Liu (1985)
1-2	3.0 E-2	Stewart & Grant (1962)
15	3.0 E-2	Stewart & Grant (1962)
15	2.5 E-2	Grant et al. (1968)
15	1.0 E-2	Liu (1985)
27	5.2 E-3	Grant et al. (1968)
36	1.5 E-1	Belyaev (1975)*
40	2.65 E-3	Liu (1985)
43	3.0 E-3	Grant et al. (1968)
58	4.8 E-3	Grant et al. (1968)
73	1.9 E-3	Grant et al. (1968)
89	3.4 E-4	Grant et al. (1968)
90	3.1 E-4	Grant et al. (1968)
100	6.25 E-4	Liu (1985)
140	3.7 E-2	Belyaev (1975)*

*In Raj (1977).

Unit Conversions

$$\begin{aligned}
 1 \text{ erg/cm}^3 \text{ sec} &= 1 \text{ cm}^2/\text{sec}^3 \text{ water} \\
 &= 10^{-4} \text{ watts/kg water} \\
 &= 10^{-7} \text{ watts/cm}^3
 \end{aligned}$$

dissipation rates of $30 \text{ cm}^2/\text{sec}^3$ or higher in the top 6 cm with winds of 10 m/sec (Lin, 1978). Raj (1977) found that wind speeds of 12 m/s (25 knots) would be required to suspend oil to a depth of two meters using only turbulence as the dispersion process.

The air-sea boundary and sea-bottom boundary are expected to be the regions of greatest energy dissipation based on velocity profile considerations. Oil-droplet concentrations will be highest near the surface (near the slick) and sediment concentrations will be highest near the bottom (in resuspension cases). The region of greatest oil-SMP interaction may then be the middle region of lowest energy dissipation, with source terms of oil-droplet and sediment input described by the boundary regions (surface and bottom) of higher energy dissipation rates. Turbulent energy dissipation rates, when known, can be readily duplicated in the laboratory as discussed in the section on experimental procedures, though only with serious scaling uncertainties.

The prediction of oil droplet size from turbulence-only models generally uses the Weber number approach. Milgram (1978) predicted that the smallest droplet possible is approximately $50 \mu\text{m}$ (while the typical droplet size is larger). Aravamuden (1981) found a similar value but found an inverse linear relationship between droplet diameter and the number of droplets. Observations around an oil spill support this inverse relationship but the minimum observed droplet size was approximately $1 \mu\text{m}$ (Shaw, 1977). The use of the Weber number approach also requires the predication of oil viscosity and oil-water interfacial surface tension over time. Neither of these physical properties is predictable strictly from oil composition.

The affect of turbulence on a coagulating suspension is complex. Hunt (1982) described this effect as two-fold. "First, it (turbulence) generates small-scale fluid shear which controls the suspended particle volume removal rate and second, disperses the discharged particle suspension which decrease the particle concentration and lowers collision and removal rates."

Emulsions

It is known from emulsion theory that without the presence of an emulsifying agent, oil-in-water emulsions (for pure compounds) are limited to a maximum concentration of about 2% and are not stable (Clayton, 1923). Liquid-liquid emulsions may be stabilized by the addition of one of three types of compounds: 1) compounds with a polar-nonpolar structure (surfactants); 2) compounds which form a protective barrier at the liquid-liquid interface (hydrophilic colloids, i.e., gelatins and gums); and 3) finely divided powders or insoluble particles (Huang and Elliot, 1977; Overbeek, 1952). The use of agitation (turbulence) alone cannot result in the formation of a stable oil-in-water emulsion but increases the interaction rate of droplets with the stabilizing compound.

Stable oil-in-water emulsions may be formed spontaneously (i.e., with no agitation) when polar compounds are present in the oil (Overbeek, 1952). Micelles are spontaneously formed by the alignment of the polar compounds into a sphere with the hydrophilic heads at the water interface and the hydrophobic tails to the center where the nonpolar oil compounds are contained. This alignment of polar-nonpolar hydrocarbons occurs in many biological systems and is the basis for the formation of cell membranes and the micelles that comprise latex and milk (Overbeek, 1952; Bretscher, 1985).

Oil-in-water emulsions formed either spontaneously or with a stabilizing agent have droplet sizes on the order of $0.1\mu\text{m}$ for pure substances with sizes increasing for nonpure compounds and in the presence of electrolytes. Oil droplets have been experimentally produced in seawater (as an unstable emulsion) with agitation in this size range as measured by filtration (Shaw, 1977).

Because oil is known to oxidize at ambient temperatures over time and its surface tension decreases (Payne et al., 1984, Payne and Phillips 1985), it is possible to hypothesize that polar products are formed in oil as it weathers (Baldwin and Daniel, 1953). This would lead to the increased possibility of spontaneous emulsion formation and/or stabilized emulsion formation. The exact

mechanism of oil-droplet formation probably involves the combined effects of turbulence, spontaneous emulsification and increased stabilization due to polar compound production and the presence of fine particles of suspended materials.

1.2.2 Sediment Transport

Sediment transport pertains to three specific topics: suspended sediment, sediment resuspension, and sediment inventory on the bottom. In order to write an oil and suspended particulate matter interaction model, the concentration of suspended sediment that might interact with oil in the water column must be known. Therefore, the "add-on" calculation for the circulation model is a sediment material balance for both the water column and the bottom. Therefore, it is necessary to address the modeling of sediment transport with respect to the differential volume element shown in Figure 1-2. The derived mathematical equations must be in a form valid for any water-phase concentration species. Thus, the mass transport equations for sediment in the water column will look the same as the equations for oil either as droplets or dissolved species.

The concentration of suspended sediment in the water column can be considered as resulting from advection and mixing within the water body and resuspension from the bottom. The former is part of the full three dimensional numerical circulation model of the water body and will include source boundary conditions such as riverine input and coastal erosion. The latter involves a sub-model of the bottom boundary layer which will provide bottom boundary conditions for the suspended sediment continuity equation and bottom friction coefficients for the sea bed to the bottom boundary layer or suspended sediment concentrations in the boundary layer resulting from resuspension (see Sections 4 and 5). The incorporation of this bottom boundary condition into the 3-D circulation model can necessarily only be performed by the circulation model.

The suspended sediment, bottom boundary layer sub-model (described in detail in Section 5) is based on Grant and Madsen (1979, 1982) and Grant and Glenn (1983). The sub-model calculates the non-linear dynamics of surface wave and current interactions in frictional bottom boundary layers. The calculated

bottom shear stress from this model (which includes moveable bed and stratification effects) is then related to sediment resuspension and transport through the Shields parameter. Inputs to this sub-model include:

1. Low frequency surface wave characteristics (amplitude, frequency and direction of the wave which most feels the bottom - that is not necessarily the most significant wave; low frequency swells resuspend sediment more easily than a steep choppy sea.)
2. Low frequency current and density profiles (from the 3-D circulation model). There is feedback from the boundary layer sub-model to the current profiles and eddy viscosity parameters.
3. Bottom sediment characteristics, including size distribution and bed form characteristics.

The theoretical mean current shear velocities calculated by all wave current models developed to date generate values relatively close to those which have been determined from field measurements (Wiberg and Smith, 1983). Wiberg and Smith (1983) used models originally developed by the late Dr. William Grant to calculate the combined effects of waves and currents to predict near bottom velocity profiles and values of boundary shear stress that agreed reasonably well with reanalyzed data collected by Cacchione and Drake (1982). As discussed in detail in Sections 4 and 5, the results for two different forms of the eddy viscosity indicated a significant enhancement of the boundary shear velocity due to the current and waves compared to the slope of the velocity profile above the wave boundary layer due to the current only. Thus, models which incorporate wave behavior as well as currents provide a much better estimate of the measure of shear velocity than that which can be obtained when only the currents are included in the calculations. In the evaluation of suspended particulate material migration, and in constructing an oil/SPM interaction model in general, it will be necessary to account for the presence of waves on the surface when estimating bottom stresses either from field data or theoretically. Estimates of sediment transport rates that ignore the interactions of waves with currents will almost certainly be too low (Wiberg and Smith, 1983; Glen, 1983; and Grant and Glen 1983).

1.2.3 Interaction of Crude Oil with Suspended Particulate Material

Interactions of oil in the water column with suspended particulate material can occur by two different mechanisms. The first mechanism is on a molecular scale with dissolved oil species sorbing from the water phase onto the suspended solids. The second mechanism is on a macroscopic scale with dispersed drops of oil colliding with the suspended solids. The resulting loaded particulates are ultimately deposited on the sea floor.

The interaction of oil with suspended particulates involves a number of mass transport processes, illustrated in Figure 1-3, which are dependent on the source terms for oil and sediment. The oil source term can be dissolution of molecular species or dispersion of drops of oil from the parent slick, and the dispersion process can be wind-induced turbulence or spontaneous emulsification (labeled 1-3, respectively, in Figure 1-3). The sediment source term occurs as the result of turbulence at the ocean floor (path 6). Another significant sediment source term in Norton Sound is the Yukon River input. The interaction of oil and suspended particles in the water column occurs by sorption of molecularly dissolved species (path 8), spontaneously dispersed drops colliding with suspended particles (path 11), and as turbulence dispersed drops also colliding with particles (path 7). The sediment returns to the sea floor (path 9) with sorbed oil or associated with oil drops, or with no oil. Oil can also transport to the sea floor as unassociated drops (path 4) or as dissolved species (path 5). The transport of unassociated drops and molecular species will occur when there is little or "no" suspended sediment or when the reaction, i.e., sticking or adsorption, does not occur at an appreciable rate relative to the transport rate. Once oil is on the sea floor, it can be further mixed into the deposited sediments by turnover mechanisms (path 10).

The mathematical description of the interaction of oil in the water column with suspended particulate matter requires both thermodynamic and kinetic information. The kinetic information must describe the strength of the oil source terms (rates), the transport (movement) of oil and sediment in the water column due to the local turbulent diffusivity, and the suspension deposition

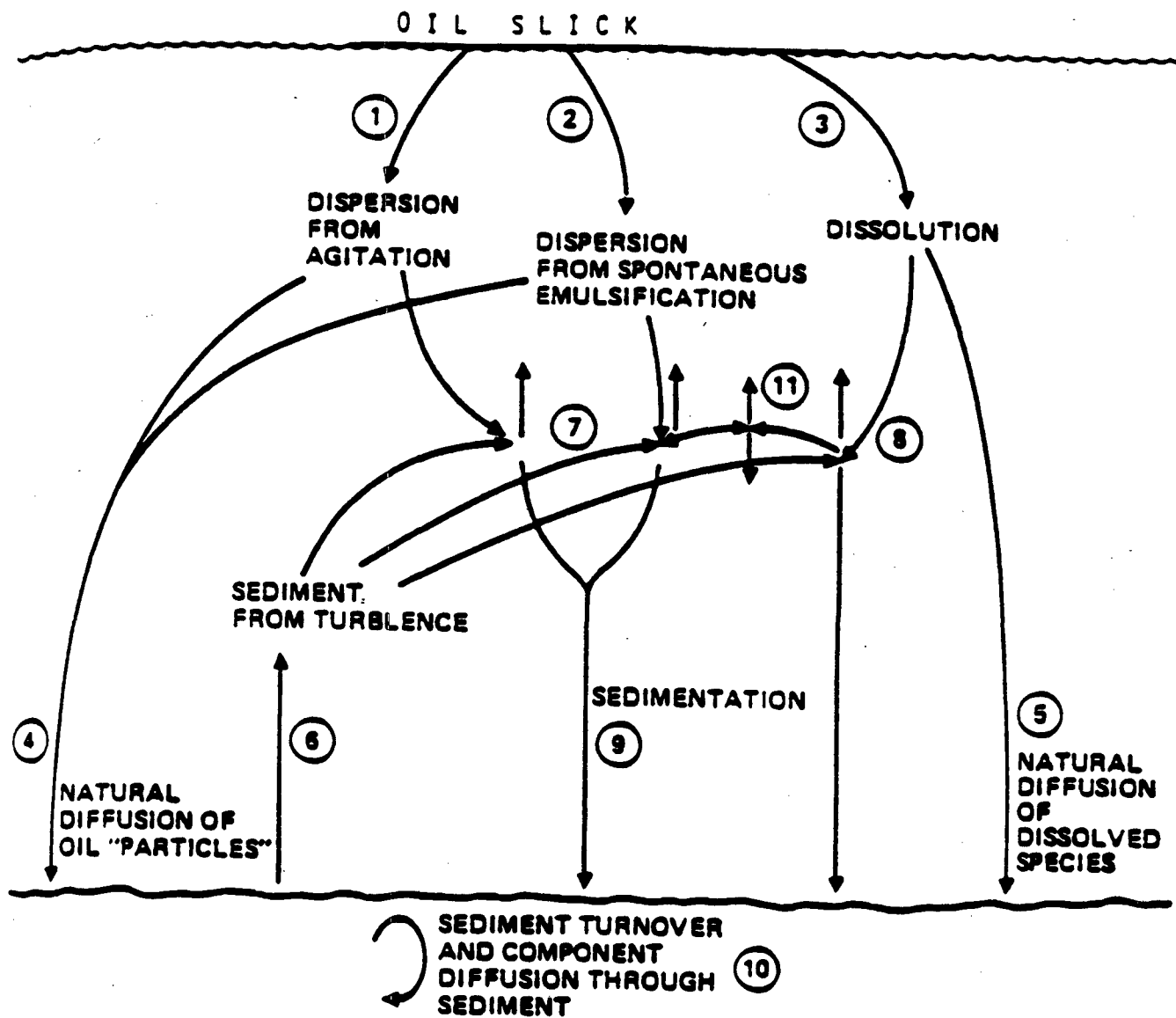


Figure 1-3. Illustrations of possible oil/SPM interactions showing transport and reaction paths. (Payne, et al., 1984)

rates of sediment on the sea floor. The thermodynamic information must describe the phase equilibrium of the molecular species for the water solid sorption. The sorption phenomena can conceptually be described the same way that vapor-liquid distributions are described by Henry's Law. Usually, for the case of dissolved hydrocarbons in the water column, the sorption ratio which relates the dissolved species concentration is a constant for very low concentrations. Also to be considered is the oil water equilibrium of dissolving species; this equilibrium has been described extensively in the open literature as a partition coefficient, or M value.

Figure 1-3 is virtually applicable to the differential volume element presented in Figure 1-2. The oil/SPM interactions are labeled numbers 7, 11, and 8, and the mathematical description of these interactions go "in" the differential volume element because they represent accumulation or change (which can be + or -) through reactions of species of interest. This is illustrated by considering dissolved compounds. The water column concentration of a hydrocarbon will change in the presence of sediment because of sorption processes. This change most likely will be described as an instantaneous reaction which requires that only a partition coefficient (thermodynamics) be used to describe this interaction. Of course, as the "plume" spreads the total concentration of hydrocarbon decreases.

The input-output processes around numbers 7, 11 and 8 (i.e., all the other numbers) are essentially fluxes which describe the arrows in and out of the differential volume element in Figure 1-2. This is especially true at the boundaries of the air-sea and sea-floor interfaces. The near-shore zone of shallow water is a special case of the sea-floor interface.

Therefore, in order to write the correct mathematical equations describing oil-SPM interactions it is necessary to be able to write a differential material balance for oil and SPM. This procedure of writing the equations yields the correct form of the mathematics to be used in the "add-on" calculation to the circulation model.

1.3 OIL/SPM INTERACTION MODEL DEVELOPMENT

The objective of the oil-droplet and suspended-particulate-matter interaction program is to quantify the reaction terms in the convection-diffusion equation for oil droplets and dissolved-oil species. The convective-diffusion equation is derived by writing a mass balance for the species of interest in a differential volume element. The result of writing the mass balance when three dimensions are considered yields the following partial differential equation for the concentration of species i :

$$\frac{\partial C_i}{\partial t} + \frac{\partial}{\partial x}(V_x C_i) + \frac{\partial}{\partial y}(V_y C_i) + \frac{\partial}{\partial z}(V_z C_i) =$$

(1-1)

$$\frac{\partial}{\partial x}\left(k_x \frac{\partial C_i}{\partial x}\right) + \frac{\partial}{\partial y}\left(k_y \frac{\partial C_i}{\partial y}\right) + \frac{\partial}{\partial z}\left(k_z \frac{\partial C_i}{\partial z}\right) + R_i$$

This partial differential equation is a mass balance which when integrated over time and space yields the concentration of species i . This equation appears in all branches of science and engineering whenever a mass balance is written. In the above equation, the left-hand side, with the exception of $(\partial C_i / \partial t)$, represents advection through the differential volume element (which is fixed in space) and the right-hand side, with the exception of R_i , describes horizontal and vertical dispersion.

This partial differential equation is the basis for discussing and describing oil and suspended-particulate-matter interactions in the water column. All of the "interaction" information is contained in the reaction term R_i above. This reaction term is a removal (output) or source (input) term for the species i . Thus, for oil-SPM interactions, it is necessary to describe what species are going to be identified and kept track of. It is not possible to quantify every single species in the system; there are simply too many. Instead, experience seems to indicate that simplifying assumptions can be made.

The reaction for oil droplets in the water column describes the rate of collision and sticking of an oil droplet with a suspended particulate, i.e., a loss of (free) oil droplet, and the settling (or rising) of an oil droplet. The reaction term R_1 for oil droplets only then is

$$R_{op} = K_{op} C_{op} C_p \quad (1-2)$$

where $K_{op} C_{op} C_p$ is the rate of collision and sticking of an oil droplet and a suspended particulate to produce an oil-particulate agglomerate. The effect of buoyancy of oil droplets or oil-SPM agglomerate appears in the vertical velocity term in the partial differential equation (1-1).

Clearly, a mass balance must also be written for unoiled sediment. The partial differential equation for suspended sediment looks exactly the same as that for C_1 . Thus, in order to predict the interaction of oil and sediment for a specific location, a prediction of sediment transport is required a priori.

A complete list of the species of interest for oil-SPM interaction prediction includes: oil droplets as a function of size, sediment size and "type," and finally oil-particulate agglomerates. Oil-particulate agglomerates refer to oil-particulate species where the particulate is composed of one, two, three, ..., individual particulate(s), and the agglomerate is the result of one oil droplet scavenging more than one particulate. There are an infinite number of species when these types of agglomerates are considered. Since it is not possible to keep track of all species even on the fastest computer (nor worthwhile), some judgement based on existing results and experimentation must be used to either eliminate species or lump species into pseudocomponents.

An explicit requirement for an oil-SPM interaction and concentration prediction is the velocity and dispersion vectors in the mass balance equation. It must be emphasized that these velocities and dispersion coefficients are not calculated from an oil-SPM model. An oil-SPM transport model only uses these

parameters to calculate where the oil and SPM are transported. These parameters come from an ocean circulation model, and if the ocean-circulation model computes salinity, then the ocean-circulation model can easily compute oil and SPM concentration in the same way (with appropriate boundary conditions).

In the discussion that follows a detailed statement of the oil and suspended-particulate-matter interaction problem is given along with the simplifying assumptions that are being pursued. A review of the literature is then given with emphasis on: particle-particle kinetics, the rate constant of these kinetics as a function of shear (and turbulence), oil droplets in water (emulsions), and the range of experimental parameters expected. Finally, in Section 2, a discussion of the results of the completed experiments is presented along with considerations on the utilization of these results and how the parameters are to be used in modeling.

1.3.1 Formal Description of Suspended Particulate Matter and Oil Interactions

The objective of the oil and suspended-particulate-matter interaction program is to describe the fate of oil in the water column when the presence of suspended particulate matter is considered. Oil exists in the water column as discrete droplets or (truly) dissolved oil species. The truly dissolved oil species can be either molecular specific species or pseudocomponents. The dissolved oil species interact with the suspended particulate by adsorbing onto the particle, while the oil droplets interact by colliding with and sticking to the particulate. The adsorption of dissolved oil species by particulate is thought to affect no change in the particle's hydrodynamic characteristics while the oil-droplet particle species might affect a change in hydrodynamic character relative to both parents.

An oil spill on the ocean surface moves as a function of environmental conditions such as wind speed, waves, and water currents. As the slick weathers, dissolved species and droplets of oil are fluxed into the water column.

At the same time sediment transport occurs due (mainly) to a flux of sediment to or from the bottom depending on wave conditions and currents. Thus, the two species, oil and particulate, interact and are transported due to the local velocity and dispersion vectors.

The mathematics which describe the water column interactions are the continuity equations for the various species. In general, this equation is

$$\frac{\partial C_i}{\partial t} + \frac{\partial}{\partial x}(V_x C_i) + \frac{\partial}{\partial y}(V_y C_i) + \frac{\partial}{\partial z}(V_z C_i) - \frac{\partial}{\partial x}(k_x \frac{\partial C_i}{\partial x}) + \frac{\partial}{\partial y}(k_y \frac{\partial C_i}{\partial y}) + \frac{\partial}{\partial z}(k_z \frac{\partial C_i}{\partial z}) + R_i = 0 \quad (1-3)$$

where C_i is the concentration of the i th species of interest, t is time, V_i are the velocity components, k_i s are the dispersion components, and R_i is the reaction term. This equation can only be solved if the velocity and dispersion components are known. Furthermore, when this equation applies to dilute species, it is not coupled back to the hydrodynamic equations. In other words if the presence of C_i does not affect the bulk density of the fluid, the (bulk) viscosity of the fluid, or any other physical property of interest, C_i depends on V and k while the converse is not true. For oil species, C_i , in the water column, this "not coupled" assumption is applied because the species are very dilute. This is apparently not the case for sediment at the bottom boundary. (See Sections 4 and 5). The continuity equation can be solved when V and k are given or specified as a function of x , y , z and time. If a circulation model is available which computes these vectors and also salinity, then it is straight forward to add the calculation procedure to consider other species. Actually, it is easier to add uncoupled species equations because (note that) salinity is coupled to the momentum equations through the bulk density. If the continuity equation for uncoupled species such as oil has to be integrated after a circulation model is run, then a considerable amount of work must be

done to "write" an integration routine, parameterize the location of the boundary, and "plot" the results.

Consider now the reaction term for oil droplets. Oil droplets leave (change their identity) the water column by colliding with and sticking to suspended particulate. The rate expression for the "reaction" is postulated to be

$$R_{op} = K_{op} C_o C_p \quad (1-4)$$

where C_o is the oil-droplet concentration, C_p is the total particulate concentration, and K_{op} is the rate constant for this "reaction." K_{op} is a function of turbulence or energy dissipation rate and is discussed in detail in the following section (1.3.2).

This interaction will result in a decrease in oil droplet concentration, i.e., $\partial C_o / \partial t$ will decrease, so $K_{op} C_o C_p$ is subtracted from the right hand side of the continuity equation (1-3) for oil droplets.

When oil-droplet bouyancy is considered the continuity equation is further modified by the "rising" velocity according to

$$V_z = V'_z + W_z \quad (1-5)$$

where V'_z is the z-component of the current velocity obtained from a (the) circulation model and W_z is the "rising" velocity. The above expression for V_z is to be used directly in the continuity equation for oil droplets.

The objective of this experimental program was to measure, verify, and gain insight on $K_{op} C_o C_p$. This work was conducted in a stirred-tank "reactor" (see Sections 2.2 and 2.4).

Now consider the suspended particulate matter in the water column. There are two types (at least) to consider: unoiled particulate, C_{pu} , and oiled particulate, C_{po} . The continuity equation for unoiled particulate also

contains a loss term due to collision with and adherence to oil droplets. Thus, the reaction term for unoiled particles is

$$R_{\text{opu}} = K_{\text{opu}} C_o C_{\text{pu}} \quad (1-6)$$

which is to be subtracted from the right hand side of the continuity equation for unoiled particulate. The settling velocity for particulate must also be included in the V_z term for particulate only. Denoting the particle settling velocity as U_z , the z-velocity component becomes

$$V_z = V'_z - U_z \quad (1-7)$$

where now a minus sign is used to denote the -z direction (settling toward the bottom).

At this point in the discussion, it should be apparent that keeping track of all kinds of species may well be impossible, especially if particulate size fractions are to be considered. However, it is only necessary to keep track of those "things" which behave differently. An example of importance which now should be considered is oiled versus unoiled particles. If the settling velocity of these two species is not appreciably different, then there is no need to consider them as separate species. The important consideration then is "appreciably different" when considered in the ocean environment. Since settling velocity is the "comparison", information on differential settling must be obtained by examining real ocean sediment to determine how sediments are size fractionated to the bottom. If it turns out that sediments with a settling velocity range of say 10% are uniformly deposited and experiments in the laboratory show that oiled versus unoiled particulate fall in this range, then there is no need to consider separate particle species. Observation appears, in a preliminary sense, to bear out the above postulate based on laboratory data only, i.e., in the absence of flocculation the observed settling rates differ very little (see Section 6.1, Payne et al. 1984, and Section 3.2.1, of this report).

The continuity equations can be integrated only when boundary conditions are applied. For the case of oil droplets, the rate of dispersion provides a "flux" boundary condition for this species at the ocean surface. The boundary condition for this species at the bottom has not been discussed. Two possibilities are $dC_o/dz = 0$ at the bottom, i.e., no transport across the bottom; or $C_o = 0$, i.e., the oil drops stick to the bottom. If sediment is being "lifted" from the bottom due to wave action, $dC_o/dz = 0$ would (probably) be satisfactory.

1.3.2 Detailed Discussion of Oil-SPM Kinetics

The rate of oil and SPM interaction, which appears as R_1 in the continuity equations, is written as

$$R_{op} = K_{op} C_o C_p \quad (1-8)$$

This equation is based on numerous research papers that have been published on the general topic of the collision frequency of particles in a fluid medium. Therefore, in order to show why this equation can be used to describe oil-SPM interactions, an abbreviated derivation is presented which also discusses how this equation is adapted to a turbulent medium.

In order for oil droplets and SPM to interact, they must collide. Once they have collided, they can "stick" to form an oil-SPM agglomerate or rebound to remain the same as before the collision. Therefore, the first step in describing the oil-SPM interaction is to describe the collision frequency of (suspended) particles in a turbulent medium.

Consider a reference frame (x, y, z) centered on a particle which is fixed in space as shown in Figure 1-4. The fluid moves past the sphere in laminar flow where the velocity in the x-direction is given by $U = -Gy$. Thus, the velocity is a function only of y and the sphere is transparent with respect to the flowing fluid. If the sphere was not transparent, then the flow of fluid around (rather than through) the sphere would have to be considered.

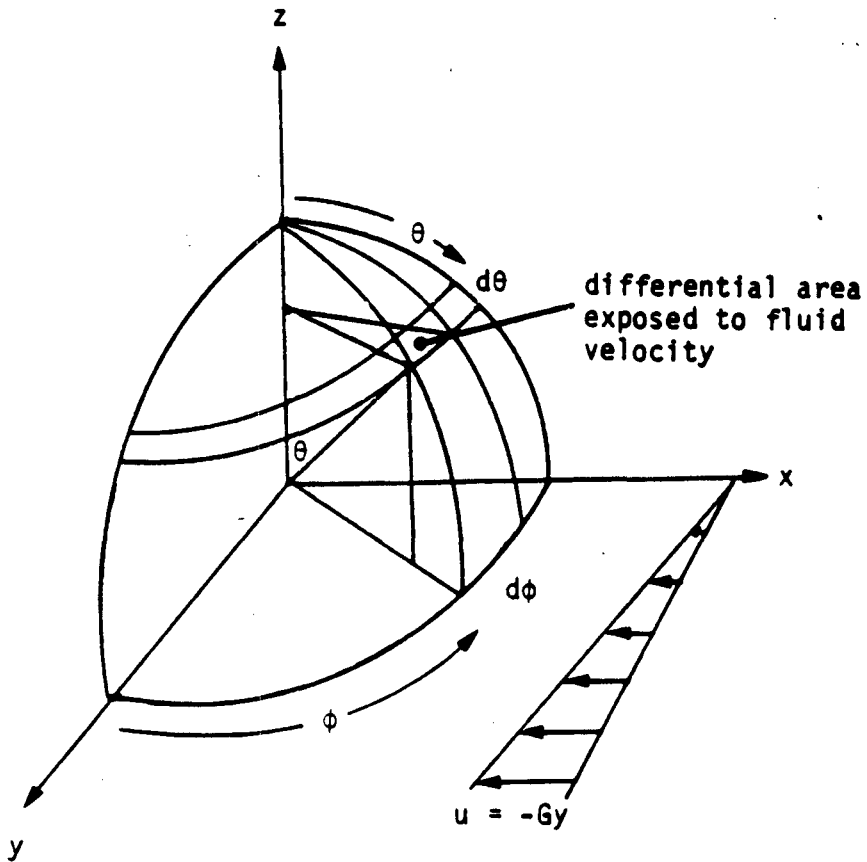


Figure 1-4. "Collision" Sphere of Radius a , which denotes the collision geometry for monodispersed spheres of diameter a . Note that a "collision" sphere is the center-to-center distance of approach that results in contact. The projected differential area onto the yz plane (normal) is to be integrated over the plane weighted by the local velocity.

The objective of the derivation is to calculate the number of spheres moving at the local fluid velocity that collide with the single sphere at the origin. Thus, it is necessary to calculate the product of the local fluid velocity (since the particles ride at this velocity) and the projected area of the sphere exposed to the local velocity. This concept can be visualized by examining Figure 1-4. Note that the velocity is zero on or near the x-axis and the projected area of the sphere in the region of the x axis is relatively large. Thus, there are relatively few collisions on the x-axis because the flow is small in this region. As the position of a flowing particle is moved off the x-axis, its fluid velocity toward the target sphere goes up and since the projected area of the target sphere is finite, collisions can occur. As the position of the moving particle changes towards $y =$ radius of the target sphere, note that the velocity is quite high which results in more particles flowing through this position, but the projected area of the target sphere is almost zero. Thus relatively few spheres collide in this region. Mathematically, the above description is worked out as follows. A differential area of the surface of a sphere of radius "a" projected onto the y-z plane is

$$dA = \{ \sin\theta(a \sin \theta d\phi) \} \{ \sin\phi(a d\theta) \} \quad (1-9)$$

or

$$dA = a^2 \sin^2 \theta \sin\phi d\theta d\phi \quad (1-10)$$

any position y can be expressed as a function of a, θ and ϕ as

$$y = a \sin\theta \cos\phi \quad (1-11)$$

Therefore, the number of particle centers passing through a sphere of radius "a" about the origin is

$$\begin{aligned} df(\theta, \phi) &= n u dA \\ &= n \{ G \cdot a \cdot \sin\theta \cos\phi \} \{ a^2 \sin^2 \theta \sin\phi d\theta d\phi \} \\ &= n G a^3 \sin^3 \theta \sin\phi \cos\phi d\theta d\phi \end{aligned} \quad (1-12)$$

where n is the number concentration of particles in the moving fluid. This is the differential collision frequency of the particles in the moving fluid with

the single particle at the origin. Integrating θ and ϕ both through 0 to $\pi/2$ for the upper octant and multiplying by 4 to get the entire "face" exposed to the moving fluid yields

$$f = \frac{4}{3} nGa^3 \quad (1-13)$$

The above expression is the collision frequency for the particles in the fluid with the single particle fixed at the origin. To get the collision frequency for all the particles multiply f by n and then divide by 2. The division by 2 must be made because otherwise the collision of i onto j and j onto i would be counted twice. Therefore, the collision frequency for a fluid containing n particles with radius "a" per unit volume in laminar shear at $G \text{ sec}^{-1}$ is

$$F = \frac{2}{3} a^3 n^2 G \quad (1-14)$$

This equation is rearranged by taking into account of the volume concentration of solids, which is

$$c = \frac{4}{3} \pi \left(\frac{a}{2}\right)^3 n \quad (1-15)$$

which when substituted into the collision-frequency equation yields

$$F = \frac{4}{\pi} ncG \quad (1-16)$$

This is the typical equation for describing the particle-particle collision frequency for a system of monodispersed particles (Manley and Mason, 1952). Note that it is first order with respect to the particle concentration because the volume concentration of solids is constant. This equation has been tested in many experiments and shown to be valid. This equation applies to oil-oil droplet and particle-particle interactions to a first approximation.

In order to apply the collision frequency equation to oil-particle interactions, the identity of two different particles must be taken into consideration. The collision frequency of two different particles is

$$F_{ij} = \frac{4G}{3} (r_i + r_j)^3 n_i n_j \quad (1-17)$$

where r_i is the radius of the i -th particle (Birkner and Morgan, 1968). Note that the shear appears in exactly the same manner as it does for the collision frequency of monodispersed particles.

The material balance, or population balance, for oil and suspended particulate can now be written using the above collision frequency equation. For oil droplets, the differential material balance is

$$\frac{dn_o}{dt} = -\alpha F = -\alpha \frac{4G}{3} (r_o + r_p)^3 n_o n_p \quad (1-18)$$

where α is introduced as the "stability" constant. This constant takes into account the efficiency of oil droplet and particle adherence, i.e., sticking (Huang, 1976). If the particles collide but do not stick, $\alpha = 0$; at the other extreme is $\alpha = 1$. The above equation is applied to the (free) oil droplet concentration as

$$\frac{dn_o}{dt} = -kG n_o n_p \quad (1-19)$$

where now k lumps α and the radius function. Thus, experimental measurements essentially determine a lumped reaction rate constant which is kG . Similar expressions apply to uncoiled sediment and an oil-particle agglomerate which is also the rate of formation of the k -th particle composed of an $i + j$ agglomerate. In order to apply the above equation to oil droplets, suspended particulate matter and the resulting agglomerates, at least three species are

identified here. Because the material balances that are actually used in calculations involve concentrations of mass rather than populations, the differential material balances are rewritten as

$$\frac{dC_i}{dt} = -kG C_i C_j \quad (1-20)$$

where k lumps all unknowns for the reaction.

The above equation relates the collision frequency to the (laminar) shear rate. In order to apply this to the problem of interest, a turbulent shear is required. Saffman and Turner (1956) present an analysis of the collision frequency in turbulent shear which results in

$$G = \left(\frac{\epsilon}{\nu}\right)^{1/2} \quad (1-21)$$

where ϵ is the (turbulent) energy dissipation per unit mass per unit time and ν is the kinematic viscosity.

Thus, the working equation for the rate of loss of the i -th particles due to collisions and sticking with the j -th particle is

$$\frac{dn_i}{dt} = -k\left(\frac{\epsilon}{\nu}\right)^{1/2} n_i n_j \quad (1-22)$$

The assumptions involved in deriving the above equation clearly do not reflect reality exactly. The relation of laminar shear and turbulent shear that is invoked requires assumptions. Clearly the particles to which the equation is to be applied are not spheres. Furthermore, the particles are distributed over a range of sizes. However, the basic form of the above equation has been shown to be applicable in many situations and was used and verified in the experimental program.

2.0 EXPERIMENTAL MEASUREMENTS OF OIL-DROPLET AND SUSPENDED-PARTICULATE-MATTER KINETICS

In this section of the report, we describe experiments that were conducted at the NOAA Kasitsna Bay Laboratory to determine the oil-SPM interaction kinetics. A brief discussion is also presented on how these results scale to the open ocean and how they can be used in conjunction with an ocean-circulation model to predict the spatial distribution of sedimented oil on the ocean floor.

2.1 BACKGROUND

Particle kinetics has been extensively described in the open literature. Essentially all of this literature can be traced back to the original work of Smoluchowski (1917). A more recent example of the application of Smoluchowski can be found in the work by Birkner and Morgan (1968). The paper by Birkner and Morgan describes a flocculation kinetics experiment which is very similar in many attributes to the oil-SPM experiment.

The collision frequency for dilute suspensions of particles can be expressed as

$$R = 1.3 \left(\frac{\epsilon}{\nu}\right)^{1/2} (r_i + r_j)^3 n_i n_j \quad (2-1)$$

when R is the collision frequency, ϵ is the energy dissipation per unit mass (of fluid) per unit time (cm^2/sec^3), ν is the kinematic viscosity (cm^2/sec), r_i is the radius of particles i present at a number density of n_i , and likewise for particles j . This equation describes only the collision frequency and nothing is implied about the "sticking" of particles.

Clearly, the above equation cannot be applied directly to oil droplets and (or) SPM. The obvious problem is that a distribution of particle sizes exists in any real situation, and the above equation is written for a specific

size. The above equation has been verified because it is possible to obtain suspensions of single-sized spheres (latex or polymer) and conduct mono-sized particle-particle kinetic experiments.

However, it is not possible to generate mono-sized oil droplets, and SPM from the ocean is definitely not single sized or spherical. Therefore, in order to apply the above equation to the kinetics of oil droplet-SPM interactions, the following assumptions are made.

1. Oil droplets in a narrow size range will behave as a mono-sized population, and
2. SPM in a narrow size range will likewise behave as a mono-sized population.

The primary reasons for "lumping" oil-droplet and suspended particulate sizes are practical. Certainly calculations can be done which consider distributions, but these would consume considerable effort. However, since the net result is to provide bounded estimates of the transport of oil rather than exact answers, a "lumping" of parameters is required. Lumping parameters is commonly done to provide a single parameter for a population, i.e., a mean versus all values. The question that then must be answered is whether the mean adequately describes the population. For the case of a true-boiling-point distillation the mean temperature of the cut "turns out" to be sufficient to be used to describe vapor pressure. Thus, lumping particle diameters over some range for the purpose of describing kinetics is assumed, but presently the range of diameters included in, for example, the 10 micron class is not known. Experiments will determine what averages and ranges are reasonable.

If the preceding two assumptions are valid, then the rate equation can be rewritten as

$$R = 1.3 \left(\frac{\epsilon}{\nu}\right)^{1/2} k n_i n_j \quad (2-2)$$

where now k "lumps" the unknown information about the particle sizes. This is the same equation as Equation 1-22, but the factor 1.3 is removed from k . This equation still does not contain information about the "sticking together of particles. It is this "sticking" together of particles, i.e., the oil-SPM agglomerate, that is important. In order to "see" the oil-SPM agglomerate, some kind of "balance" (such as a material balance) must be derived which describes the kinetics that occur.

For the experiments described here, it was (finally) decided to use the free oil-droplet number density as a direct measure of the kinetics. In order to derive this mathematically, consider that the rate of loss of free oil droplets is directly proportional to the collision frequency and sticking of oil droplets and SPM. Thus, the rate of loss of free oil droplets (or SPM) is less than (or equal to) the rate of collision between these two types of particles.

Therefore, the working equation which can describe oil-droplet and SPM interactions is

$$R = 1.3 \left(\frac{\epsilon}{\nu}\right)^{1/2} k_a C_o C_p \quad (2-3)$$

where now C_o is the concentration of oil (droplets) in the water in mg/l (or any other convenient units), C_p is the concentration of SPM in the water in mg/l, R is the rate of collision and sticking of oil droplets and SPM, and k_a is a "lumped" parameter that includes unknown information such as the "sticking" efficiency and the size dependency. Because R is the rate of loss of free oil droplets, R has units of mg (oil)/(l · sec) and the parameter k_a must have units derived from:

$$\frac{\text{mg(oil)}}{\text{l} \cdot \text{sec}} = \frac{\text{cm}^2}{\text{sec}^3} \cdot \frac{\text{sec}^{1/2}}{\text{cm}^2} k_a \frac{\text{mg(oil)}}{\text{l}} \frac{\text{mg(spm)}}{\text{l}} \quad (2-4)$$

which yields the result that k_a has units of reciprocal SPM concentration.

Application of the oil-SPM kinetic equation can be carried out in any vessel or flow situation where the independent variables can be controlled. The experimental method chosen and found to work satisfactorily here was a well-stirred vessel (with no inflow or outflow) with a known power input through a propeller. This is exactly the experimental setup used by Birkner and Morgan (1968). The objective of the experiment then is to introduce oil droplets (of a narrow size range) and SPM (of a narrow size range) into a vessel (beaker) of (stirred) water and measure the free oil-droplet counts versus time. If the concentration of the SPM is constant, i.e., its number density does not change, then

$$\frac{d C_o}{dt} = -k C_o \quad (2-5)$$

where $k = 1.3 (\epsilon/\nu)^{1/2} k_a C_p$

so that integration of the above yields

$$\ln \frac{C}{C_o^0} = -kt \quad (2-6)$$

where C_o^0 is the initial oil droplet concentration at time = 0. The experimental data, which are the oil-droplet counts normalized to the initial count, should fall on a straight line on a semi-log plot versus time if the assumptions are correct.

In order to conduct this experiment there can be no other processes occurring which affect the oil droplets or SPM. If other processes are occurring, then the appropriate differential equation must be written and solved along with the above equation. Examples of other processes are SPM loss due to settling, or SPM flocculation. Experience indicates that both of these processes can occur and must be avoided.

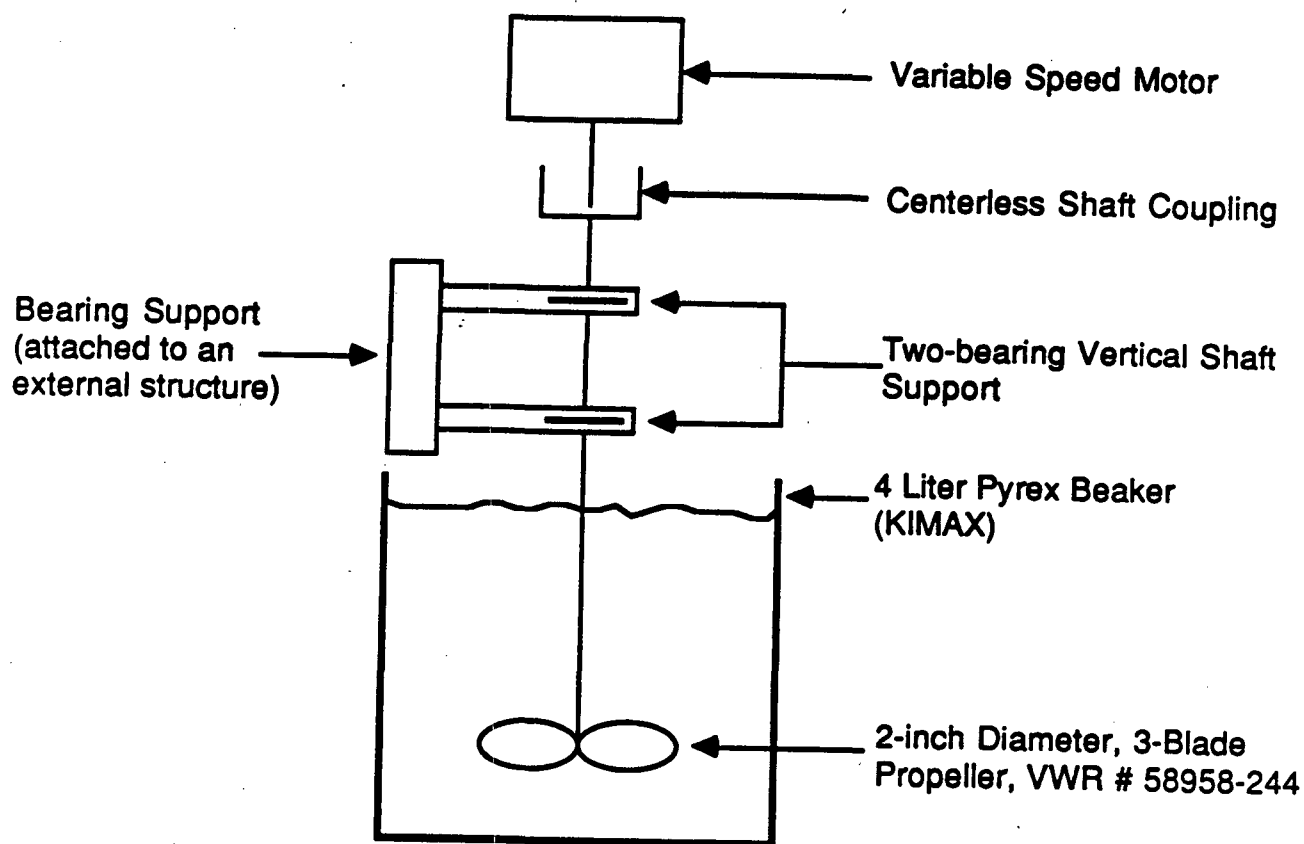
One of the most important parameters of the oil-SPM kinetics problem is the oil-droplet size (distribution). The existing open-ocean oil-weathering code contains an algorithm for dispersion of oil into the water column. However, the motivation for development of the dispersion algorithm (by Professor Mackay) was for a material balance (of oil) around the slick, not information about the oil leaving the slick. As a result, there are no acceptable models which predict oil-droplet size from a dispersing slick. Some researchers use the so-called Weber number approach which predicts oil droplets larger than 50 microns in diameter for ocean conditions. But, observations indicate that oil droplets much smaller, down around 5-10 microns, are prevalent. The mechanism which generates these small oil droplets is not known. Thus, for the purpose of conducting oil-SPM kinetic experiments, a size (range) must be chosen, and for this experimental work, 1-10 micron diameter oil droplets were used because experimental evidence seems to indicate this size range can and does occur in the ocean.

2.2 EXPERIMENTAL TECHNIQUES AND RESULTS

The experimental hardware consisted of the apparatus shown in Figures 2-1 and 2-2. Seawater was filtered through a 0.4 micron filter and added to the 4-liter vessel. The stirring motor was turned on and adjusted to maintain in suspension 53 μm sieved (Jakolof) SPM. The motor speed was approximately 400 rpm. The use of 53-micron sieved sediment is a "practice", which removes particulates that will not stay in suspension with existing (and attainable) experimental turbulence levels. An important experimental criterion is that all sediment stay suspended; otherwise, the analysis of experimental data would require the accounting of the loss of sediment from the stirred water versus time. At the same time, "natural" SPM with size distributions from 1-50 microns have been extensively documented in Alaskan coastal waters (Baker, 1983). Chemical and physical characterization data for the Jakolof Bay SPM are presented in Tables 1-1, 1-2A and 1-2B in Section 1.1.

Oil droplets were prepared with a Hamilton Beach Scovill 7-Speed Blender, model 626-3. Finding the correct combination of blending speed, volume of oil, volume of water, and "handling" required some initial testing.

Figure 2-1 Experimental Hardware Used to Determine Oil-SPM Interaction Kinetics.



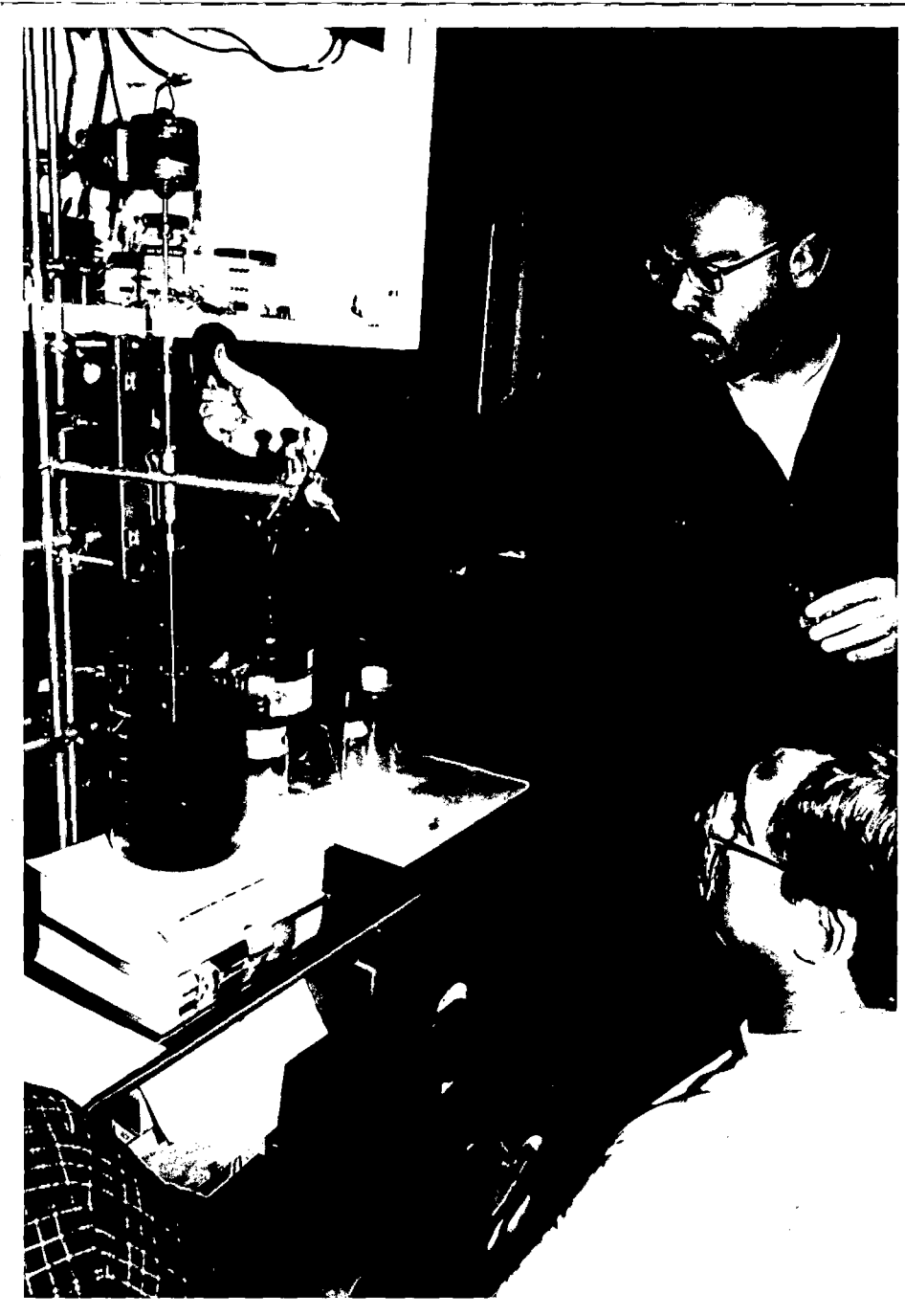


Figure 2-2. Execution of 4-liter oil/SPM interaction experiment at the NOAA Kasitsna Bay field laboratory. Time-series aliquots are being removed for total oil load and SPM determinations by microscopic, gravimetric and FID-GC analyses.

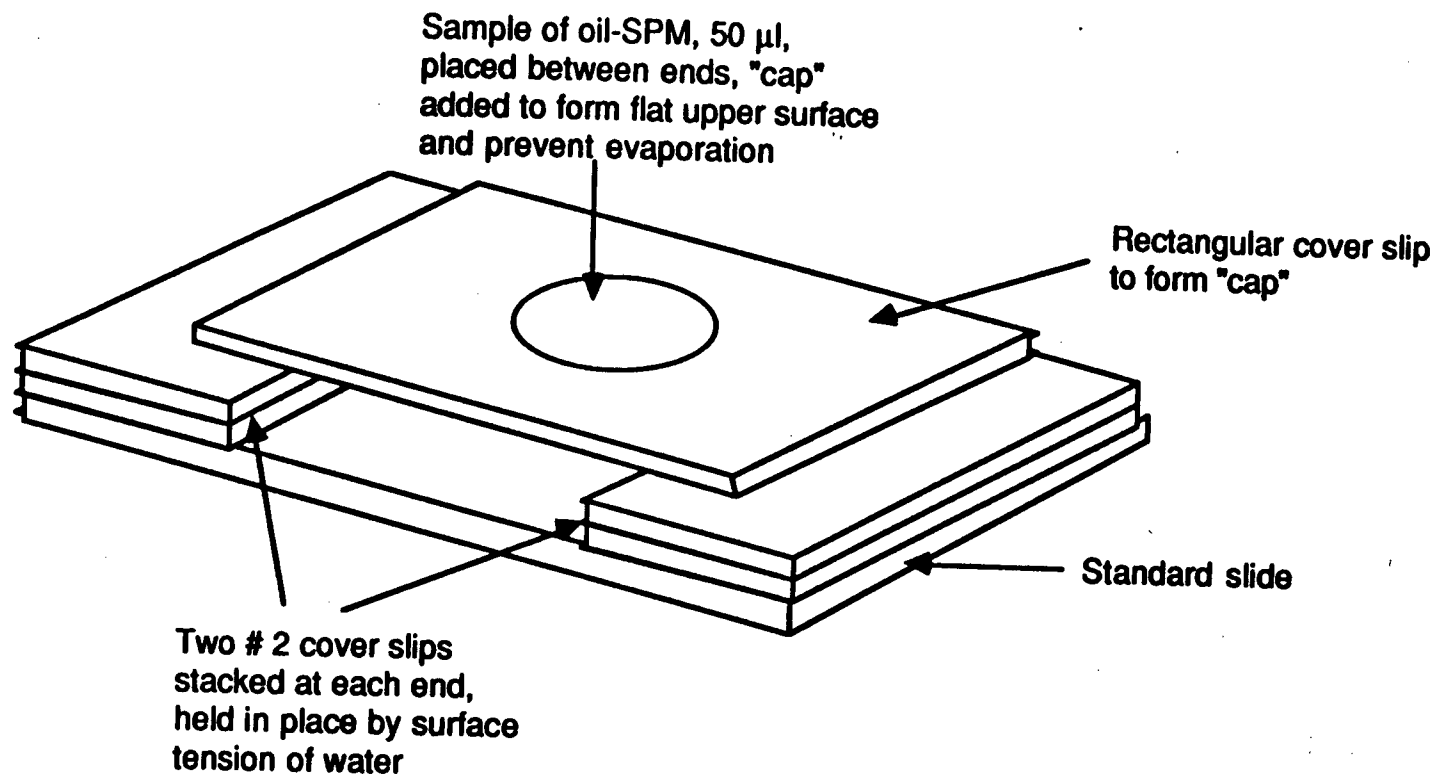
The oil droplet "recipe" was 750 ml of filtered seawater, 15 drops of crude oil from a disposable Pasteur pipet, blending at speed 6 (which was labeled "blend") for five seconds, turning off for five seconds, and then on at speed 6 for five (more) seconds. The contents of the blender were allowed to stand for five minutes and oil that floated to the surface was skimmed off with a kleenex. The "correct" recipe for producing oil droplets is determined by the production of 10-micron diameter droplets. The choice of the 10-micron diameter is based on rather scanty evidence because the actual "configuration" of oil leaving a slick has never been completely or correctly investigated. Thus, a decision was made based on the available data as noted at the end of Section 2.1. This oil droplet "recipe" yielded a final solution with droplets that remained in suspension in the water column and did not coalesce into a surface slick during the course of the experiment. As with the SPM described above, an important experimental criterion is that all oil droplets stay suspended during the experiment.

The experiment was then started (time = 0) by pouring the contents of the blender into the agitated 4-liter vessel which contained the SPM. Samples were taken for total (gross) SPM and oil loading (i.e., total oil and total SPM, not number density) at this time. Samples for microscopic examination were then taken every few minutes for up to 30 minutes.

The "visualization" of the oil droplets and particulate matter (with and without oil droplets) was carried out with visual microscopy. It was discovered (earlier) that the oil droplets would rise, even though they were quite small (5-10 microns). Stokes law predicts a rising velocity (for 5 micron diameter) of about 0.0004 cm/sec or about 1.5 cm/hour in the absence of turbulence.

Therefore, by constructing a counting chamber with cover slips as illustrated in Figure 2-3, the free oil droplets were easily seen and counted. The thickness of the water-oil-SPM sample was approximately 0.4 millimeter. Thus, the free oil drops could traverse this vertical distance in 100 seconds, and all of the free oil drops were at the water/upper-cover-slip surface while the SPM and oil-SPM agglomerates sank to the slide surface. By focusing the

Figure 2-3 Microscope Slide Arrangement for Viewing Oil Droplets and SPM.



2-9

Note: This drawing is not to scale

microscope on these free oil drops, only the free oil drops were seen because the depth-of-field focus (or lack of) caused the SPM which settled to the bottom of this water column to be completely out of focus. By adjusting the microscope focus downward (approximately 0.4 mm) the SPM and oil-SPM particles could be seen with the free oil droplets completely out of focus (not seen!). Visual counting was then conducted. The microscope used was a KYOWA #590136 with a 10x eyepiece and 10x objective. The eyepiece had a Whipple disk installed in it to aid in field definition for particle counting.

The experimental results are presented in Tables 2-1 through 2-9 and Figures 2-4 through 2-6. The experimental conditions were such that the SPM concentration (in terms of number density) was in great excess of the oil concentration. With this experimental condition, equation 2-6 applies for the purpose of data analysis. Hence, a plot of the logarithm of the relative concentration of free oil droplet numbers versus time should yield a straight line. This plot is then a test of the hypothesis represented in equation 2-6. If such a plot of the data did not yield a straight line, then further refinements or adjustments of parameters to control the experiment would have been necessary. Figure 2-4 presents the major results, which are plots of the natural logarithm of the free oil-droplet counts (normalized to the initial oil-droplet count) for four experiments. The lines plotted are least squares fits up to 14 minutes. After 15 minutes the data "bends upward" indicating a loss of the "linear" relations present in the early stages of interaction.

Note that oil loading in the water column never directly enters into the data analysis. All that is required for the oil data is relative population counts. Another requirement though is the necessity of observing enough oil droplets (under the microscope) so that statistical results and counting time can be optimized. Counts were also made of the total free SPM and the maximum number of oil drops on any SPM particle at each time interval. Four to five randomly chosen fields were counted on each slide for free oil, free SPM and oil droplets on SPM. In order to complete the counting experiment, approximately 3 hours at the microscope was required. A photographic recording procedure was not perfected for this project. As a note of record, the oil loading in these experiments was approximately 20 mg/l.

Table2-1 Thursday - November 6, 1986, 11:20 a.m.
OIL-SPM
Half Field

TIME MINUTES	COUNT 1				COUNT 2				COUNT 3				COUNT 4			
	OIL	TOTAL SPM	OIL ON SPM	MAX OIL	OIL	TOTAL SPM	OIL ON SPM	MAX OIL	OIL	TOTAL SPM	OIL ON SPM	MAX OIL	OIL	TOTAL SPM	OIL ON SPM	MAX OIL
		91				63				60				55		
0	12	34	0		12	28	0		11	35	0		17	37	0	
2	17	36	0		24	33	5	1	14*	41	2	1	22	26	2	1
4	24	32	5	3	10	24	0		16	24	3	3	7	41	2	1
6	11	25	9	4	16	23	3	1	18	30	4	1	6	32	5	2
8	7	26	2	1	9	19	6	3	9	31	7	2	4	12	9	5
10	8	52	5	1	8	54	5	1	6	30	12	6	4	41	5	4
15	3	6	4	3	3	24	9	2	4	19	13	4	4	32	19	5
20	5	18	25	7	4	17	5	2	3	15	9	7	2	14	8	5
25	-	-	-	-	-	-	-	-	-	-	-	-	-	-	-	-
30	0	29	7	7	0	18	3	3	0	19	6	3	7	23	5	2

2-11

CHI SQUARE DATA FREE OIL HALF-FIELD

TIME MINUTES	COUNT 1	COUNT 2	COUNT 3	COUNT 4	CHI SQUARE
2.0	17	24	14	22	3.26
4.0	24	10	16	7	11.84
6.0	11	16	18	6	6.80
8.0	7	9	9	4	2.31
10.0	8	8	30	4	33.52
15.0	3	3	4	4	0.29
20.0	5	4	3	2	1.43
30.0	0	0	0	7	21.00

CHI SQUARE COUNTS SPM DATA HALF-FIELD

TIME MINUTES	COUNT 1	COUNT 2	COUNT 3	COUNT 4	CHI SQUARE
0.0	34	28	35	37	1.34
2.0	36	33	41	26	3.47
4.0	32	24	24	41	6.50
6.0	25	23	30	32	1.83
8.0	26	19	31	12	9.36
10.0	52	54	30	41	8.33
15.0	6	24	19	32	17.62
20.0	18	17	15	14	0.63
30.0	29	18	19	23	3.36

Table 2-2 Thursday - November 6, 1986, 3:00 p.m.
OIL - SPM
Half Field

TIME MINUTES	COUNT 1				COUNT 2				COUNT 3				COUNT 4			
	OIL	TOTAL SPM	OIL ON SPM	MAX OIL	OIL	TOTAL SPM	OIL ON SPM	MAX OIL	OIL	TOTAL SPM	OIL ON SPM	MAX OIL	OIL	TOTAL SPM	OIL ON SPM	MAX OIL
0	-	104	-	-	-	123	-	-	-	115	-	-	-	86	-	-
1	12	73	0	-	14	47	0	-	10	52	0	-	11	42	0	-
2	9	42	0	-	10	40	2	1	10	36	0	-	7	30	0	-
3	10	37	7	4	-	27	0	-	11	63	4	2	15	61	2	1
4	3	61	2	1	-	50	1	1	8	72	11	2	9	57	3	1
5	7	49	3	2	11	58	3	1	12	52	7	1	-	48	5	2
6	3	47	3	1	9	55	5	1	9	47	0	0	4	75	6	2
8	5	48	7	1	6	43	8	2	4	43	8	2	4	30	6	3
10	2	40	7	2	6	32	6	2	3	21	9	3	3	25	7	4
15	2	18	7	3	0	22	7	2	3	46	15	4	3	50	14	6
20	0	19	3	1	2	26	10	6	3	15	12	6	2	17	6	4
25	1	47	7	2	4	67	5	2	0	22	18	9	3	13	2	2
30	2	17	4	2	-	16	11	3	1	18	7	3	4	24	3	2

2-12

CHI SQUARE DATA FOR FREE OIL

TIME MINUTES	COUNT 1	COUNT 2	COUNT 3	COUNT 4	CHI SQUARE
1.0	12	14	10	11	0.74
2.0	9	10	10	7	0.67
3.0	10	11	15	-	1.17
4.0	3	8	9	-	3.10
5.0	7	11	12	-	1.40
6.0	3	9	9	4	4.92
8.0	5	6	4	4	0.58
10.0	2	6	3	3	2.57
15.0	2	0	3	3	3.00
20.0	0	2	3	2	2.71
25.0	1	4	0	3	5.00
30.0	2	1	4	-	-

CHI SQUARE DATA FOR SPM COUNTS

TIME MINUTES	COUNT 1	COUNT 2	COUNT 3	COUNT 4	CHI SQUARE
1.0	73	47	52	42	10.41
2.0	42	40	36	30	2.27
3.0	37	27	63	61	20.26
4.0	61	59	72	57	2.16
5.0	49	58	52	48	1.17
6.0	47	55	47	75	9.36
8.0	48	43	43	30	4.34
10.0	40	32	21	25	7.06
15.0	18	22	46	50	23.53
20.0	19	26	15	117	48.34
25.0	47	67	22	3	2.07
30.0	17	16	18	24	0.00
0.0	1	1	1	1	-

Table 2-3 Friday - November 7, 1986, 5:00 p.m.
OIL-SPM
Full Field

TIME MINUTES	COUNT 1				COUNT 2				COUNT 3				COUNT 4			
	OIL	TOTAL SPM	OIL ON SPM	MAX OIL	OIL	TOTAL SPM	OIL ON SPM	MAX OIL	OIL	TOTAL SPM	OIL ON SPM	MAX OIL	OIL	TOTAL SPM	OIL ON SPM	MAX OIL
1	24	62	0	0	16	112	0	0	20	113	1	1	15	129	2	1
3	21	115	3	1	13	149	4	1	10	114	8	3	23	154	8	2
5	-	-	-	-	-	-	-	-	-	-	-	-	-	-	-	-
7	23	109	8	2	11	79	9	3	6	108	7	2	12	119	8	2
9	7	109	11	3	6	141	18	3	8	102	22	6	8	129	20	3
11	6	114	6	1	16	123	11	3	3	62	21	4	14	115	13	2
15	5	116	26	7	5	47	3	1	6	95	27	4	6	99	16	3
23	5	112	19	5	2	67	8	5	4	81	5	2	5	91	8	3
25	4	106	21	4	4	63	13	4	3	83	23	5	2	86	9	3
30	4	54	16	4	3	61	22	4	5	47	8	4	3	45	8	3

2-13

CHI SQUARE DATA FREE OIL

TIME MINUTES	COUNT 1	COUNT 2	COUNT 3	COUNT 4	CHI SQUARE
1.0	24	16	20	15	2.71
3.0	21	13	10	23	6.97
7.0	23	11	6	12	11.85
9.0	7	6	8	8	0.38
11.0	6	16	3	14	11.97
15.0	5	5	6	6	0.18
23.0	5	2	4	5	1.50
25.0	4	4	3	2	0.85
30.0	4	3	5	3	0.73

CHI SQUARE DATA SPM DATA

TIME MINUTES	COUNT 1	COUNT 2	COUNT 3	COUNT 4	CHI SQUARE
1.0	62	112	113	129	24.37
3.0	115	149	114	154	10.39
7.0	109	79	108	119	8.59
9.0	109	141	102	129	8.04
11.0	114	123	62	115	22.66
15.0	116	47	95	99	29.45
23.0	112	67	81	91	12.25
25.0	106	63	83	86	10.99
30.0	54	61	47	45	3.07

Table 2-4 Saturday - November 8, 1986, 10:45 a.m.
 OIL - SPM
 Half Field*/Full Field

TIME MINUTES	COUNT 1				COUNT 2				COUNT 3				COUNT 4			
	OIL	TOTAL SPM	OIL ON SPM	MAX OIL	OIL	TOTAL SPM	OIL ON SPM	MAX OIL	OIL	TOTAL SPM	OIL ON SPM	MAX OIL	OIL	TOTAL SPM	OIL ON SPM	MAX OIL
		74*				134*				155*				145*		
1	22	91	5	1	20	92	1	1	32	129	4	3	34	123	4	1
3	17	103	7	2	24	93	5	2	18	110	13	2	15	112	10	2
5	13	9	1	1	15	26	2	1	22	104	6	2	13	88	14	4
7	20	89	7	2	21	123	13	4	16	112	16	4	23	130	24	5
9	6	125	22	4	13	51	6	2	4	27	1	1	13	73	11	3
11	13	71	18	3	6	47	8	3	9	82	11	5	10	96	19	5
15	5	67	15	5	7	67	15	4	7	63	8	2	9	62	16	4
20	10	43	23	5	8	34	22	9	7	64	5	2	11	66	26	6
25	4	75	24	7	3	64	24	6	9	82	26	5	5	44	33	8
30	4	63	31	6	3	34	14	3	7	25	11	3	4	35	12	3

2-14

CHI SQUARE DATA FREE OIL

TIME MINUTES	COUNT 1	COUNT 2	COUNT 3	COUNT 4	CHI SQUARE
1.0	22	20	32	34	5.48
3.0	24	18	15	17	2.43
5.0	13	15	22	13	3.48
7.0	20	21	16	23	1.30
9.0	6	13	4	13	7.33
11.0	6	9	10	13	2.63
15.0	5	7	7	9	1.14
20.0	10	8	7	11	1.11
25.0	4	3	9	5	3.95
30.0	4	3	7	4	2.00

CHI SQUARE DATA FOR SPM COUNTS

TIME MINUTES	COUNT 1	COUNT 2	COUNT 3	COUNT 4	CHI SQUARE
1.0	91	92	129	123	11.11
3.0	103	93	110	112	2.11
5.0	9	26	104	88	112.23
7.0	89	123	112	130	8.50
9.0	125	51	27	73	75.94
11.0	71	47	82	96	17.38
15.0	67	67	63	62	0.32
20.0	43	34	64	66	14.39
25.0	75	64	82	44	12.45
30.0	63	34	25	35	20.71

**Table 2-5 Thursday - November 6, 1986, 10:50 a.m.
Oil Only
Full Field**

TIME MINUTES	COUNT 1	COUNT 2	COUNT 3	COUNT 4	TOTAL	CHI SQUARE
0	24	34	39	36	133	3.81
2	23	30	25	33	111	2.26
4	29	41	33	35	138	2.17
6	37	37	39	28	141	2.06
8	39	34	24	35	132	3.70
10	21	35	43	40	139	8.19
12.5	43	31	29	31	134	3.67
15	40	33	35	31	139	1.29
20	24	27	31	30	112	1.07

Table 2-6 Friday - November 7, 1986, 8:00 a.m.
Oil Only
Full Field

TIME MINUTES	COUNT 1	COUNT 2	COUNT 3	COUNT 4	CHI SQUARE
0	10	13	6	15	4.18
2	15	12	13	7	2.96
4	8	11	8	15	3.14
6	7	9	5	8	1.21
8	8	7	2	4	4.33
10	11	9	11	10	0.27
15	8	6	11	6	2.16
20	4	5	9	10	3.71
25	9	4	6	8	2.19
30	2	5	8	6	3.57

Table 2-7 Saturday - November 8, 1986, 3:20 p.m.
Oil Only
Full Field

TIME	COUNT 1	COUNT 2	COUNT 3	COUNT 4	COUNT 5	CHI SQUARE
1	22	36	12	17	18	15.81
3	19	23	21	24	28	2.00
5	24	24	27	27	22	0.76
7	19	22	28	24	19	2.55
9	17	14	20	10	20	4.49
11	22	19	26	20	19	1.64
15	20	20	16	14	27	5.11
20	13	15	24	16	28	8.69
25	13	18	17	19	20	1.68
30	17	21	23	25	15	3.41

Table 2-8 Oil/SPM Interaction and Sedimentation Experiments.

Oil/SPM Interaction and Sedimentation Experiments
Gravimetric SPM Loads and Total Oil Estimates
Kasitsna Bay, AK---November 1986

Experiment ID	Sample Description	Samp. ID rep. No. no.	Sediment Concentration (mg/liter)			Tot. Oil Concentration			Vol. Filt. (ml)	****Sample Weights (gms)****		
			Sample	Mean	Std.Dev.	FID GC Extr.	nC21 Conc. (ug/l)	Tot. Oil ESTIMATE (mg/l)		Filter + Sed.	Filter Tare	Sediment Weight
Jakolof Sed.-I (Mother Liquor)	No MeOH/DCM + MeOH/DCM		43025.0						2.0	0.10320	0.01715	0.08605
			41022.0			X	---	---	5.0	0.22260	0.01749	0.20511
Jakolof Sed.-II (Mother Liquor)	No MeOH/DCM	1	41606.7						3.0	0.14296	0.01814	0.12482
		2	41820.0	41832.2	189.4				3.0	0.14421	0.01875	0.12546
		3	42070.0						3.0	0.14400	0.01779	0.12621
	+ MeOH/DCM	1	42220.0						3.0	0.14445	0.01779	0.12666
		2	42056.7	42157.8	72.1				3.0	0.14419	0.01802	0.12617
		3	42196.7						3.0	0.14443	0.01784	0.12659
5 Nov. 1986 (Kirstein/Clary) (AM)	Pre-oil	T0	59.6						25	0.01952	0.01803	0.00149
	30 min + oil	T3	32.8						25	0.01877	0.01795	0.00082
	Final Bot. Sed.					X	---	---		0.03055	0.01830	0.01225
6 Nov. 1986 (Kirstein/Clary) (AM)	Pre-oil	T0	60.3			X	0.19	---	75	0.02208	0.01756	0.00452
	0-3 min + oil	T1	42.1			X	26.73	23.9	75	0.02021	0.01705	0.00316
	16-18 min + oil	T2	46.0			X	30.97	27.7	75	0.02048	0.01703	0.00345
	30-32 min + oil	T3	44.3			X	18.33	16.4	75	0.02232	0.01900	0.00332
6 Nov. 1986 (Kirstein/Clary) (PM)	Pre-oil	T0	52.7			X	0.48	---	75	0.02052	0.01657	0.00395
	1-3.5 min + oil	T1	44.0			X	18.75	16.8	75	0.02106	0.01776	0.00330
	15-18 min + oil	T2	41.5			X	16.62	14.8	75	0.02055	0.01744	0.00311
	30-33 min + oil	T3	43.3			X	11.7	10.5	75	0.02065	0.01740	0.00325
7 Nov. 1986 (Kirstein/Clary) 5 PM Expt.	Pre-oil	T0	57.3			X	INC	INC	75	0.02160	0.01730	0.00430
	1-3.5 min + oil	T1	54.0			X	INC	INC	75	0.02246	0.01841	0.00405
	15-18 min + oil	T2	46.0			X	INC	INC	75	0.02163	0.01818	0.00345
	30-33 min + oil	T3	50.1			X	INC	INC	75	0.02169	0.01793	0.00376
8 Nov. 1986 (Kirstein/Clary) 11 AM Expt.	Pre-oil	T0	60.0			X	INC	INC	75	0.02235	0.01785	0.00450
	1-3.5 min + oil	T1	47.6			X	26.13	23.3	75	0.02205	0.01848	0.00357
	15-18 min + oil	T2	46.3			X	20.09	17.9	75	0.02168	0.01821	0.00347
	30-33 min + oil	T3	44.8			X	INC	INC	75	0.02045	0.01709	0.00336

2-18

Table 2-9 Oil/SPM Interaction and Sedimentation Experiments.

Oil/SPM Interaction and Sedimentation Experiments
Gravimetric SPM Loads and Total Oil Estimates
Kasitana Bay, AK---November 1986

Experiment ID	Sample Description	Samp. ID No.	rep. no.	Sediment Concentration (mg/liter)			Tot. Oil Concentration			Vol. Filt. (mls)	****Sample Weights (gms)****		
				Sample	Mean	Std.Dev.	FID GC Extr.	nC21 Conc. (ug/l)	Tot. Oil ESTIMATE (mg/l)		Filter + Sed.	Filter Tare	Sediment Weight
6 Nov. 1986 Oiled Sedimentation Experiment (Kirstein/Clary) (PM) [Water Temp. = 20.5 C]	0 min settle	S0	1	43.8	42.7	5.7				50	0.01970	0.01751	0.00219
			2	35.2						50	0.01926	0.01750	0.00176
			3	49.0						50	0.02053	0.01808	0.00245
	15 min settle	S15	1	28.2	28.9	3.1				50	0.01832	0.01691	0.00141
			2	33.0						50	0.01948	0.01783	0.00165
			3	25.6						50	0.01960	0.01832	0.00128
	35 min settle	S35	1	28.2	24.3	3.7				50	0.01979	0.01838	0.00141
			2	25.2						50	0.01920	0.01794	0.00126
			3	19.4						50	0.01935	0.01838	0.00097
	60 min settle	S60	1	21.8	18.0	2.7				50	0.01828	0.01719	0.00109
			2	16.2						50	0.01950	0.01869	0.00081
			3	16.0						50	0.01875	0.01795	0.00080
	110 min settle	S110 SPM	1	8.4	13.6	5.3				50	0.01790	0.01748	0.00042
			2	20.8						50	0.01971	0.01867	0.00104
			3	11.6						50	0.01766	0.01708	0.00058
	110 min settle	S110 Bot. Sed.	1							50	0.03199	0.01808	0.01391
			2							50	0.03252	0.01747	0.01505
			3							50	0.03357	0.01797	0.01560
7 Nov. 1986 Un-oiled Sedimentation Experiment [Water Temp. = 20.5 C]	0 min stir	CT0		50.8					50	0.02112	0.01858	0.00254	
	30 min stir	CT30		49.2					50	0.02008	0.01762	0.00246	
	0 min settle	CS0	1	52.2	52.2	0.8				50	0.02048	0.01787	0.00261
			2	53.2						50	0.01968	0.01702	0.00266
			3	51.2						50	0.01899	0.01643	0.00256
	15 min settle	CS15	1	54.6	45.5	6.7				50	0.02027	0.01754	0.00273
			2	43.4						50	0.01977	0.01760	0.00217
			3	38.6						50	0.02067	0.01874	0.00193
	35 min settle	CS35	1	24.2	26.9	3.2				50	0.01797	0.01676	0.00121
			2	25.2						50	0.01840	0.01714	0.00126
			3	31.4						50	0.01857	0.01700	0.00157
	60 min settle	CS60	1	10.6	13.6	2.4				50	0.01868	0.01815	0.00053
			2	13.6						50	0.01768	0.01700	0.00068
			3	16.6						50	0.01900	0.01817	0.00083
	110 min settle	CS110 SPM	1	17.0	15.2	3.7				50	0.01840	0.01755	0.00085
2			18.6	50						0.01950	0.01857	0.00093	
3			10.0	50						0.01869	0.01819	0.00050	

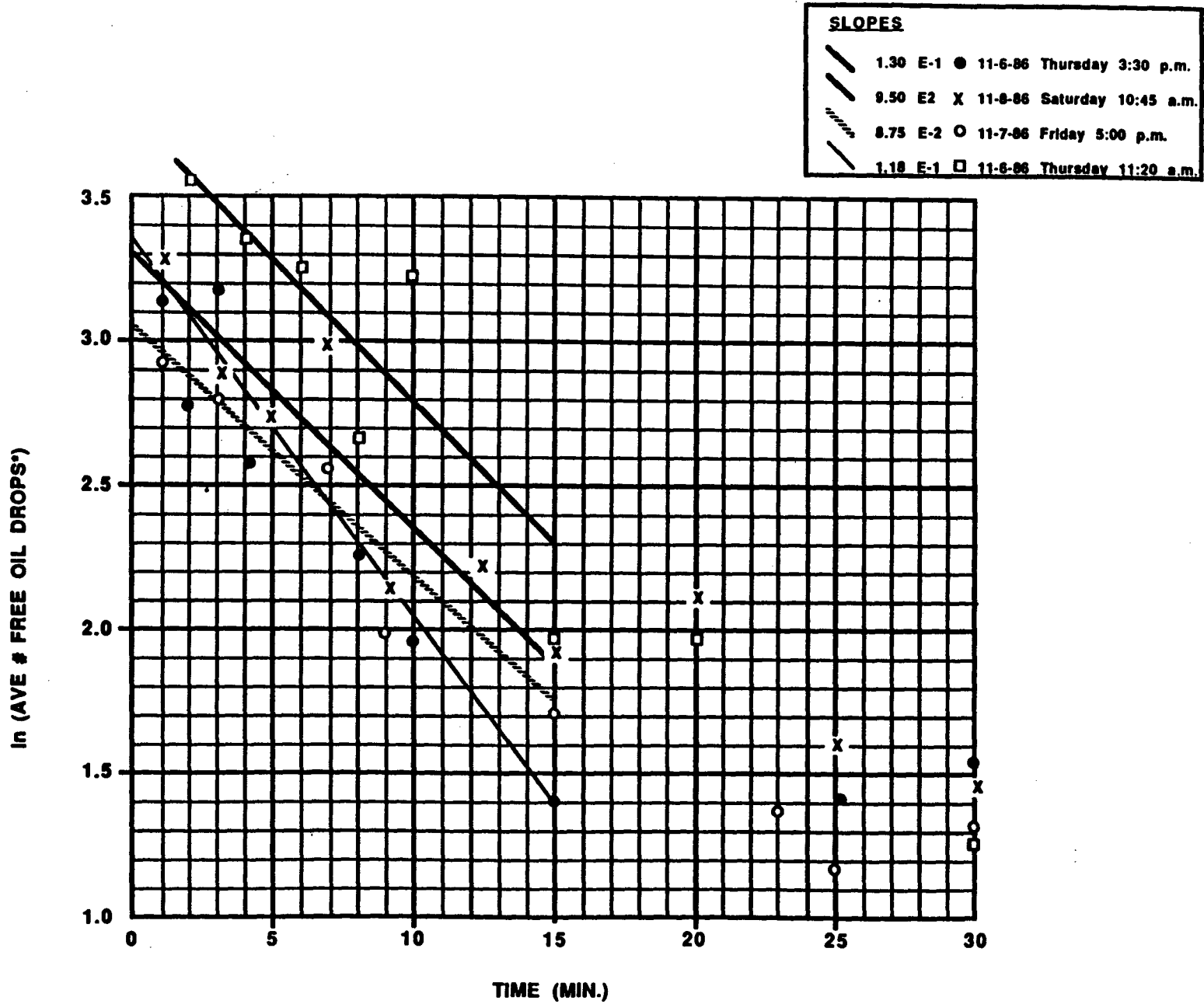


Figure 2-4 Oil-SPM Interactions Free Oil Count*

* normalized to full field counts

In (AVE # FREE OIL DROPS)

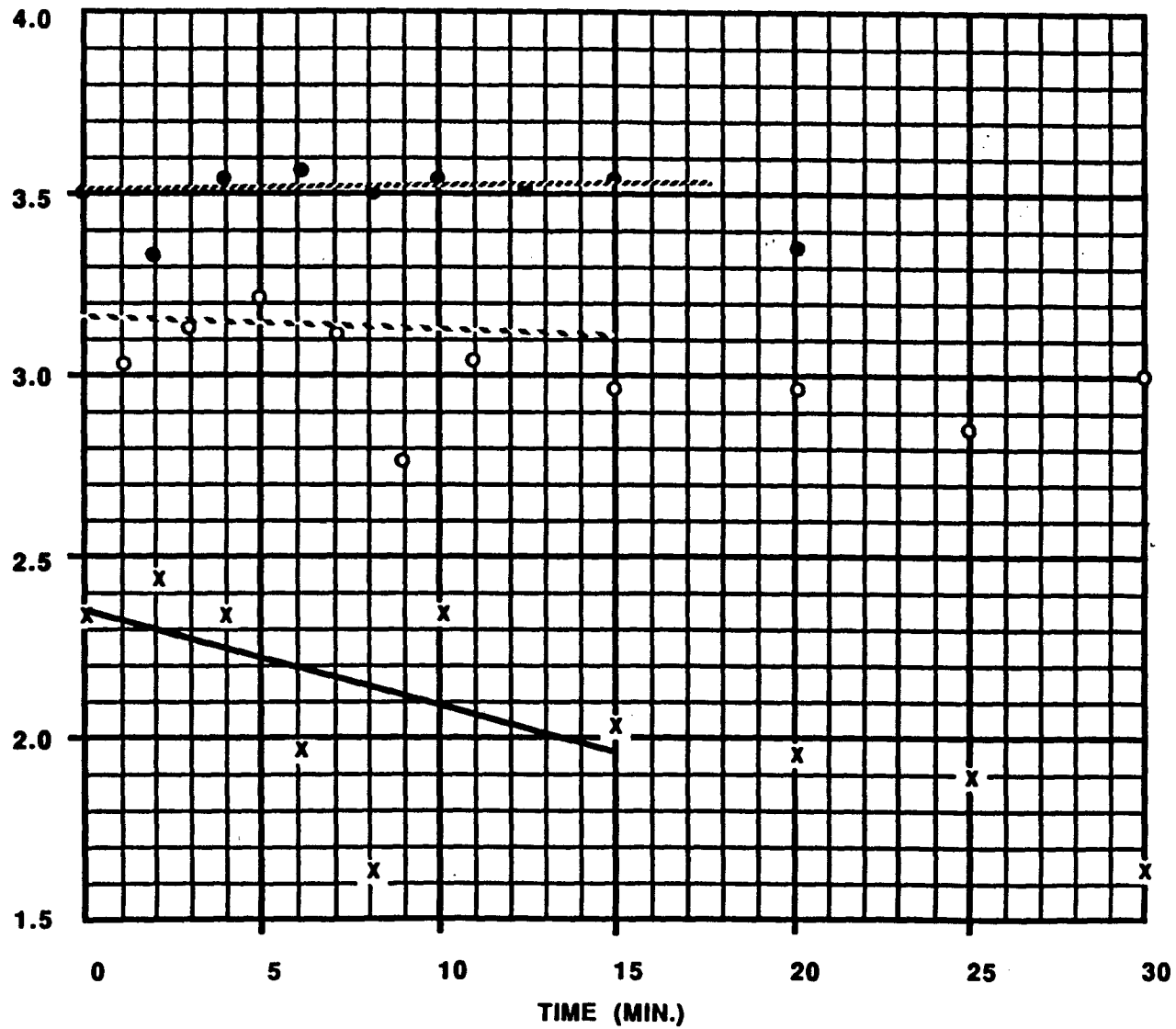


Figure 2-5 Oil Interactions (Oil Only).

SLOPES

- 3.461 E-2 ● 11-6-86 Thursday 3:30 p.m.
- 3.26 E2 X 11-8-86 Saturday 10:45 a.m.
- 1.57 E-2 ○ 11-7-86 Friday 5:00 p.m.

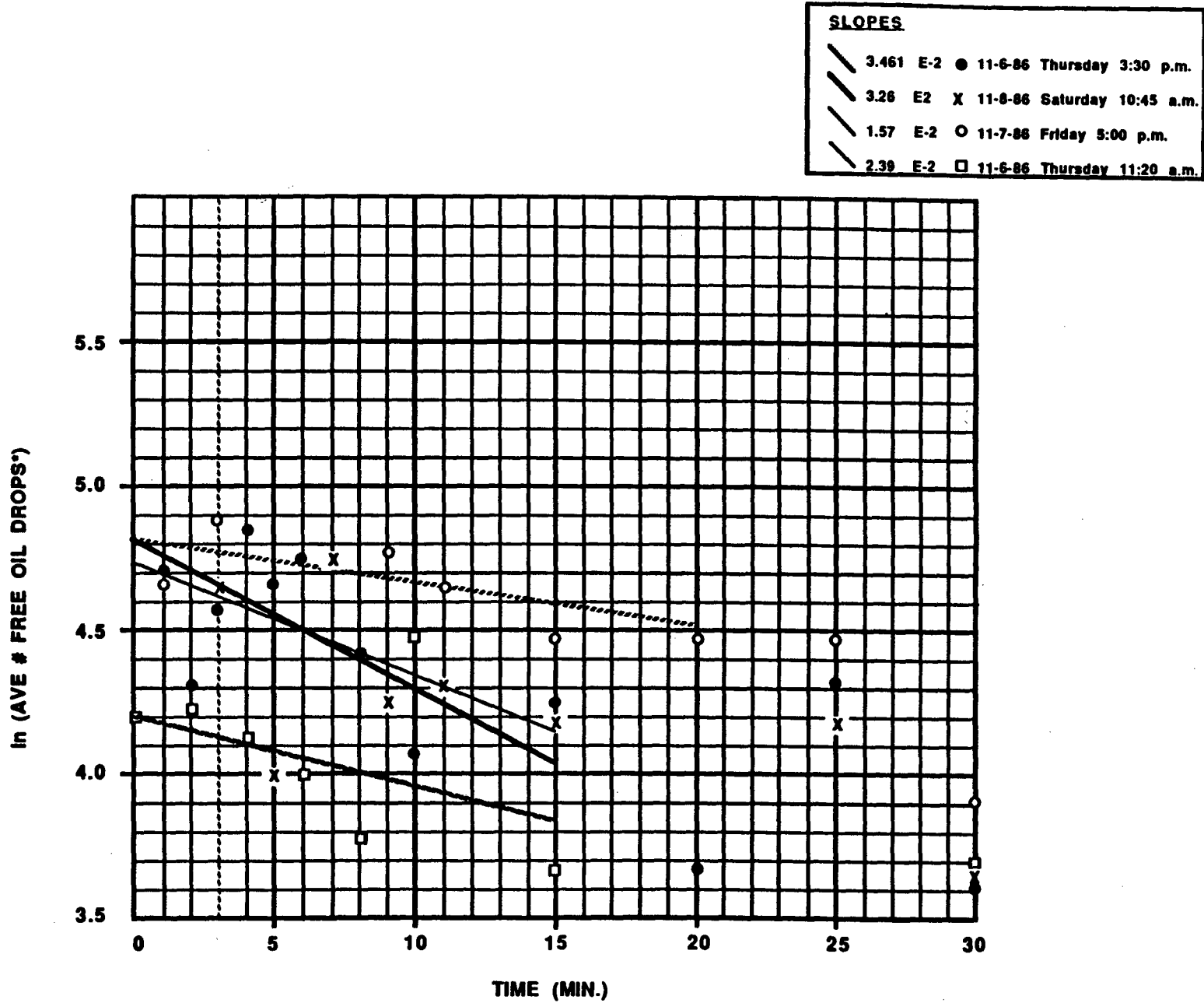


Figure 2-6 Oil-SPM Interactions Total Free SPM.

* normalized to full field counts

From the data in Figure 2-4, the interaction constant described in equation (2-5) is $k = 0.107 \text{ minutes}^{-1}$ or $0.0018 \text{ seconds}^{-1}$, which results in

$$1.3 \left(\frac{\epsilon}{\nu}\right)^{1/2} k_a C_p = 0.0018 \cdot \text{sec}^{-1} \quad (2-7)$$

From Tables 2-8 and 2-9 the sediment loading was measured to be approximately 48 mg/l, so that the above becomes

$$\left(\frac{\epsilon}{\nu}\right)^{1/2} k_a = 2.9 \times 10^{-5} \frac{1}{\text{mg} \cdot \text{sec}} \quad (2-8)$$

In order to attribute the decrease in oil-droplet number density to oil-SPM interactions, a "blank" experiment was conducted with no SPM present. These results are presented in Figure 2-5 and should yield straight lines with zero (no loss of oil droplets) slope indicating no oil-oil interaction. This appeared to be the case for two experiments while a third case yielded a slope of -0.0157. This slope is still smaller than those in Figure 2-4 (when SPM was present) where the slopes ranged from -0.0875 to -0.13.

Thus, it is concluded from these "blank" experiments that oil droplets do not interact (collide and stick) at a rate that is comparable to the oil-SPM rate.

Counts were also made of SPM at each time step to determine if SPM was flocculating significantly. The results are shown in Figure 2-6. The average slope from this graph is -0.11 indicating some flocculation is occurring, but again, not as significantly as oil-SPM interactions.

Tables 2-1 through 2-7 present the actual counting data obtained. The volume counted for each experiment was 50 μl so that the results are directly comparable on a volumetric basis. Some variation occurred in oil and SPM loading (Tables 2-8 and 2-9) but this variation will not affect the development of a rate term. Chi square tests of the data indicate that more counts should be

made in the future to insure statistical confidence. This will not be a problem (in terms of time needed per experiment) as it will not be necessary to count SPM or oil-SPM agglomerates.

The determination of the power input to the propeller (and hence the energy per unit time dissipated) was measured with the experimental hardware shown in Figures 2-7 and 2-8. A string was wound onto the stirring shaft (motor removed) and a weight attached. The (falling) mass (or weight) was then adjusted so that the shaft would rotate at the same speed at which it was driven during an experiment. This matching of speeds is crucial because the power required to drive the propeller is proportional to rate of rotation. The shaft rotation rate was measured electronically (Figures 2-8 through 2-10). Once the rotation rate had been established by adjusting the weight, the time required for the weight to fall a known distance at constant velocity was measured. From this information the power is calculated from

$$P = mgh/t \quad (2-9)$$

where the term mgh is the change in potential energy (in a gravity field). The same measurements were then taken with no water in the vessel so that the energy dissipation due to bearing friction could be subtracted. The net mass required to stir the vessel at 400 rpm was found to be 68 grams and the distance traversed was 2 feet (61 cm) in 4.5 seconds. Thus

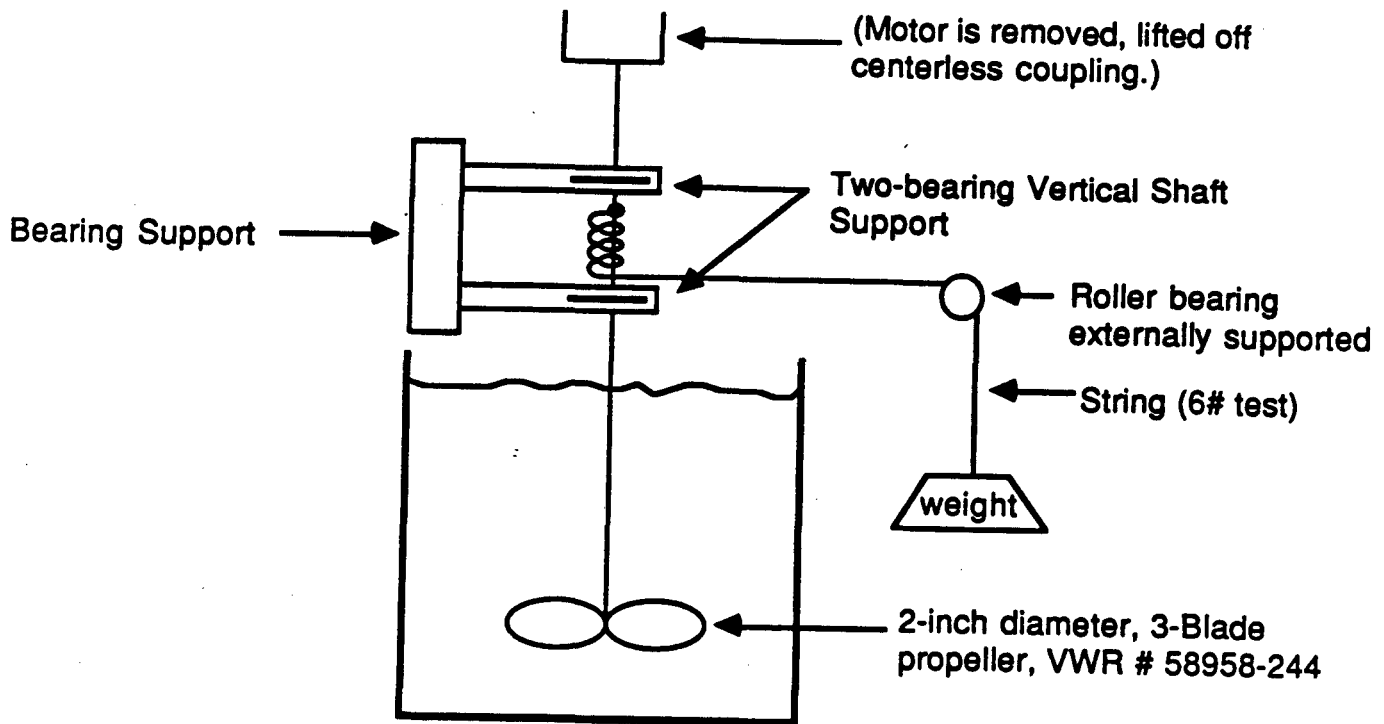
$$P = \frac{(68 \text{ grams})(980 \text{ cm/sec}^2)(61 \text{ cm})}{4.5 \text{ sec}} \quad (2-10)$$

$$P = 9.03 \times 10^5 \frac{\text{dynes} \cdot \text{cm}}{\text{sec}} \quad (2-11)$$

For a liquid volume of 3500 ml and density of 1 gm/cc,

$$\epsilon = \frac{9.03 \times 10^5 \text{ gm} \cdot \text{cm}^2 / \text{sec}^3}{(3500 \text{ cm}^3)(1 \text{ gm/cm}^3)} = 258 \frac{\text{cm}^2}{\text{sec}^3} \quad (2-12)$$

Figure 2-7 Experimental Hardware to Measure the Power Dissipated in a Stirred Vessel.



Note: The string is wound "up" on the shaft, the falling weight allowed to reach constant velocity, and the time required to traverse a vertical distance recorded.

$$\text{Power dissipated} = \frac{mgh}{\text{time}}$$

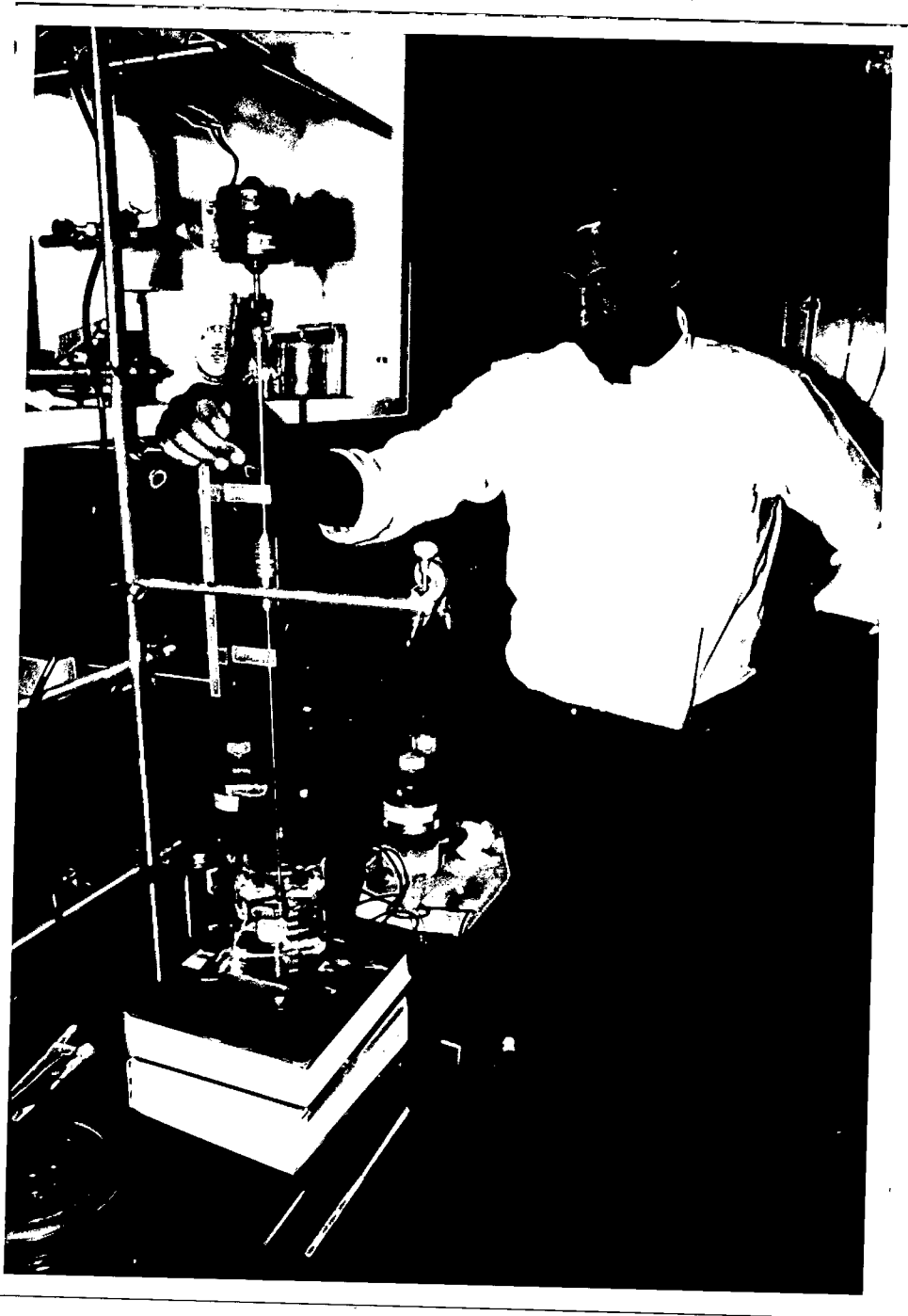


Figure 2-8. Determination of weight required to achieve 400 rpm stirring turbulence in the 4-liter beaker experiments. Note that the stirring motor is de-coupled from the propeller shaft during the falling weight drop timed experiment. Additional studies were completed without water in the beaker to quantify the effects of friction in determining the power input to the stirred chamber system.



Figure 2-9. Construction of the binary counting circuit board used to accurately measure rpm in the 4-liter beaker oil/SPM interaction experiments.



Figure 2-10. Trigger mechanism attached to the stirrer shaft and binary counting circuit board (in the background adjacent to the battery power supply) for the experimental rpm determinations.

and finally

$$\left(\frac{\epsilon}{\nu}\right)^{1/2} = \left(\frac{258 \text{ cm}^2/\text{sec}^3}{0.01 \text{ cm}^2/\text{sec}}\right)^{1/2} = 160 \text{ sec}^{-1} \quad (2-13)$$

Using this value of $(\epsilon/\nu)^{1/2}$ results in

$$k_a = \frac{2.9 \times 10^5 \frac{1}{\text{mg} \cdot \text{sec}}}{160 \text{ sec}^{-1}} \quad (2-14)$$

or

$$k_a = 1.8 \times 10^{-7} \frac{1}{\text{mg}} \quad (2-15)$$

This value of k_a then represents the term shown in equation 2-3. It is valid for the size range of particles used in its experimental determination and should not be extrapolated to other particle sizes. Extrapolation to other number densities is valid, as is extrapolation to other ϵ/ν values.

From these experiments it can be concluded that oil droplets and SPM do collide and stick in a turbulent field. It must be emphasized that these experiments were conducted with fresh (unweathered) Prudhoe Bay crude and Jakolof sediment. Only one set of experimental conditions was (repeatedly) investigated. Extrapolation to other oils, weathered Prudhoe Bay oil and other sediments is not valid. These experiments present a successful observation of oil-SPM interaction kinetics and a measured rate constant under rigorously controlled experimental conditions.

The application of the results measured in these oil-SPM experiments begins with the equation of continuity for free oil droplets.

$$\frac{\partial C_o}{\partial t} + \frac{\partial}{\partial x}(V_x C_o) + \frac{\partial}{\partial y}(V_y C_o) + \frac{\partial}{\partial z}(V_z C_o) =$$

(2-16)

$$\frac{\partial}{\partial x}(k_x \frac{\partial C_o}{\partial x}) + \frac{\partial}{\partial y}(k_y \frac{\partial C_o}{\partial y}) + \frac{\partial}{\partial z}(k_z \frac{\partial C_o}{\partial z}) + R_{op}$$

The determination of the velocity and turbulent transport coefficients and resulting integration of this equation must be accomplished by an ocean circulation model. The oil-SPM kinetic expression is R above and thus describes the rate of loss of free oil droplets in the water column (and also the production rate for oil-SPM agglomerates). R is equation 2-3 (with a - sign). This continuity equation (in the water column) requires boundary conditions for both sediment and oil droplets.

2.3 IMPLICATIONS FOR MODEL DEVELOPMENT

2.3.1 Application of Oil-SPM Kinetic Equations

The application of kinetic equations for particle-particle interactions involves some subtleties which can best be illustrated with an example. The concept that will be illustrated in this example is that of the relationship between "concentration" and "number density" and how this concept applies to the assumptions made for the Kasitsna Bay experiments conducted in November 1986. Note that the rate equation (and the working equation for the November experiments) for the free oil-drop concentration contains the sediment "concentration," i.e.,

$$\frac{dC_o}{dt} = 1.3 \left(\frac{\epsilon}{\nu}\right)^{1/2} k_a C_o C_p$$

(2-17)

Based on observations over time frames much longer than those for the November experiments (i.e., longer than 30 minutes), it was noted that the SPM does flocculate. This means that the SPM concentration as related to number density of SPM particles changes with respect to time. Using a constant value for C_p then is not strictly correct. To be correct, the value of C_p in the above rate

equation must decrease with time even though the actual SPM concentration in terms of mg/l is constant (i.e., no distinction if there are many small particles or a few large ones in suspension).

Therefore, consider how C_p could be corrected for the short timeframe of the experiments if the loss of SPM "numbers" is an experimental objective. The starting point for SPM-SPM kinetic description is the SPM collision frequency equation:

$$R = 1.3 \left(\frac{\epsilon}{\nu}\right)^{1/2} k_s n_1^2 \quad (2-18)$$

where n_1 is the number density of singlets, i.e., fresh suspended particles. This equation is the rate at which SPM particles collide with themselves, not oil drops. Now assume that every collision results in sticking to form the "doublet" as follows:



This equation describes the stoichiometry of the particles. Using this equation the rate of loss of singlets is

$$\frac{dn_1}{dt} = -2k_s n_1^2 \quad (2-20)$$

because every collision results in the loss of two particles. The rate of appearance of doublets is

$$\frac{dn_2}{dt} = +k_s n_1^2 \quad (2-21)$$

This assumes (for the sake of illustration and simplicity) that the "doublets" do not react with anything. However, a similar equation for the collision and sticking of doublets to form higher order particles can (in principle) be

written. Solving the above equation for n_1 with n_1^0 particles present at $t=0$ yields

$$n_1 = \frac{n_1^0}{1 + 2k_s n_1^0 t} \quad (2-22)$$

Note that the "material balance" or stoichiometry is preserved, i.e.,

$$n_1^0 - n_1 = 2n_2 \quad \text{for all } t \quad (2-23)$$

and as $t \rightarrow \infty$, the result for n_2 becomes

$$n_2(t \rightarrow \infty) = \frac{k_s (n_1^0)^2 t}{2k_s n_1^0 t} = \frac{n_1^0}{2} \quad (2-24)$$

But, observing this result experimentally cannot be done using "concentration" of SPM, i.e., the concentration of SPM is always the same because singlets and doublets cannot be distinguished.

Therefore, particles must be counted; simply measuring "concentration" will not work. In order to take into account the decrease in number density of SPM particles (over short time frames), an approximation can be used for the total number of SPM particles. Start with the total number of particles at any time:

$$n_T = n_1 + n_2 = \frac{n_1^0 (1 + k_s n_1^0 t)}{(1 + 2k_s n_1^0 t)} \quad (2-25)$$

and since a short timeframe is of interest, use a Taylor series approximation which yields

$$\frac{n_T}{n_1^0} = 1 - k_s n_1^0 t \quad (2-26)$$

Therefore, in the rate expression for oil, the SPM concentration should be written as (to a "better" approximation)

$$C_p = C_p^0 (1 - \bar{k}_s t) \quad (2-27)$$

where C_p^0 is the time = 0 SPM concentration in mg/l. The rate constant \bar{k}_s can be measured by counting particles. Thus, the SPM number density, not concentration, decreases linearly in time for small times. A nephelometer could be used to observe the timeframe where the SPM particle density is linear.

This example shows what the starting equations are for the particle-particle kinetics and the assumptions required. It is true that the kinetics are based on "number density," yet the primary observable is usually "concentration." There must be a relationship available which relates number density to concentration in order for open-ocean "circulation" calculations to be made. Actual observations of open-ocean SPM kinetics should be made and interpreted (i.e., fast or slow relative to oil-SPM kinetics) before a general model is derived. It is possible now to "write" the equations for all interactions; however, using these equations in a practical application is most likely impossible.

The above example also illustrates the observations that must be made and experimental variables controlled in order to obtain useable results. It is currently not possible to obtain more than one or two derived quantities (i.e., rate constants) from a particle-particle kinetic experiment. These experiments must be "controlled" so that only one event is occurring (or two at most).

2.3.2 Kinetic Algorithm Use in an Ocean Circulation Model

Now consider how the kinetic algorithm will be used in an ocean-circulation model. The ocean-circulation model will be capable of transporting material according to the mass balance equation. The kinetic algorithm will be written in a subroutine named SPMRTE (for SPM rate). The calling statement will appear as

```
CALL SPMRTE (SPMC,SPMR,EV,TSTEP,NT)
```

where SPMC is an array which contains the SPM concentrations for all fractions or types being considered, SPMR is an array which contains the SPM rates for all fractions or types (including oil drops), EV is ϵ/ν , TSTEP is the (size of) the time step and NT is the number of SPM types being considered.

Physical parameters required are the constants which relate number density to concentration for each NT type of SPM. This parameter will be named ZETA, be a dimensioned array, and be used as

$$\text{NDEN}(I)=\text{ZETA}(I)*\text{SPMC}(I) \quad (2-28)$$

with NDEN declared as REAL*4 (as required). The kinetic rate constants for the collision and sticking of component i with component j will be stored in an array KC(I,J) also declared REAL*4. These parameters must be entered before the program begins execution (i.e., similar to the way True Boiling Point distillations are entered in the oil-weathering codes). Both ZETA(I) and KC(I,J) would be passed to subroutine SPMRTE through a common block.

The calculation would proceed through a DO-LOOP to calculate the relative decrease in number density of particles through a Taylor series approximation

$$\text{ZETA}(I)=\text{ZETA}(I)*(1.-\text{KC}(I,I)*\text{TSTEP}) \quad (2-29)$$

Then the rate expressions are calculated according to

$$\text{SPMR}(I)=\text{KC}(I,J)*\text{SPMC}(I)*\text{ZETA}(I)*\text{SPMC}(J)*\text{ZETA}(J) \quad (2-30)$$

These rate arrays will be returned to the main program and then integrated. The main program also calculates how much SPM has entered (or left) the water column through the bottom boundary and likewise for oil drops at the surface. The main program also must keep track of the sediment accumulated on the bottom (i.e., a material balance of sediment on the bottom in order to keep from fluxing up something that is not there). Also, note that the boundary conditions for both sediment and oil drops are "fluxes", and algorithms for these fluxes (i.e., Grant's and Mackay's, respectively) must be encoded elsewhere.

Clearly, in programming these equations into a code, numerous "traps" will have to be included to prevent "nonsense" numbers from being generated. These traps will become apparent as real numbers are developed and calculations tried. The actual mathematics are relatively straightforward, the actual computation procedure (i.e., the integration, choosing step sizes, etc.) will be a challenge.

2.4 RESULTS OF OIL/SPM INTERACTION KINETICS DETERMINATIONS USING A 28 LITER STIRRED CHAMBER

2.4.1 Background, Required Assumptions and Limitations of Experiments

As described in the Sections 2.1 and 2.2, the experimental procedure for determining the oil-droplet and suspended-particulate interaction is based on the continuity equation in which the rate term is identified. This rate term for the interaction kinetics is first order with respect to oil-droplet concentration and first order with respect to suspended-particle concentration. The rate expression is proportional to the energy dissipation rate to the one-half power.

In the beginning of this program, the rate-determining experiments were conducted in the 28-liter stirred vessel illustrated in Figure 2-11

through 2-14. While initial experiments met with some difficulties, separatory-funnel and filtration procedures were ultimately developed to allow discrete measurements of mg/liter concentrations of dispersed oil, free SPM and oil/SPM agglomerates as a function of time (see Section 3.1 and Year One Interim Report for complete experimental details). In these experiments, the oil (fresh Prudhoe Bay crude, 2-day weathered¹ and 12-day weathered)...

¹ was introduced as a surface slick, and turbulence was provided by a propeller in much the same manner as described in Section 2.2.

One drawback to the experimental device was that its complexity and size prevented an accurate measurement of the energy dissipation rate, ϵ , such that the turbulent shear rate which is expressed as $(\epsilon/\nu)^{1/2}$ could not be experimentally determined to properly scale the kinetics expression. In order to calculate the energy dissipation rate for an experiment, the power input can be calculated from

$$P = wT \quad (2-31)$$

where w is the angular velocity of the stirrer (radians/sec) and T is the measured torque (dyne-cm) which yields the power delivered to the contents of the vessel (dyne-cm/sec). Because all of the power delivered to the stirrer is dissipated in the entire fluid mass of the vessel, the rate of energy dissipation per unit mass of fluid is

$$\epsilon = \frac{P}{V\rho} \quad (2-32)$$

¹Weathered Prudhoe Bay Crude oil was prepared by a 16 liter experimental spill in the flow-through outdoor wave-tanks at NOAA's Kasitsna Bay facility as described in Payne et al. (1984). Chemical and Physical Properties of the fresh and weathered oil are presented in Table 2-10.

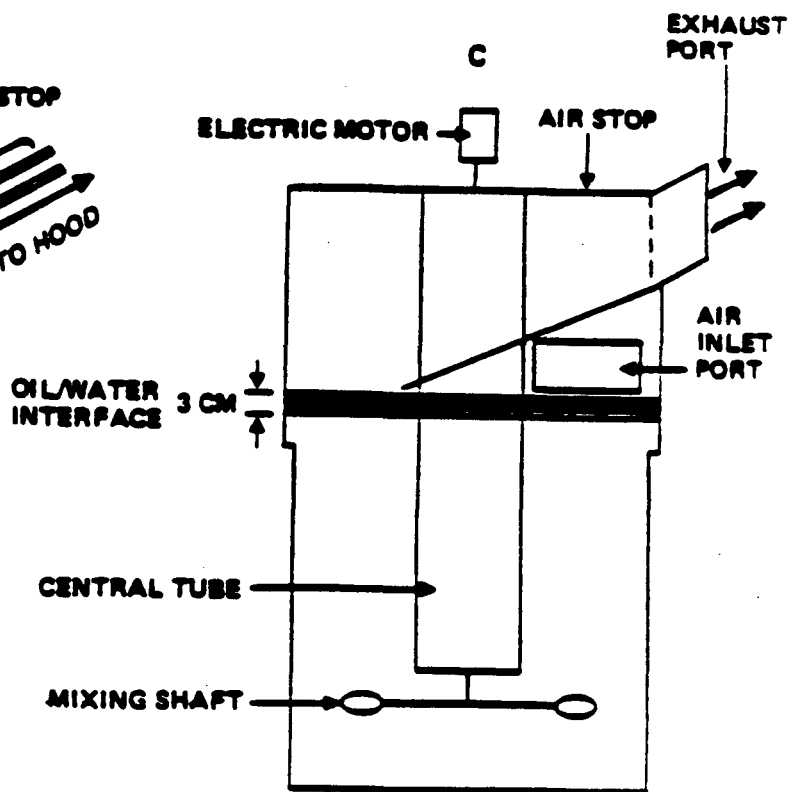
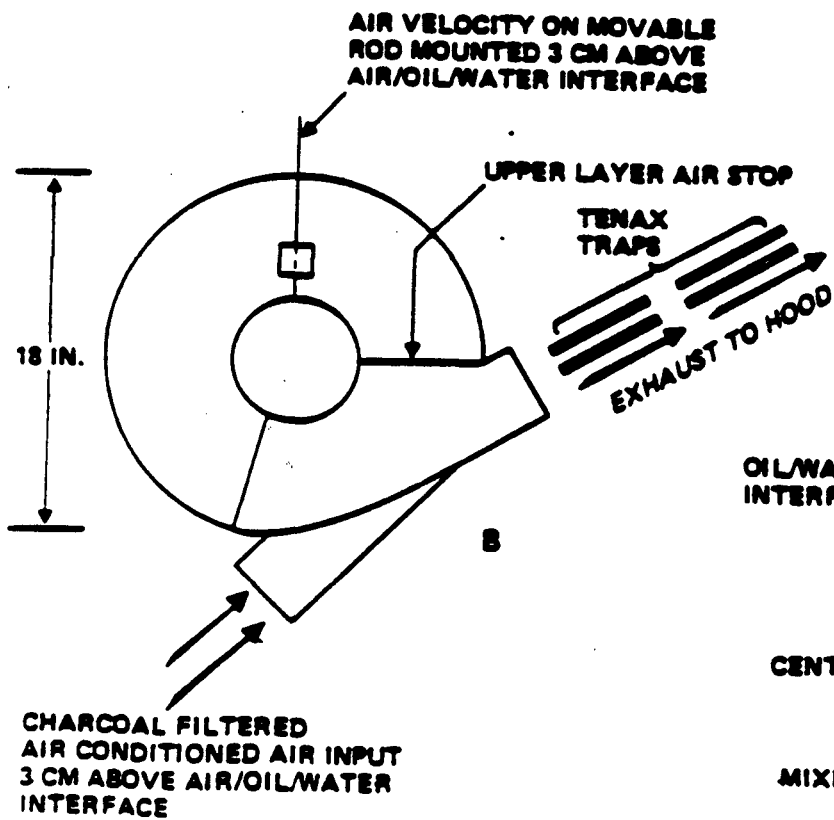
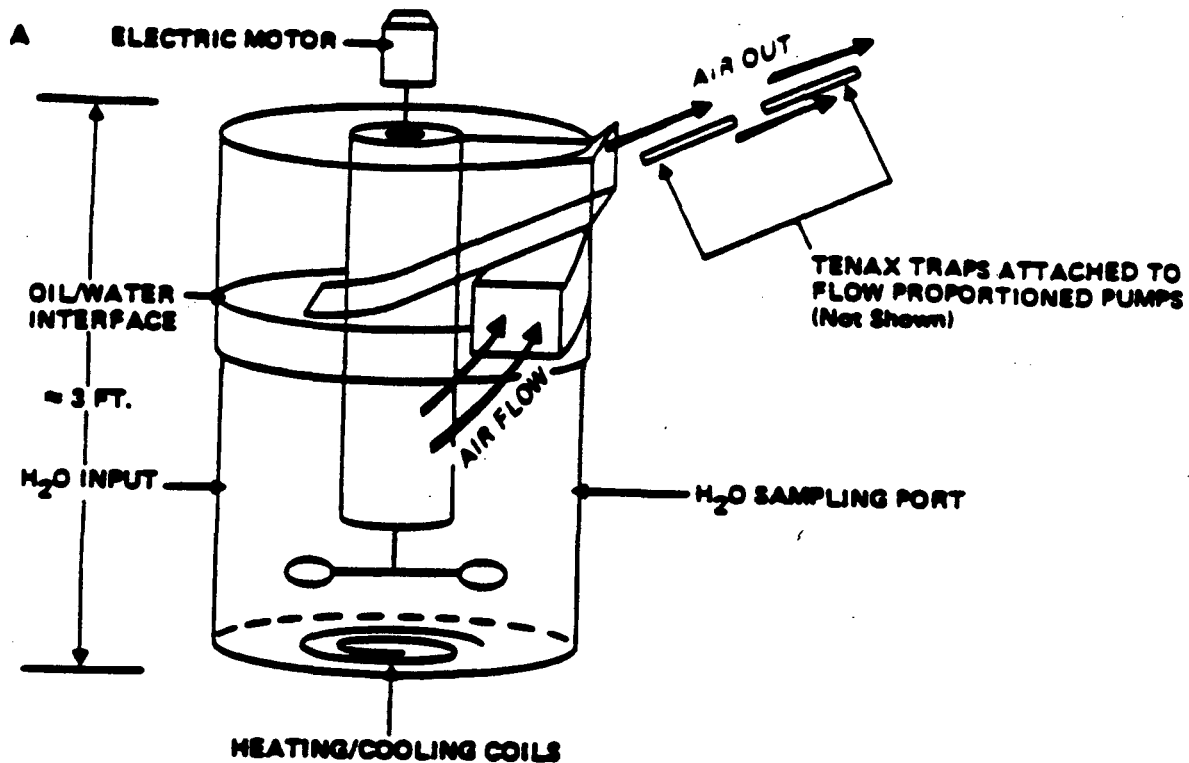


Figure 2-11. Prototype tank design for evaporation/dissolution and oil/SPM interaction experiments.



Figure 2-12. Twenty-eight liter oil/SPM interaction chamber equipped with directional air manifold and stirring motor for introduction of turbulence. Subsurface water samples are collected through the stockcocks inserted through the side of the glass chamber.

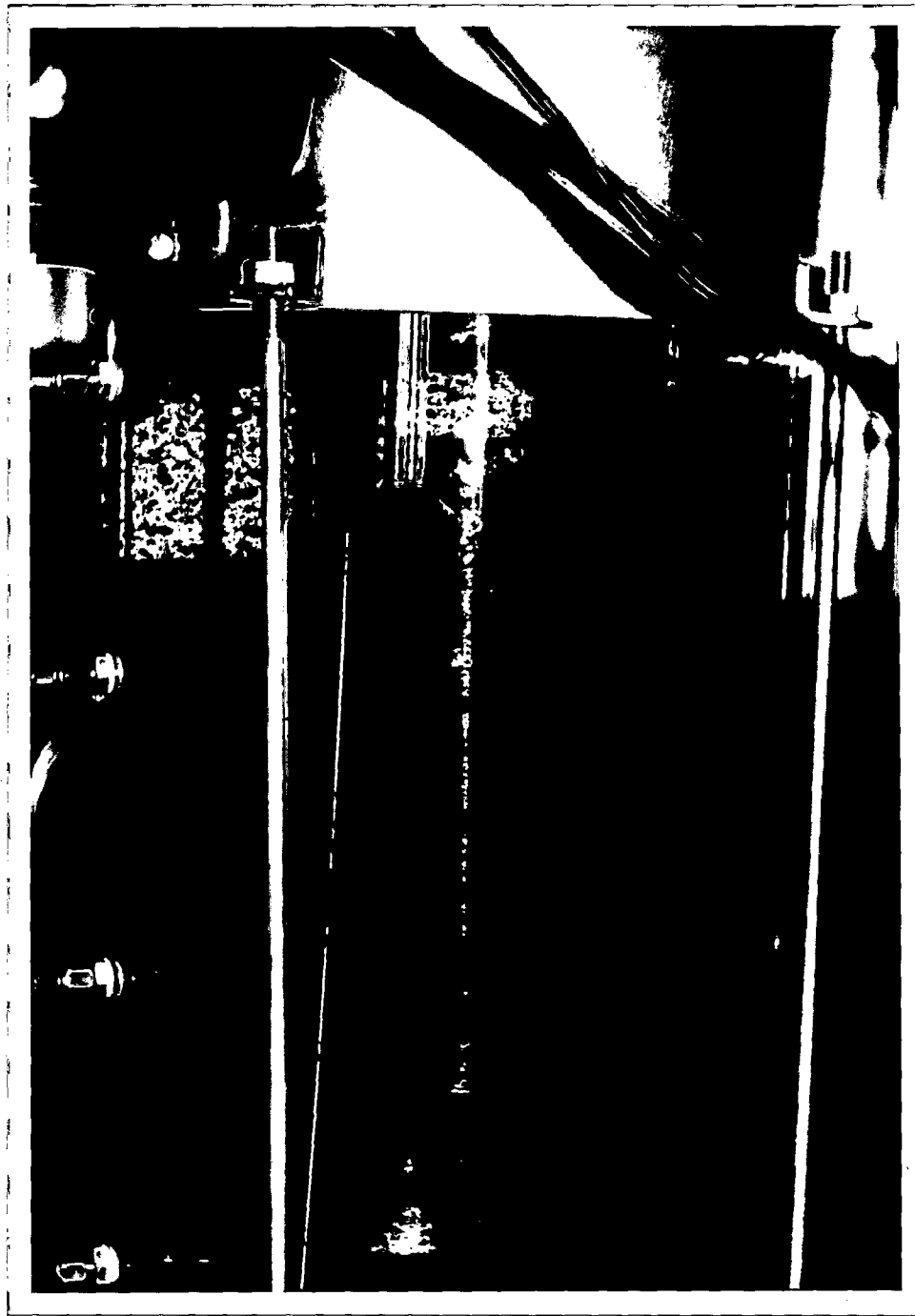


Figure 2-13. Dispersed oil droplets and SPM in the 28 liter stirred reaction chamber using 12-day weathered Prudhoe Bay crude oil and 53 μm sieved Jakolof Bay SPM.



Figure 2-14. Twenty-eight liter oil-SPM interaction chamber containing residual dispersed oil droplets and SPM two minutes after termination of stirring turbulence.

Table 2-10. Chemical and Physical Characteristics of Oil from Wave Tank #4 Oil/SPM Interaction Experiment

Time	Hydrocarbon Concentration (mg/g oil)		Interfacial Tension (dynes/cm)		Viscosity @ 38° C (centipoise)	Water Content (% by weight)
	Total Resolved	Unresolved Compounds	Oil/Water	Oil/Air		
Starting Crude	119	229	24.6	31.8	30	.30
48 hours	63.8	145	11.1	33.0	43	.17
12 days	27.5	104	11.5	34.6	800	6.3

where V is the actual volume of fluid in the vessel and ρ is the fluid density. Therefore, the working equation is

$$G = \left(\frac{e}{\nu}\right)^{1/2} = \left(\frac{P}{V\rho\nu}\right)^{1/2} \quad (2-33)$$

Attempts to install an "in-line" torque meter in the stirred chamber were unsuccessful due to serious propeller shaft alignment problems and the actual size of the apparatus. Thus, the decision was ultimately made to discontinue use of the 28-liter chamber and proceed with the smaller apparatus described in Section 2.2 where the energy dissipation rate could be successfully measured. It is significant, however, that with both systems, the turbulence in the experimental solutions (i.e., derived from the propeller rotation and any resident baffles) was just sufficient to maintain a nominal 50 mg/l suspended load of sieved (<53 μ m) particulate material from Jakolof Bay. Thus, although the applied power and contained volumes were different, it is possible (to a first approximation) to assume similar turbulence levels necessary to just maintain the SPM loads in both the 4-liter and 28-liter systems. As described in Section 2.2, the measured turbulent shear rate $(\epsilon/\nu)^{1/2}$ for the smaller system was 160 sec^{-1} . Therefore, in order to proceed with the data analyses from experiments completed in the 28-liter system, a similar value will be assumed here.

The rate of a bimolecular reaction can be measured by following the rate of disappearance of one or both of the reactants or by the rate of formation of the product. From equation 2-3 in Section 2.1 the rate, R, of oil/SPM interactions was given by

$$R = \frac{d \text{Prod}}{dt} = 1.3 (\epsilon/\nu)^{1/2} k_a C_o C_p \quad (2-34)$$

where R = rate of interaction (reactant disappearance or product formation, $\mu\text{g-oil}_{\text{SPM}}/\text{liter}\cdot\text{hr}$ or $\text{mg-oil}_{\text{SPM}}/\text{liter}\cdot\text{hr}$ with proper conversions)

Prod = measured oil-SPM agglomerate concentration ($\mu\text{g-oil}_{\text{SPM}}/\text{liter}$)

- ϵ = energy dissipation per unit mass (cm^2/sec^3)
 ν = kinematic viscosity (cm^2/sec)
 C_o = concentration of oil droplets (mg/liter)
 C_p = concentration of SPM (mg/liter)

For this derivation it should be noted that the designation $\mu\text{g-oil}_{\text{SPM}}$ (or $\text{mg-oil}_{\text{SPM}}$) represents the total mass of oil in μg (or mg) associated exclusively with the SPM phase as measured by filtration and solvent extraction of the isolated "oiled" SPM sample and FID-GC analysis of the extract. For these calculations the sum of all resolved peaks in the GC profile was used to quantify the total hydrocarbon load on the SPM (see Section 3.1 for experimental details). Thus, the term $\mu\text{g-oil}_{\text{SPM}}/\text{liter}$ represents the concentration of oil associated with all the SPM measured in a specific volume of sample.

$$\text{Since } R = \frac{\mu\text{g-oil}_{\text{SPM}}}{1 \text{ hr}} \quad (2-35)$$

$$k_a = \frac{\text{mg (oil}_{\text{SPM}}) \cdot 1}{\text{mg (oil)} \cdot \text{mg(SPM)}} = \frac{1}{\text{mg}} \quad (2-36)$$

which is dimensionally similar to what was derived for k_a in Section 2.1 (i.e., units of reciprocal concentration).

During the execution of any oil/SPM interaction experiment within the 28-liter stirred chamber, free SPM loads were observed to decrease in an exponential fashion with time due to interactions with dispersed oil droplets (not sedimentation). At the same time, total free oil droplet concentrations were observed to increase due to changes in the oil/water interfacial surface tension resulting from oil oxidation, water incorporation (into oil) and SPM coating on oil droplets (presumably affecting both interfacial surface tension and surface charge). Oiled SPM agglomerates increased in a non-linear fashion which approached some limiting value controlled by the initial SPM loading in

the experimental apparatus. These trends are shown graphically in Figure 2-15 where equations 2-37, 2-38 and 2-39 are defined to describe the time series concentrations of free oil droplets and SPM.

2.4.2 Results and Discussion of Experiments with Fresh, 2-Day Weathered, and 12-Day Weathered Prudhoe Bay Crude Oil and Jakolof Bay "SPM"

Actual free oil droplet concentration data for stirred chamber experiments with fresh, 2-day weathered and 12-day weathered Prudhoe Bay crude oil are presented in Figure 2-16. Plots of actual $\ln C_p/C_p^0$ vs time data for the three experiments are presented in Figure 2-17. From these plots it is possible to obtain values for the slope, m , in equation 2-37 and k in equations 2-38 and 2-39 which can later be used to explicitly solve for k_a the oil-SPM rate constant in equation 2-34. Values for m and k (along with correlation coefficients) for the three experiments completed in the 28 liter stirred chamber are presented in Table 2-11.

2.4.2.1 Oil/SPM Interaction Rate Constant with Fresh Prudhoe Bay Crude Oil

Rewriting equation 2-34 becomes

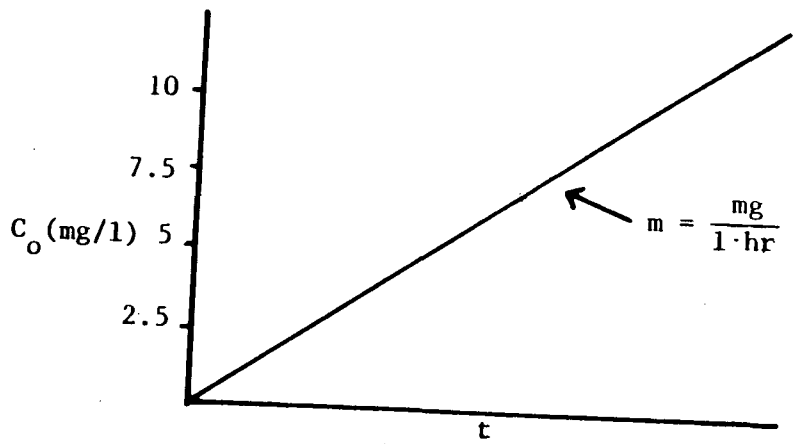
$$\frac{d\text{Prod}}{dt} = Q C_o C_p \quad (2-40)$$

where $Q = 1.3 \left(\frac{\epsilon}{\nu}\right)^{1/2} k_a$

Substituting from equations 2-37 and 2-38 yields

$$\frac{d\text{Prod}}{dt} = Q m t C_p^0 e^{-kt} \quad (2-41)$$

Re-arranging the equation and taking the integral yields



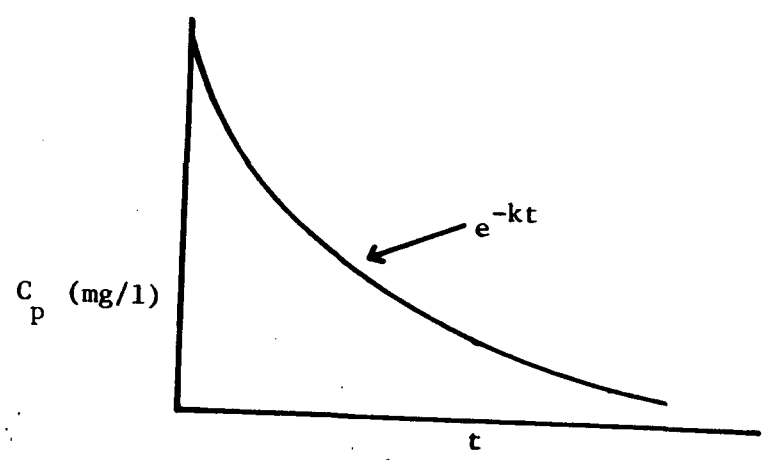
$$C_o = C_o^o + mt$$

at $t = 0$; $C_o^o = 0$

2-45

$$\therefore C_o = m \cdot t \quad (2-37)$$

where t is in hours



$$C_p = C_p^o e^{-kt} \text{ when } C_p^o \text{ equals the initial SPM load charged into the water column} \quad (2-38)$$

or

$$\ln \frac{C_p}{C_p^o} = -kt \quad (2-39)$$

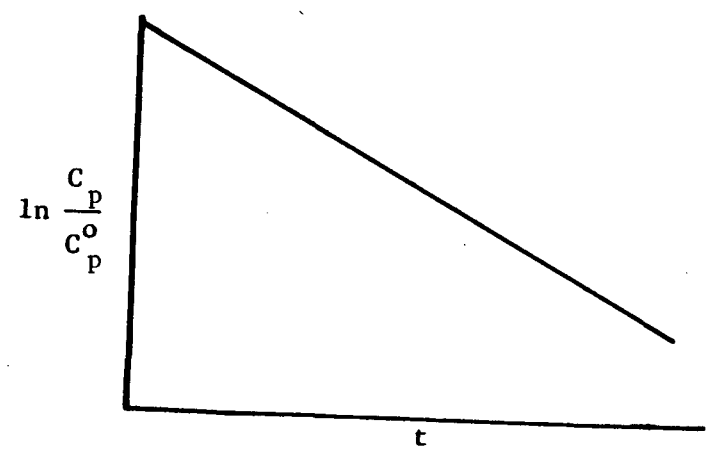
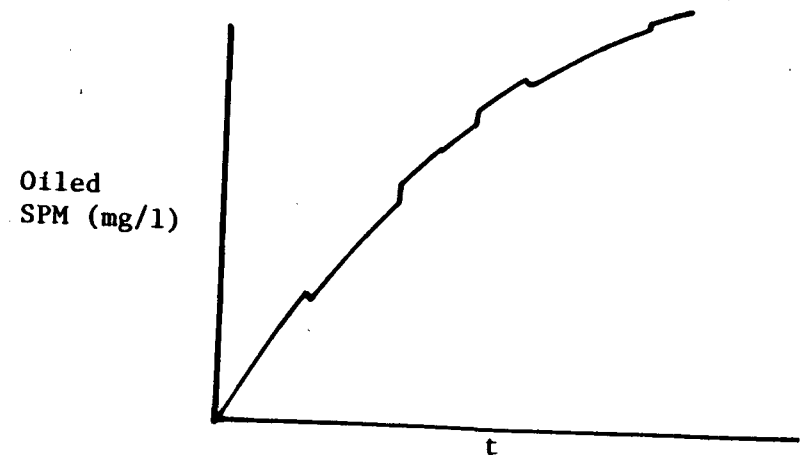


Figure 2-15 . Idealized time-series profiles of free oil (C_o), free SPM (C_p) and oiled SPM loads in 28 liter stirred chamber experiments.

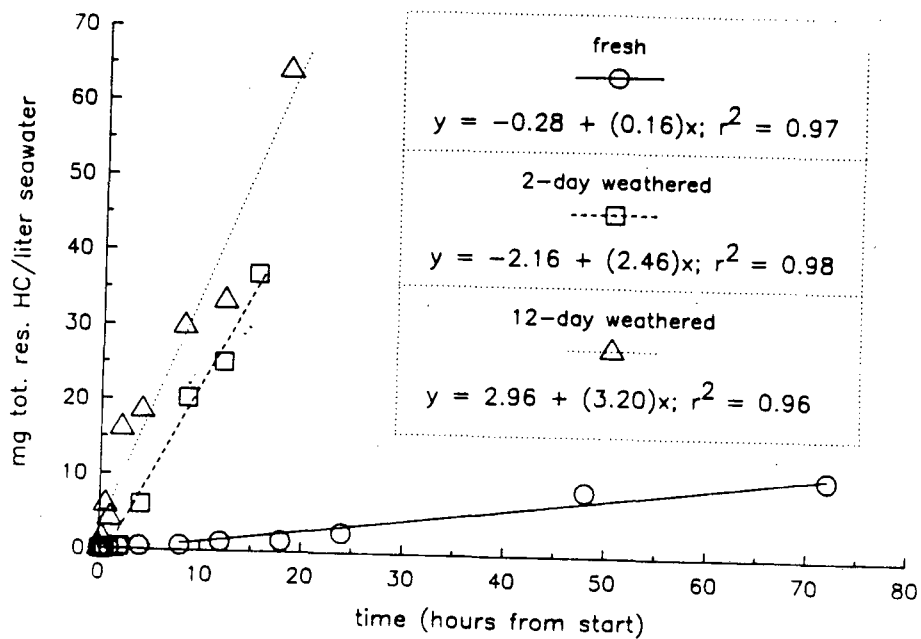


Figure 2-16. Dispersed oil concentrations (mg total resolved hydrocarbons/liter of seawater) over time (hours after the spill event) for experiments with fresh, 2-day weathered and 12-day weathered Prudhoe Bay crude oil. Linear regression lines fitted to the data and r^2 values for each set of data are included in the figure.

Ln(SPM-t/SPM-0) vs. Time
for Different Starting Oil Types

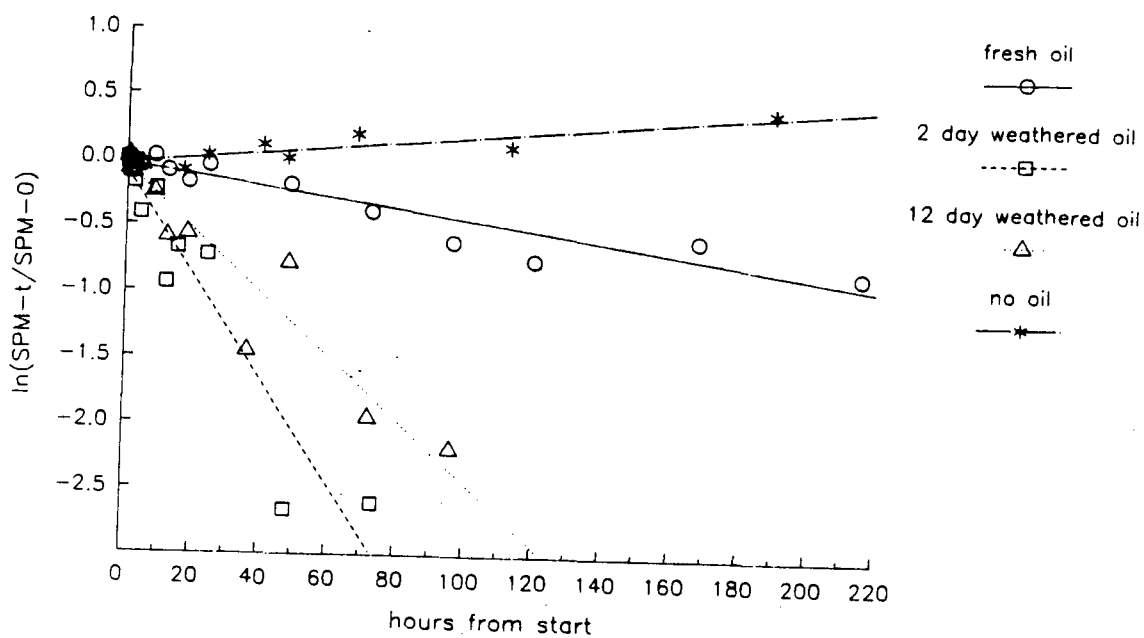


Figure 2-17. Natural logarithms of the ratios of SPM concentrations at time - "t" hours to that at time = 0 hours versus time in experiments with fresh, 2-day weathered and 12-day weathered Prudhoe Bay crude oil and no oil₂ addition. The linear regression lines fitted to the data have $r^2 \geq 0.89$ for all plots.

Table 2-11. Values for m and k (equations 2-37 through 2-39) calculated from data plots in Figures 2-16 and 2-17.

Oil Type	k_1 (hr ⁻¹)	r	m (mg/l·hr)	r
Fresh	0.0041	0.94	0.156	0.94
2-day weathered	0.0039	0.85	2.5	0.97
12-day weathered	0.0024	0.96	3.2	0.91

Note: r = correlation coefficient for linear regression lines fitted to data in Figures 2-16 and 2-17.

$$\int d\text{Prod} = QmC_p^o \int t e^{-kt} dt \quad (2-42)$$

$$\text{Prod} = QmC_p^o \left[\frac{e^{-jt} (-kt-1)}{-k^2} + \text{const} \right] \quad (2-43)$$

$$= QmC_p^o \left[\text{const} - \frac{e^{-kt} (kt+1)}{k^2} \right] \quad (2-44)$$

$$= QmC_p^o \left[\text{const} - \frac{(kt+1)}{k^2 e^{+kt}} \right] \quad (2-45)$$

At time=0, no product has been generated. Thus for Prod=0, the

$$\text{const} = \frac{1}{k^2}$$

As $t \rightarrow \infty$, equation 2-45 reduces a constant (i.e., the initial loading)

$$\text{Prod} = Q m C_p^o$$

From inspection of equation 2-45 it is apparent that a value for Q can be determined by plotting measured Product concentration ($\mu\text{g oil}_{\text{SPM}}/\text{liter}$) vs time and assigning values for Q until a reasonable fit to the data is obtained. Figure 2-18 presents such a series of computer generated curves for the fresh Prudhoe Bay crude oil plus Jakolof Sediment SPM experiment. From the figure a range of values for Q of 0.05 to 0.08 is obtained. Using the value of 160 sec^{-1} for $(\epsilon/\nu)^{1/2}$ and solving equation 2-40 yields

$$k_a = 6.7 \times 10^{-8} \text{ to } 1.3 \times 10^{-7} \text{ 1/mg}$$

$k=4.1e-3$ Fresh Oil Expt Oil Data
 Q range from 0.03 to 0.12

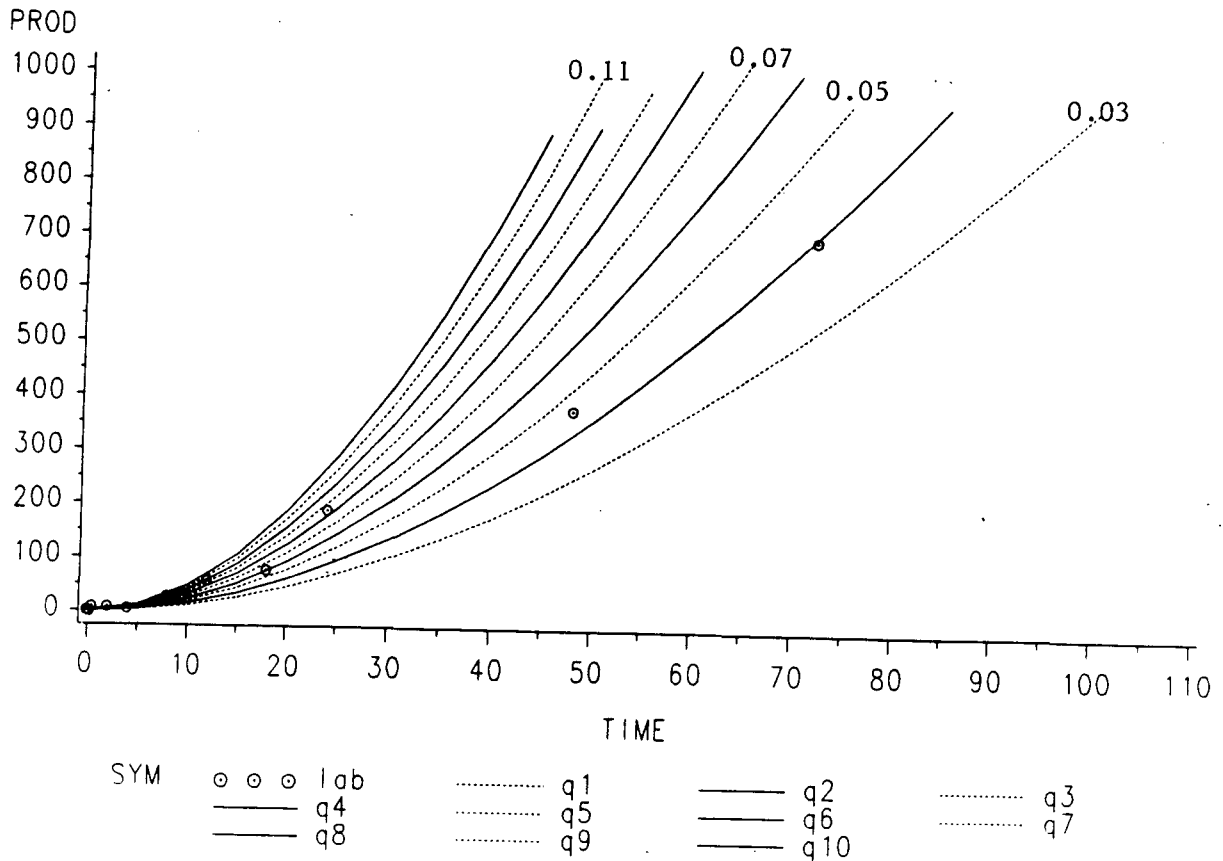


Figure 2-18. Computer generated plots of product concentrations (μg oil SPM/liter seawater) versus time (hours after spill event) for values of Q ranging from 0.03 to 0.12. Experimental data points are indicated by circles for experiment with fresh Prudhoe Bay crude oil and Jakolof Bay sediment ($\leq 53 \mu\text{m}$).

These values agree very well (within a factor of three) with the value of 1.8×10^{-7} l/mg obtained with the smaller reaction vessel described in Section 2.2. Thus, in two completely different experimental systems, using different parameters to measure the rate of reaction (free oil droplets measured by microscope versus oil-SPM agglomerates measured by selective isolation, solvent extraction and gas chromatography), very similar reaction rate constants were obtained. This very close agreement is particularly significant because it validates the overall approach of the two independent methods and adds credibility to the values obtained for the rate constant of the interaction of fresh Prudhoe Bay crude oil and $<53 \mu\text{m}$ Jakolof Bay SPM.

2.4.2.2 Oil/SPM Interaction Rate Constant with 2- and 12-Day Weathered Crude Oil

This same approach with the data sets obtained from the 28-liter stirred chamber experiments with Jakolof Bay SPM plus 2 and 12-day weathered Prudhoe Bay crude oil yielded:

$$k_a = 3.3 \times 10^{-8} \text{ l/mg for 2-day weathered oil}$$

$$k_a = 2.9 \times 10^{-8} \text{ l/mg for 12-day weathered oil}$$

These rate constants are in the same order of magnitude, but slightly lower than the rate constant obtained in the 28 liter experimental system using fresh Prudhoe Bay crude oil. Inspection of Figures 2-17 and 3-6(a), which show a more rapid decline of SPM with 2-day and 12-day weathered oil, would lead to the expectation that the more rapid decline of SPM with these weathered oils should yield a higher rate constant, k_a . In actual fact, with the 2- and 12-day weathered oil, the oil droplet concentrations in the water column were an order of magnitude higher than the oil droplet concentrations with fresh Prudhoe Bay crude oil. This reflects the lower oil/water interfacial surface tension in the weathered crude (Table 2-10) and, hence, the tendency for the oil to disperse into the water at higher oil droplet concentrations under a constant energy turbulent regime.

With dispersed oil concentrations being so much higher in the experiments with the 2- and 12-day weathered oil (see Figure 3-6(b)), any SPM which

interacted with the dispersed oil phase tended to remain in the dispersed or surface oil phase rather than remain in the SPM phase of whole water samples that were collected during experiments. Therefore, when time-series aliquots were removed from the stirred chamber and allowed to stand in the separatory funnel, the oil-SPM aggregates remained in the "floating" or dispersed oil phase and were significantly under-represented. As a result, when the formation of product in milligrams of oil associated with SPM per liter is plotted versus time, the overall maximum concentration of product is significantly under-represented. This results in smaller values for the lumped-parameter constant, Q , necessary to obtain an idealized fit to experimental data. As a result of Q being artificially small, solutions of equation 2-40 will yield values of k_a (at a constant energy dissipation rate) which are also low.

These results clearly show the efficacy of the smaller oil-SPM interaction system described in Section 2.2. Specifically, with the 4-1 system the oil droplet number density and concentration can be controlled, such that oil concentrations will not be too much in excess of the SPM phase.

- 3.0 CHEMICAL PARTITIONING AND PHYSICAL BEHAVIOR OF DISPERSED OIL DROPLETS AND OIL/SPM AGGLOMERATES
- 3.1 SEPARATION AND ANALYSIS OF SPM AND DISPERSED OIL FRACTIONS BY INHERENT DENSITY DIFFERENCES

To obtain better estimates of the discrete hydrocarbon quantities in the SPM and dispersed oil fractions, a sub-surface whole water sample was collected from the experimental chambers (at pre-determined time intervals) and placed in a glass separatory funnel that was completely filled with solution. The sample in the separatory funnel was maintained in a stationary position for a sufficient period of time (2 hrs) to allow for inherent density differences between dispersed oil droplets and SPM to produce a physical separation between the two fractions (i.e., oil droplets rise and SPM sinks in the separatory funnel). Losses of specific hydrocarbons due to volatilization of lighter fractions into an overlying head space are minimized because the separatory funnel is completely filled with sample. This sampling protocol subsequently allows for three reasonably discrete "phases" to be collected from the separatory funnel: 1) an "SPM phase" that is comprised of oiled and un-oiled SPM accumulating at the bottom of the separatory funnel, 2) a "dissolved phase" that is comprised of the water in the separatory funnel (excluding the upper oil layer) and 3) a "dispersed oil phase" that is comprised of the oil layer at the top of the separatory funnel. The "SPM" and "dissolved phases" are physically separated and extracted with methylene chloride to recover hydrocarbons. The "dispersed oil phase" is recovered with solvent rinses following removal of the "SPM" and "dissolved phases" from the separatory funnel.

Although this separatory funnel approach yields three discrete samples, a limitation in the general application of this procedure became apparent during initial experiments with oil-SPM-seawater systems. For distinctions between hydrocarbon quantities contained in the "dissolved" and "SPM phases" to be accurate, all of the SPM in a water sample must collect at the bottom of the separatory funnel. Observations during experiments indicated that a portion of the SPM often adhered to the sides of the funnel rather than sinking to the bottom. Furthermore, this trend was more pronounced when SPM particles became more "oiled". This resulted in the following limitations: 1) an underestimation of the total amount of hydrocarbons contained in the "SPM phase" of a sample (due to not only incomplete recovery of all of the SPM in the water

phase but also the possible loss of more heavily "oiled" particles that preferentially adhere to the funnel walls) and 2) an overestimation of hydrocarbon quantities in the "dissolved phase" due to inclusion of SPM adhering to the separatory funnel walls. The latter "dissolved phase" could be further misleading since it would likely contain the relatively insoluble aliphatic compounds (specifically associated with the SPM) that would not in reality exist in the "dissolved" phase of the sample. Hence, a means needed to be developed to insure that SPM particles were not included in the "dissolved phase" of a sample.

To achieve the desired separation between "dissolved" and "SPM" phases, the following general approach was adopted. After "differential phase settling" in the separatory funnel, the aqueous portion of a sample (i.e., containing both SPM and water) was vacuum filtered through a 47 mm diameter, 0.4 μm pore size polyester membrane filter (Nuclepore catalog number 181107). The resulting water filtrate (free of SPM) was then extracted with methylene chloride and analyzed for the "dissolved fraction" of hydrocarbons, and the particulate matter retained on the filter was extracted as described below to quantify the "SPM fraction" of hydrocarbons.

3.1.1 Method Validation for Polyester Filter-Vacuum Filtration Procedure

Filter blanks were processed through the entire vacuum filtration procedure to insure that: 1) the filter was resistant to the extraction solvents (i.e., methanol and methylene chloride) and did not contribute any interfering peaks during subsequent FID-GC analysis; 2) the filter would maintain its structural integrity through all manipulation steps of the filtration process plus pre- and post-filtration measurements of filter weights for determination of the exact mass of SPM filtered and extracted; and 3) the filter would not require pre-wetting with an organic solvent (e.g., methanol) to facilitate passage of aqueous solutions.

To evaluate whether the solvent rinses (i.e., methanol and methylene chloride) of the filters were sufficient to recover all of the oil from the SPM, a spike/recovery validation experiment was performed. The spiked material was prepared by mixing 40.8 mg (dry weight) of the < 53 μm sieved Jakolof sedi-

ments with 600 mls of seawater and 8.0 mls of fresh Prudhoe Bay crude oil in a 1000 ml glass beaker for 9 hours. This mixture was transferred to a separatory funnel, and differential phase separation was allowed to occur as described above. The water and SPM phase was then vacuum filtered (30 cm Hg) through a polyester filter, and the water filtrate was analyzed as the "dissolved phase" for hydrocarbons. The filter was then vacuum extracted with 10 mls of hydrocarbon-free distilled water (to remove residual seawater and salt) followed by 15 mls of methanol (to "dry" the sample) and 30 mls of methylene chloride. The combined methanol-methylene chloride filtrates were partitioned against seawater, and the resulting methylene chloride fraction was transferred to a collection flask. The remaining seawater-methanol solution was back extracted with methylene chloride, and the combined methylene chloride extracts were condensed and analyzed by capillary column FID-GC. To insure that complete extraction of the SPM had occurred, the polyester filter containing the extracted SPM was re-extracted a second time (using the vacuum technique) with an additional 30 mls of methylene chloride that was concentrated and analyzed separately.

The FID gas chromatogram of the Prudhoe Bay crude oil used in this technique validation experiment is presented in Figure 3-1a, and the chromatogram of the seawater filtrate (dissolved phase) is presented in 3-1b. Comparison of the two chromatograms demonstrates that the aliphatic n-alkanes so apparent in the parent crude oil do not appear in the "dissolved phase" of the sample. The peaks that are present in the "dissolved phase" correspond only to aromatic hydrocarbons, which are characterized by greater water solubilities (Payne et al., 1984). The FID chromatograms of the first solvent rinse of the SPM polyester filter (i.e., the normal "SPM" phase) and the second solvent rinse of the filter are presented in Figures 3-1c and 3-1d, respectively. The normal "SPM phase" (Figure 3-1c) has a chromatographic profile for n-alkanes and other aliphatic and aromatic compounds that is very similar to that of the parent crude oil (Figure 3-1a), except that the more volatile lower molecular weight components are partially missing. The latter observation reflects the

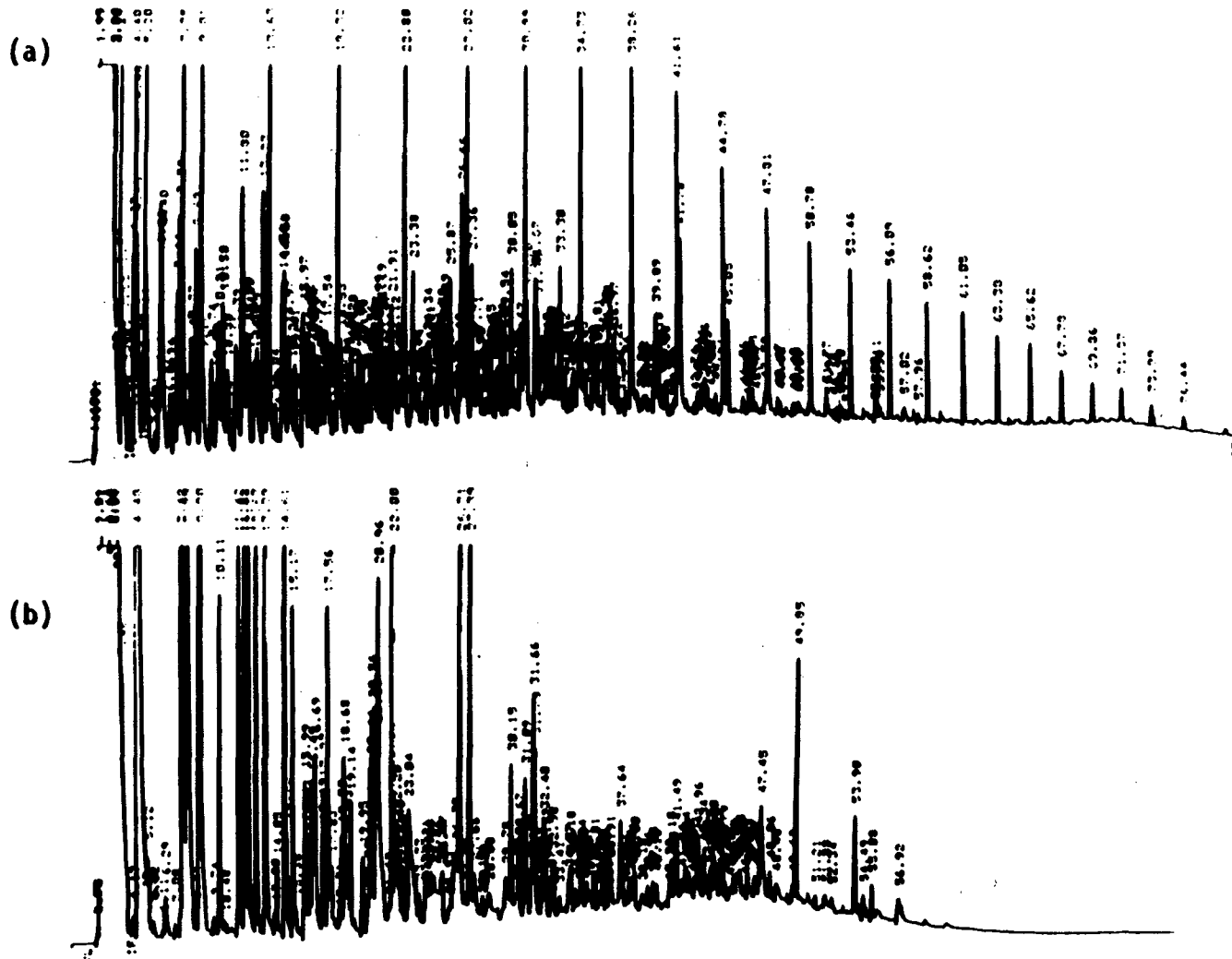
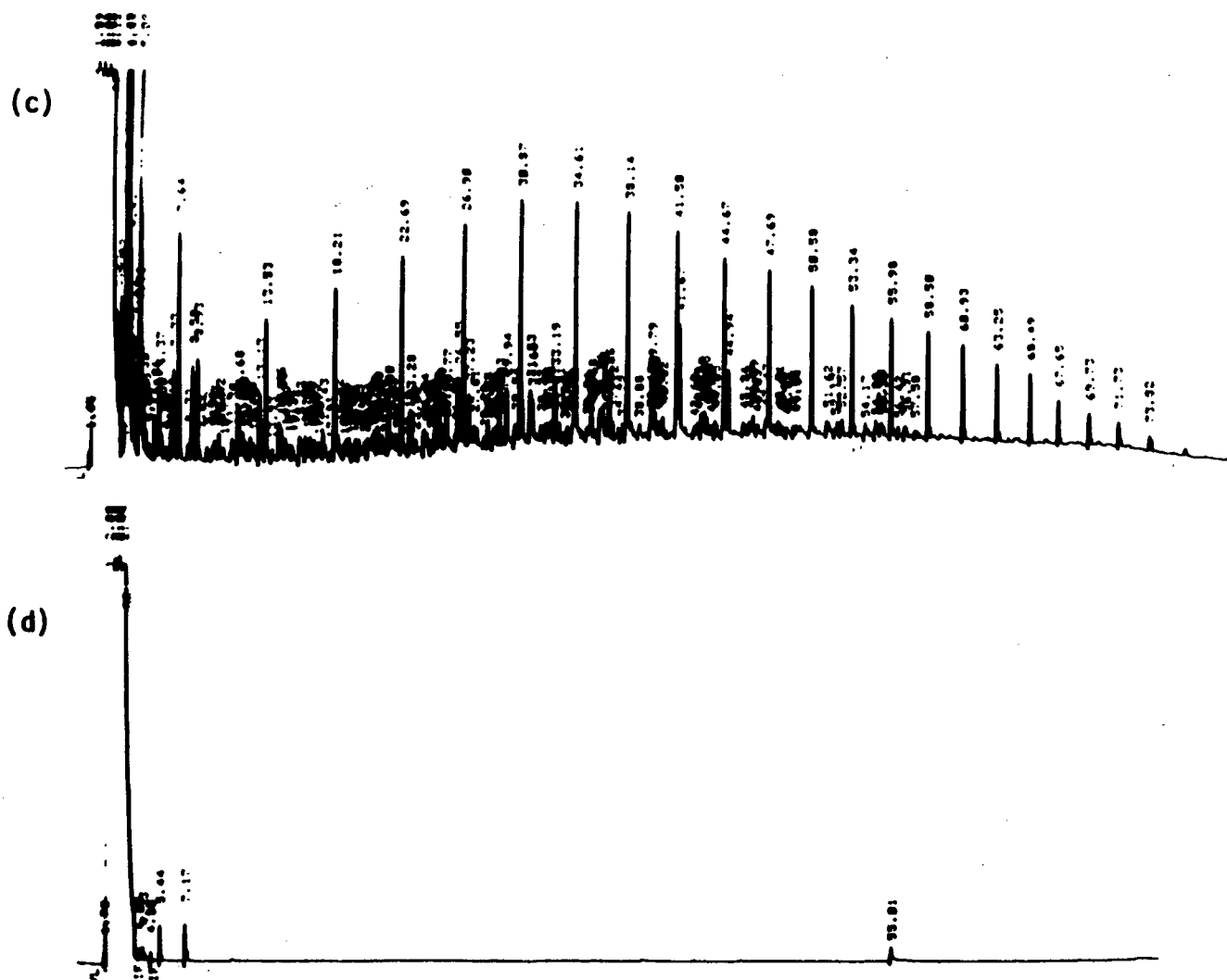


Figure 3-1a Unweathered Prudhoe Bay crude oil used for experimental oil-SPM-water system. 19.2 mg oil/1800 μ l methylene chloride; 1 μ l injected.

Figure 3-1b "Dissolved phase" from experimental oil-SPM-water system. 600 ml's sea water, 400 μ l post-injection volume, 1 μ l injected.



selective evaporation (and dissolution) of these compounds during the initial 9 hour stirring phase of the experiment when the oil-SPM-seawater system was open to the atmosphere. Because the second methylene chloride rinse of the filter (Figure 3-1d) yielded a chromatogram with essentially none of the oil indicated in Figure 3-1c, the solvent rinse sequence in the filter processing protocol (i.e., 15 mls methanol followed by 30 mls methylene chloride) appears to be nearly 100% efficient in recovering petroleum hydrocarbons that were adsorbed onto the surfaces of the SPM.

It should be emphasized that this polyester filter-vacuum filtration procedure is designed to recover hydrocarbons that are rather loosely adsorbed (i.e., "wetted") onto the surfaces of SPM particles (e.g., adsorbed oil droplets, oil films and "dissolved" compounds that have partitioned onto the SPM). The purpose of the procedure is not necessarily to extract compounds that may be more intimately associated with the internal matrices of SPM particles. However, to evaluate extraction efficiencies from "natural" sediment samples, a reference sediment containing known amounts of a variety of aromatic compounds was extracted with the polyester filter-vacuum filtration procedure. Duwamish III reference sediment supplied in the NOAA-sponsored Status and Trends Program (Dr. W. MacLeod, NOAA, Seattle) was used as a test material. To estimate procedural variability, three subsamples of this sediment (each consisting of approximately 1 gram dry weight) were extracted with the polyester filter-vacuum filtration procedure and analyzed by FID-GC. Three internal standards (d8-naphthalene, d10-acenaphthene and d12-perylene) were added to each sediment subsample immediately before extraction to estimate and correct for internal standard recoveries in the procedure. Final compound estimates from these samples were compared with values reported by the NOAA parent lab (W. MacLeod) that used the much more rigorous Status and Trends sediment extraction procedure. The latter procedure involves extraction of sediment with solvents for approximately two days, whereas the sediment with the polyester filter-vacuum filtration procedure is exposed to the extraction solvents for only approximately 60 seconds. The results of the extraction tests are summarized in Table 3-1. Keeping in mind that the polyester filter procedure involves a much less rigorous extraction sequence, the results in the table indicate that the vacuum filtration sequence is remarkably efficient for

Table 3-1. Aromatic Hydrocarbon Concentrations---Duwamish III Sediment Polyester Filter Technique vs. NOAA Status & Trends Procedure

Compound	PE filter procedure			NOAA S&T procedure			% PE filter of NOAA S&T conc.
	Mean (ng/g)	CV (%)	n	Mean (ng/g)	CV (%)	n	
naphthalene	ND	--	3	340	35	28	0
2-methylnaphthalene	82	37	3	160	19	28	51
1-methylnaphthalene	110	28	3	110	25	28	100

biphenyl	ND	--	3	36	29	28	0
2,6-dimethylnaphthalene	81	47	3	72	21	28	113
acenaphthene	233	31	3	330	13	28	71
fluorene	242	31	3	330	17	28	73
phenanthrene	1868	19	3	2300	10	28	81
anthracene	483	14	3	620	56	28	78
1-methylphenanthrene	255	13	3	210	13	28	121
fluoranthene	3201	20	3	3600	13	28	89
pyrene	3520	21	3	3900	11	28	90

benz(a)anthracene	1069	21	3	1700	12	28	63
chrysene	1273	25	3	3000	15	28	42
benzo(e)pyrene	1075	10	3	1800	11	28	60
benzo(a)pyrene	1603	19	3	2000	10	28	80
perylene	ND	--	3	600	15	28	0
dibenz[a,h]anthracene	ND	--	3	330	22	28	0

Internal Standard ID	I-Std Recovery (%)			I-Std Recovery (%)			
	Mean	CV	n	Mean	CV	n	
d8-naphthalene	39	15	3	79	11	28	
d10-acenaphthene	60	8	3	90	7	28	
d12-perylene	114	13	3	74	16	28	

 ND = not detected

recovering the specified hydrocarbons from the reference sediment samples.

3.2 UTILIZATION OF THE OIL SEPARATION TECHNIQUE IN OIL-SPM INTERACTION AND SEDIMENTATION RATE STUDIES

As discussed in Sections 2.2 and 2.4, similar oil-SPM interaction rate constants were obtained from the experiments conducted in the 4 and 28 liter reaction chambers. One of the benefits of the larger (28 liter) experimental chamber was the generation of significant quantities of oiled SPM to allow for detailed chemical characterization of oil after interaction with suspended particulate material and/or sedimentation.

To obtain information about the oil content and composition of various sample types (e.g., SPM, dispersed oil or dissolved phases), several analytical detection methods can be considered for quantitation of hydrocarbons. These methods include infrared (IR) and/or ultraviolet (UV) spectroscopy or flame ionization detector gas chromatography (FID-GC). It is worthy of note, however, that with any of these techniques, extensive wet chemistry manipulations (i.e., sample workup including gravimetric analysis, water removal, solvent extraction and solvent concentration) are required before any instrumental analysis (IR, UV or FID-GC) can be initiated.

Both IR and UV detection have major limitations that severely minimize their usefulness for the ultimate purpose of current oil-SPM model development. For example, IR requires initial sample extraction with ultrapure freon (CCl_2F_2) or carbon tetrachloride (CCl_4) or exchange of all hydrocarbons in the final sample extract into a solvent such as freon. This is required because IR uses the C-H stretch to quantify hydrocarbons such that C-H bonds in typical final extract solvents (e.g., methylene chloride, hexane, toluene) would preclude petroleum hydrocarbon analysis. Direct extraction of wet SPM samples with freon or carbon tetrachloride (without prior methanol drying) yields unacceptably poor hydrocarbon recoveries. UV suffers from the following limitations: 1) it requires that the final sample extract be in ultrapure spectrograde solvent (e.g., cyclohexane) to minimize background solvent impurity contamination; and 2) it is affected by compound specific oil-weathering losses (i.e., evaporation and/or aqueous dissolution during

experiments) of particularly sensitive aromatic ring compounds from oil or oiled-SPM. The latter weathering losses present a particular challenge for selecting appropriate standard oil mixtures to quantify experimental sample oil extracts by UV. Both IR and UV also suffer from interferences due to extraction of any natural background (e.g., biogenic) hydrocarbons in final sample extracts. However, perhaps the most severe shortcoming of both IR and UV for the stated purpose of this program regards their inability to provide information on true boiling point (TBP) cuts in oil samples. Neither IR nor UV provide any information about TBP content in samples.

In contrast to the preceding limitations, FID-GC can provide much of the required information needed to quantify the content and composition of oil in samples. Attractive properties of FID-GC include the following: 1) it is compatible with a variety of final sample extract solvents (e.g., methylene chloride, hexane, toluene); 2) it allows for potential distinction between analytical contaminants and valid sample hydrocarbons if the two occur at different chromatographic retention times; 3) it allows for evaluation and any necessary corrections to be made for compound specific weathering losses from oil during the course of experiments; 4) it allows for evaluation and possible correction for natural background (e.g., biogenic) hydrocarbons in samples; and 5) it allows for direct estimation of TBP cut content in a given sample. The latter information is derived from either an existing knowledge of FID-GC elution profiles for specific TBP cuts in oil (e.g., Payne et al., 1984) or similarly derived information for different oil types. Therefore, TBP cut as well as individual compound concentration information for sample extracts can be obtained with FID-GC. Although the following discussion of experimental FID-GC data only deals with information for specific compound or total summed compound concentrations, modifications are currently being incorporated into the SAIC FID-GC data reduction code to yield direct information about specific TBP cut concentrations in reduced sample extracts.

Using FID-GC procedures described in Payne et al., (1984) analyses were performed on numerous samples from experiments with both the 4 and 28 liter systems. Among other purposes, such measurements were utilized to determine total oil loadings in both the dispersed oil droplet and SPM phases of experiments to estimate kinetic rate constants for oil-SPM interactions. In

addition to these oil "loading" estimates, however, the combination of the membrane filter separation technique and the normal data reduction procedure for FID chromatograms of oil samples (Payne et al., 1984) allowed for detailed analyses of component-specific hydrocarbon compositions in a variety of sample types. Such samples included not only the previously described dispersed oil droplet, SPM and dissolved phases of whole water samples but also oil samples before and after "blending" to generate small oil droplets for oil-SPM kinetic rate studies (in the 4-liter system) and samples of "sedimented" SPM that were collected from the bottoms of both stirred and settling chamber studies.

Although this component specific information is not absolutely essential for kinetic or sedimentation rate estimates, it does have relevance for potential biological implications that could derive from oil-SPM interactions in aquatic environments. Specifically, the content of toxic compounds in oil droplets associated with SPM could affect aquatic biota in at least two ways: 1) oiled SPM that remains suspended in the water column can impact pelagic and epibenthic organisms that utilize filter feeding as a means of obtaining food and 2) oiled SPM that is incorporated into sediments (i.e., is "sedimented out" of the water column) can impact benthic fauna that either live in association with or ingest sedimentary material in their feeding process. Compounds of particular interest for such considerations include various aromatic hydrocarbon components (e.g., mono- and dicyclic aromatics and naphtheno-aromatics) that have been shown to be particularly toxic to impacted aquatic biota (e.g., Hyland and Schneider, 1976; Johnson, 1977; Patten, 1977). Because FID-GC analyses are routinely performed anyway to estimate "oil loadings" in various sample phases for the kinetic and sedimentation rate experiments, it is reasonable to include discussions of compound specific detailed chromatographic analyses of oil samples. Beyond the immediate scope of this project to provide input regarding oil-SPM kinetic rate estimates, such information should be of interest to MMS's long-term stated purpose of incorporating oil-SPM interaction rate estimates into "biological effects" models.

3.2.1. Oil-SPM Sedimentation Rate Studies.

Experimental studies in the 4 liter system to determine kinetic rate constants for oil droplet-suspended particulate matter (SPM) interactions have been previously discussed in section 2.2. In one of these kinetics experiments, an "add-on" study utilized the oil droplet-SPM solution generated in the experiment to evaluate the effects of oil droplet-SPM interactions on sedimentation rates of the SPM. These results are discussed below.

Sedimentation rate experiments with oiled SPM were initiated by transferring approximately 1 liter of an oil droplet-SPM-seawater solution generated at the end of an oil-SPM kinetics rate experiment to each of three vertical settling chambers (i.e., 1 liter graduated glass cylinders). Blended fresh Prudhoe Bay crude oil and 53 μm sieved Jakolof Bay sediment were used for the kinetics rate experiment. After allowing the solutions to remain undisturbed in the graduated cylinders, samples of known volume were withdrawn from a specified depth in the cylinders at time intervals of 0, 15, 35, 60, and 110 minutes. The samples were vacuum filtered (<30 cm Hg) onto pre-weighed, 0.4 μm pore size polyester membrane filters. Subsequent treatment of the filter samples for both SPM gravimetric analyses and FID-GC extraction and analyses are described in section 3.1. above. For an experimental control, an identical sedimentation experiment was performed with the same sieved Jakolof Bay sediment that had not been exposed to a solution of blended oil droplets.

The results of the measured SPM concentrations over time in the settling chambers for the experiments with and without the blended oil droplets are illustrated in Figure 3-2. Because three identical settling chambers were used in each experiment, the data points represent mean values with one standard deviation unit being indicated by vertical bars. As indicated in the figure, prior "oiling" of the SPM (i.e., during the preceding kinetics rate experiment) did not seem to substantially affect the rate at which the SPM settled out of the water column at the oil to SPM loading (ratio) considered. This may not be the case at higher relative SPM concentrations or when flocculation leading to larger oil/SPM agglomerates occurs. Additional work is currently being completed with different oil/SPM ratios, SPM types (and sizes)

SPM Concentrations: Oiled vs. Unoiled
Sedimentation Experiment--4 Liter System

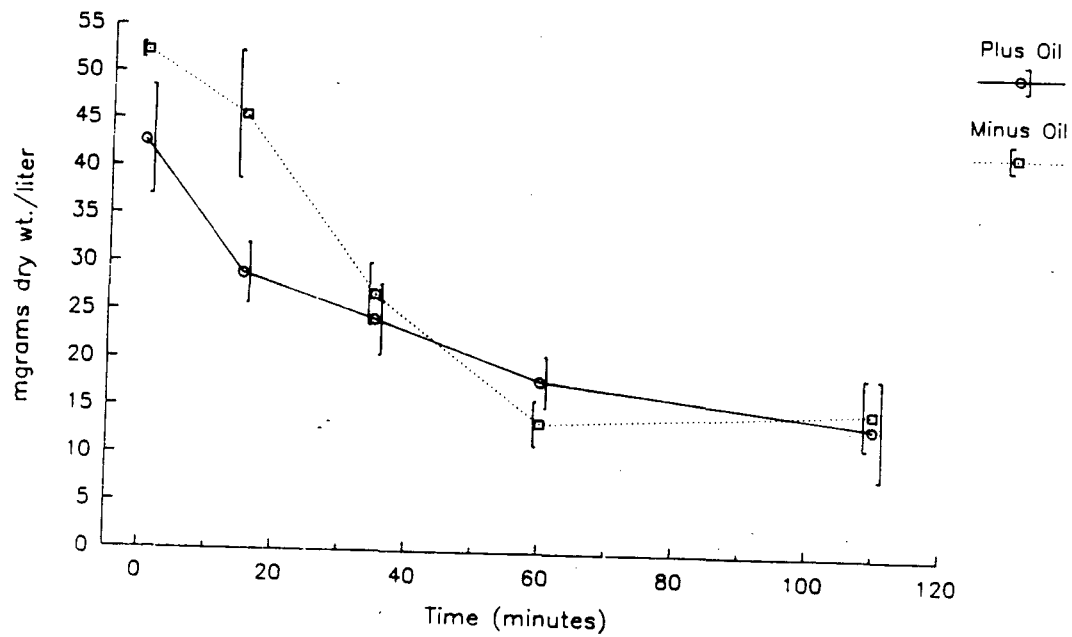


Figure 3-2. Gravimetric concentrations of SPM in sedimentation experiments conducted with oiled and unoiled Jakolof Bay sediments (sieved to $\leq 53 \mu\text{m}$). Oiled sediment was obtained from a parent oil-SPM kinetics rate experiment.

and oil types to investigate this sedimentation behavior further.

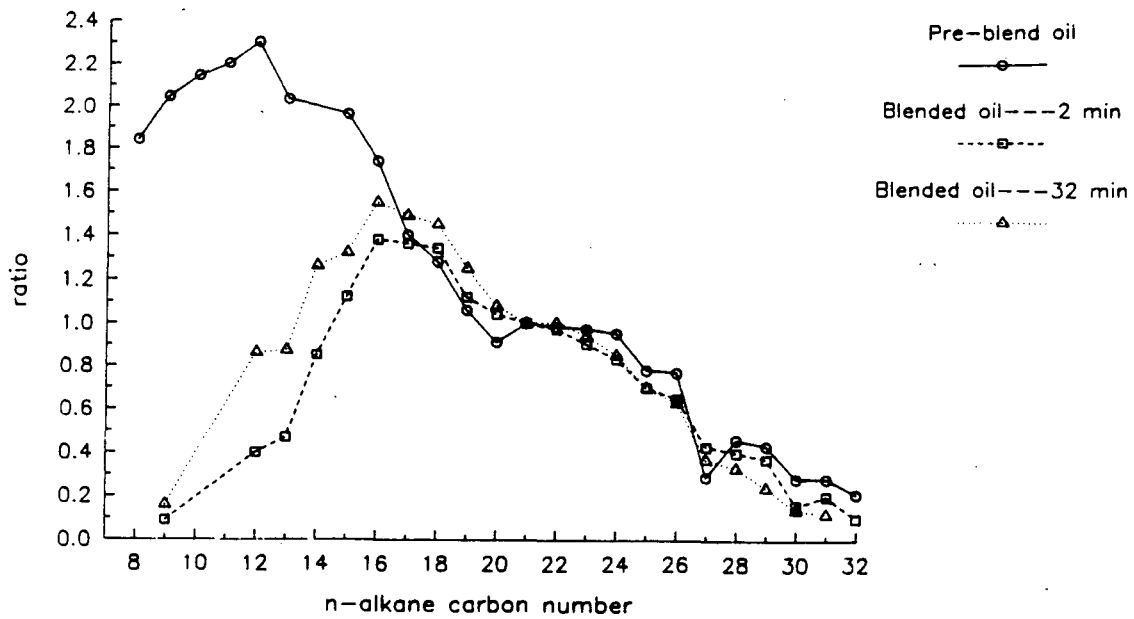
3.2.1.1. FID-GC Analyses of Oil Fractions in the Sedimentation Experiment

The compound specific composition of oil was investigated in a variety of samples from the sedimentation rate experiment in section 3.2.1. Such samples included the initial unblended and blended oil solutions used for the parent oil droplet-SPM kinetic rate experiment, oil associated with the SPM that accumulated on the floor of the sedimentation chamber after 110 minutes of settling, and oil associated with the SPM that remained suspended in the water column after 110 minutes of settling time. Individual compounds were considered in terms of 1) their absolute concentrations (e.g., 10^{-6} grams of compound per gram dry weight of SPM) and 2) the ratio of their concentrations to that of the n-alkane nC21 in the sample (i.e., compound/nC21 for both n-alkanes and aromatics). As discussed in the June 1986 quarterly progress report to MMS (SAIC, 1986), the use of concentration ratios can assist in detecting compound specific trends that might otherwise be obscured by either large absolute concentration differences between sample types (e.g., whole oil and oil associated with SPM) and/or different concentration units (e.g., per gram dry weight of sediment or per liter of seawater).

Prior to investigating compositional differences between oil contained in the various sample fractions in the sedimentation experiment, an evaluation was made of the changes in composition due to the effect of the preceding blending effort (i.e., oil in seawater in a mechanical blender) that was used to generate the dispersed oil droplets for the parent oil-SPM kinetics rate experiment. Figure 3-3 presents concentration ratios for the various n-alkane and aromatic compounds (relative to nC21) in the initial pre-blend Prudhoe Bay crude oil and the blended seawater-oil solutions at 2 and 32 minute time points in the kinetic rate experiment. Substantial losses of both n-alkanes below nC17 and the measured aromatics appeared to occur as a result of the initial mechanical blending process, but additional losses were minimal thereafter (i.e., ratios at the 2 and 32 minute time points were very similar).

The "oiled" sedimentation rate experiment in section 3.2.1. used the

Ratios: $nC(X)/nC_{21}$
 Oil Used for SPM Interaction and Sedimentation Experiments
 4 Liter System



Ratios: Aromatic Cmpd./nC₂₁
 Oil Used for SPM Interaction and Sedimentation Experiments
 4 Liter System

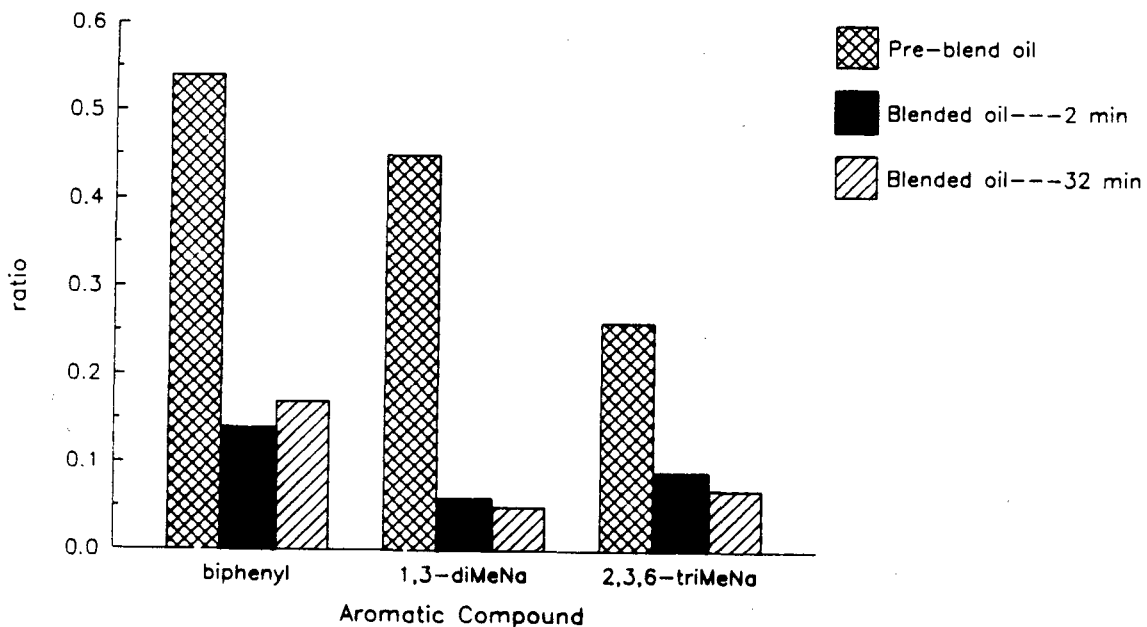
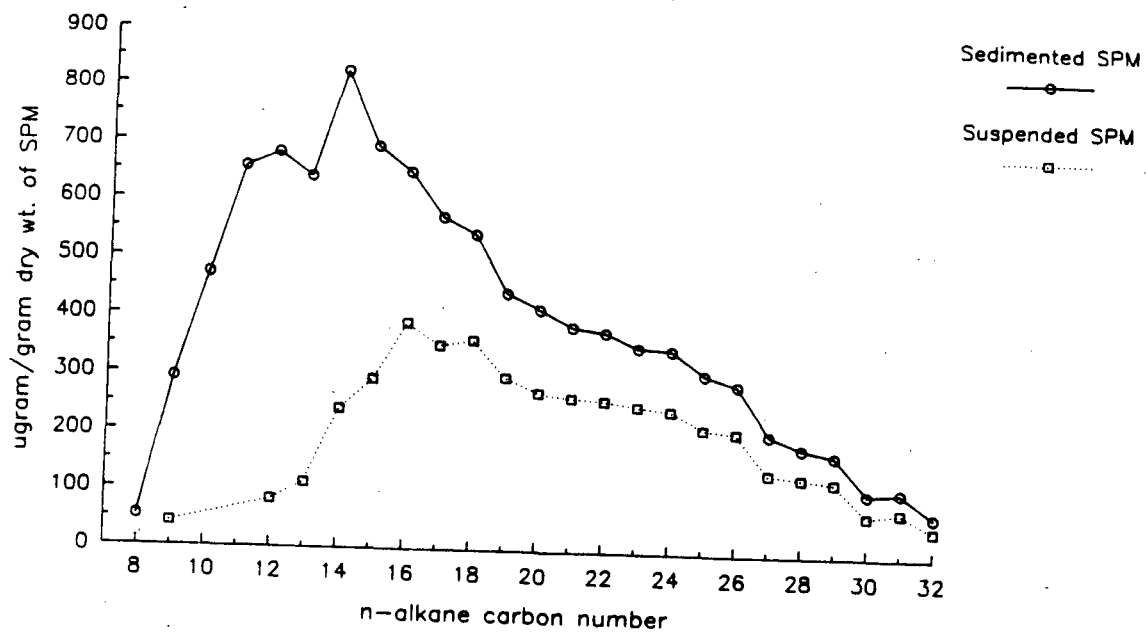


Figure 3-3. (a) Concentration ratios of n-alkanes to nC₂₁ in oil samples from the parent oil-SPM kinetics rate experiment. The seawater-oil-SPM solution from the 32 minute time point was subsequently used for the oiled SPM sedimentation experiment.
 (b) Comparable concentration ratio information for selected aromatic compounds (diMeNa = dimethylnaphthalene; triMeNa = trimethylnaphthalene).

seawater-oil-SPM solution generated at the end (32 minute time point) of one of the 4-liter reaction vessel experiments described in Section 2.2 (i.e., Table 2-2). After the sedimentation solution had remained stationary for 110 minutes in the settling chambers, samples for FID-GC analyses were collected of 1) SPM on the bottom of the chamber (i.e., SPM that had settled out of the water column during this time interval) and 2) residual suspended SPM in the water column (i.e., SPM that had remained in suspension). Figure 3-4 illustrates absolute concentrations of n-alkanes and aromatic compounds in these two SPM fractions. As indicated, the sediment on the bottom of the settling chamber had higher oil "loadings" of both n-alkanes and aromatic compounds than that remaining in suspension. Because the hydrocarbon concentrations for both the "sedimented" and "residual suspended" SPM samples are reported per gram dry weight of SPM, this indicates that higher oil loads were associated with SPM particles that settled out of the water column. Furthermore, differences between compound concentrations in the "sedimented" and "suspended" SPM fractions were greater for compounds with lower molecular weights. Ratios for the n-alkane and aromatic compounds relative to nC21 are presented in Figure 3-5. Information from this ratio eliminates any uncertainty in interpreting chemical fractionation trends that might be obscured by differences in absolute concentration values and illustrates that the chemical fractionation trends evident in Figure 3-4 are still valid. Because oil droplets associated with both the "sedimented" and "suspended" SPM fractions should be subject to comparable tendencies for dissolution losses of compounds into the ambient water, the enhanced retention of both the aromatic and lower molecular weight n-alkane compounds in the "sedimented" SPM may reflect the existence of larger oil droplets associated with the SPM fraction that "settled out" of the water column (i.e., larger droplets will have smaller surface to volume ratios, which will favor slower rates of compound dissolution into the adjacent water phase).

Similar trends in the compound specific fractionation of oil associated with "residual suspended" and "settled" SPM phases have been observed in stirred chamber experiments with the larger 28 liter system (Section 3.2.2.3. below). Higher absolute concentrations of aliphatic and aromatic compounds have been observed in SPM that has a tendency to sink out of the water column. Furthermore, examination of compound/nC21 ratios indicates that compounds with

Sediment Concentrations: n-alkanes
Sedimentation Experiment--From 4 Liter System



SPM Concentrations: Aromatics
Sedimentation Experiment--From 4 Liter System

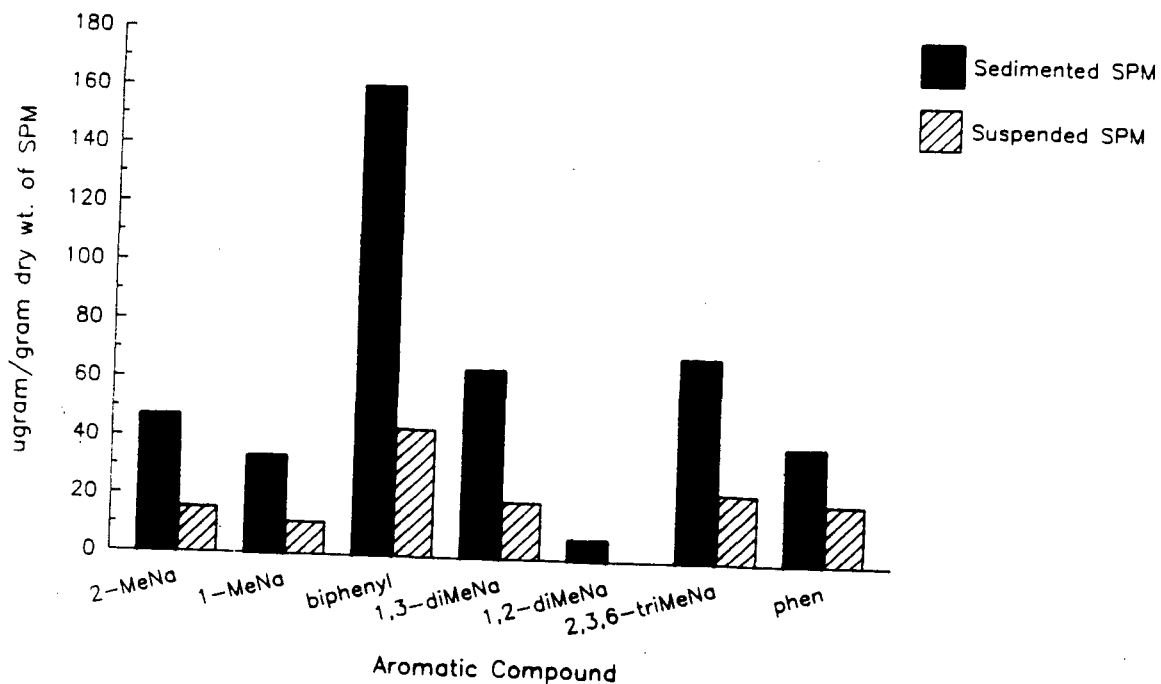
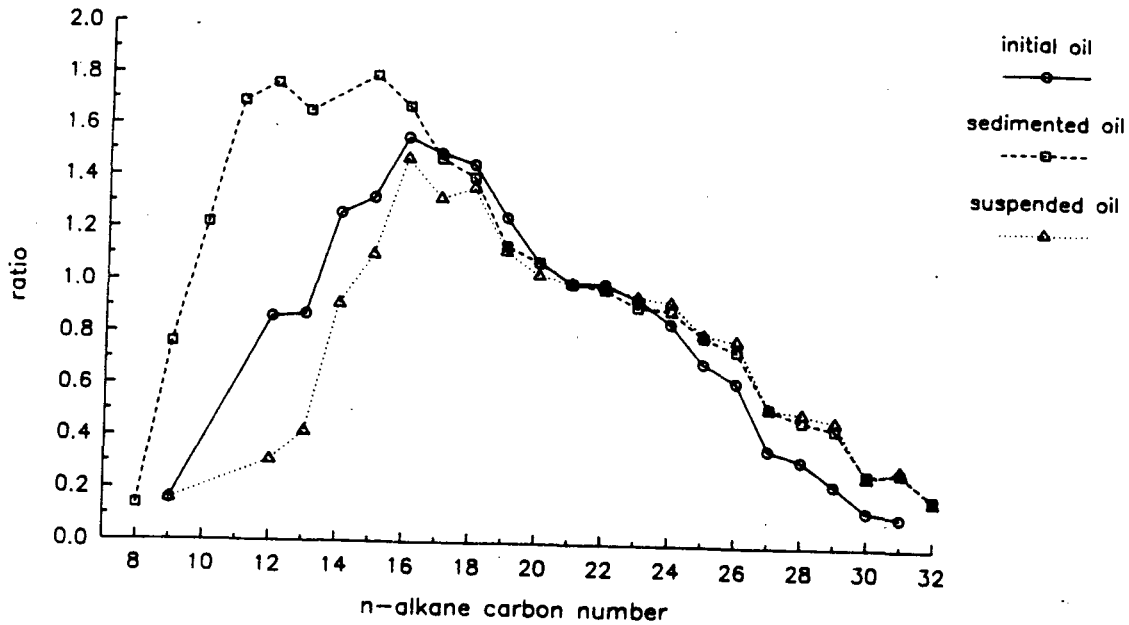


Figure 3-4. (a) Absolute concentrations of n-alkanes associated with "sedimented" and "residual suspended" SPM fractions after 110 minutes of settling in the oiled sedimentation experiment. (b) Comparable concentrations for aromatic hydrocarbons (MeNa - methylnaphthalene; diMeNa - dimethylnaphthalene; triMeNa - trimethylnaphthalene; phen - phenanthrene).

Ratios: $nC(X)/nC_{21}$
Sedimentation Experiment--From 4 Liter System



Ratios: Aromatic Cmpd./nC₂₁
Sedimentation Experiment--From 4 Liter System

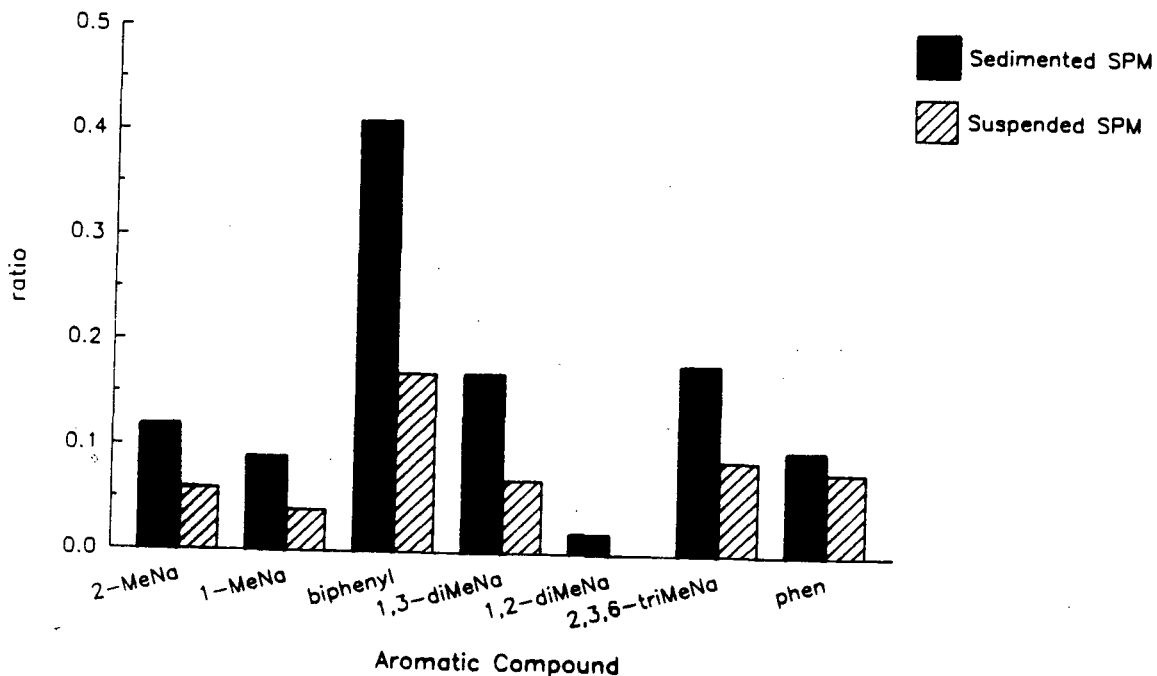


Figure 3-5. (a) Concentration ratios of n-alkanes to nC₂₁ in the initial blended oil (2 minutes after blending) and the final "sedimented" and "residual suspended" SPM after 110 minutes of settling in the oiled sedimentation experiment. (b) Comparable concentration ratio information for selected aromatic compounds (see Figure 3-4(b) for compound identification).

higher water solubilities (e.g., aromatics and lower molecular weight n-alkanes) have a greater relative enhancement in the oil fractions of the "sedimented" as opposed to "residual suspended" SPM. This higher absolute "loading" and selective enhancement of more toxic hydrocarbon compounds (e.g., various di- and tricyclic aromatics) in "sedimenting" SPM phases can have important biological implications for bottom fauna. This would be particularly true for organisms inhabiting areas where such "oiled" SPM might become concentrated in the surface sediments.

3.2.2. SPM Load and Hydrocarbon Information from Oil-SPM Interaction Studies with the 28 Liter Stirred Chamber System.

One advantage of the larger 28 liter test chamber presented in section 2.4. (i.e., as opposed to the 4 liter chamber discussed in section 2.2.) is the total volume of experimental solution available to be sampled. The larger total solution volume allows for not only larger sample volumes to be collected at any one time but also multiple samples to be collected over longer sampling time periods. While experiments in the 28 liter chamber do suffer from certain experimental limitations (section 2.4.1.), it has been determined that estimates of oil-SPM interaction rate constants for fresh Prudhoe Bay crude oil and 53 μm sieved Jakolof Bay sediments can yield comparable values with both the 4 and 28 liter systems (section 2.4.2.1.).

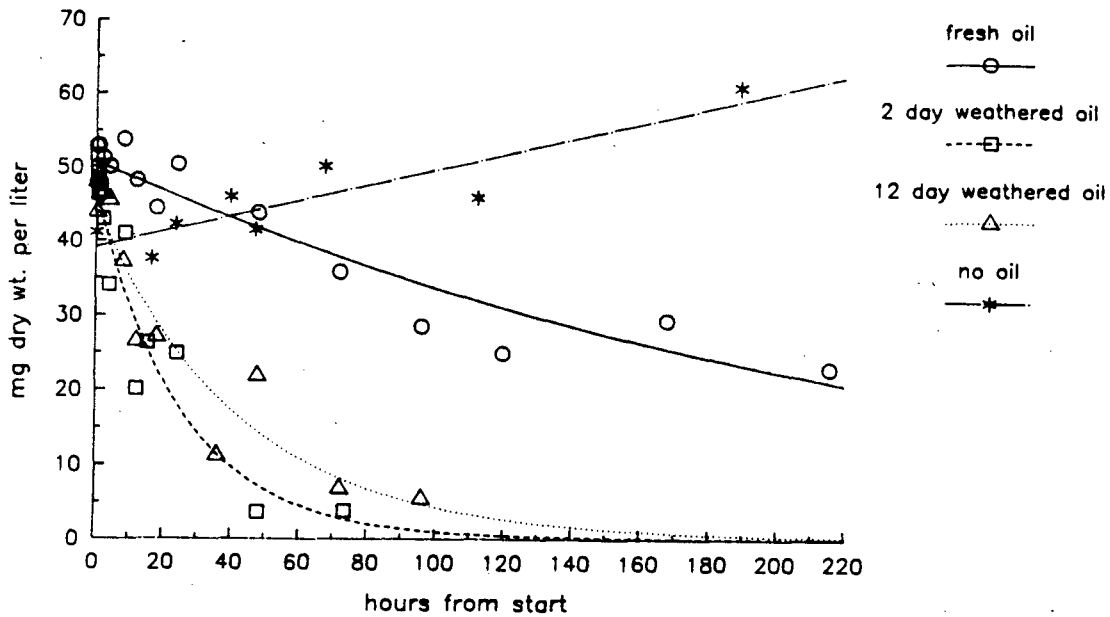
As discussed in section 2.4., three experiments were performed in the 28 liter system with seawater, 53 micron sieved Jakolof Bay sediment and either fresh, 2-day weathered or 12-day weathered Prudhoe Bay crude oil. As a control, a fourth experiment was conducted with the Jakolof sediment and seawater, but without any addition of oil to the system. Sample collection and processing protocols used in these experiments are discussed in section 3.1. Estimation of rate constants for oil-SPM interactions from these experiments has already been presented in section 2.4. A further discussion regarding SPM load and hydrocarbon measurements during the course of these experiments is presented here.

3.2.2.1. Effect of Prior Weathering History of Prudhoe Bay Crude Oil on SPM Loads and Dispersion of Oil into the Water Column over Time.

Figure 3-6a illustrates SPM loads over time in the water column of the four experiments in the 28 liter system. For the SPM type used and the turbulence level provided to the system, there appeared to be little or no tendency for the SPM load to decline in the absence of oil. In fact, the SPM load actually increased with time (after 60-80 hours) due to processes that appeared to be related to activities of microorganisms that were observed with light microscopy in the system. Although microscope facilities were not available during the experiments with the three types of Prudhoe Bay crude oil, there was no indication of microorganism-mediated processes affecting SPM loads in these experiments. The presence of toxic hydrocarbon compounds derived from the oil (e.g., dissolved aromatics) may have inhibited the growth of microorganisms in the latter systems.

The levels of SPM declined over time in all three experiments with the crude oil (Figure 3-6a). Because SPM was not observed to accumulate on the floor or walls of the chamber during the experiments, the declining SPM loads were indicative of incorporation of the SPM into the dispersed oil droplets and/or the surface oil slick. In contrast to the system receiving fresh crude oil, the rate of decline in the SPM load in the water column was much accelerated in the presence of both the 2-day and 12-day weathered oils. Because the abundance of polar compounds typically increases in weathered oils due to reactions such as photochemical and microbial oxidation (e.g., Payne and Phillips, 1985; Karrick, 1977), the more rapid declines in SPM loads with weathered oil may have resulted from enhanced interactions between the SPM and a weathered oil phase that was characterized by greater surface charge characteristics than that of fresh crude oil. Certainly the oil/water interfacial surface tension was much lower with the weathered versus fresh oil (11 vs. 25 dynes/cm; see Table 2-10) and this did enhance oil droplet dispersion. In fact, it is quite possible that the more rapid decline in SPM loads with the weathered oils may be found in the relative dispersion rates for the three oils into the water column. Levels of dispersed oil (as measured by concentrations

SPM Concentrations vs. Time for Different Starting Oil Types



Total Resolved Hydrocarbons--Dispersed Oil Phase for Different Starting Oil Types

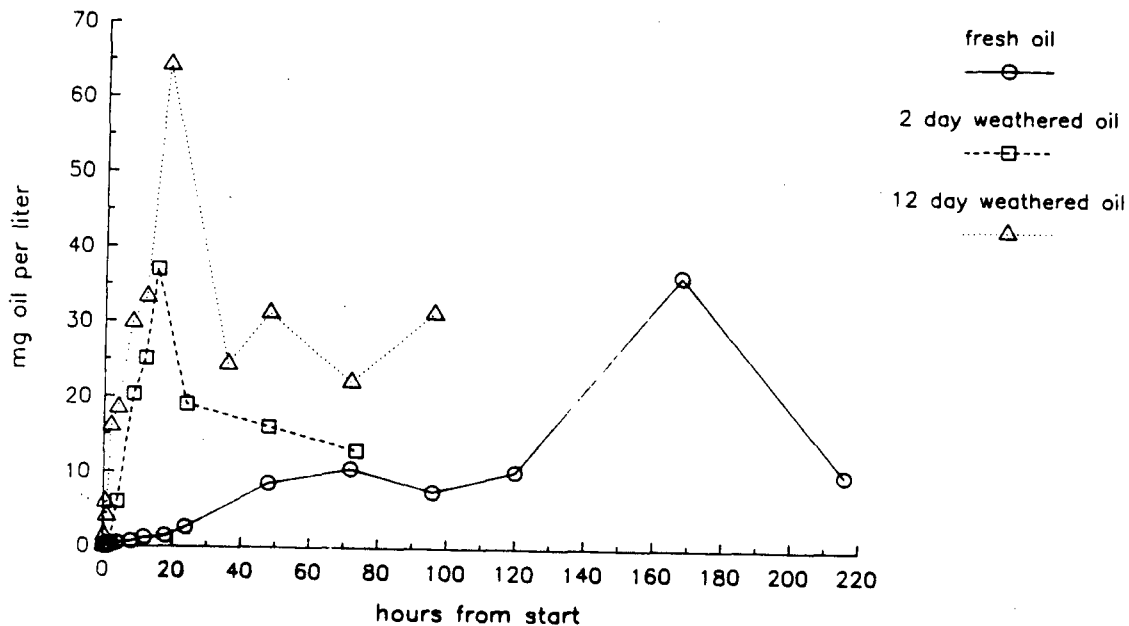


Figure 3-6. (a) SPM loads over time in experiments with fresh, 2-day weathered and 12-day weathered Prudhoe Bay crude oil and with no oil addition in the 28 liter stirred chamber system with continuous stirring. Exponential regression lines are fitted to data points for the three oil types ($r^2 \geq 0.89$ for each line) and a linear regression line is fitted to the data for no oil addition. The energy dissipation rate (ϵ) in these experiments was estimated to be approximately $260 \text{ ergs/cm}^3\text{-sec}$ for the duration of each experiment. (b) Dispersed oil concentrations in the corresponding experiments with oil.

of total resolved hydrocarbons) over time in the three experiments are illustrated in Figure 3-6b. The maximum concentration for fresh oil was not observed until approximately 170 hours after the initial spill event. In contrast, maximum concentrations with the 2-day and 12-day weathered oils were observed approximately 15-18 hours after the spill event. Consequently, the higher levels of dispersed oil at early time points in the experiments with the weathered oils may have been responsible for the more rapid disappearance of SPM from the water column.

In the experiments with 2-day and 12-day weathered oil, concentrations of dispersed oil began to decline when SPM loads in the water column fell below approximately 25 mg dry weight per liter. Although at a much later time in the experiment, a similar decline in dispersed oil levels also appeared to occur with fresh oil when the SPM load reached approximately 25 mg dry weight per liter. Huang and Elliot (1977) noted that the stability of oil-in-water emulsions can be dramatically affected by direct interactions between dispersed oil droplets and SPM particles. Specifically, SPM particles can associate with (or "coat") the oil-water interfaces of oil droplets due to surface charge properties of both the SPM particles and the oil droplets. Such coatings of SPM can then "armor the oil droplets against coalescence", thus increasing the stability of oil-in-water emulsions (i.e., dispersed oil droplets). This increased stability imparted to dispersed oil droplets can be directly related to absolute concentrations of SPM in a water column. For example, at SPM concentrations either above or below some critical level, the stability of the "SPM-coated" dispersed oil droplets declines. At SPM concentrations below this critical level, the reservoir of SPM particles in the water column available to interact with oil droplets is insufficient to adequately coat the oil droplets to the degree necessary to enhance droplet stability. Under such circumstances the dispersed oil droplets would rise to the surface and recombine into the surface slick, rather than remain in the water column. This scenario could explain the declines in dispersed oil concentrations observed in all three experiments when SPM loads fell below approximately 25 mg dry weight per liter. Although not pursued in our experiments, Huang and Elliott (1977) note that the stability of dispersed oil droplet suspensions in the water column will also decline at high SPM loads (e.g., >200 mg/liter). At these high SPM loads, the specific gravity of oil-SPM agglomerates will be increased (due to greater SPM

inclusions in the agglomerates) to the point that their specific gravity is greater than that of the liquid medium. Thus, the oil-SPM agglomerates can sink out of the water column and thereby lower dispersed oil concentrations in the water column.

3.2.2.2. Distribution of Oil Between Dispersed, Dissolved and SPM Phases in Experiments With Fresh, 2-day and 12-day Weathered Oil.

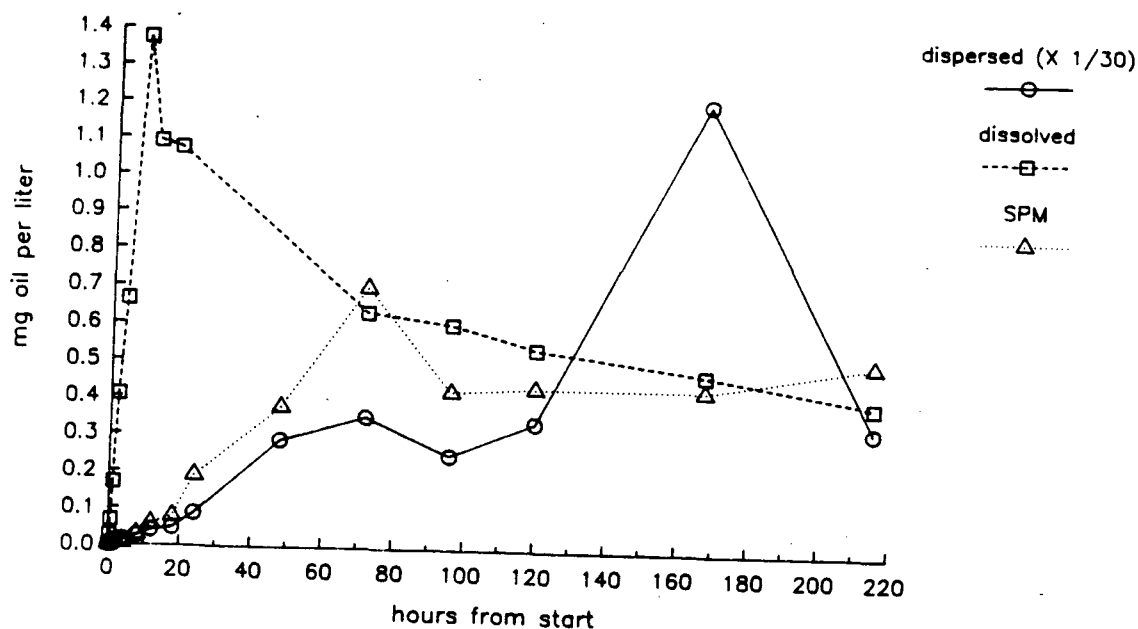
Concentrations of oil (measured as total resolved hydrocarbons) over time in the dispersed oil, SPM and dissolved phases in the experiments with fresh, 2-day and 12-day weathered oil are presented in Figure 3-7. In all three experiments the majority of the oil in the whole water samples was always contained in the dispersed oil phase. It must be noted, however, that the hydrocarbon composition in the dissolved phase was always radically different from that in the dispersed oil and SPM phases. Aromatic compounds were the only hydrocarbons ever detected in dissolved phase samples. In contrast, aliphatic compounds were consistently the most abundant hydrocarbons observed in the dispersed oil and SPM phases of samples, although aromatic compounds were also detected. As for relative concentration levels in those phases with a similar predominance of aliphatic compounds (i.e., the dispersed oil and SPM phases), it should be noted that total resolved hydrocarbon concentrations on a per liter seawater basis were consistently greater in the dispersed oil phase.

It has been noted that only aromatic compounds were detected in the dissolved phases of whole water samples, whereas aliphatic components were dominant (although aromatics were present) in all samples of surface oil, dispersed oil, and SPM samples that had either "settled out" or remained suspended in the water column. The similar aliphatic character of the latter sample phases suggests that direct dispersed oil droplet-SPM interactions were the primary route by which the oil hydrocarbons became associated with the SPM particles.

3.2.2.3. FID-GC Analyses of Oil Fractions in the SPM and Dispersed Oil Phases of Experiments in the 28 Liter System.

In a manner analogous to that described in the preceding sedimentation experiments, compound specific differences were investigated in the dispersed

Total Resolved Hydrocarbon Concentrations Fresh Oil



Total Resolved Hydrocarbon Concentrations 2 Day Weathered Oil

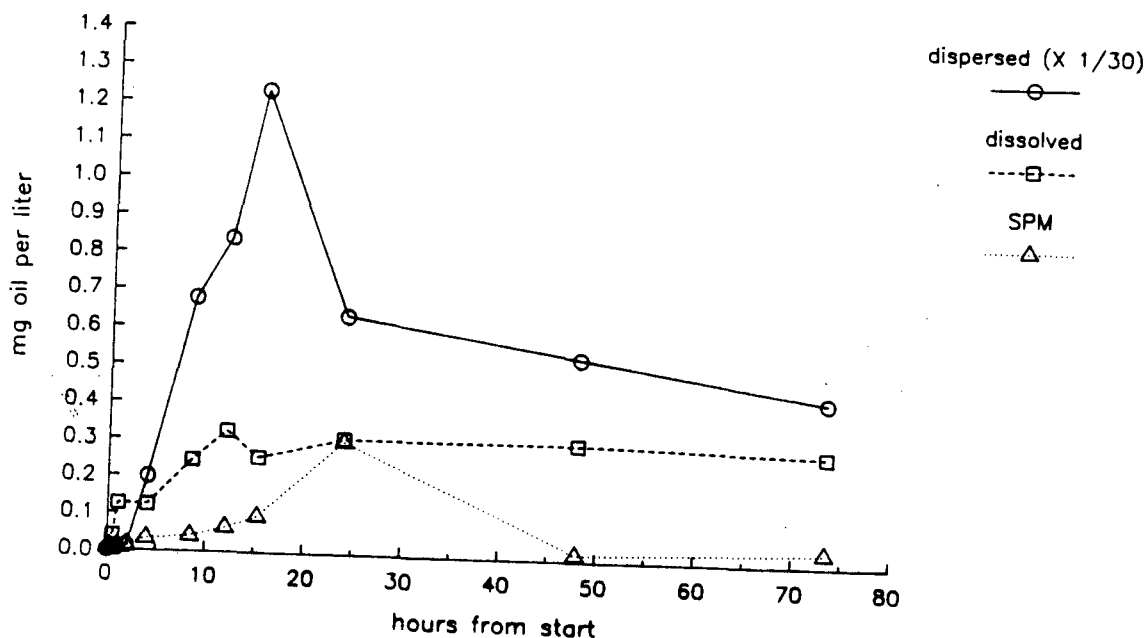


Figure 3-7. (a) Concentrations of oil (i.e., total resolved hydrocarbons) over time in the dispersed oil, dissolved and SPM phases of whole water samples from experiments with Prudhoe Bay crude oil in the 28 liter stirred chamber system. The energy dissipation rate (ϵ) in the experiments was estimated to be approximately 260 ergs/cm³-sec. Fresh Prudhoe Bay crude oil.
 (b) Comparable information with 2-day weathered oil.

Total Resolved Hydrocarbon Concentrations 12 Day Weathered Oil

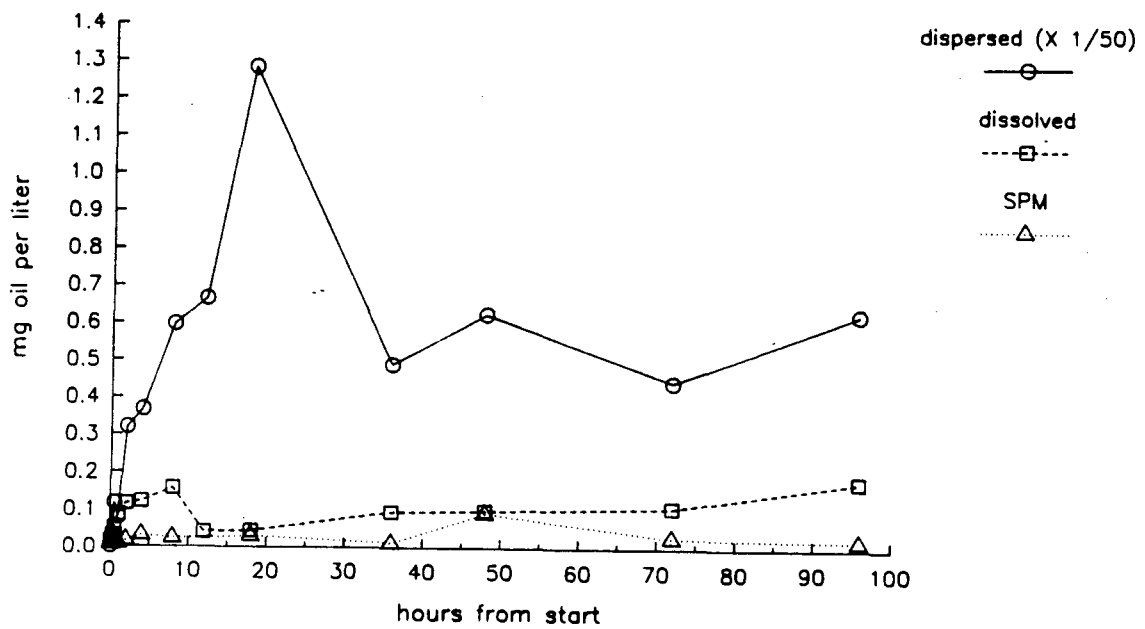
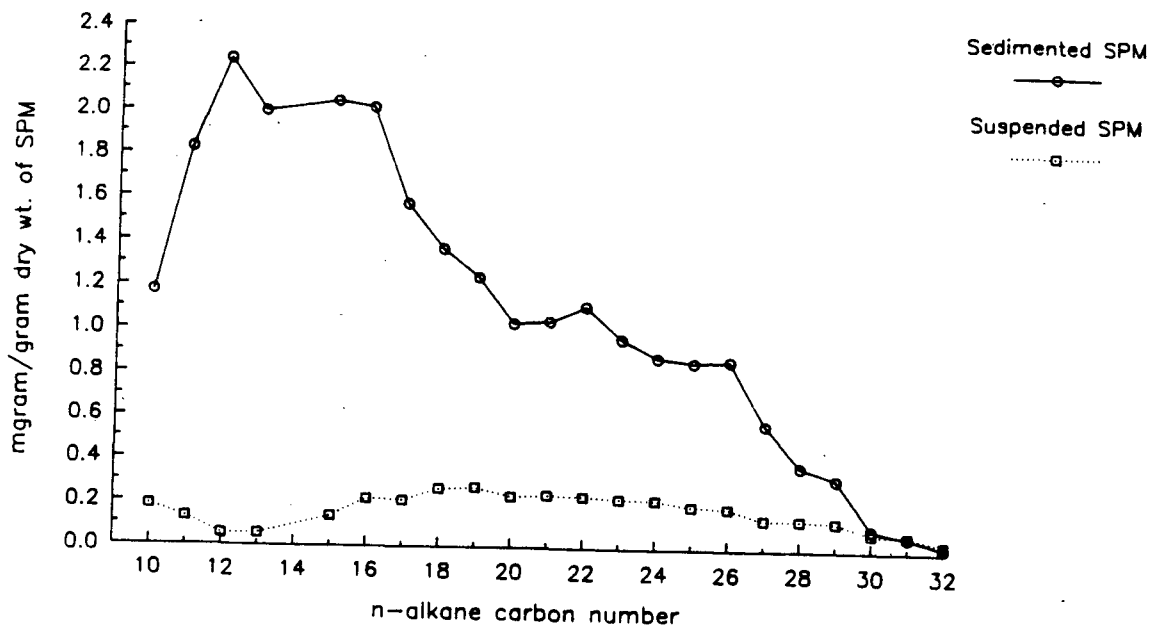


Figure 3-7. (c) Comparable information with 12-day weathered oil.

and SPM phases of samples collected during experiments in the 28 liter system. Similar compound specific trends to those reported in section 3.2.1.1. were observed. For example, Figure 3-8 illustrates absolute concentrations (per gram dry weight) of individual n-alkanes and aromatic compounds in SPM that had "settled out" of the water column as well as SPM that remained suspended at 73.5 hours after the spill event in the experiment with 2-day weathered crude oil. Much higher concentrations of both the n-alkanes and aromatics were observed in the "sedimented" SPM. Furthermore, ratios of the specific compounds to nC21 (Figure 3-9) indicate a distinct relative enhancement of both the low molecular weight n-alkanes and the aromatic compounds in the SPM fraction that had "settled out" of the water column.

In both the sedimentation and large volume stirred chamber experiments (Sections 3.2.1. and 3.2.2., respectively), it is noteworthy that hydrocarbon compositions in SPM that "settled out" of the water column had compound specific compositions that more closely resembled that in the dispersed oil as opposed to the "residual suspended" SPM remaining at the end of the sedimentation experiment. Because SPM that "settles out" originates from the initial SPM in the water column, one might expect "settled" bottom sediment to have a similar oil composition to that of the "residual suspended" SPM. Results from both the sedimentation and large volume stirred chamber experiments indicate, however, that "sedimented" oil (i.e., that which could be transported to bottom sediments in natural environments) might be less subject to dissolution losses of lower molecular weight compounds than would be expected from hydrocarbon compositions in particulate phases that remain suspended. Microscopic examination of sedimented oil/SPM agglomerates has suggested that the larger flocs of oiled SPM contain discrete 5-10 μm oil droplets that are less subject to lower molecular weight compound dissolution (compared to thin oil coatings on residual SPM) due to their lower surface to volume ratios. This subject was not pursued further due to limitations of funds and the desire to pursue phenomena that could more readily be modeled. Although such chemical partitioning has not been modeled to date, it may have particular relevance for predictions of effects of oiled particulate phases on benthic fauna.

Sediment Concentrations: n-alkanes
 2 Day Weathered Oil--28 Liter System
 73.5 Hours Post-Spill



SPM Concentrations: Aromatics
 2 Day Weathered Oil--28 Liter System
 73.5 Hours Post-Spill

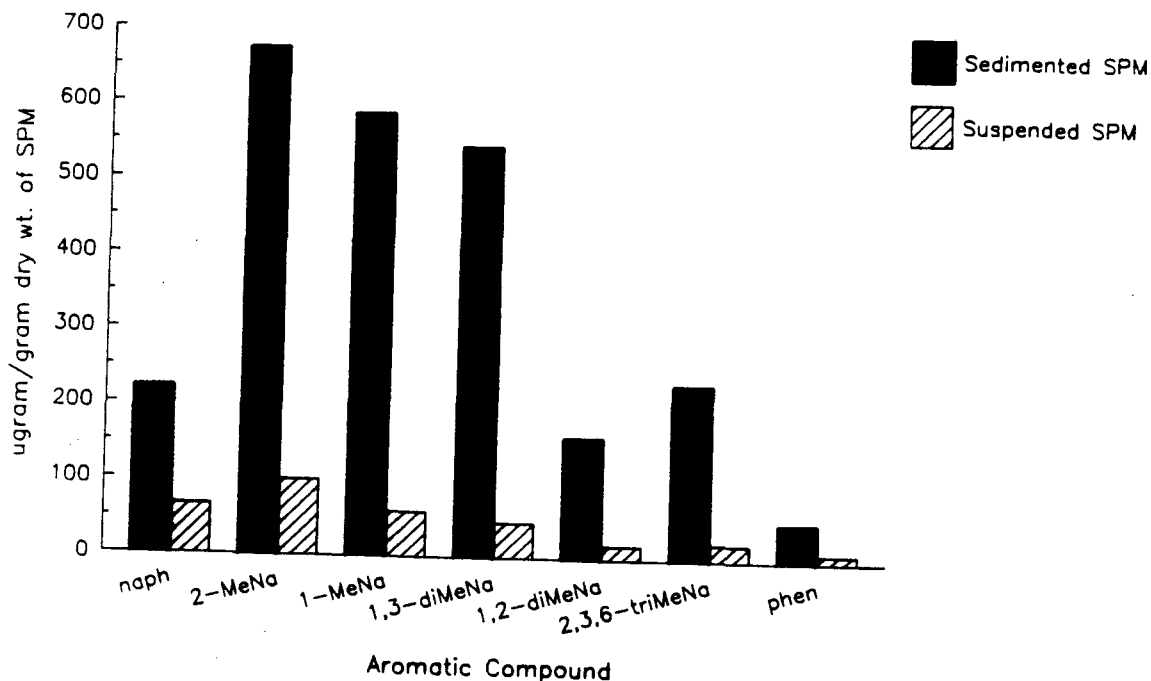
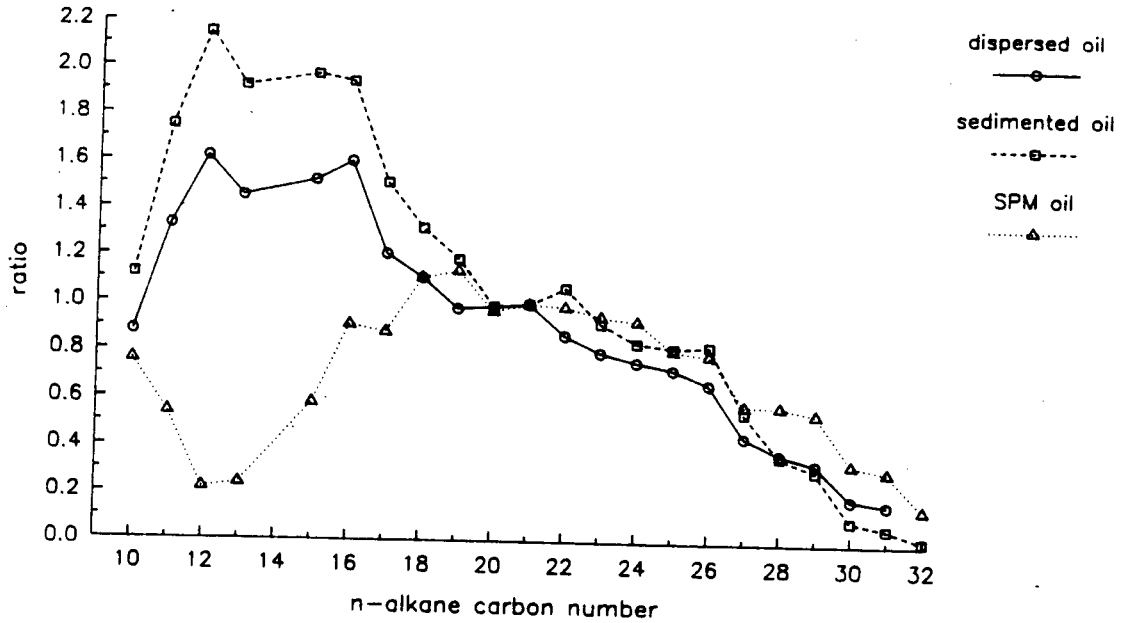


Figure 3-8. (a) Absolute concentrations of n-alkanes associated with "sedimented" and "residual suspended" SPM fractions at the final sampling time in the 28 liter stirred chamber experiment with 2-day weathered Prudhoe Bay crude oil. (b) Comparable concentrations for selected aromatic compounds (naph = naphthalene; see Figure 3-4 (b) for other compound identification).

Ratios: $nC(X)/nC_{21}$
 2 Day Weathered Oil--28 Liter System
 73.5 Hours Post-Spill



Ratios: Aromatic Cmpd./nC₂₁
 2 Day Weathered Oil--28 Liter System
 73.5 Hours Post-Spill

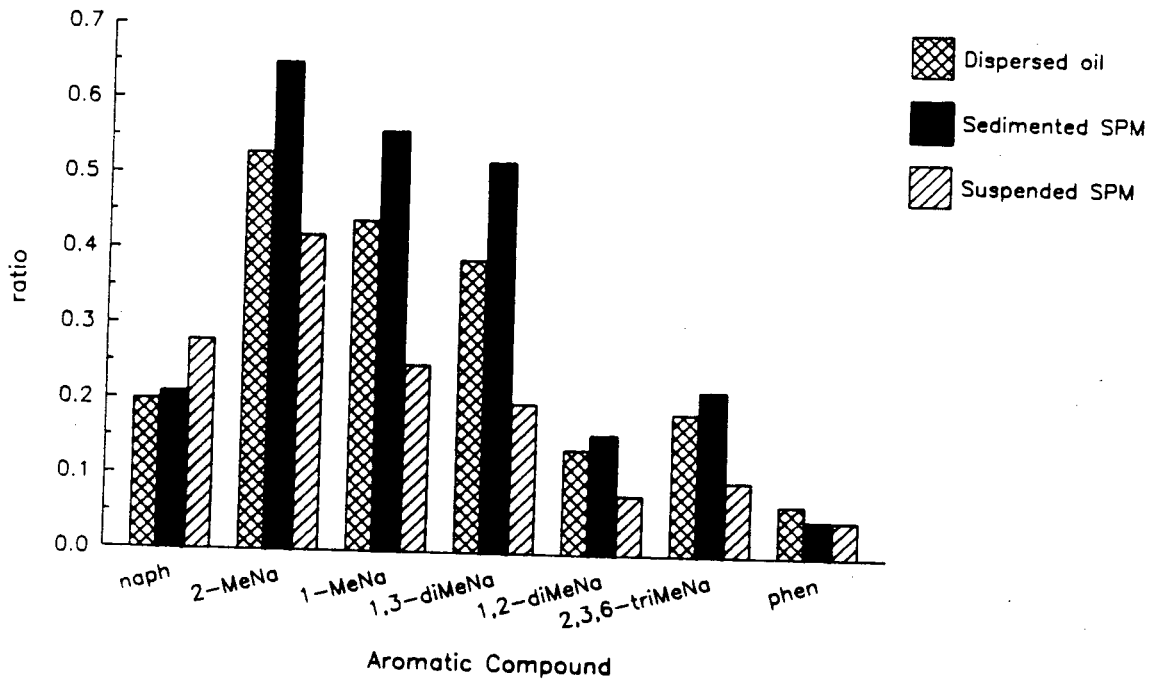


Figure 3-9. (a) Concentration ratio information for n-alkanes to nC₂₁ from the experiment in Figure 3-8.
 (b) Comparable information for aromatic compound ratios in Figure 3-8.

3.3 PARTITIONING OF DISSOLVED PETROLEUM HYDROCARBONS BETWEEN SEDIMENT AND WATER

When a chemical compound becomes dissolved into water in the presence of suspended particulate matter, a portion of the compound will adsorb onto the particulates. The extent to which this adsorption takes place is typically described by an adsorption isotherm, such as the Langmuir equation, the BET equation, or the Freundlich equation. In natural systems, however, the adsorptive capacity of the solids is invariably orders of magnitude greater than the solid phase concentration (O'Conner and Connolly, 1980). Under these (dilute) conditions the equilibrium concentrations of the compound in the aqueous and solid phases are related by,

$$K_p = \frac{C_s}{C_w} = \frac{\text{solid phase concentration}}{\text{aqueous phase concentration}}$$

where K_p is called the partition coefficient. The magnitude of this coefficient depends on the characteristics of the compound and the adsorbing solids.

The experiment described below was performed in order to measure the partition coefficient of hydrocarbons present in Prudhoe Bay crude oil.

Experimental Procedure

"Oil accommodated seawater" was prepared by placing one liter of unweathered Prudhoe Bay crude oil and one liter of seawater into a separatory funnel. The funnel was then allowed to equilibrate for several days.

The sediment utilized for the experiments was obtained from the upper intertidal zone of Jakolof Bay. This sediment was initially filtered through a 54 μm geological sieve and then allowed to settle in a beaker for approximately 2 1/2 hours. The settled sediment was saved, the aqueous phase discarded.

A 300 ml aliquot of the "oil accommodated seawater" was vacuum filtered through a 0.4 μm pore size polyester filter to remove small dispersed oil

droplets. Approximately 1.02 grams of sediment was then added to the water in a separatory funnel. The mixture was then allowed to equilibrate for 12 hours. Occasionally, the separatory funnel was agitated to resuspend the sediments.

After equilibration, the settled SPM (at the bottom of the separatory funnel) was carefully removed onto a polyester filter. The aqueous phase was vacuum filtered through another filter and then extracted twice with 100 ml of methylene chloride. The filters then received vacuum filtrations of the following solutions 1) tapwater, 2) 10 ml methanol, and 3) 30 ml methanol chloride. These filtrates were collected in a separatory funnel, partitioned against 100 ml of seawater, and the remaining aqueous phase extracted with 100 ml of methylene chloride.

The resulting extract (of the aqueous and particulate phases) were reduced in volume and analyzed by FID-GC.

Experimental Results

The results of partitioning experiment are presented in Table 3-2. Additional compounds (not listed in Table 3-2) were detected in one phase but not the other. This fact is due to the detection limits of the GC and to the partitioning behavior of the hydrocarbons. The measured partition coefficients range from 4.1 to 380.

Implications for Suspended Particulates

The results above can be used to calculate concentrations of aromatic hydrocarbons in suspended sediment of the type used with the conditions employed in the experiment. Additional studies with dissolved components from different true boiling point (distillate) cuts of Prudhoe Bay crude oil and a variety of other SPM types are being continued.

Table 3-2 Partitioning Experiment Results.

Retention Time (min)	Compound I.D.	Water phase concentration ($\mu\text{g/g}$)	Sediment phase concentration ($\mu\text{g/g}$)	Partition coefficient, K
4.88	toluene	1.1		
7.84	ethyl benzene	0.067	6.1	5.5
8.17	m, p-xylene	0.21	0.84	12.5
9.10	o-xylene	0.14	2.7	12.9
10.79	--	0.004	0.57	4.1
22.24	naphthalene	0.026	0.55	138.
26.99	2-methyl naphthalene	0.005	0.69	26.5
27.68	1-methyl naphthalene	0.016	1.9	380.
31.95	--	0.053	1.4	87.5
			0.67	12.6

4.0 MODELING OF PHYSICAL PROCESSES INVOLVED WITH THE INTERACTION OF OIL DROPLETS AND SPM IN THE WATER COLUMN

4.1 WATER COLUMN PROCESSES

The modeling of the advection, mixing and interaction of oil droplets and SPM in the water column requires the consideration of a number of interacting physical processes. If the problem is reduced to predicting the distribution of oil and SPM concentrations, without considering interactions, then only the inputs of material from oil spills at the surface and from resuspension of sediment from the bottom need to be defined and modeled. The interior water column advection and mixing are described by the three-dimensional mass conservation equation which determines the concentrations as functions of space and time. Oil and SPM occur in the water column with size-class distributions with the smaller oil-droplet and sediment grain sizes predominating. This is because fine-grain sands and silts are more likely than coarse sands to be resuspended from the bottom under the action of bottom currents, and smaller oil droplets seem to be more readily dispersed into the water column from surface oil slicks (Bouwmeester and Wallace, 1986). Even if there is no interaction between particles, the non-linear form of the mass-conservation equation and the dependence of the sinking (rising) velocity on the particle size and density (buoyancy) means that each size class requires a separate equation. This is illustrated by the one-dimensional mass conservation equation (i.e. neglecting horizontal advection and mixing) for the concentration of SPM, C_i , with mean diameter d_i ;

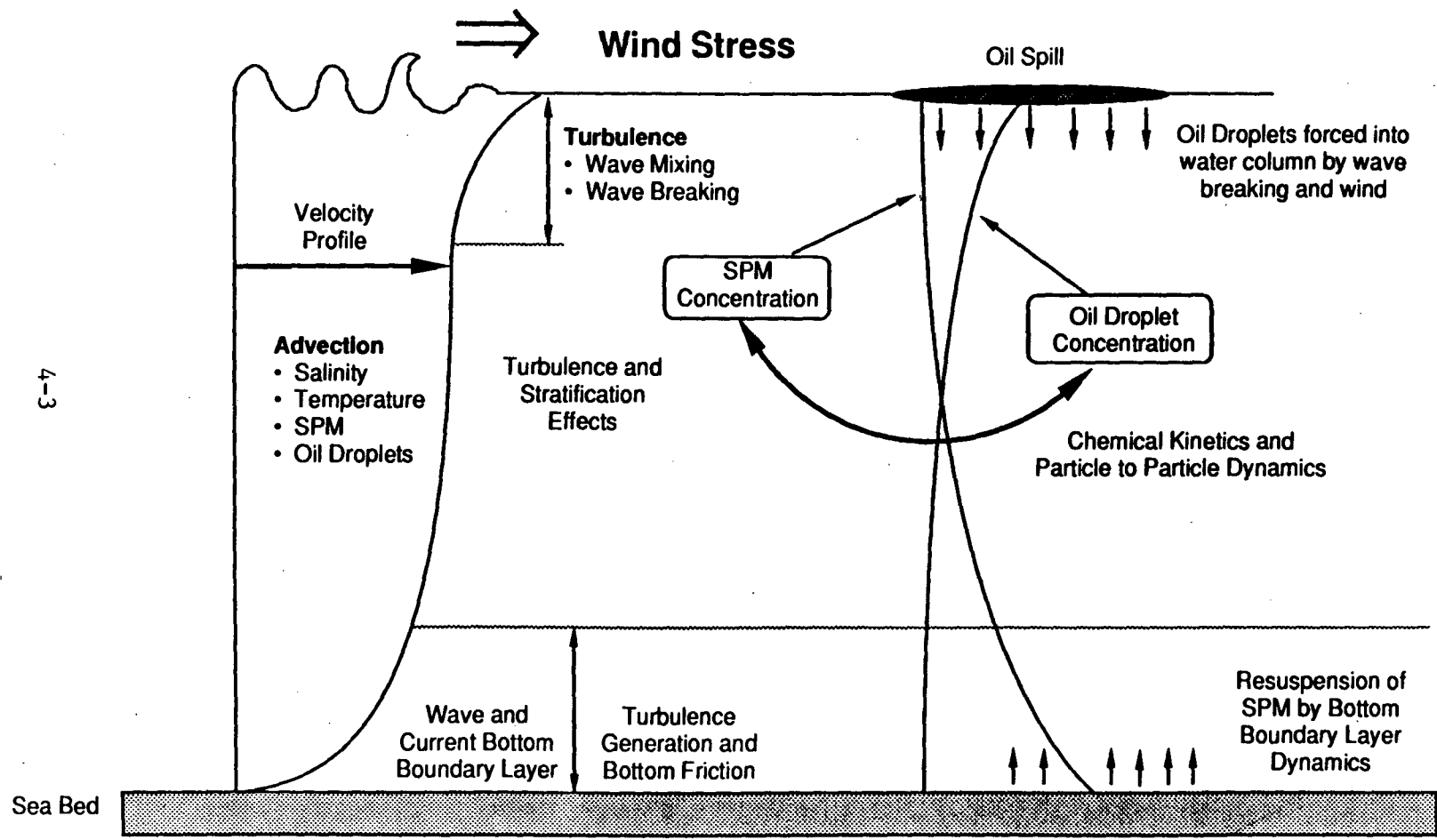
$$\frac{\partial C_i}{\partial t} + (w + w_{fi}) \frac{\partial C_i}{\partial z} - \frac{\partial}{\partial z} (\nu_{ts} \frac{\partial C_i}{\partial z}) = 0 \quad (4-1)$$

where w = is the vertical fluid velocity, ν_{ts} is the vertical turbulent eddy diffusivity, w_{fi} is the fall velocity of the particle, usually given by Stoke's Law (equation 5-11), and z is the vertical coordinate, + upwards. This equation (4-1) is applied separately to each size class of particles and oil droplets present in the water column. If the particles interact through coagulation and flocculation then an interaction term, R_i , must be included on the

right hand side of equation 4-1. This term, R_i , represents the source of particles due to the coagulation of particles of different smaller sizes to produce a particle of effective diameter d_i and the break-up of larger particle conglomerates by turbulence to produce particles of size class, i . It also represents sinks due to coagulation of particles of size class i with other particles and the break up of particles which remove them from size class i . The interaction of particles is usually approximately modeled by kinetic relationships similar to those discussed in Sections 1 and 2. Thus, if even only a few size classes, i , are modeled, the deterministic bookkeeping on particle concentrations in each size class becomes quite complex. In recent years a stochastic approach to modeling the transport of interacting particles of multiple size classes has been proposed and used successfully to model coagulation processes (Mercier, 1985) and turbulent reacting flows (Pope, 1979; 1981; 1982). This method is discussed in more detail below.

A schematic of the processes acting in the water column is shown in Figure 4-1. In simplest terms SPM is input from the sea bed by the bottom boundary dynamics (or riverine sources which are not explicitly discussed here) and oil droplets are input from the oil slick by surface layer processes. Both input conditions involve surface waves and wind. The physics of bottom boundary layer are quite well understood due to the theoretical models of Grant and Madsen (1979, 1982) and involve the non-linear interaction of surface wave oscillatory currents with steady or low-frequency currents (i.e. tidal or wind forced) in the bottom boundary layer. The entrainment of oil by the action of waves and the wind driven surface turbulent boundary layer is not well understood. Most of the evidence comes from wind tunnel and flume experiments (Bouwmeester and Wallace; 1985; 1986) where there are problems of consistent scaling for the turbulence and the waves compared with the ocean. However, there is indication that the turbulence introduced by breaking waves facilitates the production of small oil-droplets beneath a slick. There have been some attempts to model the formation and depth of penetration of oil droplets due to breaking waves (Aravamudan et al., 1982; Mackay et al., 1982) but the development of a solid theory is limited by the lack of knowledge and quantification of turbulence generated by breaking waves.

Water Column



4-3

Figure 4-1 Sketch of water column processes affecting the distribution of oil and SPM.

4.2 BOUNDARY CONDITIONS

As far as the model of advection and mixing of oil and SPM in the water column is concerned, the boundary submodels provide the flux of material to the water column. This is expressed as

$$\nu_{ts} \frac{\partial C}{\partial z} = F \text{ at } z = z_T \quad (4-2)$$

where F is the vertical flux, usually expressed as a vertical velocity multiplied by a concentration, and z_T is a level just below the surface or just above the bottom. The concentrations; C , and the turbulent diffusivity of the interior and boundary layer models should match at $z = z_T$. In addition for the bottom boundary layer model the current velocity, u , and the turbulent viscosity, ν_t , should also match the interior circulation model at $z = z_T$ (see Section 5 for details). Equation 4-2 provides the boundary conditions for equation 4-1 or its 3-D equivalent assuming a level bottom.

The physical processes that resuspend sediment are as follows: the near bottom oscillatory currents generated by surface waves combine with the low frequency currents in the bottom wave-current boundary layer to enhance bottom friction above that felt by a steady current alone. The enhanced bottom friction has two effects: the first is to increase the skin friction on the bed so that sediment grains are more readily placed in suspension, and the second is to increase the turbulence and hence the eddy viscosity and diffusivity in the boundary layer.

If the shear stress on the bed initiates sediment motion, then this moving bed under the action waves and steady currents has the effect of further enhancing the effective bottom friction. The initiation of sediment movement is dependant on the grain size of the sediments. Thus, smaller particles are more readily moved than larger particles. Once in motion particles can be mixed upwards by the turbulence in the boundary layer. Boundary layer turbulent mixing is proportional to the bottom shear stress velocity. This, in turn is a

function not only of the skin friction but of friction due to the larger scale bedforms such as ripples or bed formations due to biological activity. Sediment in motion near the bed which is not mixed up into the boundary layer is known as bedload transport, and its presence introduces density stratification very close to the bottom which has the effect of suppressing the mixing. Thus, there are a number of competing effects in the calculation of sediment transport and vertical SPM flux to the water column. These account for the complexity of the iteration procedures used to calculate the initiation of sediment motion, bottom boundary layer turbulent coefficients and SPM flux in the Grant, Madsen and Glenn model described in Section 5. The major limitation of this theory is that it only applies to non-cohesive sediments such as sand. There is currently no equivalent theory for cohesive sediments, and thus this bottom boundary layer model should be used with care when even small amounts of clays are present in the bottom sediment. A review of bottom boundary layer dynamics and models is given by Grant and Madsen, (1986).

Surface boundary layer turbulence and mixing under the combined effects of wind, waves and background currents is not well understood. Surface waves which are not breaking are not turbulent since the wave velocity field is irrotational. In the bottom boundary-layer it is the interaction of the wave currents with the bottom in the wave boundary layer that generates turbulence. Thus breaking waves are required to inject oil and turbulent energy below the surface. Most of the studies on this problem have been done in wind-wave flumes where incompatibilities of the scaling of wave motion (by Froude Number) and turbulence (by Reynolds Number) make application to the ocean surface uncertain. The principal result of the laboratory studies of Bouwmeester and Wallace (1985, 1986) was that small oil droplets (25 μ m diameter) predominate in the water column due to dispersal from a surface oil slick by breaking waves. Larger droplets tend to return to the surface due to buoyancy. There do not seem to be any systematic studies of oil entrainment rates as functions of sea-state, composition and age of the oil. Clearly the rate of breaking of the steepest waves will determine the rate of input of oil droplets to the surface layer. This can be estimated from wave spectra (Longuet-Higgins, 1969). This implies a certain intermittency in both space and time by the entrainment mechanisms. Note that breaking waves are in the short period part of the spectrum

(i.e. wind-waves), whereas waves that generate bottom turbulence correspond to long waves (i.e. swell) that have wavelengths greater than half the water depth. Thus, both sea and swell (i.e. the complete wave spectrum) are required to generate input data for both top and bottom boundary conditions. There are no current formulations which satisfactorily describe the flux of oil droplets from a surface slick to the water column due to wind and wave action. As a result, further laboratory experiments on this problem are being conducted by Delft Hydraulics Laboratory under a separate MMS contract. A literature review by Delvigne et al., (1986) discusses some possible formulations for calculating dissipation rates and eddy viscosities due to intermittently breaking waves.

4.3 WATER COLUMN PROCESSES

The mixture of oil droplets and SPM in the water column is acted upon by the advection and turbulence of the fluid, and it undergoes transformations due to coagulation. The simplest possible model of oil and SPM transport would consist of three equations similar to 4-1, one for oil droplets of similar diameter, one for SPM of a single size class and one for oil-SPM agglomerates. Only dissimilar particles could interact. Thus, the coagulation of oil droplets to form larger droplets or the coagulation of SPM particles or oiled-SPM particles would be prohibited. This, of course, does not happen in natural environments, so such an approach is only likely to be approximately true for very low concentrations of oil droplets with SPM containing no clays or organic matter (i.e. fine sand grains) so that SPM particles are unlikely to stick together even if they collide. As noted, this is not very realistic, and if reactions are allowed to occur, then different ranges of size classes for oil droplets, SPM and oiled-SPM are required. Solving a large number of equations of type 4-1 with complex source and sink terms for each particle class quickly becomes prohibitive in computer costs (Pope, 1981). Alternative methods using Monte Carlo techniques to solve the transport equation for the joint probability density function (pdf) for particle concentrations has proved effective for reacting constituents in a turbulent fluid (Pope, 1979; 1981). Mercier (1985) applied Pope's methods to modeling the transport and dispersion of sewage sludge from an outfall including coagulation of the particles and settling.

It is not the purpose of this section to present the theory and solution methods for the pdf transport equation, but rather to indicate that conventional finite difference or element methods are impractical if the reactions (coagulation) between different particle size classes and different particle-types are to be treated in a reasonable manner. The details of the pdf transport equation, coagulation formulations, and the Monte Carlo solution method, which should be readily adaptable to the oil-SPM problem, are given by Mercier (1985). However, brief descriptions of the concepts behind the stochastic pdf transport model and the mechanisms that promote coagulation in a turbulent fluid, are presented in the following paragraphs.

The control volume of a finite difference transport model has horizontal dimensions of the order of a few kilometers and depth of a few meters. The turbulence length scale which is the Kolmogorov length scale, ℓ (approximately 1 mm to 1 cm) defines the smallest volume element that is completely mixed. The joint pdf for a particular control volume is represented by an ensemble of N elements, each of which "contains" separate representative concentrations of each constituent. Elements can be considered as approximately equal-sized, completely mixed, lumps of fluid, with characteristic length and time scales given by the turbulence scales. The Monte Carlo method manipulates the ensemble of elements so as to simulate the corresponding evolution of the joint pdf which is governed by the pdf transport equation. Thus, the statistics of the ensemble are equivalent to the statistics of the pdf. The result is that the mean concentration of a constituent over N elements is equivalent to the mean concentration of that constituent in the control volume such as might be determined by a conventional equation 4-1. Each control volume is spatially uniform or equivalently homogenous from a statistical perspective. Therefore, the element volumes have no relative position within the volume. The element set represents typical constituent concentrations that one would obtain if N samples, with volumes of order ℓ^3 were taken at random points throughout the assumed homogenous control volume.

The Monte Carlo technique simulates the effects of that physical processes of advection, turbulent mixing and settling have on the ensemble of elements in each control volume as well as the effects on the ensemble of

reactions in "composition" space. One of the advantages of this pdf approach is that the source and sink term, R_1 , does not have to be specifically modeled (i.e. it appears in the equation in closed form Mercier, 1985; Pope 1979; 1981). The distribution of particle sizes in natural waters is approximated by:

$$g(d) = Ad^{-4} \quad (2\mu\text{m} < d < 100\mu\text{m}) \quad (4-3)$$

where $g(d)$ is the number of particles per unit fluid volume of diameter d and A is a constant (Mercier, 1985). Therefore particles at the lowest end of the size range tend to predominate. The coagulation of particles depends upon their collision rate. Mechanisms which cause particles to collide are Brownian motion, fluid shear and differential sedimentation. Collision rates, derived by assuming rectilinear motion of particles, are modified by fluid shear generated by the motions and short range attractive van der Waals forces and repulsive electrostatic double-layer forces. These are taken into account by collision efficiency functions which modify the collision rates for the various mechanisms. Mercier (1985) discusses the formulation for the collision frequencies due to the three mechanisms and solves the equations numerically. He shows that coagulation by all three mechanisms is dominated by particles of the smallest size. Thus, larger particles are more likely to collide with smaller particles than with particles of similar size. The coagulation equations can be incorporated into the source terms of the pdf transport equation and solved using Monte Carlo techniques for transport through composition space (i.e. changes in number density of particle size classes due to coagulation).

This section is very brief introduction to the complexities of modeling reactive transport of suspended particles. The reader is referred to Mercier's Thesis for a more complete and rigorous discussion.

4.4 COMPONENT MODELS OF OIL-SPM TRANSPORT AND FATE

The previous sections have discussed surface and bottom boundary layer and water column processes affecting the modeling of the interaction and transport of oil and SPM. However, to construct a model of oil-SPM transport, hori-

zontal spacially varying processes need to be considered as is indicated by the sketch in Figure 4-2. Thus a coastal sea model will have open boundaries for which deep ocean conditions need to be prescribed. This includes tides, specification of salinity, temperature and SPM concentrations at minimum. A fully three dimensional circulation model is required to predict the velocity field which advects the constituents in the 3-D transport model. Current velocities and winds will move and disperse the oil slick at the surface. Other inputs include river sources of brackish water and SPM, and SPM input from coastal erosion. Finally the surface wave field including deep water swells as well as wind seas for input to the bottom boundary layer sediment resuspension model and the surface wave-breaking mixing model will be required.

The model components of a complete 3-D oil-SPM transport model are represented by the box diagram in Figure 4-3. The space dimensionality (1, 2 or 3-D) and physical basis of each model component are indicated. Thus, "mass conservation" indicates that the major equations of this component are derived from the law of mass conservation (i.e. equation 4-1) and "dynamical" means that momentum conservation equations (i.e. the prediction of current velocities) are required. All models and external inputs are assumed to be time dependent. The arrows indicate the transfers of information between model components.

It can be seen that the 3-D circulation model is the central component in that it supplies velocities and mixing coefficients to most of the other components which in turn supply boundary conditions. There is a requirement that surface and bottom velocities as well as turbulent coefficients match at appropriate levels within the boundary layers. Thus, the interactions between the boundary sub-models and the circulation model are essentially non-linear. The 3-D circulation model will usually predict salinity and temperature fields because horizontal density gradients modify wind-forced currents and vertical density gradients (stratification) suppress the turbulent mixing processes.

Since the surface wave model needs to calculate low frequency (i.e. swell) waves for the bottom boundary layer model, it may cover a much larger area than any given coastal circulation model. Thus a model of Norton Sound

Plan View

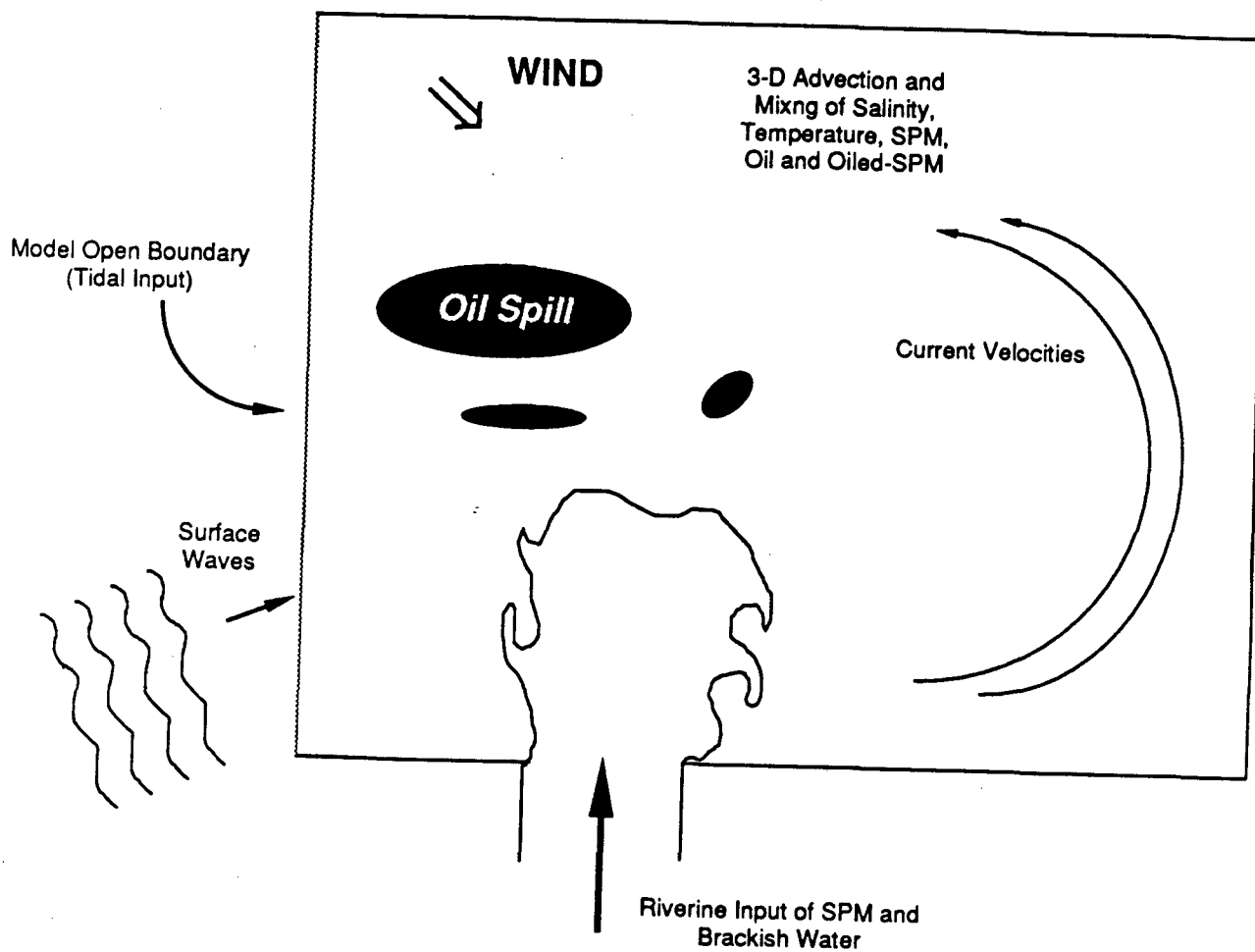


Figure 4-2 Sketch of a plan view of oil-SPM transport processes.

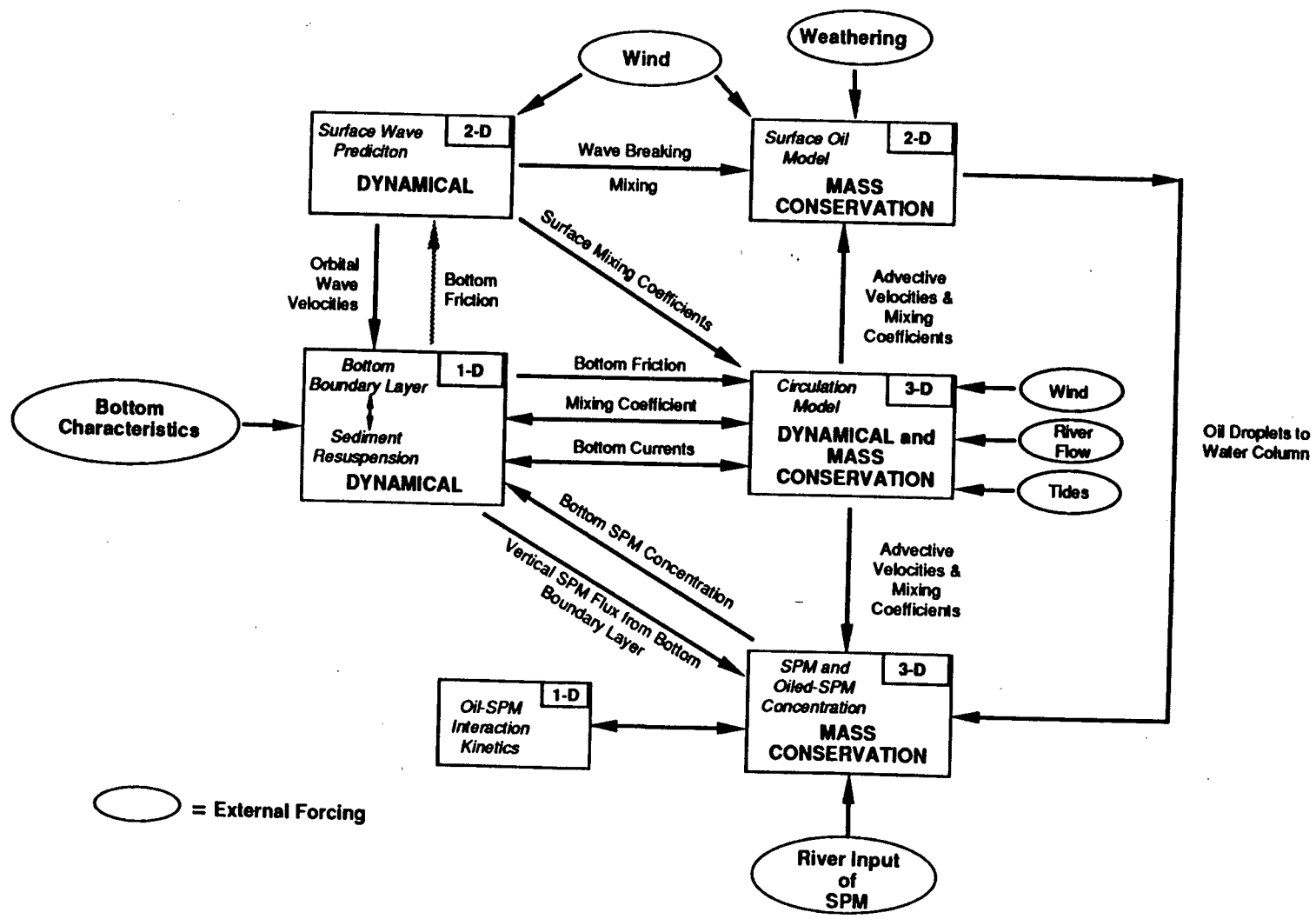


Figure 4-3 Component Models of a 3-D Oil-SPM Transport Model

would probably require a wave prediction model that includes the deep water of the Bering Sea. An example of a parametric wave prediction model is given by Gunther et al., (1979) and a recent review of wind-wave prediction models is given by Sobey (1986). If the oil-SPM model is used in a hindcast mode then wave spectra, preferably directional, could be obtained from offshore wave-rider buoys and (with assumptions on uniformity) directly input into the boundary layer models.

As a result of these analyses, it now appears that it may be more appropriate to use the pdf formulation of the transport equation (solved by Monte Carlo methods discussed above) for the oil-SPM transport model. This would especially be the case if the model is to include representative size classes of oil droplets and SPM as well as different coagulation mechanisms. For this reason as well as the complexity of the boundary conditions, the Oil-SPM transport model should probably be a separate model from the circulation model even though the circulation model provides the 3-D velocity and turbulence fields to drive this model.

The complete oil-SPM transport model as represented by Figure 4-3 does not exist and not all components have satisfactory models at present. Even though the bottom-boundary layer model, described in detail in the next section, is now well established it has not yet been incorporated into continental shelf circulation models. The stochastic transport model for reactive particles is a completely new technique for oceanography. Formulations for surface layer mixing due to wave breaking and Langmuir circulations are not well established. Therefore it is recommended that the development of the model proceed in stages. Possible development scenarios are as follows:

1. Incorporate Grant/Madsen bottom boundary layer model for bottom friction into 3-D circulation model. Determine effects on wind-driven flow for storm conditions. Spectra from wave-rider buoys could be used as input.
2. Attempt application of parametric wind-wave/swell models to areas of interest. When possible, use hindcast wave conditions for specific storm events to evaluate modeled wave spectra using wave-rider data.

3. Develop stochastic oil-SPM reactive transport model based on Mercier (1985) in simple 1-D form and apply to Kasitsna Bay Laboratory experiments to test the realism of the coagulation formulations.
4. Formulate, and devise laboratory tests for a model of the generation of oil droplets (including size distribution) from an oil slick by wind and breaking waves.
5. Develop projects 3 and 4 along with the bottom boundary layer/sediment resuspension model for a 1-D (depth) model of the water column under an oil slick. Horizontal uniformity of depth, current velocity, wave fields and bottom characteristics would be assumed and motion would be relative to the oil slick (i.e. the coordinate system would be fixed in the oil slick.) Surface wave data could be obtained from project 2 or from wave-rider. This model would in effect be a 1-D version of the complete oil-SPM transport model (Figure 4-3). It would allow the interactions of the component models to be properly incorporated and experimented upon, without being prohibitive in computer costs. The limitations and approximations due to the 1-D assumption should not be unduly restrictive.
6. Develop 5 into complete 3-D model incorporating the 3-D circulation model and expanding the stochastic transport model to 3-D. This model may require extensive super computer resources even for a relatively small area such as Norton Sound.

5.0 APPLICATION OF THE GRANT-MADSEN BOUNDARY LAYER MODEL TO A MODEL OF SUSPENDED PARTICULATE TRANSPORT

5.1 INTRODUCTION

The Grant-Madsen-Glenn boundary layer model provides a method for estimating bottom stress in the presence of waves and currents, including treatments of movable bed roughness, initiation of sediment motion, sediment suspension, and stratification by suspended sediments. The foundation of the work is the treatment of waves in the presence of a steady current, presented by Grant and Madsen (1979). The theory divides the near-bottom boundary layer into two regions: 1) a thin layer, typically two to twenty centimeters thick, in which the energy of the eddies is controlled by the wave motion, and 2) a broader region, with a thickness on the order of meters, where the eddy energy is related only to the non-oscillatory part of the current. Using this assumption, the bottom shear stress is calculated, and eddy viscosities are determined for the two regions. These are used to predict near-bottom velocity profiles under combined wave and current flows.

Another component of the present model is the movable bed roughness model of Grant and Madsen (1982). It predicts the physical boundary roughness due to bedforms and moving sediment, which depend on the skin friction shear stress generated by the flow. The bed roughness model contributes to the estimate of total shear stress by modifying the effective drag coefficient of the bed.

The application of the Grant and Madsen model to sediment transport was performed by Glenn (1983) and Grant and Glenn (1983a). This model uses the Grant-Madsen (1979) wave-current interaction model and the Grant-Madsen (1982) bed roughness model, in combination with empirically derived relations for initiation of sediment motion and semi-empirical models of near-bed suspended sediment concentration, to represent the vertical distribution and transport of suspended sediment in conditions representative of the continental shelf. The model includes the damping influence of stable stratification by suspended sediment on turbulence in the boundary layer, with consequent reduction of mean boundary shear stress under certain conditions. They also developed a full Ekman layer model under waves and currents. The near-bottom model is currently

being applied explicitly to sediment transport problems by a student of Grant and Madsen, Margaret Goud. She has added a bedload transport estimate and an estimate of load and transport in the outer Ekman layer, and has investigated the uncertainties in sediment load and transport predictions based on the assumptions in the model.

The fundamental advance by Grant and Madsen was the treatment of waves as they affect boundary layer flow, which is critical for prediction of sediment transport on the continental shelf. The Grant-Madsen-Glenn sediment transport model (hereafter referred to as GMG) combines this representation of wave-current interaction with a combined theoretical and empirical representation of the sediment dynamics to yield a relatively simple but powerful predictive model of sediment transport. However, it should be emphasized that the GMG model is only applicable where the effects of breaking waves (e.g., the surf zone) do not penetrate to the bottom boundary layer. The GMG model would have to be modified to be useful when water depths are less than approximately 3-4 wave heights (i.e., the depth at which breaking waves "penetrate" to the bottom).

The following discussion will provide a brief synopsis of the elements of the Grant-Madsen-Glenn model, with emphasis on the application of the model as the boundary condition to a circulation-transport model. The discussion is by no means comprehensive, and the reader is referred to the three technical reports prepared by Grant and Glenn (1983a,1983b,1983c) for a complete treatment of the derivation of the theory, discussion of the assumptions and uncertainties, and the solution procedure, including Fortran code.

In Section 5.2, the relevant fluid and sediment dynamics will be discussed, followed in Section 5.3 by a flow chart of the model, with examples of results. Section 5.4 will be a discussion of the model's uses and limitations as an element of a numerical model of continental shelf sediment transport.

5.2 MODEL ELEMENTS

5.2.1 Boundary Layer Hydrodynamics

The bottom boundary layer is the region of the flow that is significantly influenced by bottom stress, which may be limited to a small fraction of the water column, depending on the water depth, the strength of the flow, and the time scales of motion. A boundary layer can be described most effectively by a length scale, δ which represents the height of the boundary layer, and a velocity scale, u_* . The so-called friction velocity u_* is defined by:

$$u_* = \left(\frac{\tau_0}{\rho}\right)^{1/2}$$

where τ_0 is the bottom stress and ρ is the fluid density. By scaling the momentum equation, it can be shown that

$$d = O\left(\frac{u_*}{\omega}\right)$$

where O means "on the order of" and ω is the dominant frequency of motion, which may be the orbital frequency of waves, the tidal frequency, or the Coriolis frequency, f , depending on the flow.

Because surface gravity waves have frequencies far higher than tides or geostrophic currents, the boundary layers associated with them are orders of magnitude thinner. In environments where there are significant currents as well as surface waves, it is convenient to divide the boundary layer into two regions, a narrow region that is strongly influenced by the waves and relatively weakly by the current, and a broad region that is influenced only by the current. The length and velocity scales of the "wave-current" boundary layer are designated δ_{cw} and u_{*cw} and those of the "current" boundary layer are denoted δ_c and u_{*c} .

The turbulence in the wave boundary layer will thus tend to be more intense than that in the current boundary layer, principally because of the strong vertical velocity gradients associated with the small vertical length scale of the wave boundary layer. Thus the velocity scale u_{*cw} will often be much larger than u_{*c} . It should be pointed out, however, that u_{*cw} is associ-

ated with an oscillatory stress, and the mean stress, reflected in the value of u_{*c} is essentially constant across the wave-current boundary layer.

It has long been recognized that the turbulent flux of momentum can be represented effectively in the turbulent boundary layers by coefficients of eddy viscosity ν_t of the form

$$\nu_t = \kappa u_* z$$

where κ is von Karman's constant ($\kappa = 0.41$) and z is the vertical distance from the bed. This formulation leads to the familiar logarithmic velocity profile in the vicinity of the bed. The Grant-Madsen (1979) formulation assumes this form for the eddy viscosity in order to solve for the flow in the wave-current and current boundary layers. Although the details of the oscillatory boundary layer flow are not of interest in a model of the low-frequency currents, the wave motions largely determine the value of u_{*cw} and a solution for the oscillatory boundary layer motion is required to establish the value of u_{*cw} given the wave and current parameters. Based on arguments about the nature of turbulence production in boundary layers, Grant and Madsen (1979) define

$$u_{*cw} = \left| \frac{\tau_c}{\rho} + \frac{\tau_{w,max}}{\rho} \right|^{1/2}$$

where τ_c and τ_w are stress components due to the mean and the wave components, each of which includes the interaction terms between the currents and the waves.

The expression for τ_w is obtained by solving for the oscillatory velocity, and using the closure relation

$$\tau_w = \kappa u_{*cw} z \frac{\partial u}{\partial z}$$

to obtain an expression for τ_w in terms of u_{*cw} and the wave parameters. An expression for τ_c is obtained by defining a friction factor f_{cw} using a quadratic drag law:

$$\tau_0 = \frac{1}{2} \rho f_{cw} |u|u$$

where τ_0 is the mean bottom shear stress and u is a representative velocity in the wave-current boundary layer, time-averaged over the wave period. τ_c and u_{*cw} are each written in terms of the mean and wave-induced currents and the friction factor. These expressions are combined to yield an implicit expression for f_{cw} , which is then used to solve for u_{*cw} and u_{*c} .

The derivation of the solution for the friction factor, and therefore the shear velocities, is more involved than this discussion warrants; it is detailed in Grant and Madsen (1979). The solutions for the wave velocity and the friction factor are included in a short appendix to this report. It should be pointed out here that u_{*c} and u_{*cw} depend on the orbital velocity of the dominant waves, the wave frequency, the mean current velocity in the boundary layer, the relative angle between the waves and currents, and the bottom roughness (see appendix for formula). The mean velocity in the boundary layer, represented by the symbol u_a , is used as an iteration parameter, starting from an initial estimate or guess, with the iterations ending when the velocity at a reference level z_r above the wave boundary layer matches the value determined from the model of the overlying flow.

The mean velocity profiles in the wave-current and current boundary layers are solved by assuming steady flow and constant stress, so that:

$$\nu_{t,cw} \left(\frac{\partial u_c}{\partial z} \right) = |u_{*c}| u_{*c} \quad z_0 < z < \delta_{cw} \quad (5-1)$$

$$\nu_{t,c} \left(\frac{\partial u_c}{\partial z} \right) = |u_{*c}| u_{*c} \quad \delta_{cw} < z < z_r \quad (5-2)$$

where

$$\nu_{t,cw} = \kappa u_{*cw}^2 \quad z \leq \delta_{cw} \quad (5-3)$$

$$\nu_{t,c} = \kappa u_{*c} z \quad z > \delta_{cw} \quad (5-4)$$

and

$$\delta_{cw} = 2 \frac{\kappa u_{*cw}}{\omega} \quad (5-5)$$

The solutions to these equations are simply:

$$u(z) = \frac{1}{\kappa u_{*c}} \left(\frac{u_{*c}}{u_{*cw}} \right) \ln \frac{z}{z_0} \quad z \leq \delta_{cw} \quad (5-6)$$

$$u(z) = \frac{1}{\kappa u_{*c}} \ln \frac{z}{z_{0c}} \quad z > \delta_{cw} \quad (5-7)$$

where z_0 is the roughness length, the calculation of which is discussed below, and z_{0c} is the apparent roughness length of the outer flow, defined by

$$\frac{z_{0c}}{z_0} = \left(\frac{\delta_{cw}}{z_0} \right)^{\left(1 - \left| \frac{u_{*c}}{u_{*cw}} \right| \right)} \quad (5-8)$$

which is obtained by matching the solutions at δ_{cw} . Note that the effect of the wave on the flow above the wave boundary layer is an increase in the roughness length z_{0c} ; u_{*c} is greater in the presence of waves because the steady current "feels" a rougher boundary.

5.2.2 Initiation of Sediment Motion

Sediment motion is initiated when the combined wave and current boundary shear stress felt by the seafloor is greater than the critical shear stress for moving sediment. The boundary shear stress τ_0 defines the effects of turbulence on the flow in the boundary layer; this stress results from the viscous interaction of the fluid with the solid boundary and from the turbulence generated due to pressure gradients introduced by roughness elements on the bottom. These two components of the boundary shear stress are referred to as skin fric-

tion and form drag. The medium sand and smaller grains which are of primary interest in suspended sediment transport are not set in motion by the pressure gradients which make up the form drag component. For the purposes of this model, initial sediment motion is considered to result from the skin friction component, denoted by the symbol τ'_0 , whereas turbulent transport of mass and momentum in the boundary layer is governed by the total boundary shear stress.

A sediment grain responds essentially instantaneously to turbulent fluctuations. Therefore, critical shear stress for initiation of motion might be expected to be related to the skin friction component of the maximum boundary shear stress τ_{0cw} . In controlled lab settings initiation of motion and bedload transport in oscillatory flow were found to be quite successfully predicted using the maximum shear stress (Madsen and Grant, 1976, pp 18-28, 40-45). In those cases, the bed was flat, so the maximum shear stress was equal to the skin friction shear stress. In the model, the skin friction component of the maximum combined boundary shear stress is used for all initiation of motion and bedload transport predictions.

A commonly used empirical criterion for determining the critical shear stress for initiation of motion of non-cohesive sediments is the Shields parameter, which is defined:

$$\psi = \frac{\tau'_0}{(s - 1)\rho g d} \quad (5-9)$$

The numerator represents the force trying to move the particle and the denominator represents the gravitational force (per unit area) on the particle, which resists motion ($s = \rho_{sed}/\rho$, ρ_{sed} = grain density, g = gravity, and d = grain diameter). When the critical value of Shields parameter for the grains in the bed is exceeded by the flow, sediment is put into motion. The critical value is designated ψ_c .

Critical values for the Shields parameter have been determined empirically in a series of laboratory experiments, beginning with those used to generate the original Shields Diagram (Shields, 1936). That original diagram

plotted ψ_c vs the boundary Reynolds number $R_* = u_* d / \nu$; this was reformulated by Madsen and Grant (1976) to make the independent variable a function of sediment and fluid properties only. The modified Shields Diagram plots ψ vs a non-dimensional sediment parameter S_* where

$$S_* = \frac{d}{4\nu} \sqrt{(s - 1)gd} \quad (5-10)$$

The original flume experiments on which the diagram was based were performed using only large grain size material, corresponding to grain diameters of medium sand or larger ($R_* > 1$ and $S_* > 1$). Later investigators did experiments with grains as $d = .0016$ cm (medium silt) (White, 1970) and extended the Shields Diagram from $R_* = 1.0$ to $R_* = 0.05$. These results have been adapted to the S_* formulation; the result is Figure 5-1. This figure shows the initiation of motion criterion which is used in this model. The initiation of motion criterion can be increased by biological adhesion of sediment grains (Grant, Boyer and Sanford, 1982) or plastic cohesion, due to the presence of clays in even small quantities. This is especially true for silt-sized grains, so interpretation of sediment load and transport results must be made with this uncertainty in mind.

5.2.3 Sediment Suspension

Once sediments are dislodged from the seabed, they are available for transport upward by turbulent eddies. As described above, the strength of these eddies governs the mixing of mass and momentum in the boundary layer and is determined by the boundary shear stress, τ_0 . Mixing occurs because vertical eddies are transporting high-concentration fluid up and low-concentration fluid down, so that there is a net upward flux of sediment based on the concentration gradient. This flux is balanced by the tendency of the sediment to fall out of suspension due to gravitational force.

The tendency of the sediment to fall is measured by the particle fall velocity w_f and is determined to first order by balancing the submerged particle weight with the fluid drag on the particle. For grains smaller than fine

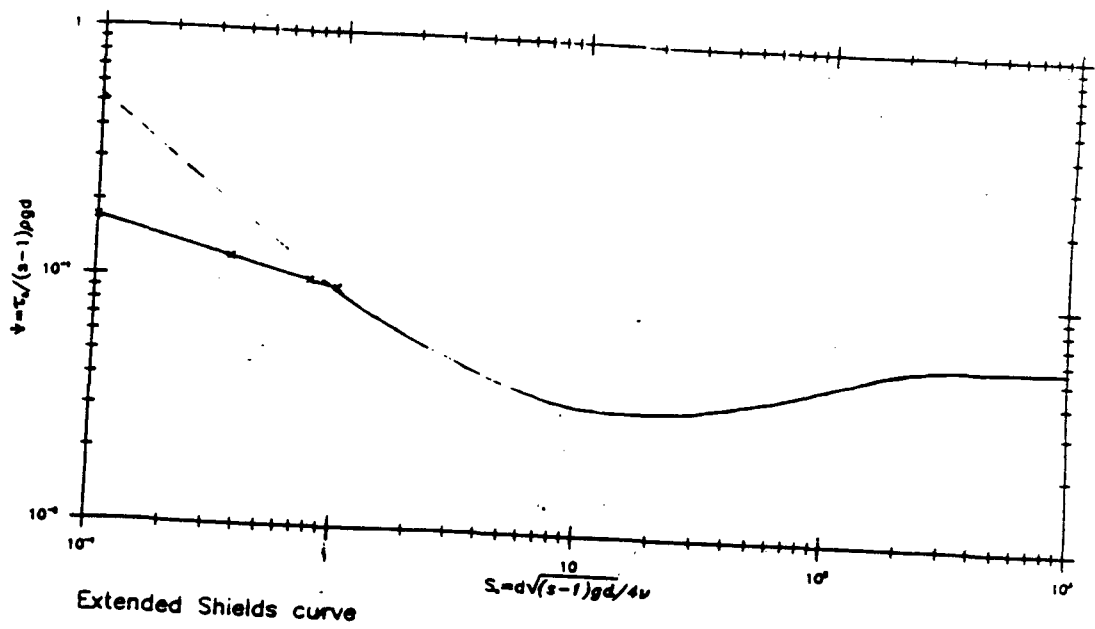


Figure 5-1. Modified Shields Diagram, extended to include fine grain data (modified from Madsen and Grant, 1976)

sand (diameter of 0.012 cm), Stokes drag law holds and the fall velocity is given by:

$$\frac{w_f}{[(s-1)gd]^{1/2}} = \frac{2}{9} S_*^2 \quad (5-11)$$

the particle. The fall velocity of a particle in the field, however, can be affected by flocculation or biological aggregation.

The distribution of sediment in the water column is governed by the conservation of mass equation for sediment:

$$\frac{\partial C}{\partial t} - w_f \left(\frac{\partial C}{\partial z} \right) + \frac{\partial}{\partial z} \langle C'w' \rangle = 0 \quad (5-12)$$

where C_n is volumetric sediment concentration and $\langle C'w' \rangle$ represents the Reynolds averaged turbulent fluctuation of sediment. Analogous to the eddy viscosity representation for turbulent stress, turbulent mixing of sediment can likewise be modeled using an eddy diffusivity, so that

$$\langle C'w' \rangle = \nu_{ts} \left(\frac{\partial C}{\partial z} \right) \quad (5-13)$$

Experimental evidence indicates that the eddy diffusivity and viscosity have similar forms in boundary layer, and ν_{ts} can be written as

$$\nu_{ts} = \frac{\nu_t}{\gamma} = \frac{\kappa}{\gamma} u_* z \quad (5-14)$$

where γ is an empirical parameter, assumed to be 0.74, based on Businger and Arya (1974). The GMG model assumes steady state conditions, with a balance between upward turbulent diffusion and fall velocity, thus Equation 5-12 simplifies to

$$-w_f C + \nu_{ts} \left(\frac{\partial C}{\partial z} \right) = 0 \quad (5-15)$$

which is satisfied by

$$C(z) = C_0 \left(\frac{z}{z_0}\right)^{-\frac{\gamma w_f}{\kappa u_{*cw}}} \quad z_0 < z < \delta_{cw} \quad (5-16)$$

$$C(z) = C_{\delta_{cw}} \left(\frac{z}{\delta_{cw}}\right)^{-\frac{\gamma w_f}{\kappa u_{*c}}} \quad z > \delta_{cw} \quad (5-17)$$

where C_0 is a reference sediment concentration, discussed below, and $C_{\delta_{cw}}$ is the concentration at the top of the wave-current boundary layer, determined from Equation 5-16.

Note that the GMG model assumes zero net vertical flux of sediment, since the fall velocity exactly balances the turbulent flux. This constraint is not valid for application of the GMG model as a boundary condition to a time-dependent transport model, and a slight modification is required to generalize the model to conditions of non-zero vertical flux. This is discussed in Section 5.4.

5.2.4 Reference Sediment Concentration

The reference concentration C_0 is calculated using the form suggested by Smith and McLean(1977):

$$C_0 = C_{bed} \left(\frac{\gamma_0 S}{1 + \gamma_0 S}\right) \quad (5-18)$$

where C_{bed} is the bed concentration of the grain. γ_0 is an empirical reference concentration parameter of order 10^{-3} . S is the normalized excess skin friction

$$S = \frac{\tau'_0 - \tau_c}{\tau_c} = \frac{\psi'}{\psi_c}$$

The primes refer to the skin friction component of the total boundary shear stress. The skin friction component is determined by calculating the combined

wave/current friction factor f_{cw} using the dominant grain size as the bottom roughness scale rather than the physical boundary roughness which includes the effect of ripples and sediment in motion. To handle the presence of waves in this model, the instantaneous normalized excess shear stress is used to calculate instantaneous reference concentrations which are then averaged over a wave period to find the mean reference concentration.

The reference concentration is directly dependent on the critical shear stress, as determined by the Shields parameter. However, the Shields parameter is an empirical value based on laboratory flume experiments on single grain-size sands. Mixed grain sizes and biological binding or mixing, as found in field situations, may affect the critical shear stress.

5.2.5 Suspended Sediment Stratification Effects

The vertical gradient of suspended sediment results in stable stratification in the boundary layer, which causes a partial suppression of turbulence and a reduction in the eddy viscosity and diffusivity. The GMG model uses the form developed by Businger and Arya (1974) for stable stratification in the atmospheric boundary layer, in which turbulence was related to the Monin-Obukov length, which in the case of suspended sediment can be approximated:

$$L = \frac{|u_*|^3}{\kappa g (s - 1) w_f C(z)} \quad (5-19)$$

where s is the specific gravity of the suspended sediment and the concentration represents the total concentration for all grain sizes considered.

The sediment concentration profile is coupled with the velocity profile through modification of the eddy viscosity and diffusivity to reflect the effect of stratification on turbulent energy:

$$\nu_t = \frac{\kappa u_* z}{1 + \beta \frac{z}{L}} \quad (5-20)$$

$$\nu_{ts} = \frac{\kappa u_* z}{\gamma + \beta \frac{z}{L}} \quad (5-21)$$

where β is an empirical stratification parameter, assumed to be 4.7 (Businger and Arya, 1974). The Monin-Obukov length L becomes smaller as the suspended sediment stratification increases, which causes a reduction in the viscosity and diffusivity. The dependence of the eddy coefficients on stratification causes the vertical profiles of velocity and suspended sediment to vary with increasing stratification. The solution for velocity and suspended sediment must therefore be approached iteratively, with corrected values of ν_t and ν_{ts} coming from estimates of the concentration distribution $C(z)$.

The solutions for the velocity and suspended sediment profiles, with the inclusion of the stratification correction are as follows:

$$u(z) = \frac{1}{\kappa u_* c} \left[\ln \frac{z}{z_{0c}} + \int_{\delta_{cw}}^z \frac{1}{L} dz \right] \quad z > \delta_{cw} \quad (5-22)$$

$$C(z) = C_{\delta_{cw}} \left(\frac{z}{\delta_{cw}} \right)^{-\frac{\gamma w_f}{\kappa u_* c}} \exp - \left(\frac{\beta w_f}{\kappa u_* c} \int_{\delta_{cw}}^z \frac{1}{L} dz \right) \quad z > \delta_{cw} \quad (5-23)$$

The effects of stratification are shown in the second term on the right hand side of Equation 5-22 and in the exponential term in Equation 5-23. Because the high energy of the eddies in the wave boundary layer is expected to keep that region well mixed, the stratification correction is not included in the calculation of the velocity below δ_{cw} . The velocity and concentration profiles inside the wave boundary layer are therefore given by the neutral solutions, Equations 5-6 and 5-16.

5.2.6 Bedload and Suspended Sediment Transport

Transport of sediment in the near-bottom layer is calculated by numerically integrating the product of the predicted concentration and velocity profiles:

$$q_{s, \text{sus}} = \int_{z_0}^z C(z)u(z)dz \quad (5-24)$$

For sediment larger than medium-coarse silt, most transport is expected to be confined to the near-bottom layer.

Bedload is not expected to be a significant portion of the total load in the wave-dominated shelf flows over beds of sand and silt on which this study focuses. It is estimated using a semi-empirical bedload formula as outlined in the following paragraphs; this estimate is sufficiently accurate for the purposes of this model. Since the bedload is assumed to travel in the direction of the wave-current shear stress, however, and the suspended load direction is controlled by the current, the bedload could be a major contributor for some size classes in the direction of the wave.

The bedload is calculated using the Meyer-Peter and Muller (1948) formulation, an empirical formula based on an extensive set of laboratory experiments:

$$q_{s, \text{bed}} = 8[d\sqrt{(s-1)gd}](\psi' - \psi_c)^{3/2} \quad (5-25)$$

where the Shields parameter is calculated using the skin friction value of the shear stress. We want to apply this equation, which was formulated for steady, unidirectional flow, to the combined wave/current flow. For this, we assume, as we do for the reference concentration calculation, that the response time for the sediment is small relative to the unsteady time scale (as demonstrated in Madsen and Grant, 1976) and that the maximum shear stress in each direction dominates the boundary shear stress. This estimate will be larger than the actual bedload, but will provide a reasonable scale for comparison with the suspended load to see if the bedload is significant.

Since we assume that the maximum boundary shear stress in the direction of the current is equal to the sum of the wave shear stress and current shear stress, we likewise assume that the maximum boundary shear stress in the

opposite direction ($\tau_{cw,neg}$) can be calculated by subtracting the current shear stress from the wave shear stress ($\tau_{cw,neg} = \tau_{w,max} - \tau_c$). (Codirectionality has again been assumed for ease of discussion.) If we assume that the maximum shear stress in each direction occurs for 1/2 the wave period, we overestimate the bedload transport in each direction; however, to 'time average' the transport we subtract the value in the negative direction from that in the positive direction, cancelling most of the error. To calculate total bedload transport, we determine for each grain size class n the following:

$$q_{s,bed,n} = 8[d_n \sqrt{(s-1)gd_n}]((\psi' - \psi_{c,n})^{3/2} - (\psi_- - \psi_{c,n})^{3/2}) \quad (5-26)$$

where ψ_- is the Shields parameter in the negative direction, based on τ_{cw} .

5.2.7 Bottom Roughness

The calculation of the velocity profile inside the wave boundary layer (Equation 5-6), depends explicitly on the physical bottom roughness length z_0 . This length is also necessary for the calculation of the friction factor f_{cw} on which the calculation of the shear velocities depends. Its value is therefore of fundamental importance.

A model for movable bed roughness under a combined wave and current flow was developed by Grant and Madsen (1982), and that work will be described briefly here. Their model is used in GMG.

The physical roughness felt by the near-bottom flow is the sum of the three components: 1) the roughness due to the individual grain diameters in the bed (skin friction); 2) the roughness due to ripples and mounds on the sea-floor (form drag); and 3) a roughness associated with dissipation due to sediment in motion in the near-bed layer. The effect of these elements will be parameterized in terms of a Nikuradse equivalent sand grain roughness, As used here, the roughness height is expressed in terms of the three elements listed above so that the total roughness height is:

$$k_b = k_{b,gr} + k_{b,rip} + k_{b,s.t.} \quad 5-(27)$$

where the three terms on the right hand side represent the roughness due to grains, ripples, and sediment transport, respectively.

The grain roughness, $k_{b,gr}$ is represented by the grain diameter d . For a flat bed, the grain roughness is the only roughness element, and the skin friction is the total roughness. In most continental shelf situations, however, there are either hydrodynamically or biologically generated roughness elements at least an order of magnitude greater than the grain size, so that this element can be neglected. It should be noted, however, that the sand grain size is the appropriate roughness length for the skin friction component of the total boundary shear stress, on which initiation of motion and bedload calculations depend.

The form drag component of shear stress is generated by the formation of eddies in the wake of the roughness element and the reattachment of the flow between elements. The roughness is dependent on the shape and distribution of the elements. Grant and Madsen (1982) derive an expression for roughness associated with a two-dimensional wave-generated ripple with height equal approximately to its length:

$$k_{b,rip} = 27.7\eta\left(\frac{\eta}{\lambda}\right) \quad (5-28)$$

where η and λ are ripple height and length.

The dimensions of the ripple are best determined from direct observation of the seafloor in the region in question. When this is impossible, or when the roughness is in transition, empirical bedform formulas can be used. The model used in this work, since the cases of interest are wave-dominated, is a model of wave-generated ripples discussed in Grant and Madsen (1982). For boundary shear stress only slightly greater than that needed to initiate motion, Grant and Madsen found that ripples change only slightly with changing shear stress, in what they refer to as 'equilibrium range'. At higher shear stresses, ripples grow smaller rapidly as they are washed out. The shear stress where this process begins is designated by a breakoff Shields parameter:

$$\psi_B = 1.8S_*^{0.6}\psi_c \quad (5-29)$$

where S_* is a non-dimensional grain diameter (Equation 5-10) and ψ_c is the critical Shields parameter for initiation of motion. The empirical relationships for ripple geometry under waves given by Grant and Madsen are:

$$\frac{\eta}{A_b} = 0.22\left(\frac{\psi'}{\psi_c}\right)^{-0.16}$$

$$\psi_c < \psi' < \psi_B$$

$$\frac{\eta}{\lambda} = 0.16\left(\frac{\psi'}{\psi_c}\right)^{-0.04}$$

and

$$\frac{\eta}{A_b} = 0.48S_*^{0.8}\left(\frac{\psi'}{\psi_c}\right)^{-1.5}$$

$$\psi' > \psi_B$$

$$\frac{\eta}{\lambda} = 0.28S_*^{0.6}\left(\frac{\psi'}{\psi_c}\right)^{-1}$$

These values are used in Equation 5-28 to calculate ripple roughness in the model.

The roughness associated with sediment transport is based on arguments advanced by Owen (1964) that the wake structure around sediment grains in the near-bed transport layer cause the flow to feel a roughness proportional to the thickness of the layer. This concept was applied by Smith and McLean (1977) to steady flow in the Columbia River and by Grant and Madsen (1982) to oscillatory flow. Grant and Madsen derive an expression for the layer thickness by balancing the initial kinetic energy of a particle put into motion with the potential energy at its highest elevation. The roughness length they derive, using data from Carstens, et al, 1969) is expressed:

$$k_{b\ s.t.} = 11.1(s + C_m)d\psi_c \left[\left(\frac{\psi'}{\psi_c}\right)^{1/2} - 0.7 \right]^2 \quad (5-30)$$

where $C_m = 0.5$ is the coefficient of added mass of a sphere.

The roughness length z_0 in fully turbulent flows as considered in the model is equal to $k_b/30$. The expression used for the roughness length is

therefore given:

$$z_0 = \left(\eta_{\text{rip}} \frac{\eta_{\text{rip}}}{\lambda_{\text{rip}}} \right) + 5.3(s + C_m) d \psi_c \left[\left(\frac{\psi'}{\psi_c} \right)^{1/2} - 0.7 \right]^2 + \frac{d}{30} \quad (5-31)$$

The three terms on the right hand side represent, respectively, ripple roughness ($z_{0,\text{rip}}$), sediment transport roughness ($z_{0,\text{s.t.}}$), and grain size roughness.

5.3 RUNNING THE GMG MODEL

The interconnections of these disparate elements, and the generation of the results, might be better understood by using a step-by-step examination of how the boundary layer model works. The computational procedure, as discussed in the preceding sections and applied here, is traced in Figure 5-2. Each line in the flow chart is labelled, and those labels are referred to in this discussion.

There are three inputs (Line 1) to the model at each point: (1) current velocity (u_r) at some height within the current boundary layer and above the wave boundary layer, (2) wave climate, consisting of maximum wave bottom velocity (u_b) and wave excursion amplitude (A_b) (or, equivalently, wave height (H) and period (T) and water depth (h)), and (3) sediment size (d), density and texture. (For simplicity, co-directional wave and current and a single grain size bed are assumed in this discussion.) The example presented is a moderate storm wave, with a 26 cm/sec current measured one meter above the bottom, which is composed of coarse silt. The model input parameters are as follows:

u_b : 40 $\frac{\text{cm}}{\text{sec}}$	A_b : 96 cm.
H : 2.6 meter	T : 15 seconds
h : 50 meters	
u_r : 26 $\frac{\text{cm}}{\text{sec}}$	z_r : 1.0 meter
d : 0.006 cm.	ρ_s 2.65 $\frac{\text{gm}}{\text{cm}^3}$

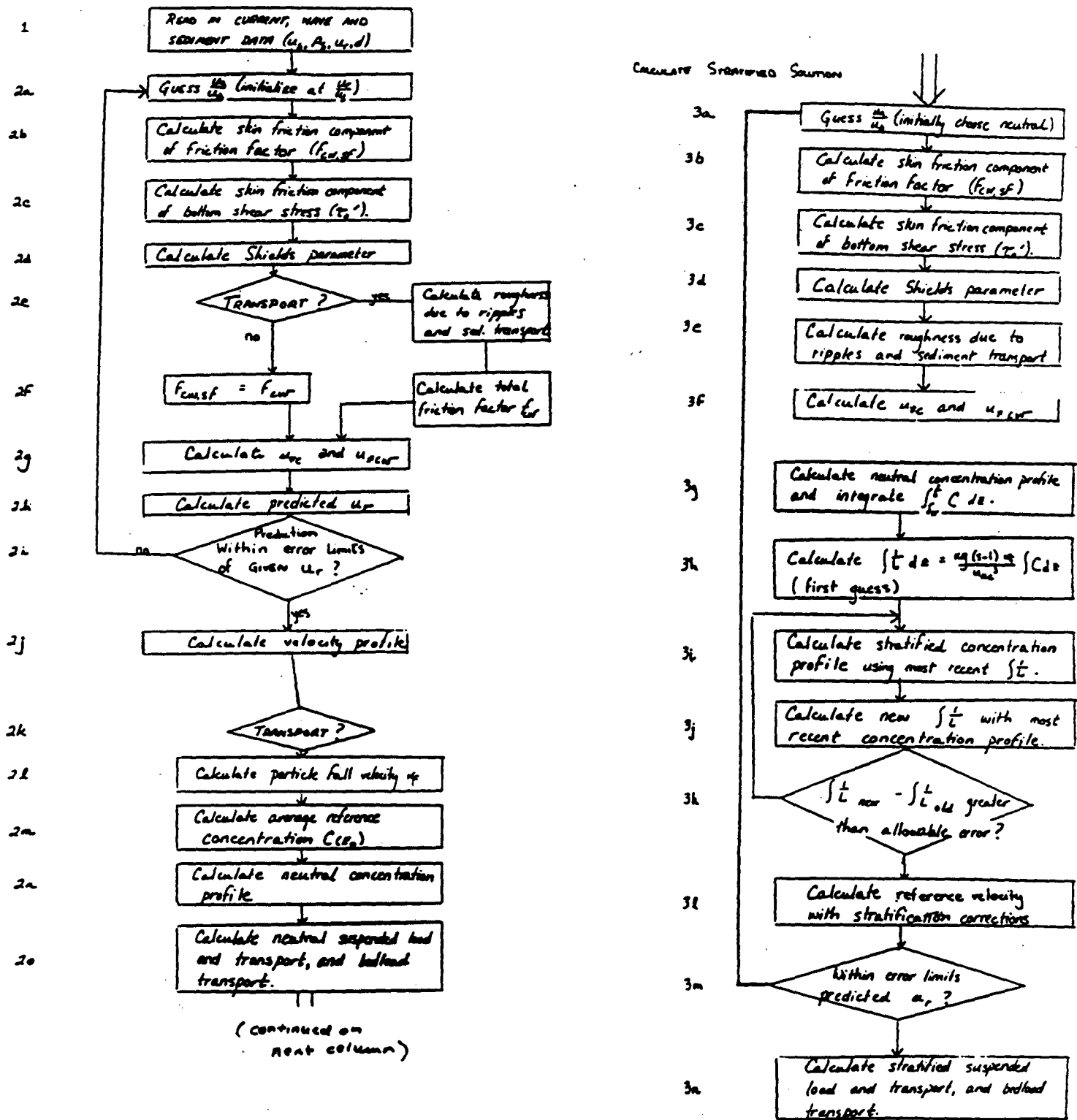


Figure 5-2. Flow chart tracing computational procedure for boundary layer model. Labels are referred to in text

The first step in the model is to make a guess at the current contribution to boundary shear stress on the bottom (Line 2a). This is represented as u_a/u_b , where u_a represents the mean velocity at some unspecified height within the wave boundary layer. The model makes an initial guess that $u_a/u_b = u_r/u_b$.

This shear stress estimate is used with the grain roughness (d) in the equation for the friction factor (found in Section 5.5) to calculate the skin friction component of the friction factor ($f_{cw, sf}$; Line 2b). That friction factor is necessary to test for initiation of sediment motion. It is used to calculate the skin friction component of the maximum bottom shear stress τ_0' and, from that, the Shields parameter for the flow (Equation 5-9). If the Shields parameter is less than the critical value for the sediment on the seafloor, no sediment moves (Lines 2c - 2e). In that case, the skin friction shear stress is the same as the total shear stress. If sediment is moving, however, and no bed roughness was specified as input, the boundary roughness due to ripples and sediment transport is calculated according to Equation 5-31, and that roughness is used in the friction factor equation to calculate the total friction factor f_{cw} (Line 2f). The total f_{cw} is used to calculate the mean and maximum shear velocities (see Section 5.5). From these, the first guess at the predicted reference velocity is calculated using Equations 5-6 and 5-7 (Line 2h). If the predicted velocity is not acceptably close to the given reference velocity (as it will certainly not be on the initial try), the model chooses another value of u_a/u_b , and proceeds again through the steps just described. If the predicted value was too low, the value of u_a/u_b is multiplied by a factor of 2.05; if too high, the parameter is halved. Iterations continue until the predicted and given currents match. At that point, the neutral velocity profile is calculated using Equations 5-6 and 5-7 (Line 2j).

If sediment was put in motion, the sediment concentration profile is calculated, first without including stratification corrections to either velocity or concentration profiles. The particle fall velocity is determined and the sediment reference concentration is determined from Equation 5-18. These are used in Equations 5-16 and 5-17 (neglecting the exponential term in the latter) to calculate the sediment concentration profile (Line 2n).

Finally, the velocity and concentration profiles are integrated to determine the neutral load and transport predictions. The estimated bedload is calculated using Equation 5-26.

The neutral results for the wave case described above are shown in Table 5-1. Note that the value of u_a drops by a factor of three from the first guess. Most of the roughness is generated by ripples (compare $z_{0,rip}$ vs. $z_{0,s.t.}$), and the additional roughness increases the friction factor significantly (compare $f_{cw,sf}$ vs. f_{cw}). The wave-current shear velocity is more than twice the current shear velocity. The predicted bedload transport is insignificant compared with the suspended transport. The predicted neutral velocity and concentration profiles are shown in Figures 5-3 (a) and (b).

The stratified calculation begins, as does the neutral one, with a guess of u_a/u_b . Initially, the value which produced the neutral case solution is used. This results in a prediction of reference velocity which is higher than the given reference velocity, since stratification increases velocities above the wave boundary layer. The same steps as for the neutral case are followed through calculation of the shear velocities at Line 3f. At this stage, the calculation of the stratification-corrected concentration profile begins.

First, the concentration profile without the stratification correction is calculated, as for the neutral case. That profile is used to determine Monin-Obukov Length (Equation 5-19), which is substituted into Equation 5-23 to get a revised estimate of the concentration profile (lines 3g and 3h). This provides a revised estimate of the integrated Monin-Obukov Length (Lines 3i-3j). If the difference between the old and new integrated M-O Length values is greater than the allowable error, the new value is used to calculate another revised concentration profile. These iterations (Lines 3i-3k) continue until the integrated M-O Length values converge.

Once the concentration profile is determined for this u_a/u_b value, the

Neutral results for sample run			
$\frac{u_a}{u_b}$.203	$f_{cw,sl}$	4.745×10^{-3}
ψ'_m	0.5657	ψ_c	0.1226
z_0	8.837×10^{-2} cm	$z_{0,rip}$	6.226×10^{-2} cm
$z_{0,c}$	1.432 cm	$z_{0,s.t.}$	2.591×10^{-2} cm
f_{cw}	2.907×10^{-2}		
u_{*c}	2.46 cm/sec	u_{*cw}	5.802 cm/sec
δ_{cw}	11.13 cm	$\frac{\ell_a}{\delta}$	16.41 m
susp. load	$.6294 \frac{cm^2}{cm^2}$		
susp. tran	$22.65 cm^3/cm/sec$	bedload	$.0663 cm^3/cm/sec$

Table 5-1. Some results for neutral, near-bottom model run for a moderate storm wave on the continental shelf, as described in text. Load and transport are calculated for near-bottom layer, designated $z < \frac{\ell_a}{\delta}$

Near Bottom Wave and Current Model
 Mod.storm wave,silt
 13-apr-87

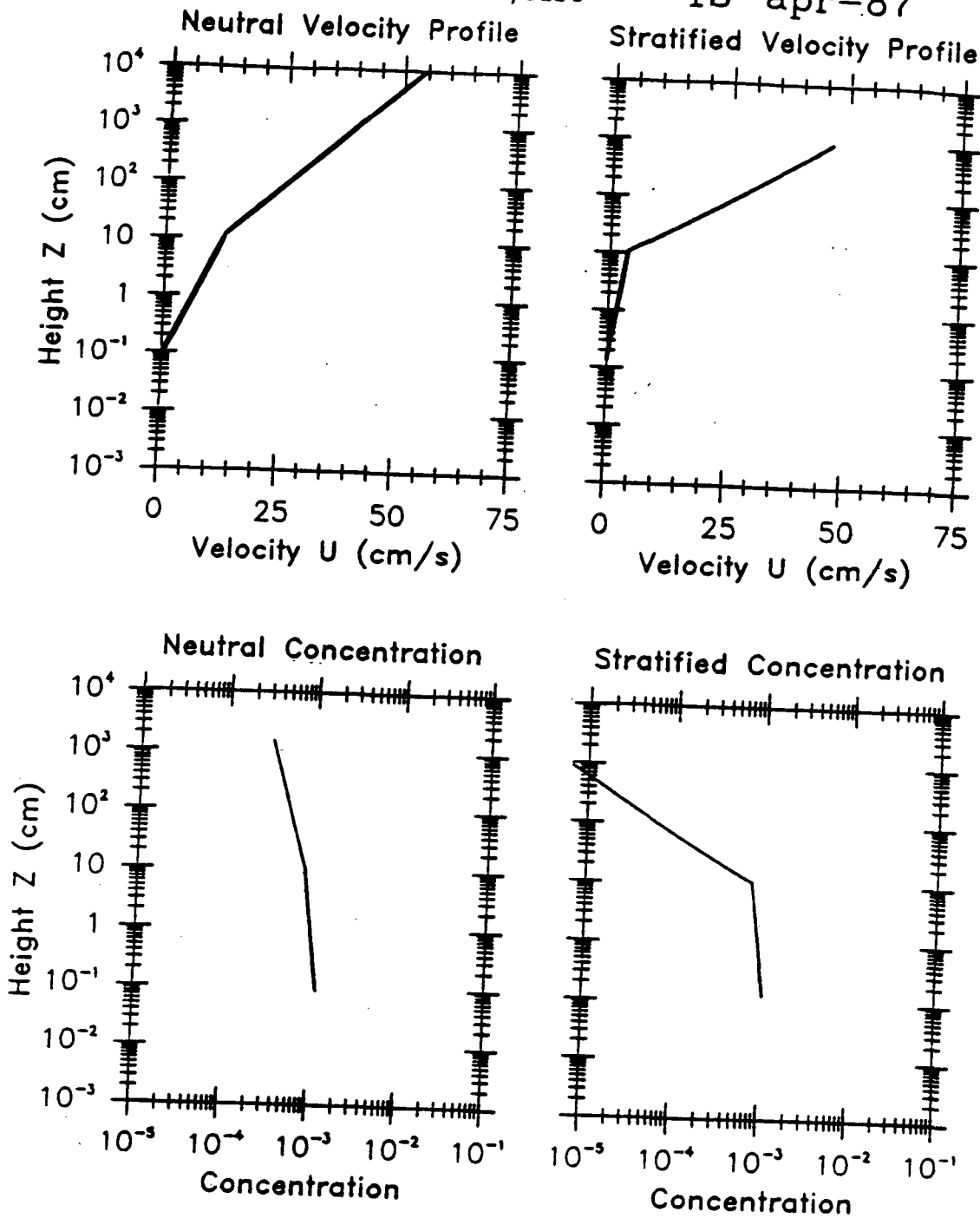


Figure 5-3. Predicted neutral and stratified velocity and concentration profiles to a height $z = \frac{L}{8}$ for a moderate storm wave with a reference current of 26 cm/sec

new reference velocity prediction including stratification effects can be calculated using Equation 5-22. As in the neutral case, if the predicted and given values are outside acceptable error limits, iterations of Lines 3a-3m begin again with a revised u_a/u_b value. Once the velocity values converge, the final stratified velocity and concentration profiles and the transport and load predictions are calculated.

The stratified results for the wave case described above are shown in Table 5-2 and Figures 5-3 (c) and (d). Compare these with the neutral case results shown in Table 5-1 and Figure 5-3 (a) and (b). The sharp drop in concentration and increase in velocity above the wave boundary layer can be seen by comparing the neutral and stratified profiles in Figure 5-3.

The largest changes from the neutral case result from the reduced current shear velocity: u_{*c} is approximately one-half the neutral value. For this reason, $\delta_c/6$ drops to 9.4 m in the stratified case from 16.4 m, and the suspended load and transport drop by an order of magnitude or more.

Parameters which reflect only wave boundary layer conditions change much less: The wave-current shear velocity u_{*cw} and wave boundary layer height δ_{cw} are essentially the same; the roughness prediction rises slightly in the stratified case because the ripples are left intact by the smaller current shear stress; the sediment transport roughness drops somewhat. Bedload transport drops by only 25%, but is still insignificant compared with suspended transport.

5.4 APPLICATION TO A SUSPENDED PARTICULATE FLUX MODEL

While the GMG model solves for steady-state distribution of velocity and suspended sediment, it can be applied to time-dependent problems if the vertical scale of the boundary layer is small enough that the vertical flux divergence terms are much larger than the time-dependence of the currents and suspended sediments within the boundary layer. This condition is satisfied if the GMG model extends over a small fraction of the total boundary layer height,

Stratified results for sample run			
$f_{cw, sf}$	4.861×10^{-3}	$\frac{u_a}{u_b}$.0539
ψ'_m	0.4448	ψ_c	0.1226
z_0	1.317×10^{-1} cm	$z_{0, rip}$	1.135×10^{-1} cm
$z_{0, c}$	3.646 cm	$z_{0, s. t.}$	1.7937×10^{-2} cm
f_{cw}	3.659×10^{-2}		
u_{*c}	1.418 cm/sec	u_{*cw}	5.702 cm/sec
δ_{cw}	10.95 cm	$\frac{L_a}{\delta}$	9.45 m
susp. load	$0.0373 \frac{cm^3}{cm^2}$		
susp. tran	$0.7430 \frac{cm^3}{cm/sec}$	bedload	$.0482 \frac{cm^3}{cm/sec}$
Predicted u_r , with $\frac{u_a}{u_b} = 0.203$:			39.0 cm/sec

Table 5-2. Some results for stratified near-bottom model run for a moderate storm wave, strong current, and a silt bed on the continental shelf. Load and transport are calculated for near-bottom layer, designated $z < \frac{L_a}{\delta}$. Predicted velocity on bottom line is the result for the neutral current shear stress

for instance:

$$z_r \leq 0.1 \frac{u_{*c}}{f}$$

For practical application, z_r can be as little as a few meters, thus minimizing the errors due to neglecting time-dependence in the boundary layer.

The GMG model can provide an estimate of the bottom stress and the near-bed suspended load, based on the input of the directional wave data, sediment size and texture in the bed, and the velocity at the matching level. From the standpoint of a circulation model, it can be thought of as a black box model of the effective bottom drag coefficient. However, in order for the model to be used for prediction of vertical flux of suspended sediment into the domain of the overlying model, a minor modification must be made of the equation for suspended sediment distribution.

The modification is made as follows: Rather than assuming that there is zero vertical flux of sediment, the vertical flux is allowed to vary depending on the concentration at the matching level z_r between the boundary layer model and the outer flow model. At that level, the concentration of suspended sediment is specified, based on conditions in the overlying model, which in turn is subject to the vertical flux condition of the GMG boundary layer model. Considering for simplicity a simple current boundary layer without stratification, the solution for a steady-state sediment distribution is

$$C(z) = C_1 + C_2 \left(\frac{z}{z_0}\right)^{-\frac{\gamma w_f}{\kappa u_{*c}}}$$

where C_1 and C_2 are constants. When the vertical flux is zero, C_1 is zero and the solution is the same as in GMG. For application to a suspended particulate flux model, C_1 is not zero, but rather it is adjusted to satisfy the condition at the top of the boundary layer.

The bottom boundary condition will remain the same, so that $C = C_0$ at $z = z_0$. This gives

$$C(z) = C_1 + (C_0 - C_1) \left(\frac{z}{z_0}\right)^{-\frac{\gamma w_f}{\kappa u_* c}}$$

Satisfying the boundary condition that $C = C_r$ at $z = z_r$, where C_r is specified by the overlying model, gives

$$C_1 = \frac{C_r - C_0 \left(\frac{z_r}{z_0}\right)^{-\frac{\gamma w_f}{\kappa u_* c}}}{1 - \left(\frac{z_r}{z_0}\right)^{-\frac{\gamma w_f}{\kappa u_* c}}}$$

Generalizing the result to the case of a wave-current boundary layer and a current boundary layer, we have to match the solutions at δ_{cw} , obtaining

$$C_1 = \frac{C_r - C_0 \sigma_s \sigma_r}{1 - \sigma_s \sigma_r}$$

where

$$\sigma_s = \left(\frac{\delta_{cw}}{z_0}\right)^{-\frac{\gamma w_f}{\kappa u_* cw}}$$

and

$$\sigma_r = \left(\frac{z_r}{\delta_{cw}}\right)^{-\frac{\gamma w_f}{\kappa u_* c}} \exp - \frac{\beta w_f}{\kappa u_* c} \int_{\delta_{cw}}^{z_r} \frac{1}{L} dz$$

This solution will have to be iterated several times, since the stratification correction will change, depending on the value of C_1 . The Monin-Obukov length L will not depend on the total concentration, but only on the z -dependent part, so

$$L = \frac{|u_*|^3}{\kappa g (s - 1) w_f (C(z) - C_1)}$$

The vertical flux of sediment is constant across the boundary layer, and it is simply equal to $-C_1 w_f$. If C_1 is positive, the flux is downward, and if C_1 is negative, the flux is upward.

With this modification of the GMG model, the suspended sediment flux as well as the stress are determined at the top of the boundary layer, based on matching the velocity and the concentration at z_r . Suspended sediment of multiple size classes or a single size class can be considered with equal facility, depending on the needs of the model.

5.4.1 Interfacing With a Wave Prediction Model

The GMG model requires the orbital velocity and frequency of wave motion near the bottom. This may not be the spectral peak, because shorter waves will be attenuated with depth according to the short wave particle excursion relation:

$$u_b = \frac{H}{2} \frac{\omega}{\sinh kh} \quad (5-32)$$

where H = trough-to-crest wave height, k is wave number and h is water depth. It is a straightforward matter to integrate a model-derived wave spectrum to determine the peak near-bottom oscillatory current as a function of sea state.

5.4.2 Problems

The single most difficult problem with the GMG model is the estimation of near-bottom sediment concentration C_0 . This quantity has only been arrived at empirically; there is no theoretical basis for its estimation. The problem is far worse in the case of cohesive sediments than non-cohesive sediments, since the threshold for resuspension is not well known, and resuspension is strongly dependent on biological processes. For particles finer than sandy silt, the properties of suspended sediment become very difficult to quantify.

Another problem area is the question of stratification-induced stabil-

ity. While the concept is well-documented for thermal stratification in atmospheric boundary layers, there is still some uncertainty in application to suspended sediment. The matching zone between the wave-current and current boundary layers appears to be particularly sensitive to stratification effects, and more research is required to ascertain the proper means of representing the stabilizing influence of stratification.

As a final difficulty, it should be noted that the GMG model is not readily compatible with the open ocean oil weathering code. Therefore, elements of the GMG model are unlikely to be incorporated into the oil weathering code at this time.

5.5 APPENDIX: FRICTION FACTOR, SHEAR STRESS AND SHEAR VELOCITY SOLUTIONS

The characteristic boundary shear stresses and shear velocities are calculated from the instantaneous boundary shear stress. The instantaneous boundary shear stress is defined in GMG using a quadratic drag law:

$$\tau_0 = \frac{1}{2} \rho f_{cw} (u^2 + v^2) \left[\frac{u}{(u^2 + v^2)^{1/2}}, \frac{v}{(u^2 + v^2)^{1/2}} \right] \quad (5-33)$$

where u , v are the x , y components of a combined wave and current reference velocity close to the bottom (though we are, for the moment, assuming that the wave and near-bottom current are collinear in the x -direction). f_{cw} is the combined wave and current friction factor. The characteristic shear stress in the wave boundary layer ($\tau_{0cw} = \rho u_{*cw}^2$) is defined as the maximum value of Equation 5-33. For the current boundary layer, $\tau_{0c} (= \rho u_{*c}^2)$ is calculated by time averaging equation 5-33. The solutions for the shear velocities are:

$$u_{*cw} = \left[\frac{1}{2} f_{cw} \alpha \left(\frac{u_a}{u_b} \right) \right]^{1/2} u_b \quad (5-34)$$

$$u_{*c} = \left[\frac{1}{2} f_{cw} V_2 \left(\frac{u_a}{u_b} \right) \right]^{1/2} u_b \quad (5-35)$$

where ϕ is the angle between the wave and current directions, α and V_2 are functions of the maximum and time-averaged velocities, respectively, in the wave-current boundary layer. u_a is a representation of the velocity of the mean flow in the wave boundary layer, so u_a/u_b is a representation of the relative strength of the mean versus the maximum oscillatory flow in the wave boundary layer. The value of f_{cw} is determined using these definitions and the wave velocity profile. The value of f_{cw} is calculated implicitly with the equation:

$$\left[0.097 \left(\frac{k_b}{A_b} \right)^{1/2} \frac{K}{f_{cw}^{3/4}} \right]^2 + 2 \left[0.097 \left(\frac{k_b}{A_b} \right)^{1/2} \frac{K}{f_{cw}^{3/4}} \right] \left[\frac{V_2}{2\alpha^{1/4}} \right] \cos\phi_c = \frac{\alpha^{3/4}}{4} - \frac{V_2^2}{4\alpha^{1/2}} \quad (5-36)$$

where α and V_2 are functions of the maximum and mean velocities in the wave boundary layer, respectively. A_b is the bottom excursion amplitude for the wave, defined:

$$A_b = \frac{u_b}{\omega} \quad (5-37)$$

and K is derived from the equation for the wave velocity, defined below, and is defined:

$$K = \frac{1}{2\zeta_0^{1/2}} \frac{1}{(\ker^2 2\zeta_0^{1/2} + \operatorname{kei}^2 2\zeta_0^{1/2})^{1/2}}$$

The solution for the wave momentum equation inside the wave boundary layer is not explicitly of interest for the present problem, though it is necessary for the calculation of the boundary shear stress. The solution is:

$$u_w = u_b \left[1 + \frac{\ln\xi + 1.154 + i\frac{\pi}{2}}{\ker 2\xi_0^{1/2} + \operatorname{kei} 2\xi_0^{1/2}} e^{i\omega t} \right] \quad (5-38)$$

where $\xi = x/\delta_{cw}$ and $\xi_0 = x_0/\delta_{cw}$. Ker and kei are Bessel Functions: tabulated solutions to a particular form of differential equation. The derivation and background for the wave velocity profile and friction factor equation are covered in some detail in Grant and Madsen, 1979.

6.0 EXECUTIVE SUMMARY

The objective of this study was to characterize the nature of oil/suspended particulate material (SPM) interactions such that predictive mathematical formulations could be derived and (ultimately) incorporated into an open-ocean oil spill trajectory and circulation model. Dispersed oil droplet/suspended particulate material (SPM) interactions provide a potential mechanism for transport of spilled oil to benthic marine environments. Section 1 of this report contains a detailed review of previous field and laboratory studies and our knowledge of the mechanisms involved (including uncertainties on oil droplet dispersion, turbulence requirements, sediment flux, and oil/SPM interaction kinetics).

Oil and SPM interactions occur through two primary mechanisms: 1) oil droplets colliding with suspended particulate material and 2) molecular sorption of dissolved species. Chromatographic profiles presented in Section 1 (Figure 1-1) illustrate the selective partitioning of intermediate and higher molecular weight aliphatic (Fig. 1-1A) and polynuclear aromatic (Fig. 1-1D) hydrocarbons onto suspended particulate material. The chromatograms also demonstrate the concomitant selective lower molecular weight (one ring) aromatic hydrocarbon dissolution (Fig. 1-1G) into the water column.

The parameters and/or conditions that might influence the rate of "reaction" between dispersed oil droplets and SPM are numerous and include: concentrations of dispersed oil and SPM, size distributions of the oil droplets and SPM, composition of the oil and SPM, the extent of previous weathering and dissolution of individual components from the dispersed oil droplets, and the turbulence required for mixing. Data from field and laboratory studies suggest that SPM sorption of truly dissolved components is not important to the overall mass balance of oil from a spill; however, such adsorption may be important for biological considerations.

As initially envisioned, this program was initiated to examine the rate of oil/SPM interactions for the purpose of developing a mathematical model to predict the potential for sedimentation of components of spilled crude oil

and refined petroleum products. The development of a model for this interaction was intended as an "add on" calculation (or sub-routine) to a general circulation model that addresses both vertical and horizontal transport. All circulation models are essentially solutions to momentum transport equations, and sediment transport depends on ocean circulation for modeling purposes.

An appropriate three dimensional mass balance equation for the concentration of a given species i yields the following partial differential.

$$\frac{\partial C_i}{\partial t} + \frac{\partial}{\partial x}(V_x C_i) + \frac{\partial}{\partial y}(V_y C_i) + \frac{\partial}{\partial z}(V_z C_i) -$$

$$\frac{\partial}{\partial x}\left(k_x \frac{\partial C_i}{\partial x}\right) + \frac{\partial}{\partial y}\left(k_y \frac{\partial C_i}{\partial y}\right) + \frac{\partial}{\partial z}\left(k_z \frac{\partial C_i}{\partial z}\right) + R_i = 0 \quad (6-1)$$

This equation allows for calculation of a mass balance that yields the concentration of species i when integrated over time and space. This equation appears in numerous branches of science and engineering when mass balance considerations are encountered. In the equation, the left-hand side, with the exception of $\partial C_i / \partial t$, represents advection through a differential volume element that is fixed in space. The right-hand side, with the exception of R_i , describes horizontal and vertical dispersion. This partial differential equation is the basis for discussing and describing oil and suspended particulate material interactions in the water column. All of the "interaction" information is contained in the reaction term R_i . This reaction term can be either a removal (output) or source (input) term for the species i . Thus, for oil/SPM interactions, it is necessary to describe what species are going to be identified and kept track of. It is not possible to quantify every single species in the system; there are simply too many. Instead, experience seems to indicate that simplifying assumptions can be made.

When these equations are applied with specific boundary conditions (e.g., bottom topography, shoreline, and weather), a specific 3-D circulation

model is obtained. These models are "huge" because the large number of equations and the form of the boundary conditions make it impossible to "simplify" the mathematics. In essence, every differential element of the model affects every other differential element. Integrating an existing circulation model with the inputs of oil at the air-sea interface and sediment from the bottom and shoreline (including rivers) will yield a description of oil and SPM transport and the interaction of these two additional "species". These species will not affect general circulation in any way because their presence does not significantly affect momentum transport. Thus, the fate of oil and SPM depends on circulation (and weather), but circulation does not depend on oil and SPM. The defining equations for oil and SPM are thus decoupled and essentially "ride along" as the momentum equations are solved.

The reaction for oil droplets in the water column describes the rate of collision and sticking of an oil droplet with a suspended particulate (i.e., a loss of a "free" oil droplet) and the settling (or rising) of an oil droplet. The reaction term R_i for oil droplets can then be described by

$$R_{op} = K_{op} C_{op} C_p \quad (6-2)$$

where $K_{op} C_{op} C_p$ is the rate of collision and sticking of an oil droplet and a suspended particulate to produce an oil-particulate agglomerate. The effect of buoyancy of oil droplets or oil-SPM agglomerates appears in the vertical velocity term in equation 6-1.

Details of the complete derivation of the mathematics required to generate the rate equation for oil droplet/SPM interactions are presented in Sections 1.2 and 1.3. From these derivations the collision frequency for dilute suspensions of particle (SPM and oil) interactions can be expressed as

$$R = 1.3 \left(\frac{\epsilon}{\nu}\right)^{1/2} (r_i + r_j)^3 n_i n_j \quad (6-3)$$

when R is the collision frequency, ϵ is the energy dissipation per unit mass (of fluid) per unit time (cm^2/sec^3), ν is the kinematic viscosity (cm^2/sec), r_i is the radius of particles i present at a number density of n_i , and likewise

for particles j . This equation describes only the collision frequency. Nothing is implied about the "sticking" of particles. Essentially, the interactions are modeled on a particle/particle basis where number densities for both species (discrete oil droplets and suspended particulates) are required. That is, the "concentrations" or number densities of the two reactants are related to the rate of interaction (collision and sticking) as described in equation 6-3.

Clearly, the above equation cannot be applied directly to oil droplets and (or) SPM. The obvious problem is that a distribution of particle sizes exists in any real situation, and the above equation is written for a specific size class only. Therefore, in order to apply the equation to the measured kinetics of oil/SPM interactions it is necessary to assume that oil droplets in a narrow size range will behave as a mono-sized population, and that SPM in a narrow size range will likewise behave as a mono-sized population. The rationale for these assumptions and their impact on the mathematics of model development are considered in detail in Section 2. If these assumptions are valid, then the rate equation can be rewritten as

$$R = 1.3 \left(\frac{\epsilon}{\nu}\right)^{1/2} k n_i n_j \quad (6-4)$$

where k now "lumps" the unknown information about the particle sizes.

Experimental application of the oil/SPM kinetic equation can be carried out in any vessel or flow situation where the independent variables can be controlled. The experimental methods found to work satisfactorily in this program utilized well stirred vessels (with no inflow or outflow) with a known power input through a propeller. By introducing oil droplets of a narrow size range and SPM of a narrow size range into the stirred vessel and measuring the free oil droplet counts versus time, it was possible to generate rate constant data for the oil/SPM interaction. Under the experimental conditions chosen to comply with the modeling (mathematical) requirements, the concentration of SPM

remained constant (i.e., its number density did not change). Thus, the rate of change of free oil droplets, C_o , could be defined as

$$\frac{d C_o}{dt} = -k C_o \quad (6-5)$$

where $k = 1.3 (\epsilon/\nu)^{1/2} k_a C_p$. Integration of equation 6-5 yields

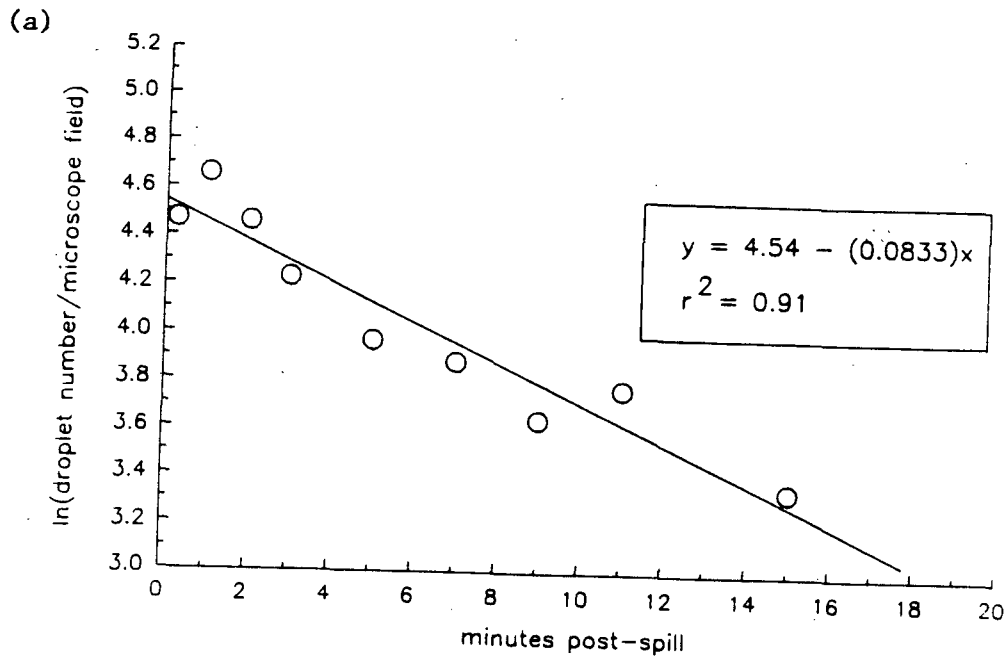
$$\ln \frac{C}{C_o^0} = -kt \quad (6-6)$$

where C_o^0 is the initial oil droplet concentration at time = 0. The experimental data, which are the free oil droplet counts normalized to the initial count, should fall on a straight line on a semi-log plot versus time if the assumptions are correct.

Sections 2.2 through 2.4 contain results and discussions of experimental data on the interaction of fresh and weathered Prudhoe Bay crude oil with representative SPM types. Figure 6-1 is representative of the linear regression analysis of free oil droplet disappearance for the interaction of fresh Prudhoe Bay crude oil and Grewingk Glacier till. These data were derived from photomicroscopic analysis (i.e., counting) of declines in free oil droplet numbers over time (e.g., see Figure 6-2). Concomitantly, the formation of multiple oil/SPM agglomerates and their settling due to density increases could be documented as a function of time (e.g., see oil-SPM agglomerates in the photograph in Figure 6-3). Using photomicroscopy to obtain rate data on the formation of oil/SPM agglomerates is a much more difficult task (compared to monitoring disappearance of free oil droplets) because of depth of field focusing problems with the microscope and the complex distributions of SPM and discrete oil droplets within the oil/SPM flocs or agglomerates.

Much more detailed experimental results with fresh and weathered Prudhoe Bay crude oil and a representative suspended particulate material are presented in sections 2.2 and 2.4. For these more extensive experiments, the

In(OIL DROPLET NUMBER) vs. TIME
 30 July 1987---Experiment A
 fresh Prudhoe Bay crude oil + Grewingk till



In(OIL DROPLET NUMBER) vs. TIME
 29 July 1987---Experiment B
 fresh Prudhoe Bay crude oil ONLY

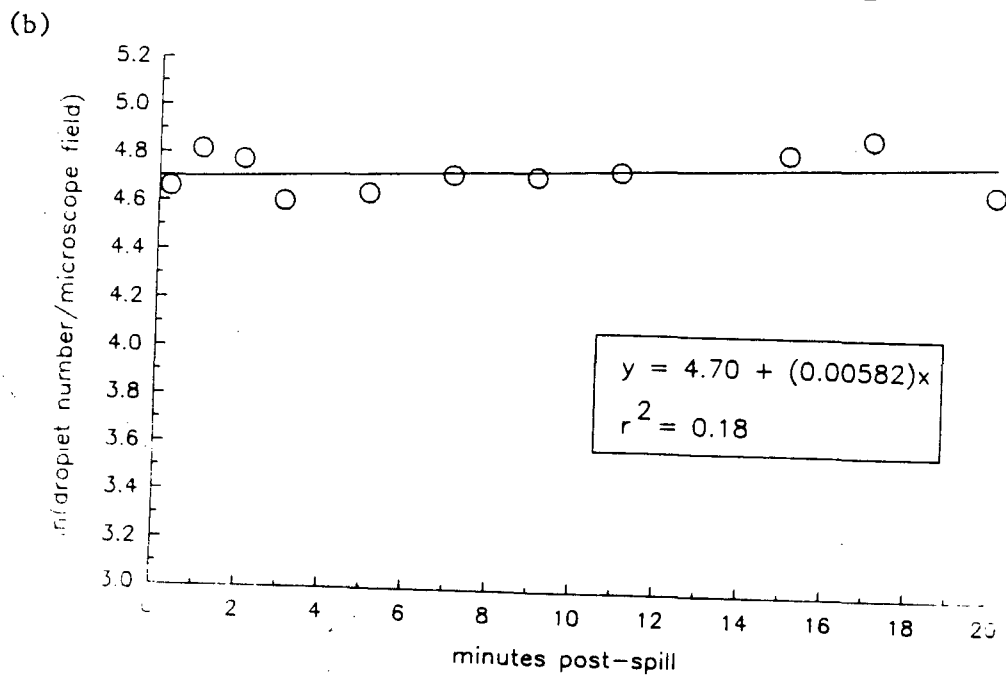


Figure 6-1. Plots of ln(oil droplet number density) vs time for experiments with fresh Prudhoe Bay crude oil and Grewingk Glacier till. The energy dissipation rate constant (ϵ) was approximately 260 ergs/cm³sec in each experiment. (a) oil plus glacial till. (b) oil only.

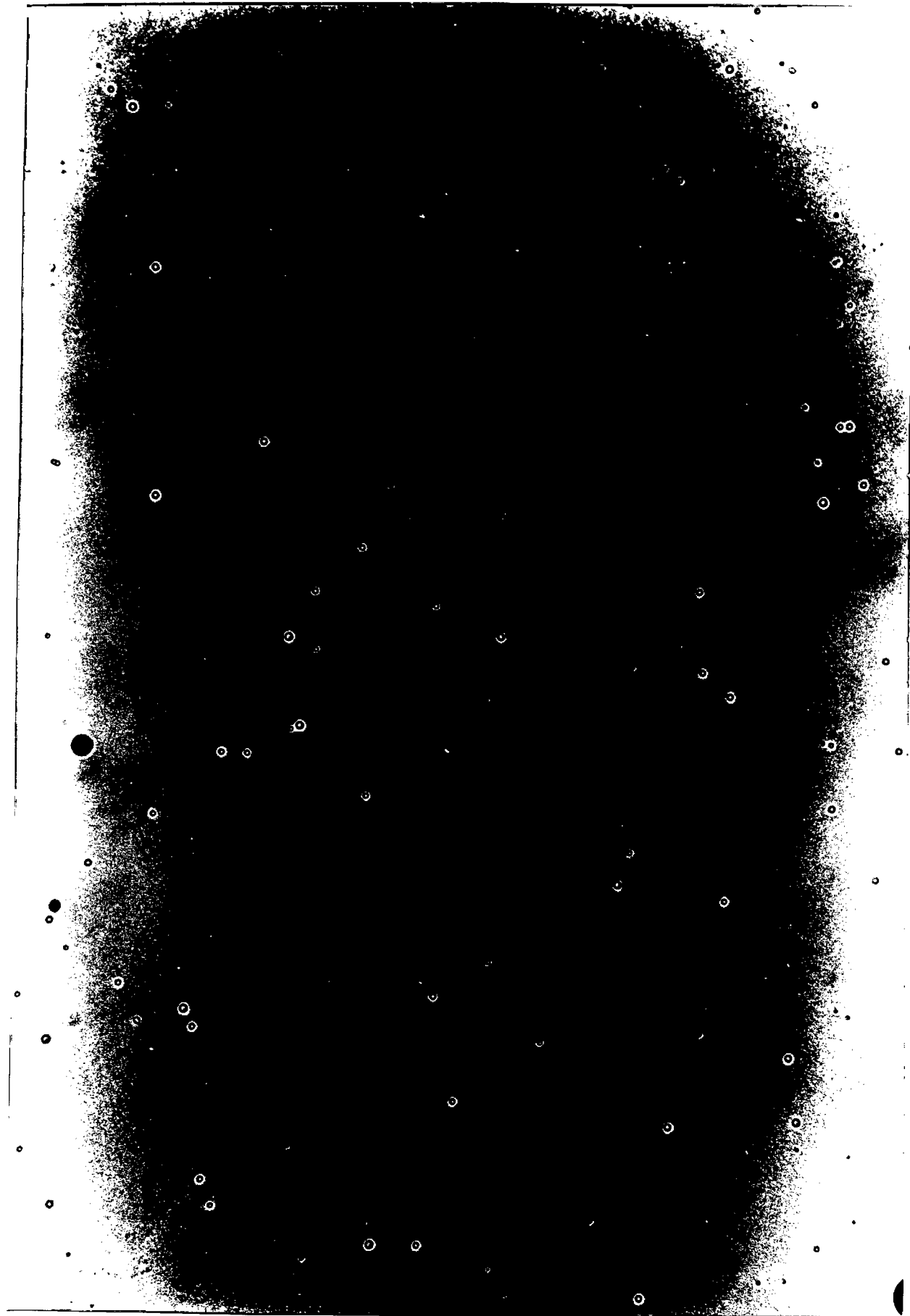


Figure 6-2. Photomicrograph of blended oil droplets on the microscope slide at 2 minutes into a stirred vessel experiment with an energy dissipation rate (ϵ) of approximately 260 ergs/cm³ sec. Size scale for 50 microns = \longleftrightarrow .

A photomicrograph showing numerous dark, irregularly shaped agglomerates of oil droplets and Grewingk Glacial till SPM. The agglomerates vary in size and shape, with some appearing as small, dense clusters and others as larger, more elongated or branched structures. The background is light and contains many smaller, individual particles.

Figure 6-3. Photomicrograph of oil droplet-Grewingk Glacial till SPM agglomerates on the microscope slide at 5 minutes into a stirred vessel experiment. Energy dissipation rate and size scale are as in Fig. 6-2.

suspended particulate material was selected to represent observed grain size distributions (1 to 53 μm) and relatively high total organic carbon (TOC) burdens characteristic of Alaskan Outer Continental Shelf (OCS) waters (Baker, 1983). Because of the difficulty in collecting large (kg) quantities of "natural" SPM in the open ocean, $\leq 53 \mu\text{m}$ sieved-fractions of selected intertidal sediments from lower Cook Inlet were used for most of the studies. The "SPM" so obtained was characterized by X-ray diffraction (for mineralogy), total organic carbon (TOC) loading, grain size distributions and background compound-specific organic composition by flame ionization detector gas chromatography (FID-GC). These SPM characterizations are presented in Tables 1-2A and 1-2B in Section 1.1.

Rates of oil/SPM interactions under carefully controlled conditions of turbulence were obtained for fresh Prudhoe Bay crude oil and SPM derived from Jakolof Bay using two completely independent analytical techniques. Both the rate of disappearance of "free" oil droplets (as measured by light microscopy; see Section 2.2) and the formation of oil-SPM agglomerates (quantified by physical separation, solvent extraction and FID-GC; see Section 2.4) yielded oil/SPM interaction rate constants that agreed reasonably well ($k = 0.67 \times 10^{-7}$ to 1.8×10^{-7} l/mg) with the different experimental approaches. For these experiments the turbulence (as measured by the energy dissipation rate) was approximately $260 \text{ ergs/cm}^3 \text{ sec}$.

Section 3 contains the results of detailed chemical compositional analyses of dispersed oil droplets, dissolved components, oiled SPM and sedimented oil/SPM agglomerates. Quite clearly, selected oil weathering patterns due to evaporation, dissolution and compound specific adsorption are observed. The FID-GC data that are presented can ultimately be used to compare computer-predicted oil weathering behavior from the Open Ocean Oil Weathering Code (Payne, et al., 1984) with observed oil-weathering behavior from the stirred chamber experiments. The chromatograms and reduced data illustrate that the 1-10 μm sized oil droplets used in the experiments undergo very rapid evaporation/dissolution weathering (even during the blending/oil droplet generation process). Substantial losses were observed for all components in boiling point ranges of 107° to 393° F (distillate cuts 1 through 11 as described by

Payne et al., 1984). Those compounds remaining (after droplet generation) also showed selective partitioning behavior, and enrichment or enhancement of both intermediate and higher molecular weight aliphatics and aromatics was observed in the sedimented particle agglomerates as opposed to residual (less than 1 μm) suspended phases remaining in the water column following the cessation of stirring (i.e., turbulence) in the experimental system (i.e., settling column studies). Interestingly, little or no enhancement in settling velocities of the oil-SPM agglomerates was noted using fresh Prudhoe Bay crude oil and Jakolof Bay-SPM under the conditions examined. Additional work is currently under way to further investigate sedimentation rates at varying oil/SPM ratios with different oil and SPM types.

Section 4 contains a discussion of the potential computer requirements (and limitations) for modeling oil/SPM interactions within the context of a full three-dimensional open-ocean circulation model. As discussed, there are several possible approaches including finite element circulation models based on conservation of mass and energy as well as probability distribution functions (PDFs) that might be used to approximate the problem. Finally, Section 5 presents an overview of the late Dr. William Grant's contribution to modeling of the bottom boundary layer and sediment resuspension/transport as controlled by non-linear wave and current interactions.

It is significant that several important program elements (e.g. wave and current induced sediment resuspension and transport, breaking wave induced oil droplet dispersion, and turbulent energy dissipation rate predictions for the open ocean) are all areas of on going Ph.D.-level research at major universities, oceanographic institutions and private laboratories. As a result, there are still many gaps in our knowledge, and at this time it appears to be premature to believe that a fully operational three-dimensional ocean circulation model that incorporates all of the desired interaction terms (e.g., oil droplet dispersion, sediment resuspension for all size classes of sediment, oil/SPM collisions as a function of oil and SPM loadings and turbulence, etc.) is possible in the very near future. In any case, extensive computer capabilities and resources may be required to ultimately develop predictive models that incorporate all of the variables and stochastic processes involved.

Therefore, a more pragmatic approach may be the development of a one-dimensional model that would be more useful in providing information which to a first approximation could be used to assess the potential impact of a hypothetical oil spill in SPM-rich waters. In the conceptualization and development of such a model, one must eventually ask, "What will this model ultimately be used for, and by whom? How can an environmental studies manager use the results of this study and the model to assess and predict environmental damage and response to a near-shore oil spill? In other words, what is the logical end product for this research?"

In the course of answering these questions, it has become apparent that it may not be appropriate (or even possible) to directly couple the oil/SPM interaction model with a fully developed three-dimensional circulation model. Instead, as research and model development progressed, the need for a stand-alone one-dimensional code that could run on a Personal Computer became more apparent. If such a stand alone program were to be developed, what should it contain?

Ideally, the model should be not only very user friendly but also capable of accepting user input that includes at least the following:

- o anticipated sea state
- o oil type and time from initiation of spill
- o weather conditions
- o anticipated suspended particulate loads and types

The model would then request a wind speed to which (to the best of our ability and what is currently attainable through the open literature) near-surface energy dissipation rates might be assigned or correlated. Ideally, it would be nice to estimate the relation between wind-induced sea-surface turbulence (potentially represented by Beaufort Sea Scales for which the user has some intuitive feel) and near surface and mid-depth energy dissipation rates. Then, based on the user specified sea-state, an energy dissipation rate could be selected from available published data (representative values are presented

in section 1.2.1). This energy dissipation rate would then be matched to measured oil/SPM interaction rate constants from the current (i.e., Section 2) and ongoing laboratory studies.

An accounting of the dispersion of discrete oil droplets from a surface oil slick (i.e., by droplet size, number density, interfacial surface tension, specific gravity, etc.) has yet to be successfully accomplished. This is still an area of active research being pursued by other investigators. As an initial starting point, however, a dispersed oil flux into a water column must be assumed (or assigned) to provide material for SPM interactions. This topic is currently being investigated by Delft under contract to MMS.

For the purposes of an oil-SPM interaction model, potentially important user-defined properties of SPM that would be desirable may include:

- o total organic carbon (TOC) content
- o microscopic size fractionation
- o mineralogical composition
- o general surface morphology
- o electron microscopic characterization of the ≤ 53 μm size fraction (Payne et al., 1984).

In designing a mathematical model and experiments to provide data for its verification and implementation, it quickly becomes apparent that there are more variables to consider than can be reasonably accounted for. For example, Section 2 deals just with the mathematics necessary to generate rate constants for the interaction of single sized oil droplets and one size of SPM particles. Obviously, simplifying assumptions are required to model a mixture of varying oil droplet and SPM sizes. There are also inherent experimental difficulties in trying to complete measurements of oil and suspended particulate material interactions. For example, should only one size of oil droplets be examined? How are the oil droplets to be generated, and can that process be related to environmental conditions? Furthermore, can the interaction rate constants be correlated with open ocean conditions (which are also the subject of intense ongoing research) to develop adequate descriptive mathematical models.

In summary, model development to adequately describe and predict oil-SPM interaction phenomena and their relation to contributing environmental variables is a complex undertaking from both conceptual and experimental standpoints. While all of the difficulties entailed in such an effort have not been resolved, it is felt that the results of the present program provide much useful information and a good foundation toward further model development. As a simpler and more realistic point of departure, an experimentally verifiable one-dimensional model (with certain simplifying assumptions) now appears to be achievable. Further laboratory and modeling efforts are being directed at its development and implementation in a PC-based form which will have more immediate utility for environmental studies management needs.

7.0 BIBLIOGRAPHY

- Adams, C. E., and G. L. Weatherly. 1981. Some Effects of Suspended Sediment Stratification on an Oceanic Bottom Boundary Layer. *J. Geophys. Res.* 86:4161-4172.
- Aravamudan, K. S., K. Raj, and G. Marsh. 1981. Simplified Models to Predict the Breakup of Oil on Rough Seas, 1981 Oil Spill Conference.
- Atlas, R. M., M. I. Venkatesan, I. R. Kaplan, R. A. Feely, R. P. Griffiths, R. Y. Morita. 1983. Distribution of Hydrocarbons and Microbial Populations Related to Sedimentation Processes in Lower Cook Inlet and Norton Sound, Alaska. *Arctic* 36:251-261.
- Baker, E.T., 1983. Suspended particulate matter distribution, transport, and physical characteristics in the North Aleutian Shelf and St. George Basin lease areas. Final Report submitted to National Oceanic and Atmospheric Administration, NOAA Project No. R7120897. 134p.
- Baldwin, R. R., and S. G. Daniel. 1953. The Solubility of Gases in Lubricating Oils and Fuels. *J. Petroleum Inst.*, 39(351):105-124.
- Bassin, J. J., T. Ichiye. 1977. Flocculation Behavior of Suspended Sediments and Oil Emulsions, *J. Sed. Petrol.* 47:671-677.
- Birkner, F. B., and J. J. Morgan. 1968. Polymer Flocculation Kinetics of Dilute Colloidal Suspensions, *Am. Waterworks Assoc. Journal*, 60:175.
- Boehm, P. D. in press. Transport and transformation processes regarding hydrocarbon and metal pollutants in OCS sedimentary environments. Background paper prepared to Interagency Committee on Ocean Pollution Research Development and Monitoring; Predictive Assessment for Studies of Long-Term Impacts of OCS Activities, Louisiana Universities Marine Consortium, Chauvin LA.
- Boehm, P. D. and D. L. Fiest. 1980. Aspects of the Transport of Petroleum Hydrocarbons to the Offshore Benthos During the IXTOC-1 Blowout in the Bay of Campeche. Pages 207-236 In Proceedings of a Symposium, Preliminary Results from the September 1979 Researcher/Pierce IXTOC-1 Cruise (June 9-10, 1980 Key Biscayne, FL). Office of Marine Pollution Assessment, National Oceanic and Atmospheric Administration.
- Boehm, P. D., D. L. Fiest, and A. Elskus. 1981. Comparative Weathering Patterns of Hydrocarbons from the Amoco Cadiz Oil Spill Observed at a Variety Of Coastal Environments. Pages 159-173 In Proceedings of the Interatinal Symposium, Amoco Cadiz Fates and Effects of the Oil Spill. Centre Oceanogique de Bretagne, Brest (France).
- Boehm, P. D., D. L. Fiest, D. Mackay, and S. Patterson. 1982. Physical-chemical Weathering of Petroleum Hydrocarbons from the IXTOC I Blowout: Chemical Measurements and Weathering Model. *Environmental Science and Technology*, 16:498-505.

- Bouwmeester, Reinier J. B. and Roger B. Wallace. 1985. The break-up of an oil film due to wind-wave action. In: Proceedings of the Eighth Annual Arctic Marine Oilspill Program, Dept. of Civil Engineering, Michigan State University. pp. 14-25.
- Bouwmeester, Reinier J. B. and Roger B. Wallace. 1986. Oil entrainment by breaking waves. In: Proceedings of the Ninth Arctic Marine Oilspill Program Technical Seminar, Dept. of Civil Engineering, Michigan State University. pp. 39-49.
- Bretscher, M. S., 1985. The Molecules of the Cell Membrane. Scientific American, 253(4):100.
- Businger, J. A., and S. P. S. Arya. 1974. Height of the mixed layer in the stably stratified planetary boundary layer. Adv. Geophys., 18A, 73-92.
- Cacchione, D. A., and D. E. Drake. 1979. Sediment Transport in Norton Sound Physical Chemistry of the Emulsifying Agent. Pages 426-438 In Proc. International Congress Surface Activity.
- Carstens, M. R., R. M. Nielson, and H. D. Altinbilek. 1969. Bed forms generated in the laboratory under oscillatory flow: analytical and experimental study. Tech. Memo. 28, U.S. Army Corps. Engr., Coastal Eng. Rsch. Ctr.
- Clayton, W. 1983. The Theory of Emulsions and Emulsification, Blaksitions, Sons and Co.
- Davies, J. T. 1957. A Quantitative Kinetic Theory of Emulsion Type 1, Physical Chemistry of the Emulsifying Agent. Pages 426-438 In Proc. International Congress Surface Activity.
- deLappe, B. W., R. W. Riseborough, J. C. Shropshire, W. R. Sisteck, E. F. Letterman, D. R. deLappa, and J. R. Payne. 1979. The Partitioning of Petroleum Related Compounds Between the Mussel Mytilus californianus and Seawater in the Southern California Bight. Draft Final Report II-15.0, Interdial Study of the Southern California Bight, submitted to Bureau of Land Management, Washington, D.C.
- DeLvigne, G. A. L., J. A. Roelivink, and C. E. Sweeney. 1986. Research on Vertical Turbulent Dispersion of Oil Droplets and Oil Particles: Literature Review. OCS Study MMS 86-0029, 138 pp.
- Drake, D. E. 1976. Suspended Sediment Transport and Mud Deposition on Continental Shelves. Pages 127-158 In D.J. Stanley and D.J. Swift (eds.) Marine Sediment Transport and Environmental Management. Wiley-Interscience, New York, N.Y.
- Eganhouse, R. P. and J. A. Calder. 1976. The solubility of medium molecular weight aromatic hydrocarbons and the effects of hydrocarbon co-solutes and salinity. Geochim. Cosmochim. Acta, 40:555-561.

- Feely, R. A., J. D. Cline, G. L. Massoth. 1978. Transport Mechanisms and Hydrocarbon Adsorption Properties of Suspended Matter in Lower Cook Inlet. In: Environmental Assessment of the Alaskan Continental Shelf. Annual Report to Outer Continental Shelf Environmental Assessment Program, Environmental Research Laboratories, National Oceanographic and Atmospheric Administration, Boulder, CO 8:11-72.
- Feely, R. A., G. S. Massoth, A. J. Paulson, M. F. Lamb, and E. A. Martin. 1981. Distribution and elemental composition of suspended matter in Alaskan Coastal Waters. NOAA Technical Memorandum ERL PMEL-27. 119 pp.
- Forrester, W. D. 1971. Distribution of suspended oil particles following the grounding of the tanker Arrow. J. Mar. Res. 29:151-170.
- Gad, J. 1978. Arch. Anat. Physiol. p. 181.
- Gearing, J. N. and P. J. Gearing. 1983. Effects of suspended load and solubility on sedimentation of petroleum hydrocarbons in controlled estuarine ecosystems. Can. J. Fish. Aquatic Sci. (submitted).
- Gearing, J. N., P. J. Gearing, T. Wade, J. G. Quinn, H. B. McCarty, J. Farrington, and R. F. Lee. 1979. The rates of transport and fates of petroleum hydrocarbons in a controlled marine ecosystem and a note on analytical variability. Pages 555-565 In Proceedings of the 1979 Oil Spills Conference. American Petroleum Institute. Washington, D.C.
- Grant, H. L., H. L. Moilliet, and W. M. Vogel. 1968. Some Observations of the Occurrence of Turbulence In and Above the Thermocline. J. Fluid Mech., 34(3):443-448.
- Grant, W. D., O. S. Madsen. 1979. Combined Wave and Current Interaction with a Rough Bottom. J. Geophys. Res 84(C4):1797-1808.
- Grant, W. D., O. S. Madsen. 1982. Moveable Bed Roughness in Unsteady Oscillatory Flow. J. Geophys. Res 87(C1):469-81.
- Grant, W. D., S. M. Glenn. 1983a. A continental shelf bottom boundary layer model. Volume 1: Theoretical model development, Technical Report to the American Gas Association. 167 pp.
- Grant, W. D., S. M. Glenn. 1983b. A continental shelf bottom boundary layer model. Vol. II: Model/data comparison. Technical report to the American Gas Association, 63 pp.
- Grant, W. D., S. M. Glenn. 1983c. A continental shelf bottom boundary layer model. Vol. III: Users manual. Technical report to the American Gas Association, 189 pp.
- Grant, W. D., L. Boyer, and L. P. Sanford. 1982. The effects of bioturbation on the initiation of motion of intertidal sands. J. Mar. Res. 40:659-677.
- Grant, W. D., O. S. Madsen. 1986. The continental shelf bottom boundary layer. AMM. Rev. Fluid Mechanics, 18, 265-306.

- Grant, W. D., H. L. Moilliet, and W. M. Vogel. 1968. Some observations of the occurrence of turbulence in and above the thermocline. *J. Fluid Mech.* 34:443-448.
- Gleen, D. R. et al. 1982. Fate of chemically dispersed oil in the sea. A report on two field experiments. Report EPS4-EC-82-5, Environmental Impact Control Directorate, Canada.
- Griffiths, R. P. and R. Y. Morita. 1980. Study of microbial activity and crude oil-microbial interactions in the waters and sediments of Cook Inlet and the Beaufort Sea. Final Report to the NOAA OCSEAP office, Juneau, Alaska.
- Groves, M. J. 1978. Spontaneous emulsification. *Chemistry and Industry* 12:417.
- Gundlach, E. R., K. J. Finklerstein, and J. L. Sadd. 1981. Impact and persistence of IXTOC-1 oil on the South Texas Coast, Pages 477-485, In: Proceedings of the 1981 Oil Spills Conference. American Petroleum Institute, Washington, D.C.
- Gunther, H., W. Rosenthal, T. J. Weare, B. A. Worthington, K. Hasselmann, J. A. Ewing. 1979. A Hybrid Parametrical Wave Prediction Model. *J. Geophys. Res.* 84(C9):5727-38.
- Gurwitsch. 1913. *Wissenschaftliche Grundlagen der Erdolbearbeitung.* Translation by Moore, London. Chapman and Hall, Ltd.
- Hann, R. W., Jr. 1977. Fate of oil from the supertanker Metula. Pages 476-473, In: Proceedings of the 1977 Oil Spills Conference. American Petroleum Institute, Washington, D.C.
- Hayes, M. O., E. R. Gundlach, and L. D'Ozouville. 1979. Role of dynamic coastal processes in the impact and dispersal of the Amoco Cadiz oil spill. (March, 1978) Brittang, France. Pages 193-198, In: Proceedings of the 1979 Oil Spills Conference. American Petroleum Institute, Washington, D.C.
- Huang, C. P. 1976. Solid-solution Interface: Its Role in Regulating the Chemical Composition of Natural Waters. In: *Transport Processes in Lakes and Oceans.*
- Huang, C. P. and H. A. Elliott. 1977. The stability of emulsified crude oils as affected by suspended particles. In: *Fate and Effects of Petroleum Hydrocarbons in Marine Ecosystems and Organisms.* (Wolfe, D.A., ed.) Pergamon Press, Oxford. pp. 413-420.
- Hunt, J. R. 1982. Self-similar Particle-size Distributions During Coagulation. Theory and experimental verification. *J. Fluid Mech.*, 122:169.
- Hunt, J. R. 1981a. Particle dynamics in Seawater: implication for predicting the fate of discharged particles. *Environ. Sci. Technol.* 16:303-09.

- Hyland, J. L. and E. D. Schneider. 1976. Petroleum hydrocarbons and their effects on marine organisms, populations, communities, and ecosystems. In: Proceedings of the Symposium on Sources, Effects and Sinks of Hydrocarbons in the Aquatic Environment. The American Institute of Biological Sciences. American University, Washington, D.C. pp. 464-506.
- Inman, D. L. and C. E. Nordstrom. 1977. On the tectonic and morphologic classification of coasts. *J. Geol.* 79:1-21.
- Johansson, S., U. Larsson, and P. D. Boehm. 1980. The Tsesis oil spill impact on the pelagic ecosystem. *Mar. Pollution Bull.* 11:284-293.
- Johnson, F. G. 1977. Sublethal biological effects of petroleum hydrocarbon exposures: bacteria, algae, and invertebrates. In: Effects of Petroleum on Arctic and Subarctic Marine Environments and Organisms. Volume II. Biological Effects. (Malins, D.C., ed.) Academic Press, New York. pp. 271-318.
- Jordan, R. E. and J. R. Payne. 1980. Fate and Weathering of Petroleum Spills in the Marine Environment. A Literature Review and Synopsis. Ann Arbor Science Publishers, Inc. Ann Arbor, Michigan. 174 p.
- Kaminski and McBain. 1949. *Proc. Royal. Soc. A* 198:447.
- Karickhoff, S. W. 1981. Semi-empirical estimation of sorption of hydrophobic pollutants on natural sediments and soils. *Chemosphere* 10:833-846.
- Karickhoff, S. W., D. S. Brown, and T. A. Scott. 1979. Sorption of hydrophobic pollutants on natural sediments. *Water Research* 13:241-248.
- Karrick, N. L. 1977. Alterations in Petroleum Resulting from Physicochemical and Microbiological Factors. In: Effects of Petroleum on Arctic and Subarctic Marine Environments and Organisms. Volume I. Nature and Fate of Petroleum. (Malins, D.C., ed.) Academic Press, New York. pp. 225-299.
- Kolpack, R. L. 1971. Biological and oceanographic survey of the Santa Barbara Channel oil spill, 1969-1970, Vol. II, Physical, Chemical, and Geological Studies, Allen Hancock Foundation, University of Southern California, Los Angeles, California.
- Leibovich, S. 1975. A Natural Limit to the Containment and Removal of Oil Spills at Sea, *Ocean Engineering*, Vol. 3.
- Leibovich, S. and J. L. Lundey. 1981. A Theoretical Appraisal of the Joint Effects of Turbulence and of Langmuir Circulations on the Dispersion of Oil Spilled in the Sea, U.S. Dept. of Transportation, Washington, D.C.
- Lin, J. T., M. Gad-el-Hak, and H. T. Liu. 1978. A Study to Conduct Experiments Concerning Turbulent Dispersion of Oil Slicks. U.S. Coast Guard Rpt. CG-D-54-78.

- Lin, Jung-Tai et al. 1978. A Study to Conduct Experiments Concerning Turbulent Dispersion of Oil Slicks. U.S. Dept. of Transportation, Washington, D.C.
- Liu, S. K. 1985. Range of Turbulent Energy Dissipation Rates in Arctic Seas, Personal Communication.
- Liu, S. K. and J. J. Leendertse. 1982. Modeling of tides and circulation in the Bering/Chukchi Sea, Part 1. Preliminary analysis of simulation results. Draft report for National Oceanic and Atmospheric Administration, Juneau, Alaska.
- Liu, S. K. 1983. Letter (RAND) to T. Laevastu.
- Longuet-Higgins, M. S. 1969. On Wave Breaking and the Equilibrium Spectrum of Wind-Generated Waves. Proc. Roy. Soc. London, A310, 151-159
- Mackay, D., A. Bobra, and D. W. Chan. 1982. Vapor pressure correlations for low-volatility environmental chemicals. Environ. Sci. Technol. 16:645-649.
- Mackay, D., and K. Hossain. 1983. An Exploratory Study of Naturally and Chemically Dispersed Oil, Department of Chemical Engineering and Applied Chemistry, University of Toronto (internal paper).
- Madsen, O. S., and W. D. Grant. 1976. Quantitative description of sediment transport by waves. Proc. Coastal Engr. Conf., 15th, 2, 1093-1112. J. Phys. Oceanogr., 7:248-255.
- Malinky, G. and D. G. Shaw. 1979. Modeling the association of petroleum hydrocarbons and sub-arctic sediments. Pages 621-624, In: Proceedings of the 1979 Oil Spills Conference, American Petroleum Institute, Washington, D.C.
- Manley, R. St. J., and S. G. Mason. 1952. Particle Motions in Sheared Suspensions. II. Collisions of Uniform Spheres. J. of Colloid Science, 7:354
- McAuliffe, C. D. 1966. Solubility in water of paraffin, cycloparaffin, olefin, acetylene, cycloolefin, and aromatic hydrocarbons. J. Phys. Chem., 70:1267-1275.
- McAuliffe, C. D. et al. 1975. Chevron Main Pass Block 41 Oil Spill: Chemical and biological investigations. Proceedings of the Joint Conference on Prevention and Control of Oil Spills, San Francisco, 1975.
- McManus, D. A., V. Kolla, D. M. Hopkins, and C. H. Nelson. 1977. Distribution of bottom sediments on the continental shelf, North Bering Sea. U.S. Geological Survey Professional Paper 759-C.
- Means, J. C., S. G. Wood, J. J. Hassett, and W. C. Banwart. 1980. Sorption of polynuclear aromatic hydrocarbons by sediments and soils. Environ. Sci. Technol. 14:1524.

- Mercier, R. S. 1985. The Reactive Transport of Suspended Particles: Mechanisms and Modeling. Doctoral Dissertation, Joint Program in Oceanography and Ocean Engineering, Massachusetts Institute of Technology and Woods Hole Oceanographic Institution WHOI-85-23.
- Meyer-Peter, E. and R. Muller. 1948. Formulas for Bed-Load Transport. Proc. Intl. Assn. Hydraulic Struc. Tsch., 2nd, 39-64.
- Meyers, P. A. and J. G. Quinn. 1973. Association of hydrocarbons and mineral particles in saline solutions. Nature 244:23-24.
- Milgram, J. H. et al. 1978. Effects of Oil Slick Properties on the Dispersion of Floating Oil into the Sea. U.S. Dept. of Transportation, Washington, D.C.
- Muench, R. D. and K. Ahlnas. 1976. Ice movement and distribution in the Bering Sea from March to June 1974. J. Geophys. Res. 81:4467-4476.
- Muench, R. D., R. B. Tripp, and J. D. Cline. 1981. Circulation and hydrography of Norton Sound. Pages 77-97, In: D. W. Hood and J. A. Calder (eds.), The Eastern Bering Sea Shelf: Oceanography and Resources, Vol 1, U.S. Dept. of Commerce, Washington, D.C.
- Munk, W. H. 1947. A Critical Wind Speed for Air-Sea Boundary Processes, J. Marine Resources, VI(1-3).
- Nelson, C. H. and J. S. Creager. 1977. Displacement of Yukon-derived sediment from Bering Sea to Chukchi Sea during Holocene time. Geol. 5:141-146.
- NRC (National Research Council). 1985. Oil in the Sea, Inputs, Fates, and Effects. National Academy Press, Washington, D.C.
- O'Melia, C. 1980. Aquasols: The behavior of small particles in aquatic systems. Environ. Sci. Technol., 14:1052.
- Overbeek, J. Th. G. 1952. Stability of Hydrophobic Colloids and Emulsions. In: Colloid Science, Vol. 1; (H.R. Kruyt, ed.). Elsevier Publishing Co., New York.
- Owen, M. W. 1977. Problems in modeling the transport, erosion, and deposition of cohesive sediments. Pages 515-537, In: E. D. Goldberg, I. N. McCave, J. J. O'Brien, and T. H. Steele (eds.), The Sea, Vol. 6, Interscience, New York, NY.
- Owen, P. R. 1964. Saltation of uniform grains in air. J. Fluid Mech., 20:225-242.
- Parker, P. L. and S. Macko. 1978. An intensive study of the heavy hydrocarbons in the suspended particulate matter in seawater. Chapter 11, In: The South Texas Outer Continental BLM Study. Bureau of Land Management, Washington, D.C.

- Patten, B. G. 1977. Sublethal biological effects of petroleum hydrocarbon exposures: fish. In: Effects of Petroleum on Arctic and Subarctic Marine Environments and Organisms. Volume II. Biological Effects. (Malins, D.C., ed.) Academic Press, New York. pp. 319-335.
- Pavlou, S. P. and R. N. Dexter. 1979. Distribution of polychlorinated biphenyls (PCB) in estuarine ecosystems. Testing the concept of equilibrium partitioning in the marine environment. Environ. Sci. Technol. 13:65.
- Payne, J. R., B. D. Kirstein, D. McNabb Jr., J. L. Lambach, R. I. Redding, R. E. Jordan, W. Hom, C. deOliveira, G. S. Smith, D. M. Baxter, and R. Gaegel, 1984. Multivariate Analysis of Petroleum Weathering in the Marine Environment--Subarctic. In: Environmental Assessment of the Alaskan Continental Shelf--Final Reports of principal investigators. Vol 21 and 22. U.S. Department of Commerce, National Oceanic and Atmospheric Administration, Juneau, AK.
- Payne, J. R., B. E. Kirstein, R. F. Shokes, N. L. Guinasso, L. Carver, K. R. Fite, R. E. Jordan, P. J. Mankiewicz, G. S. Smith, W. J. Paplawsky, T. G. Fanara, and J. Lambach. 1980. Multivariate analysis of petroleum weathering under marine conditions. Interim Quarterly Report Submitted to National Oceanic and Atmospheric Administration, Juneau, Alaska.
- Payne, J. R., B. E. Kirstein, R. F. Shokes, N. L. Guinasso, L. Carver, K. R. Fite, R. E. Jordan, P. J. Mankiewicz, G. S. Smith, W. J. Paplawsky, T. G. Fanara, and J. Lambach. 1981. Multivariate analysis of petroleum weathering in the marine environment-subarctic. Annual Report submittal to National Oceanic and Atmospheric Administration, Juneau, Alaska.
- Payne, J. R., B. E. Kirstein, G. D. McNabb, Jr., J. L. Lambach, R. T. Redding, R. E. Jordan, W. Hom, C. deOliveira, G. S. Smith, D. M. Baxter, and R. Gaegel. 1984. Multivariate analysis of petroleum weathering in the marine environment-subarctic. Final Report to National Oceanic Atmospheric Administration, Juneau, Alaska.
- Payne, J. R., and D. McNabb Jr. 1984. Weathering of Petroleum in the Marine Environment. Marine Technology Society Journal, 18(3):24-42.
- Payne, J. R. and C. R. Phillips. 1985a. Petroleum Spills in the Marine Environment. The Chemistry and Formation of Water-in-Oil Emulsions and Tar Balls. Lewis Publishers, Inc. Chelsea, Michigan. 148 p.
- Payne, J. R., and C. R. Phillips. 1985b. Photochemistry of Petroleum in Water. Environmental Science and Technology, 19(7):569-579.
- Payne, J. R., C. R. Phillips, and W. Hom. 1987. Transport and transformations: water column processes. Background paper for Interagency Committee on Ocean Pollution Research Development and Monitoring; Predictive Assessment for Studies of Long-Term Impacts of OCS Activities. Louisiana Universities Marine Consortium, Chauvin, Louisiana.

- Poirier, O. A., and G. A. Thiel. 1941. Deposition of Free Oil by Sediments Settling in Sea Water, Bulletin of the American Association of Petroleum Geologists, Vol. 25, No. 12, pp. 2170-2180.
- Pope, S. B. 1979. The Relationship Between the Probability Approach and Particle Models for Reaction in Homogeneous Turbulence. Combustion and Flame, 35:41-45.
- Pope, S. B. 1981. A Monte Carlo Method for the PDF Equations of Turbulent Reactive Flow. Combustion Science and Technology, 25:159-174.
- Pope, S. B. 1982. An improved Turbulent Mixing Model. Combustion Science and Technology, 28:131-145
- Quinn, J. G. In press. Sedimentation of petroleum in the marine environment. Background paper prepared for the National Academy of Science, Petroleum in the Marine Environment. National Academy of Sciences, Washington, D.C.
- Raj, P. K. 1977. Theoretical Study to Determine the Sea State Limit for the Survival of Oil Slicks on the Ocean. U.S. Coast Guard Rpt. CG-61505A.
- Raschevsky. 1928. Z. Phys. 46:585.
- Sadd, J. L., E. R. Gundlach, W. Ernst, and G. I. Scott. 1980. Distribution, size, and oil content of tar mats and the extent of buried oil along the South Texas Shoreline. Pages 14-20, In: Research Planning Institute Report to the National Oceanic and Atmospheric Administration, Office of Marine Pollution Assessment, Boulder, Colorado.
- Saffman, P. G. and J. S. Turner. 1956. On the Collision of Drops in Turbulent Clouds. J. of Fluid Mechanics, 1:16.
- Seuss, E. 1968. Calcium carbonate interactions with organic compounds. Ph.D. Thesis. Lehigh University.
- Sharma, G. D., F. F. Wright, J. J. Burns, and P. C. Burbank. 1974. Sea surface circulation, sediment transport, and marine mammal distribution, Alaska Continental Shelf: ERTS Final Report, Natl. Tech. Serv. Report E74-10711.
- Shaw, D. G. 1977. Hydrocarbons in the Water Column, In: Fates and Effects of Petroleum Hydrocarbons in Marine Ecosystems and Organisms (D.A. Wolfe, ed.).
- Shonting, D. H., P. Temple, and J. Roklan. 1970. The Wind Wave Turbulence Observation Program (WAVTOP), U.S. Coast Guard Rpt. CG-D-68-79.
- Smith, J. D. and S. R. McLean. 1977a. Spatially averaged flow over a wavy surface. J. Geophys. Res. 32:1735-1746.

- Smith, J. D. and S. R. McLean. 1977b. Boundary layer adjustments to bottom topography and suspended sediment. Pages 123-152, In: J. C. J. Nihoul (ed.), Bottom Turbulence. Elsevier Scientific Publishing Co., The Netherlands.
- Sobey, R. J. 1986. Wind-Wave Prediction. Ann. Rev. Fluid Mechanics 18, 169-172.
- Stackelburg, W., Klockner and Mohrhauer. 1949. Kolloidzshr 115:53.
- Steen, W. C., D. F. Paris, and G. L. Baughman. 1978. Partitioning of selected polychlorinated biphenyls to natural sediments. Water Research 12:655.
- Stewart, R. W. and H. L. Grant. 1962. The Determination of the Rate of Dissipation of Turbulent Energy Near the Sea Surface in the Presence of Waves. J. of Geophysical Research, 67(8):3177.
- Straughn, D. 1977. Biological survey of intertidal areas in the straits of Magellan in January, 1975, five months after the Metula oil spill. Pages 247-260, In: D. A. Wolfe (ed.), Fate and Effects of Petroleum Hydrocarbons in Marine Organisms and Ecosystems. Pergamon Press, Inc., Elmsford, NY.
- Sutton, C. and J. A. Calder. 1974. Solubility of higher-molecular-weight n-paraffins in distilled water and seawater. Environ. Sci. Technol., 8:654-647.
- Sutton, C. and J. A. Calder. 1975. Solubility of alkylbenzenes in distilled water and seawater at 25.0°C. J. of Chem. and Eng. Data, 20:320-322.
- Venkatesan, N. I., M. Sandstrom, S. Brenner, E. Ruth, J. Bonilla, I. R. Kaplan, and W. E. Reed. 1981. Organic geochemistry of surficial sediments from the eastern Bering Sea. Pages 389-409, In: D. W. Hood and J. A. Calder (eds.), The Eastern Bering Sea Shelf: Oceanography and Resources. U.S. Department of Commerce, Washington, D.C.
- Wade, T. L. and J. G. Quinn. 1979. Incorporation, distribution, and fate of saturated petroleum hydrocarbons in sediments from a controlled marine ecosystem. Mar. Environ. Res. 3:15.
- Wallace, R. B., T. M. Rushlow and R. J. B. Bouwmeester. 1986. In situ measurement of oil droplets using an image processing system. In: Proceedings of the Ninth Arctic Marine Oilspill Program Technical Seminar, Department of Civil and Environmental Engineering, Michigan State University. pp. 421-431.
- White, S. J. 1970. Plane bed thresholds of fine grained sediments. Nature, 228:152-153.
- Wiberg, P. and J. D. Smith. 1983. A comparison of field data and theoretical models for wave-current interactions at the bed on the continental shelf. Continental Shelf Research 2:147-162.

Winters, J. K. 1978. Fate of petroleum derived aromatic compounds in seawater held in outdoor tanks. Chapter 12, In: South Texas Outer Continental Shelf BLM Study. Bureau of Land Management, Washington, D.C.

Zurcher, F. and M. Thuer. 1978. Rapid weathering processes of fuel oil in natural waters: Analyses and interpretations. Environ. Sci. Technol., 12: 838-843.

APPENDIX A

COMPOUND SPECIFIC HYDROCARBON CONCENTRATIONS
FROM 28 LITER STIRRED CHAMBER EXPERIMENTS

HYDROCARBON CONCENTRATIONS FROM STIRRED CHAMBER EXPERIMENTS—UCH, Total Resolved, and Total n-alkanes

FID-GC Hydrocarbons with Retention Times Greater Than or Equal to n-C10

Fresh Prudhoe Bay Crude Oil and Jakolof Bay Sediments

Time from start (hrs)	Surface Oil—Hydrocarbon Concentrations (ug/g of oil)				Dispersed Phase Hydrocarbon Concentrations (ug/liter sea water)				Hydrocarbon Concentrations (ug/liter sea water)				SPM Phase SPM Load (ug dry wt./l)		Hydrocarbon Concentrations (ug/g dry weight)				Dissolved Phase Hydrocarbon Concs. (ug/liter)			
	UCH+Tot.Res.	UCH	Tot.Res.	Tot.n-alk.	UCH+Tot.Res.	UCH	Tot.Res.	Tot.n-alk.	UCH+Tot.Res.	UCH	Tot.Res.	Tot.n-alk.	UCH+Tot.Res.	UCH	Tot.Res.	Tot.n-alk.	UCH+Tot.Res.	UCH	Tot.Res.	UCH+Tot.Res.	UCH	Tot.Res.
0.00	232211.5	187838.0	44373.5	28976.9	0.0	0.0	0.0	0.0	2.0	0.0	2.0	0.4	52.9	38.2	0.0	38.2	7.1	0.0	0.0	0.0	0.0	0.0
0.25					37.4	0.0	37.4	32.4	0.0	0.0	0.0	0.0	50.1	0.0	0.0	0.0	0.0	25.6	0.0	25.6	0.0	0.0
0.50					607.0	528.8	78.2	65.0	61.5	52.4	9.1	5.2	53.0	1160.7	989.2	171.5	98.2	67.2	0.0	67.2	0.0	0.0
1.00					571.2	500.9	70.3	49.1	NA	NA	NA	NA	47.7	NA	NA	NA	NA	169.4	0.0	169.4	0.0	0.0
2.00					1341.2	1118.0	223.2	157.4	55.7	47.1	8.6	5.1	51.3	1085.3	917.7	167.6	99.5	552.0	144.6	407.4	0.0	0.0
4.00					2763.1	2275.1	488.0	305.5	45.2	38.9	6.3	4.5	50.1	901.4	776.4	125.0	89.7	664.0	0.0	664.0	0.0	0.0
8.00					4429.0	3710.8	718.2	494.6	173.8	145.2	28.6	16.9	53.8	3229.6	2698.7	530.9	314.4	1707.9	334.5	1373.4	0.0	0.0
12.00					8018.7	6748.5	1270.2	813.3	348.8	290.0	58.8	34.2	48.2	7236.0	6016.0	1220.0	710.2	1364.4	273.9	1090.5	0.0	0.0
18.00					1489.4	0.0	1489.4	1140.7	539.5	460.7	78.8	63.6	44.4	12150.7	10377.0	1773.7	1433.2	1365.3	292.0	1073.3	0.0	0.0
24.00					17350.8	14684.3	2666.5	1382.7	929.1	739.4	189.7	126.7	50.4	18435.3	14671.6	3763.7	2513.1	—	299.3	NA	NA	NA
48.00					34598.8	25973.2	8625.6	5347.4	1974.9	1597.9	377.0	217.3	43.8	45089.7	36481.3	8608.4	4961.0	—	518.9	NA	NA	NA
72.00	292309.6	244567.0	47742.6	31615.0	54444.5	43819.2	10625.3	5898.2	4032.9	3328.7	704.2	398.8	35.9	112336.5	92721.5	19615.0	11110.0	1362.9	726.9	636.0	0.0	0.0
96.00					33198.0	25615.9	7582.1	4354.4	1301.4	876.8	424.6	272.5	28.7	45344.9	30550.5	14794.4	9494.8	1217.6	612.5	605.1	0.0	0.0
120.00					38406.5	28089.5	10317.0	5286.2	997.5	559.3	438.2	287.0	25.0	39900.0	22372.0	17528.0	11480.0	1500.7	957.9	542.8	0.0	0.0
168.00	52203.9	28704.3	23499.6	15262.4	15777.4	121453.0	36321.7	21778.1	1475.3	1039.5	435.8	287.4	29.5	50010.2	35237.3	14772.9	9742.4	1705.2	1225.8	479.4	0.0	0.0
216.00	129510.9	105011.0	24499.9	15994.4	51518.9	41491.1	10027.8	6390.4	1288.7	775.4	513.3	338.5	23.0	56030.4	33713.0	22317.4	14717.4	2035.6	1633.8	401.8	0.0	0.0

2 Day Weathered Prudhoe Bay Crude Oil and Jakolof Bay Sediments

Time from start (hrs)	Surface Oil—Hydrocarbon Concentrations (ug/g of oil)				Dispersed Phase Hydrocarbon Concentrations (ug/liter sea water)				Hydrocarbon Concentrations (ug/liter sea water)				SPM Phase SPM Load (ug dry wt./l)		Hydrocarbon Concentrations (ug/g dry weight)				Dissolved Phase Hydrocarbon Concs. (ug/liter)				
	UCH+Tot.Res.	UCH	Tot.Res.	Tot.n-alk.	UCH+Tot.Res.	UCH	Tot.Res.	Tot.n-alk.	UCH+Tot.Res.	UCH	Tot.Res.	Tot.n-alk.	UCH+Tot.Res.	UCH	Tot.Res.	Tot.n-alk.	UCH+Tot.Res.	UCH	Tot.Res.	UCH+Tot.Res.	UCH	Tot.Res.	
0.00	80034.3	54659.6	25374.7	12132.0	3.3	0.0	3.3	0.0	18.9	14.0	4.9	2.5	51.6	366.3	270.5	95.7	49.2	NA	NA	NA	NA	NA	
0.25					NA	NA	NA	NA	42.5	34.8	7.7	4.8	49.3	861.5	705.1	156.4	97.0	NA	NA	NA	NA	NA	
0.50					973.1	815.5	157.6	107.0	17.0	14.4	2.6	2.0	46.4	367.0	310.8	56.3	42.5	40.5	0.0	40.5	0.0	0.0	
1.00					1027.0	842.3	184.7	120.0	41.1	33.5	7.7	5.5	46.8	879.1	715.6	163.5	116.9	126.1	0.0	126.1	0.0	0.0	
2.00					2202.7	1822.9	379.8	213.3	72.4	59.8	12.6	6.6	43.0	1684.0	1391.2	292.8	153.0	NA	NA	NA	NA	NA	
4.00					32580.8	26568.6	6012.2	3559.8	197.1	164.2	32.9	22.7	34.1	5780.1	4815.2	964.8	666.2	123.5	0.0	123.5	0.0	0.0	
8.50					96012.5	75667.0	20345.5	11595.8	262.9	221.1	41.8	33.5	41.0	6412.2	5392.7	1019.5	816.5	449.2	203.4	245.8	0.0	0.0	
12.00					144588.0	119426.0	25162.0	14383.8	403.0	337.4	65.6	49.6	20.2	19950.5	16703.0	3247.5	2454.8	458.4	133.1	325.3	0.0	0.0	
15.25					184452.7	147484.0	36968.7	22587.8	434.2	337.4	96.8	55.5	26.4	16447.0	12780.3	3666.7	2103.8	581.9	325.4	256.5	0.0	0.0	
24.00					105936.7	86856.1	19080.6	10631.1	1464.3	1162.7	301.6	166.7	25.0	58572.0	46508.0	12064.0	6666.1	580.7	271.8	308.9	0.0	0.0	
48.00					86464.7	70336.7	16128.0	9808.5	102.0	82.6	19.4	11.2	3.6	28325.0	22944.4	5380.6	3115.5	640.9	330.6	310.3	0.0	0.0	
73.50	78402.6	58111.7	20290.9	11060.8	62759.8	49718.2	13041.6	6458.5	150.5	113.5	37.0	13.8	3.8	39597.4	29868.4	9728.9	3639.1	628.3	335.9	292.4	0.0	0.0	
														Bot. Sed. (71.5 hr)	247373.8	202545.0	44828.8	24930.1					

12 Day Weathered Prudhoe Bay Crude Oil and Jakolof Bay Sediments

Time from start (hrs)	Surface Oil—Hydrocarbon Concentrations (ug/g of oil)				Dispersed Phase Hydrocarbon Concentrations (ug/liter sea water)				Hydrocarbon Concentrations (ug/liter sea water)				SPM Phase SPM Load (ug dry wt./l)		Hydrocarbon Concentrations (ug/g dry weight)				Dissolved Phase Hydrocarbon Concs. (ug/liter)				
	UCH+Tot.Res.	UCH	Tot.Res.	Tot.n-alk.	UCH+Tot.Res.	UCH	Tot.Res.	Tot.n-alk.	UCH+Tot.Res.	UCH	Tot.Res.	Tot.n-alk.	UCH+Tot.Res.	UCH	Tot.Res.	Tot.n-alk.	UCH+Tot.Res.	UCH	Tot.Res.	UCH+Tot.Res.	UCH	Tot.Res.	
0.00	114082.1	91197.9	22884.2	13432.4	225.9	195.4	30.5	23.2	50.8	44.4	6.5	4.6	48.0	1058.8	924.0	134.8	96.5	60.2	44.8	15.4	0.0	0.0	
0.25					7015.6	5627.7	1387.9	833.4	27.1	19.0	8.1	4.9	43.9	616.2	432.3	183.8	112.3	82.2	51.5	30.7	0.0	0.0	
0.50					27352.0	21522.2	5829.8	3432.9	38.0	29.4	8.6	4.3	48.8	778.5	602.7	175.8	88.7	75.8	23.6	52.2	0.0	0.0	
1.00					18654.2	14631.9	4022.3	2533.8	34.6	25.9	8.7	5.5	46.4	745.0	558.0	187.1	117.5	153.3	66.6	86.7	0.0	0.0	
2.00					57322.7	41277.5	16045.2	10061.8	51.5	34.9	16.6	9.6	46.4	1109.5	752.6	356.9	207.0	188.7	71.8	116.9	0.0	0.0	
4.00					78602.9	60147.2	18455.7	11423.7	166.5	134.8	31.7	16.3	45.5	3699.3	2962.6	696.7	358.9	290.6	167.6	123.0	0.0	0.0	
8.00					108237.6	78410.9	29826.7	18491.8	96.7	72.6	24.1	14.7	37.2	2598.4	1951.6	646.8	393.8	559.4	401.6	157.8	0.0	0.0	
12.00					140206.8	106929.0	33277.8	21281.4	NA	NA	NA	NA	26.5	NA	NA	NA	NA	245.8	203.4	42.4	0.0	0.0	
18.00					452846.3	388693.0	64153.3	20770.2	123.5	92.4	31.1	19.5	27.2	4540.0	3398.1	1141.9	717.6	333.9	288.9	45.0	0.0	0.0	
36.00					87688.0	63252.1	24435.9	17033.0	60.4	47.1	13.2	8.0	11.2	5391.1	4208.9	1182.1	712.9	453.7	357.8	95.9	0.0	0.0	
48.00					136798.8	105588.0	31210.8	20457.9	547.3	454.6	92.7	65.1	21.9	24990.9	20758.0	4232.9	2974.3	380.4	280.6	99.8	0.0	0.0	
72.00					43177.5	21025.7	22151.8	15368.2	134.1	105.5	28.6	14.7	6.8	19720.6	15514.7	4205.9	2106.5	554.6	444.5	110.1	0.0	0.0	
96.00	83399.9	66896.2	16503.7	10123.7	31290.2	0.0	31290.2	23495.9	98.3	76.9	21.4	11.1	5.4	18207.4	14240.7	3966.7	2033.0	610.4	430.1	180.3	0.0	0.0	
														Bot. Sed. (96.0 hr)	6403.8	5380.8	1023.0	672.6					

HYDROCARBON CONCENTRATIONS FROM STIRRED CHAMBER EXPERIMENTS

n-alkanes (nC10 through nC32), pristane, and phytane

SURFACE OIL—Concentrations per gram of oil

Unweathered Prudhoe Bay Crude Oil and Jakolof Bay Sediments

Unweathered Prudhoe Bay Crude Oil and Jakolof Bay Sediments

Time from start (hrs)	FID-CC Run:		Surface Oil—Hydrocarbon Concentrations (ug/g of total oil)													Surface Oil—Hydrocarbon Concentrations (ug/g of total oil)																				
	Place	Time	Visual Alk.Max	nC10	nC11	nC12	nC13			nC14	nC15	nC16	nC17	pristane	nC18	phytane	nC19	nC20	nC21			nC22	nC23	nC24	nC25	nC26	nC27	nC28	nC29	nC30	nC31	nC32				
							nC13	nC14	nC15										nC21	nC22	nC23															
0.00	KB	Jun-85	C11,C13	2969.6	2914.0	2976.5	2908.2	2324.0	2033.7	1990.1	1608.1	NA	1307.5	403.6	1162.6	983.6	972.3	953.1	706.5	792.4	628.9	607.3	548.2	337.9	256.6	Tr	Tr	Tr	Tr	Tr	Tr	Tr	Tr			
0.25																																				
0.50																																				
1.00																																				
2.00																																				
4.00																																				
8.00																																				
12.00																																				
18.00																																				
24.00																																				
48.00																																				
72.00	KB	Jun-85	C14	2598.7	2813.8	3028.0	2911.1	2465.8	2210.6	2470.7	1772.8	NA	1373.8	571.0	1234.4	1125.2	1161.9	1189.6	910.7	1026.8	820.0	823.7	772.4	448.7	456.2	Tr	Tr	Tr	Tr	Tr	Tr	Tr	Tr	Tr		
96.00																																				
120.00																																				
168.00	LJ	Mar-86	C13	983.7	1576.9	1420.7	1527.4	1159.2	1140.8	1037.3	831.8	473.1	837.6	376.6	726.5	630.0	593.5	547.0	501.8	473.4	401.7	368.2	252.7	231.1	200.0	170.7	137.9	95.2								
216.00	LJ	Mar-86	C13	966.8	1728.0	1616.0	1746.2	1308.9	1321.5	1169.6	978.3	542.0	912.5	367.5	757.4	650.2	596.2	515.6	456.0	411.4	333.5	310.3	208.5	173.5	173.3	129.3	129.1	82.6								

2 Day Weathered Prudhoe Bay Crude Oil and Jakolof Bay Sediments

2 Day Weathered Prudhoe Bay Crude Oil and Jakolof Bay Sediments

Time from start (hrs)	FID-CC Run:		Surface Oil—Hydrocarbon Concentrations (ug/g of total oil)													Surface Oil—Hydrocarbon Concentrations (ug/g of total oil)																				
	Place	Time	Visual Alk.Max	nC10	nC11	nC12	nC13			nC14	nC15	nC16	nC17	pristane	nC18	phytane	nC19	nC20	nC21			nC22	nC23	nC24	nC25	nC26	nC27	nC28	nC29	nC30	nC31	nC32				
							nC13	nC14	nC15										nC21	nC22	nC23															
0.00	LJ	Jun-86	C11-C14	811.5	1022.6	1047.0	971.5	1041.5	947.0	843.5	794.3	499.3	642.2	275.4	531.1	470.5	461.4	469.5	413.5	388.4	322.1	278.5	182.9	121.7	118.7	93.1	87.3	72.2								
0.25																																				
0.50																																				
1.00																																				
2.00																																				
4.00																																				
8.50																																				
12.00																																				
15.25																																				
24.00																																				
48.00																																				
73.50	LJ	Jun-86	C11-C13	678.4	929.7	1021.5	953.3	975.2	924.3	802.6	760.8	483.5	651.3	281.2	560.0	455.6	415.0	400.3	337.0	310.0	248.6	222.2	132.6	92.9	70.5	47.9	42.1	29.2								

12 Day Weathered Prudhoe Bay Crude Oil and Jakolof Bay Sediments

12 Day Weathered Prudhoe Bay Crude Oil and Jakolof Bay Sediments

Time from start (hrs)	FID-CC Run:		Surface Oil—Hydrocarbon Concentrations (ug/g of total oil)													Surface Oil—Hydrocarbon Concentrations (ug/g of total oil)																				
	Place	Time	Visual Alk.Max	nC10	nC11	nC12	nC13			nC14	nC15	nC16	nC17	pristane	nC18	phytane	nC19	nC20	nC21			nC22	nC23	nC24	nC25	nC26	nC27	nC28	nC29	nC30	nC31	nC32				
							nC13	nC14	nC15										nC21	nC22	nC23															
0.00	KB	Feb-86	C13	244.8	720.2	1101.4	1045.6	BI	957.2	1088.0	870.6	527.7	795.3	419.2	768.1	807.8	641.9	699.4	610.2	644.6	525.4	430.8	239.8	281.7	241.8	Tr	Tr	Tr	Tr	Tr	Tr	Tr				
0.25																																				
0.50																																				
1.00																																				
2.00																																				
4.00																																				
8.00																																				
12.00																																				
18.00																																				
36.00																																				
48.00																																				
72.00																																				
96.00	KB	Feb-86	C13-C14	64.7	401.4	775.4	803.6	BI	888.7	878.4	630.2	365.3	646.1	301.2	511.0	411.8	482.9	480.0	462.1	425.5	384.0	319.7	282.3	197.2	159.2	180.8	106.9	72.1								

HYDROCARBON CONCENTRATIONS FROM STIRRED CHAMBER EXPERIMENTS

n-alkanes (nC10 through nC32), pristane, and phytane

DISPERSED OIL PHASE—Concentrations per liter of sea water

Unweathered Prudhoe Bay Crude Oil and Jakolof Bay Sediments

Unweathered Prudhoe Bay Crude Oil and Jakolof Bay Sediments

Time from start (hrs)	FID-GC Run:		Dispersed Oil Phase Hydrocarbon Concentrations (ug/l of sea water)													Dispersed Oil Phase Hydrocarbon Concentrations (ug/l of sea water)														
	Place	Time	Visual Alk.Max	nC10	nC11	nC12	nC13	nC14	nC15	nC16	nC17	pristane	nC18	phytane	nC19	nC20	nC21	nC22	nC23	nC24	nC25	nC26	nC27	nC28	nC29	nC30	nC31	nC32		
0.00	KB	Jun-85	—	0.0	0.0	0.0	0.0	0.0	0.0	0.0	0.0	0.0	0.0	0.0	0.0	0.0	0.0	0.0	0.0	0.0	0.0	0.0	0.0	0.0	0.0	0.0	0.0	0.0	0.0	
0.25	KB	Jun-85	C16	Tr	Tr	Tr	1.0	2.3	2.8	3.3	3.2	1.4	2.8	1.5	2.7	2.3	2.3	1.7	1.8	1.4	1.4	1.1	Tr	Tr	Tr	Tr	Tr	Tr	0.0	
0.50	KB	Jun-85	C16	0.9	1.0	1.5	2.9	4.9	5.0	5.7	5.4	2.7	4.7	2.4	4.6	3.4	3.8	4.0	3.0	3.5	2.9	2.7	2.3	1.4	1.5	Tr	Tr	Tr	0.0	
1.00	KB	Jun-85	C16	1.7	1.7	2.1	2.8	3.7	3.5	5.2	4.1	3.9	3.7	2.7	3.2	2.4	2.5	2.5	1.8	2.1	1.7	1.6	1.2	0.9	0.9	Tr	Tr	Tr	0.0	
2.00	KB	Jun-85	C15,C16	2.9	4.3	7.7	11.7	13.3	14.8	16.1	12.5	6.7	11.1	5.2	8.8	10.7	6.3	6.5	4.5	6.0	4.9	4.6	5.0	2.4	2.2	1.3	Tr	Tr	0.0	
4.00	KB	Jun-85	C15,C16	7.3	13.1	22.2	29.7	28.4	31.9	28.7	20.3	7.5	18.7	6.2	13.3	15.5	12.9	11.1	9.4	11.7	7.9	8.2	7.1	4.1	3.8	Tr	Tr	Tr	0.0	
8.00	KB	Jun-85	C14	19.4	29.9	40.5	48.3	41.3	40.6	44.4	30.6	7.2	26.8	8.7	21.3	21.7	18.8	19.7	14.1	16.5	13.8	13.9	12.6	7.7	7.2	5.4	Tr	Tr	0.0	
12.00	KB	Jun-85	C13,C14	39.0	54.4	73.3	81.7	71.0	71.5	73.7	57.9	24.6	49.7	BI	39.1	26.1	15.9	31.5	30.1	28.0	17.7	21.4	7.3	8.9	9.8	5.0	Tr	Tr	0.0	
18.00	LJ	Apr-86	C13,C15	NA	NA	NA	NA	NA	NA	NA	85.2	42.1	75.6	30.4	68.5	60.9	56.3	53.4	49.9	45.3	36.9	31.7	20.0	13.0	12.1	Tr	Tr	Tr	0.0	
24.00	KB	Jun-85	C13	120.9	167.0	188.0	186.9	134.2	142.9	118.0	80.6	23.2	31.6	29.8	BI	26.5	30.1	29.4	24.4	20.4	14.3	12.1	13.1	10.1	4.4	Tr	Tr	Tr	0.0	
48.00	KB	Feb-86	C13	287.7	375.9	433.2	413.7	BI	413.1	448.8	322.4	193.0	302.5	131.4	255.6	244.4	260.3	214.6	220.6	208.6	182.8	164.2	105.0	95.1	78.8	51.4	Tr	Tr	0.0	
72.00	KB	Jun-85	C13	527.7	626.3	680.0	643.6	478.5	465.5	466.7	334.5	148.8	275.9	94.7	BI	95.8	159.4	178.2	133.8	172.2	128.6	110.1	155.0	58.8	Tr	Tr	Tr	Tr	0.0	
96.00	LJ	May-86	C13	260.8	332.5	376.8	452.0	392.7	363.9	333.6	308.7	194.6	262.9	110.1	221.8	186.4	166.1	155.5	130.9	119.6	100.0	89.3	60.7	40.3	Tr	Tr	Tr	Tr	0.0	
120.00	LJ	May-86	C13	328.2	422.5	458.4	547.9	475.8	458.2	409.7	374.2	232.8	317.0	133.9	275.7	254.4	211.0	199.1	162.2	138.1	105.0	90.0	58.8	Tr	Tr	Tr	Tr	Tr	0.0	
168.00	KB	Feb-86	C13	1310.3	1714.8	1920.2	1765.5	BI	1710.6	1747.2	1302.1	825.8	1175.3	502.1	1032.0	898.1	858.9	1024.4	752.5	878.4	587.8	626.4	455.9	361.9	341.7	209.4	Tr	Tr	Tr	0.0
216.00	LJ	Mar-86	C13	348.1	623.6	608.9	674.4	528.1	571.9	509.3	414.6	252.8	403.7	166.8	313.8	267.8	244.0	218.3	188.1	166.8	134.0	119.5	77.5	66.3	64.9	47.2	47.2	27.1	0.0	

2 Day Weathered Prudhoe Bay Crude Oil and Jakolof Bay Sediments

2 Day Weathered Prudhoe Bay Crude Oil and Jakolof Bay Sediments

Time from start (hrs)	FID-GC Run:		Dispersed Oil Phase Hydrocarbon Concentrations (ug/l of sea water)													Dispersed Oil Phase Hydrocarbon Concentrations (ug/l of sea water)													
	Place	Time	Visual Alk.Max	nC10	nC11	nC12	nC13	nC14	nC15	nC16	nC17	pristane	nC18	phytane	nC19	nC20	nC21	nC22	nC23	nC24	nC25	nC26	nC27	nC28	nC29	nC30	nC31	nC32	
0.00	KB	Feb-86	—	0.0	0.0	0.0	0.0	0.0	0.0	0.0	0.0	0.0	0.0	0.0	0.0	0.0	0.0	0.0	0.0	0.0	0.0	0.0	0.0	0.0	0.0	0.0	0.0	0.0	0.0
0.25	KB	Feb-86	C15	3.4	5.1	6.7	7.2	BI	9.2	8.4	7.9	5.2	7.5	3.4	6.6	6.7	5.0	4.9	4.7	4.5	3.7	3.4	2.2	1.9	1.8	0.9	Tr	Tr	0.0
1.00	KB	Feb-86	C14,C15	3.9	6.1	8.2	8.2	BI	10.7	11.5	8.4	5.2	7.9	4.1	6.9	6.7	5.8	5.5	4.4	4.5	3.9	3.5	2.4	2.1	1.9	1.3	Tr	Tr	0.0
2.00	KB	Feb-86	C14	7.1	11.0	15.2	16.6	BI	19.6	21.2	15.0	10.3	15.8	8.5	12.0	13.2	10.7	9.6	8.5	7.8	6.5	3.2	3.5	3.3	1.7	Tr	Tr	Tr	0.0
4.00	KB	Feb-86	C13	156.2	236.3	285.5	259.2	BI	260.3	280.3	211.0	140.6	203.5	103.9	185.3	156.9	147.3	158.0	141.3	169.2	111.0	116.4	87.5	70.4	64.5	40.6	42.2	Tr	0.0
8.50	KB	Feb-86	C13	733.5	969.8	1129.4	960.8	BI	886.0	892.2	659.4	390.1	587.5	306.9	530.4	480.9	484.8	478.2	474.5	453.3	355.1	328.4	244.1	142.3	194.4	Tr	Tr	Tr	0.0
12.00	KB	Feb-86	C12	813.0	1098.5	1252.2	1089.4	BI	1068.8	1137.4	823.8	472.6	742.1	400.2	736.5	641.8	672.2	627.5	688.9	691.1	545.7	405.4	316.8	201.0	Tr	Tr	Tr	99.5	Tr
15.25	KB	Feb-86	C13	1181.1	1631.4	1878.8	1632.5	BI	1723.2	1781.1	1349.4	803.8	1256.8	527.6	1109.9	1029.7	985.8	996.7	938.6	918.3	806.0	727.4	490.8	406.4	361.1	232.8	Tr	Tr	Tr
24.00	KB	Feb-86	C13	633.9	893.6	1043.1	931.2	BI	957.4	967.8	732.1	479.0	665.2	326.2	544.9	484.9	466.0	426.1	360.8	306.8	230.0	177.4	94.4	76.7	Tr	0.0	0.0	0.0	0.0
48.00	KB	Feb-86	C13	512.0	726.4	850.1	753.3	BI	733.0	767.0	578.3	343.8	517.7	233.2	475.8	408.0	402.6	422.4	475.0	401.1	347.3	311.6	209.7	172.2	151.6	90.9	Tr	Tr	0.0
73.50	KB	Feb-86	C13	284.5	426.4	521.2	465.7	BI	490.5	514.3	389.1	246.6	357.8	182.1	315.7	317.6	321.8	280.8	257.1	243.0	235.4	215.2	145.8	122.7	109.2	61.6	54.8	Tr	0.0

12 Day Weathered Prudhoe Bay Crude Oil and Jakolof Bay Sediments

12 Day Weathered Prudhoe Bay Crude Oil and Jakolof Bay Sediments

Time from start (hrs)	FID-GC Run:		Dispersed Oil Phase Hydrocarbon Concentrations (ug/l of sea water)													Dispersed Oil Phase Hydrocarbon Concentrations (ug/l of sea water)													
	Place	Time	Visual Alk.Max	nC10	nC11	nC12	nC13	nC14	nC15	nC16	nC17	pristane	nC18	phytane	nC19	nC20	nC21	nC22	nC23	nC24	nC25	nC26	nC27	nC28	nC29	nC30	nC31	nC32	
0.00	KB	Feb-86	C16	Tr	0.4	0.8	1.2	1.7	2.0	2.3	2.1	1.3	2.1	0.9	1.8	1.6	1.4	1.4	1.2	1.2	1.1	1.1	0.8	Tr	Tr	Tr	Tr	Tr	
0.25	KB	Feb-86	C13,C14	12.0	42.5	70.8	71.9	BI	70.2	75.9	55.6	34.5	55.9	25.5	45.8	39.6	36.5	38.4	33.0	31.0	29.5	18.6	15.1	24.1	10.1	Tr	Tr	8.5	Tr
0.50	KB	Feb-86	C13	65.9	208.6	323.8	307.6	BI	301.3	320.6	225.8	138.6	218.3	89.8	180.5	164.9	164.5	126.8	148.9	120.1	107.3	92.5	61.0	50.7	42.5	Tr	Tr	Tr	0.0
1.00	KB	Feb-86	C13	43.8	141.4	217.6	217.0	BI	192.5	223.3	159.6	104.0	153.0	64.4	138.0	129.5	111.9	117.7	106.5	100.0	85.0	78.7	55.9	49.5	42.6	27.9	Tr	Tr	0.0
2.00	LJ	Mar-86	C13	216.2	791.8	1008.8	1139.2	928.7	975.1	835.4	703.0	392.1	640.9	275.9	559.6	477.9	445.5	382.7	322.4	267.3	213.4	197.3	121.0	105.2	87.3	70.2	55.8	Tr	0.0
4.00	LJ	Mar-86	C13	233.6	882.9	1164.9	1349.3	1069.2	1081.5	968.8	765.8	467.2	775.9	316.0	693.0	530.0	484.0	421.4	344.7	303.6	233.9	205.6	128.3	111.8	92.5	76.1	62.6	Tr	0.0
8.00	LJ	Mar-86	C13	365.2	1395.3	1822.4	2135.6	1721.0	1711.7	1577.2	1352.7	678.4	1214.7	493.8	1045.2	890.7	797.4	651.6	563.5	485.4	384.6	352.9	219.6	199.3	170.6	136.6	113.9	79.4	Tr
12.00	LJ	Mar-86	C13	382.7	1558.3	2116.1	2415.2	2011.0	1972.6	1821.1	1550.2	865.7	1442.5	582.8	1317.3	1017.3	929.2	790.4	655.2	569.4	445.0	401.2	253.4	218.8	182.6	154.0	123.2		

HYDROCARBON CONCENTRATIONS FROM STIRRED CHAMBER EXPERIMENTS

n-alkanes (nC10 through nC32), pristane, and phytane

SPM PHASE—Concentrations per gram dry weight of sediment

Unweathered Prudhoe Bay Crude Oil and Jakolof Bay Sediments

Unweathered Prudhoe Bay Crude Oil and Jakolof Bay Sediments

Time from start (hrs)	SPM Load (ng dry wt./l)	SPM Phase Hydrocarbon Concentrations (ug/g dry weight)												SPM Phase Hydrocarbon Concentrations (ug/g dry weight)												
		nC10	nC11	nC12	nC13	nC14	nC15	nC16	nC17	pristane	nC18	phytane	nC19	nC20	nC21	nC22	nC23	nC24	nC25	nC26	nC27	nC28	nC29	nC30	nC31	nC32
		0.00	52.9	2.6	2.0	Tr	Tr	Tr	Tr	Tr	0.9	Tr	Tr	Tr	Tr	Tr	0.8	0.8	Tr	Tr	Tr	Tr	Tr	0.0	Tr	Tr
0.25	50.1	Tr	Tr	0.0	0.0	0.0	0.0	0.0	0.0	0.0	0.0	0.0	0.0	0.0	0.0	0.0	0.0	0.0	0.0	0.0	0.0	0.0	0.0	0.0	0.0	0.0
0.50	53.0	4.1	3.5	2.5	3.7	6.6	7.0	8.2	9.2	5.6	8.4	5.2	8.0	7.2	7.1	6.3	5.3	4.8	3.9	3.3	3.6	1.7	1.5	Tr	Tr	0.0
1.00	47.7	NA	NA	NA	NA	NA	NA	NA	NA	NA	NA	NA	NA	NA	NA	NA	NA	NA	NA	NA	NA	NA	NA	NA	NA	NA
2.00	51.3	0.0	Tr	Tr	2.6	5.7	6.5	7.8	8.9	5.6	7.9	4.7	7.4	6.8	7.0	6.1	5.4	4.8	4.2	3.7	4.7	2.5	2.5	2.0	2.9	Tr
4.00	50.1	0.0	0.0	Tr	2.9	6.9	7.8	8.9	9.9	6.0	8.5	4.8	7.5	6.8	6.6	5.6	4.4	3.6	2.8	2.4	2.5	1.4	1.4	Tr	Tr	Tr
8.00	53.8	0.0	1.9	7.2	16.6	BI	26.6	26.3	28.4	17.0	22.9	14.6	19.1	18.1	18.7	16.8	14.6	13.0	11.4	10.3	10.6	6.6	5.8	4.3	5.6	3.4
12.00	48.2	Tr	5.9	22.7	44.6	BI	65.0	59.2	61.2	36.9	30.7	34.3	42.1	39.3	42.0	38.0	32.6	27.9	24.7	19.7	16.9	12.2	11.7	7.2	9.4	6.8
18.00	44.4	45.0	62.3	82.1	100.9	BI	105.9	132.6	100.0	51.0	94.0	32.4	81.0	63.3	66.5	66.3	49.5	58.8	45.4	49.0	44.5	25.4	23.1	Tr	Tr	Tr
24.00	50.4	65.5	98.8	158.7	203.5	208.2	223.8	228.7	177.6	86.9	161.2	76.4	132.7	99.4	105.4	111.9	99.0	103.2	65.9	78.0	83.3	40.2	36.4	31.9	Tr	Tr
48.00	43.8	212.4	324.8	457.0	521.8	452.2	448.1	465.9	325.2	164.9	293.8	155.4	NA	149.2	159.6	166.0	146.0	156.9	131.3	102.3	115.2	53.7	66.2	Tr	Tr	Tr
72.00	35.9	409.2	751.6	1044.4	1177.3	1016.2	967.1	989.8	716.2	386.4	602.8	278.1	NA	349.5	414.0	430.9	331.6	411.1	355.6	319.0	158.3	96.6	98.7	Tr	Tr	Tr
96.00	28.7	287.0	656.6	741.8	844.2	754.8	844.9	763.4	657.3	394.0	686.4	328.6	578.5	492.8	455.2	412.1	352.9	315.9	251.8	225.5	144.8	123.1	107.3	81.5	65.2	45.4
120.00	25.0	405.8	898.6	957.7	1091.6	951.1	1053.6	932.9	828.8	466.4	753.0	317.1	635.8	546.8	492.1	432.4	379.9	349.7	290.5	269.5	165.7	150.9	131.8	112.2	82.0	60.5
168.00	29.5	247.8	602.3	716.6	873.4	779.6	910.1	836.6	702.1	401.7	716.2	311.3	598.9	506.6	460.1	392.0	343.5	317.5	260.4	236.8	152.1	138.5	120.3	105.3	78.6	52.0
216.00	23.0	311.1	828.0	1032.9	1209.5	1176.9	1355.4	1285.4	1171.7	582.3	1063.8	464.5	919.1	815.1	734.4	653.2	554.4	499.8	397.1	361.6	227.9	207.0	182.6	144.6	118.3	79.2

2 Day Weathered Prudhoe Bay Crude Oil and Jakolof Bay Sediments

2 Day Weathered Prudhoe Bay Crude Oil and Jakolof Bay Sediments

Time from start (hrs)	SPM Load (ng dry wt./l)	SPM Phase Hydrocarbon Concentrations (ug/g dry weight)												SPM Phase Hydrocarbon Concentrations (ug/g dry weight)												
		nC10	nC11	nC12	nC13	nC14	nC15	nC16	nC17	pristane	nC18	phytane	nC19	nC20	nC21	nC22	nC23	nC24	nC25	nC26	nC27	nC28	nC29	nC30	nC31	nC32
		0.00	51.6	4.4	3.7	1.7	1.1	1.5	2.5	6.1	4.6	2.1	3.9	2.0	3.9	3.1	2.7	2.4	2.2	2.1	2.0	Tr	2.2	Tr	Tr	Tr
0.25	49.3	6.0	4.1	1.6	Tr	2.4	4.1	6.1	6.8	3.1	6.8	3.3	7.2	6.3	5.9	5.4	5.2	4.6	4.3	3.9	4.3	3.6	4.4	Tr	5.3	Tr
0.50	46.4	3.7	2.7	Tr	1.2	2.3	3.8	5.3	6.3	3.1	6.1	2.8	5.4	4.0	2.8	Tr	Tr	Tr	Tr	Tr	Tr	Tr	Tr	Tr	0.0	0.0
1.00	46.8	5.3	4.4	2.8	2.7	4.8	7.5	10.0	11.0	5.7	11.4	5.5	11.1	10.0	8.9	8.0	7.2	5.9	4.8	3.5	Tr	Tr	Tr	Tr	Tr	0.0
2.00	43.0	6.3	4.9	2.5	2.6	7.1	7.4	9.9	9.3	8.1	10.1	7.2	10.4	9.4	8.7	8.3	8.1	7.7	7.4	6.4	6.6	5.5	8.2	Tr	9.8	Tr
4.00	34.1	16.8	15.0	12.1	17.9	16.2	40.1	45.9	50.2	20.0	56.7	21.1	54.0	50.7	47.9	45.2	47.0	45.0	39.7	37.2	28.6	Tr	Tr	Tr	Tr	0.0
8.50	41.0	29.0	31.1	34.7	39.2	BI	58.2	57.9	57.2	33.4	62.4	28.0	60.3	57.3	54.2	53.5	49.1	45.3	39.0	32.1	23.3	Tr	Tr	Tr	Tr	Tr
12.00	20.2	54.1	41.5	43.3	77.7	BI	157.5	222.4	211.1	141.4	226.1	112.7	192.4	175.2	160.9	155.1	148.8	136.9	116.3	96.1	65.0	52.7	46.0	Tr	Tr	Tr
15.25	26.4	38.3	43.2	64.0	86.4	BI	132.9	181.4	166.1	110.0	176.2	89.0	148.3	140.2	135.2	129.7	122.6	119.5	99.9	91.2	58.0	51.0	47.9	Tr	Tr	Tr
24.00	25.0	55.4	107.9	283.5	354.1	BI	513.5	612.5	496.6	326.3	483.8	273.3	427.9	379.5	408.8	365.3	400.7	337.3	229.9	296.0	210.5	167.9	163.5	Tr	85.2	Tr
48.00	3.6	170.1	119.0	41.0	38.1	BI	174.2	239.3	282.4	191.2	355.6	170.1	325.6	365.3	270.1	230.8	177.2	135.0	96.0	69.3	Tr	Tr	Tr	Tr	Tr	0.0
73.50	3.8	183.4	128.6	53.7	56.4	BI	138.3	218.7	212.1	145.8	267.1	153.3	274.0	232.7	239.9	237.1	227.0	222.1	195.4	189.7	139.7	138.1	131.3	Tr	73.9	Tr
(73.50)	Bot. Sed. (ug/g)	1172.0	1827.2	2244.1	2000.7	BI	2048.6	2018.2	1575.4	999.6	1372.4	734.3	1243.3	1029.4	1041.9	1111.5	963.5	879.4	858.5	869.6	574.0	381.6	326.3	Tr	Tr	Tr

12 Day Weathered Prudhoe Bay Crude Oil and Jakolof Bay Sediments

12 Day Weathered Prudhoe Bay Crude Oil and Jakolof Bay Sediments

Time from start (hrs)	SPM Load (ng dry wt./l)	SPM Phase Hydrocarbon Concentrations (ug/g dry weight)												SPM Phase Hydrocarbon Concentrations (ug/g dry weight)													
		nC10	nC11	nC12	nC13	nC14	nC15	nC16	nC17	pristane	nC18	phytane	nC19	nC20	nC21	nC22	nC23	nC24	nC25	nC26	nC27	nC28	nC29	nC30	nC31	nC32	
		0.00	48.0	1.0	1.5	2.3	5.6	13.5	15.6	16.0	13.8	8.2	11.3	5.4	8.1	5.7	4.0	3.0	2.2	Tr	Tr	Tr	Tr	Tr	Tr	Tr	0.0
0.25	43.9	3.5	2.7	1.9	3.7	10.1	13.6	16.5	10.0	14.8	7.1	11.6	8.3	5.6	3.9	2.8	2.0	Tr	0.0	0.0	0.0						
0.50	48.8	3.2	2.4	Tr	2.1	4.6	7.1	9.4	10.5	5.3	10.9	4.9	10.1	9.1	7.6	6.1	4.6	3.2	Tr	Tr	Tr	Tr	Tr	Tr	Tr	Tr	Tr
1.00	46.4	4.1	3.2	2.1	3.3	6.9	10.2	13.7	12.8	6.9	12.6	5.9	11.4	10.1	9.0	7.9	6.0	4.7	3.1	Tr	Tr	Tr	Tr	Tr	Tr	0.0	0.0
2.00	46.4	6.5	5.4	3.9	5.2	BI	13.9	19.2	16.7	12.6	17.0	9.2	13.6	13.1	12.0	12.1	11.0	10.6	9.2	8.1	6.7	5.2	5.7	Tr	5.1	Tr	
4.00	45.5	9.4	7.0	5.7	8.5	BI	19.7	30.0	26.2	21.2	27.5	15.9	27.3	27.4	22.4	20.4	19.5	17.8	16.0	12.7	11.1	10.9	Tr	Tr	9.0	Tr	
8.00	37.2	11.1	8.1	6.7	15.1	BI	46.1	60.8	51.0	37.7	49.3	25.2	37.1	28.4	20.8	NA	NA	NA	NA								
12.00	26.5	11.3	8.3	NA	NA	NA	NA	NA	NA	NA	NA	NA	NA	NA	NA	NA	NA	NA	NA	NA	NA	NA	NA	NA	NA	NA	NA
18.00	27.2	10.0	8.5	7.0	13.0	35.2	50.3	67.4	71.0	52.8	69.3	38.9	63.7	54.6	49.2	46.9	40.3	35.1	28.1	24.7	17.2	15.3	15.8	Tr	13.1	Tr	
36.00	11.2	32.4	23.9	14.4	25.2	BI	38.6	77.2	71.7	49.1	76.9	40.2	71.4	59.5	NA	NA	NA	NA									
48.00	21.9	73.0	87.3	135.1	174.2	BI	227.9	273.1	235.0	147.4	230.0	109.7	196.9	161.9	149.9	141.6	137.2	119.2	112.5	77.1	66.8	63.1	Tr	Tr	Tr	Tr	
72.00	6.8	102.3	75.2	33.9	54.4	BI	157.8	215.6	179.3	116.8	176.3	77.0	153.1	126.6	121.9	119.1	110.9	100.6	85.7	77.7	52.6	49.8	47.2	Tr	Tr	Tr	
96.00	5.4	103.2	75.5	37.4	76.7	BI	193.2	262.1	226.9	153.6	236.6	114.7	192.2	151.9	NA	NA	NA	NA									
(96.00)	Bot. Sed. (ug/g)	4.07	21.72	42.63	45.95	BI	48.31	51.97	40.31	22.85	43.88	22.58	38.32	42.60	38.48	41.49	35.98	34.95	30.72	29.45	16.87	15.41	13.18	11.27	Tr	Tr	

HYDROCARBON CONCENTRATIONS FROM STIRRED CHAMBER EXPERIMENTS

Identifiable aromatics

SURFACE OIL—Concentrations per gram of oil

Unweathered Prudhoe Bay Crude Oil and Jakolof Bay Sediments

Time from start (hrs)	FID-GC Run:		Surface Oil							
	Place	Time	Hydrocarbon Concentrations (ug/g of total oil)							
			Naph	2-MeNa	1-MeNa	2,6-diMeNa	1,3-diMeNa	1,2-diMeNa	2,3,6-triMeNa	Phenanth
0.00	KB	Jun-85	233.1	1087.6	737.9	Tr	276.2	Tr	Tr	NA
0.25										
0.50										
1.00										
2.00										
4.00										
8.00										
12.00										
18.00										
24.00										
48.00										
72.00	KB	Jun-85	190.1	1101.1	659.4	Tr	261.4	Tr	Tr	NA
96.00										
120.00										
168.00	LJ	Mar-86	NA	542.2	BI	323.2	269.9	129.8	110.0	118.9
216.00	LJ	Mar-86	210.2	581.1	BI	350.2	288.8	130.6	94.4	135.7

2 Day Weathered Prudhoe Bay Crude Oil and Jakolof Bay Sediments

Time from start (hrs)	FID-GC Run:		Surface Oil							
	Place	Time	Hydrocarbon Concentrations (ug/g of total oil)							
			Naph	2-MeNa	1-MeNa	2,6-diMeNa	1,3-diMeNa	1,2-diMeNa	2,3,6-triMeNa	Phenanth
0.00	LJ	Feb-86	213.1	384.6	235.2	387.8	295.6	145.5	155.2	Tr
0.25										
0.50										
1.00										
2.00										
4.00										
8.50										
12.00										
15.25										
24.00										
48.00										
73.50	LJ	Feb-86	170.8	350.2	219.3	307.9	268.6	109.6	132.0	Tr

12 Day Weathered Prudhoe Bay Crude Oil and Jakolof Bay Sediments

Time from start (hrs)	FID-GC Run:		Surface Oil							
	Place	Time	Hydrocarbon Concentrations (ug/g of total oil)							
			Naph	2-MeNa	1-MeNa	2,6-diMeNa	1,3-diMeNa	1,2-diMeNa	2,3,6-triMeNa	Phenanth
0.00	KB	Feb-86	132.0	366.9	284.9	BI	266.2	89.1	130.0	70.6
0.25										
0.50										
1.00										
2.00										
4.00										
8.00										
12.00										
18.00										
36.00										
48.00										
72.00										
96.00	KB	Feb-86	18.3	217.3	199.5	BI	211.6	68.2	95.7	39.2

HYDROCARBON CONCENTRATIONS FROM STIRRED CHAMBER EXPERIMENTS

Identifiable aromatics

DISPERSED OIL PHASE—Concentrations per liter of sea water

Unweathered Prudhoe Bay Crude Oil and Jakolof Bay Sediments

Time from start (hrs)	FID-GC Run:		Dispersed Oil Phase							
	Place	Time	Hydrocarbon Concentrations (ug/l of sea water)							
			Naph	2-MeNa	1-MeNa	2,6-diMeNa	1,3-diMeNa	1,2-diMeNa	2,3,6-triMeNa	Phenanth
0.00	KB	Jun-85	0.0	0.0	0.0	0.0	0.0	0.0	0.0	0.0
0.25	KB	Jun-85	0.0	0.0	0.0	0.0	0.0	0.0	0.0	0.0
0.50	KB	Jun-85	0.0	0.0	0.0	0.0	0.0	0.0	0.0	0.0
1.00	KB	Jun-85	0.0	0.0	0.0	0.0	Tr	0.0	Tr	0.0
2.00	KB	Jun-85	0.0	1.1	0.8	Tr	0.8	0.0	0.6	1.2
4.00	KB	Jun-85	1.4	6.1	4.5	1.1	2.2	0.8	1.1	0.8
8.00	KB	Jun-85	NA	14.4	8.2	Tr	4.1	Tr	2.0	0.0
12.00	KB	Jun-85	4.1	28.6	17.9	Tr	7.4	Tr	Tr	3.9
18.00	LJ	Apr-86	Tr	NA	BI	24.5	18.9	7.9	10.8	8.5
24.00	KB	Jun-85	21.8	74.0	49.1	3.8	11.0	5.9	5.7	8.9
48.00	KB	Feb-86	62.0	142.7	115.4	BI	101.8	38.0	49.5	Tr
72.00	KB	Jun-85	76.1	282.6	181.2	Tr	58.0	15.9	Tr	32.1
96.00	LJ	May-86	57.5	122.8	BI	125.3	104.9	51.1	56.9	30.0
120.00	LJ	May-86	75.5	149.0	BI	147.0	129.5	64.0	71.6	36.3
168.00	KB	Feb-86	306.5	573.9	477.2	BI	418.3	138.7	196.2	66.0
216.00	LJ	Mar-86	81.3	186.7	BI	137.0	113.7	50.6	41.4	41.7

2 Day Weathered Prudhoe Bay Crude Oil and Jakolof Bay Sediments

Time from start (hrs)	FID-GC Run:		Dispersed Oil Phase							
	Place	Time	Hydrocarbon Concentrations (ug/l of sea water)							
			Naph	2-MeNa	1-MeNa	2,6-diMeNa	1,3-diMeNa	1,2-diMeNa	2,3,6-triMeNa	Phenanth
0.00	KB	Feb-86	0.0	0.0	0.0	0.0	0.0	0.0	0.0	0.0
0.25			NA	NA	NA	NA	NA	NA	NA	NA
0.50	KB	Feb-86	Tr	1.4	0.7	BI	1.3	0.4	1.1	Tr
1.00	KB	Feb-86	0.4	1.7	1.1	BI	1.6	0.6	1.1	Tr
2.00	KB	Feb-86	Tr	1.7	2.5	BI	3.6	1.2	2.8	0.6
4.00	KB	Feb-86	13.2	79.6	67.8	BI	67.9	25.4	36.8	14.3
8.50	KB	Feb-86	81.5	322.5	276.8	BI	230.6	78.5	118.4	44.0
12.00	KB	Feb-86	81.3	384.5	326.6	BI	276.4	104.3	136.9	66.7
15.25	KB	Feb-86	145.4	584.5	479.8	BI	440.6	154.9	218.6	122.3
24.00	KB	Feb-86	121.4	351.2	286.9	BI	254.2	79.4	122.9	42.6
48.00	KB	Feb-86	87.8	272.3	223.1	BI	192.6	67.7	94.6	45.9
73.50	KB	Feb-86	65.6	171.3	140.1	BI	126.2	43.8	62.2	22.4

12 Day Weathered Prudhoe Bay Crude Oil and Jakolof Bay Sediments

Time from start (hrs)	FID-GC Run:		Dispersed Oil Phase							
	Place	Time	Hydrocarbon Concentrations (ug/l of sea water)							
			Naph	2-MeNa	1-MeNa	2,6-diMeNa	1,3-diMeNa	1,2-diMeNa	2,3,6-triMeNa	Phenanth
0.00	KB	Feb-86	0.0	0.0	0.0	0.0	Tr	0.0	Tr	0.0
0.25	KB	Feb-86	7.7	23.5	18.6	BI	17.7	6.4	8.8	4.6
0.50	KB	Feb-86	35.2	106.6	82.0	BI	75.0	25.8	37.9	16.3
1.00	KB	Feb-86	20.2	89.7	51.6	BI	50.2	17.0	25.6	14.7
2.00	LJ	Mar-86	62.7	366.1	BI	245.7	202.1	90.8	73.5	100.8
4.00	LJ	Mar-86	67.2	415.9	BI	287.0	222.1	109.3	87.8	109.0
8.00	LJ	Mar-86	119.0	663.4	BI	475.0	367.4	185.9	153.9	173.4
12.00	LJ	Mar-86	66.9	759.1	BI	550.4	427.2	198.0	160.5	230.5
18.00	LJ	Sep-85	NA	NA	NA	BI	839.4	207.3	415.9	Tr
36.00	LJ	Mar-86	Tr	499.9	BI	386.1	340.0	245.1	107.2	187.2
48.00	LJ	Mar-86	Tr	673.9	BI	510.0	419.6	369.4	154.2	197.6
72.00	LJ	Mar-86	0.0	425.8	BI	341.6	302.2	233.3	98.0	159.3
96.00	LJ	Apr-86	Tr	461.1	BI	510.2	387.5	Tr	210.0	177.2

HYDROCARBON CONCENTRATIONS FROM STIRRED CHAMBER EXPERIMENTS

Identifiable aromatics

SPM PHASE—Concentrations per gram dry weight of sediment

Unweathered Prudhoe Bay Crude Oil and Jakolof Bay Sediments

Time from start (hrs)	SPM Load (mg dry wt./l)	SPM Phase							
		Hydrocarbon Concentrations (ug/g dry weight)							
		Naph	2-MeNa	1-MeNa	2,6-diMeNa	1,3-diMeNa	1,2-diMeNa	2,3,6-triMeNa	Phenanth
0.00	52.9	0.0	0.0	0.0	0.0	0.0	0.0	0.0	0.0
0.25	50.1	0.0	0.0	0.0	0.0	0.0	0.0	0.0	0.0
0.50	53.0	Tr	1.1	Tr	BI	Tr	0.0	Tr	Tr
1.00	47.7	NA	NA	NA	NA	NA	NA	NA	NA
2.00	51.3	0.0	Tr	Tr	BI	Tr	0.0	Tr	0.9
4.00	50.1	0.0	Tr	Tr	BI	Tr	0.0	Tr	Tr
8.00	53.8	Tr	4.0	3.6	BI	4.4	1.1	3.3	1.4
12.00	48.2	Tr	7.9	8.2	BI	9.6	2.9	8.2	2.6
18.00	44.4	0.0	14.5	Tr	BI	9.5	Tr	8.4	Tr
24.00	50.4	Tr	60.0	38.2	BI	24.1	Tr	Tr	15.3
48.00	43.8	28.2	180.3	109.0	BI	56.3	11.8	28.5	31.3
72.00	35.9	76.3	431.1	294.8	BI	118.3	Tr	79.4	76.5
96.00	28.7	37.3	197.8	BI	147.4	152.7	68.4	62.5	72.5
120.00	25.0	62.7	281.8	BI	214.5	209.4	89.4	80.3	84.5
168.00	29.5	39.5	221.6	BI	176.8	172.1	131.0	64.2	77.7
216.00	23.0	Tr	252.2	BI	231.1	238.5	95.2	93.9	98.6

2 Day Weathered Prudhoe Bay Crude Oil and Jakolof Bay Sediments

Time from start (hrs)	SPM Load (mg dry wt./l)	SPM Phase							
		Hydrocarbon Concentrations (ug/g dry weight)							
		Naph	2-MeNa	1-MeNa	2,6-diMeNa	1,3-diMeNa	1,2-diMeNa	2,3,6-triMeNa	Phenanth
0.00	51.6	Tr	Tr	Tr	BI	Tr	0.0	0.0	0.0
0.25	49.3	Tr	Tr	Tr	BI	Tr	0.0	0.0	Tr
0.50	46.4	Tr	Tr	Tr	BI	Tr	0.0	0.0	Tr
1.00	46.8	Tr	Tr	Tr	BI	Tr	0.0	Tr	Tr
2.00	43.0	Tr	Tr	1.2	BI	Tr	0.0	Tr	Tr
4.00	34.1	0.0	Tr	Tr	BI	Tr	0.0	Tr	0.0
8.50	41.0	0.0	Tr	7.1	BI	11.8	Tr	Tr	Tr
12.00	20.2	0.0	Tr	13.7	BI	21.1	Tr	Tr	Tr
15.25	26.4	0.0	Tr	16.6	BI	23.4	Tr	14.1	Tr
24.00	25.0	0.0	62.1	69.0	BI	97.9	32.9	72.0	Tr
48.00	3.6	53.6	113.8	57.3	BI	53.1	Tr	30.2	Tr
73.50	3.8	67.1	101.3	60.4	BI	47.7	Tr	23.1	Tr
(73.50)	Bot.Sed.	223.4	674.6	587.6	BI	545.2	162.0	232.5	51.8

12 Day Weathered Prudhoe Bay Crude Oil and Jakolof Bay Sediments

Time from start (hrs)	SPM Load (mg dry wt./l)	SPM Phase							
		Hydrocarbon Concentrations (ug/g dry weight)							
		Naph	2-MeNa	1-MeNa	2,6-diMeNa	1,3-diMeNa	1,2-diMeNa	2,3,6-triMeNa	Phenanth
0.00	48.0	0.0	Tr	Tr	BI	Tr	0.0	Tr	0.0
0.25	43.9	0.0	Tr	Tr	BI	Tr	0.0	Tr	Tr
0.50	48.8	0.0	Tr	Tr	BI	Tr	0.0	Tr	Tr
1.00	46.4	0.0	1.5	Tr	BI	Tr	0.0	Tr	Tr
2.00	46.4	Tr	4.3	2.5	BI	2.9	Tr	1.6	2.4
4.00	45.5	Tr	5.4	4.2	BI	5.3	2.0	3.3	5.2
8.00	37.2	0.0	5.2	5.1	BI	8.0	Tr	4.7	8.1
12.00	26.5	0.0	NA	NA	BI	NA	NA	NA	NA
18.00	27.2	0.0	Tr	Tr	BI	Tr	0.0	Tr	Tr
36.00	11.2	Tr	Tr	5.5	BI	11.5	Tr	6.6	7.0
48.00	21.9	Tr	Tr	17.1	BI	37.9	Tr	25.6	Tr
72.00	6.8	Tr	Tr	Tr	BI	17.5	Tr	Tr	Tr
96.00	5.4	Tr	40.9	24.2	BI	38.0	Tr	22.6	Tr
(96.00)	Bot.Sed.	Tr	Tr	2.39	BI	4.41	1.01	3.14	Tr

HYDROCARBON CONCENTRATIONS FROM STIRRED CHAMBER EXPERIMENTS

Identifiable aromatics (Note: ND observed aliphatics)

DISSOLVED PHASE—Concentrations per liter of sea water

Unweathered Prudhoe Bay Crude Oil and Jakolof Bay Sediments

Time from start (hrs)	FID-GC Run:		Dissolved Phase Hydrocarbon Concentrations (ug/l of sea water)										Dissolved Phase Hydrocarbon Concentrations (ug/l of sea water)					
	Place	Time	Toluene	Ethylbenz	p-Xylene	o-Xylene	Camene	n-Propylbenz	Mesitylene	Naph	2-MeNa	1-MeNa	2,6-diMeNa	1,3-diMeNa	1,2-diMeNa	2,3,6-triMeNa	Fluorene	Phenanth
0.00	KB	Jun-85	0.0	0.0	0.0	0.0	0.00	0.00	0.00	0.0	0.0	0.0	0.00	0.00	0.00	0.00	0.00	0.00
0.25	LJ	Apr-86	9.0	0.7	3.2	1.7	Tr	Tr	Tr	1.4	1.0	0.9	0.30	0.33	Tr	0.00	Tr	Tr
0.50	KB	Jun-85	20.4	4.6	17.6	10.0	Tr	Tr	0.61	3.0	2.0	1.7	0.00	Tr	0.00	0.00	0.00	0.00
1.00	LJ	Apr-86	74.1	5.5	13.9	11.2	0.48	0.61	0.87	1.7	3.6	3.3	1.20	1.18	0.37	Tr	0.47	0.49
2.00	KB	Jun-85	230.0	14.9	49.3	28.2	1.09	1.35	1.42	12.8	8.7	7.4	1.51	0.69	Tr	0.00	0.82	0.00
4.00	KB	Jun-85	380.3	BI	88.5	48.5	1.50	2.36	2.38	24.1	15.7	13.4	2.65	1.15	1.63	Tr	1.02	0.00
8.00	KB	Jun-85	749.5	54.8	176.5	100.3	4.41	5.38	6.03	38.7	25.1	22.4	3.78	1.74	2.45	0.85	2.69	Tr
12.00	KB	Jun-85	629.1	43.9	133.0	83.3	3.65	4.11	4.79	22.8	17.6	16.2	2.57	1.22	1.53	Tr	1.56	Tr
18.00	KB	Jun-85	595.6	43.1	135.3	84.8	3.35	3.84	4.50	27.5	19.7	18.3	2.53	1.01	1.79	Tr	1.68	Tr
24.00	KB	Jun-85	BI	15.6	57.6	38.1	1.40	1.60	2.07	23.0	15.1	14.0	2.24	1.05	Tr	0.00	1.97	Tr
48.00	KB	Jun-85	BI	26.2	82.1	61.0	2.36	2.73	3.26	34.8	19.1	19.0	3.30	1.47	1.62	0.70	2.68	Tr
72.00	KB	Jun-85	BI	35.9	120.8	92.5	3.98	4.78	6.03	59.9	31.2	29.1	5.44	2.37	1.09	1.23	3.90	0.62
96.00	KB	Feb-86	95.7	19.9	60.9	56.6	2.61	3.16	5.07	39.3	15.0	17.8	1.52	4.98	1.80	1.19	2.89	1.13
120.00	KB	Feb-86	55.4	13.8	50.9	45.4	2.05	2.09	4.24	40.3	13.5	17.4	1.09	4.48	1.59	1.25	3.25	1.05
168.00	KB	Feb-86	18.0	9.5	36.8	31.8	1.53	1.82	3.76	42.8	16.2	18.0	1.45	4.33	1.58	1.31	5.27	1.22
216.00	KB	Feb-86	4.7	4.7	20.5	24.4	1.13	1.45	3.71	29.7	13.9	16.1	1.48	4.91	1.79	1.71	7.63	0.85

2 Day Weathered Prudhoe Bay Crude Oil and Jakolof Bay Sediments

Time from start (hrs)	FID-GC Run:		Dissolved Phase Hydrocarbon Concentrations (ug/l of sea water)										Dissolved Phase Hydrocarbon Concentrations (ug/l of sea water)					
	Place	Time	Toluene	Ethylbenz	p-Xylene	o-Xylene	Camene	n-Propylbenz	Mesitylene	Naph	2-MeNa	1-MeNa	2,6-diMeNa	1,3-diMeNa	1,2-diMeNa	2,3,6-triMeNa	Fluorene	Phenanth
0.00			NA	NA	NA	NA	NA	NA	NA	NA	NA	NA	NA	NA	NA	NA	NA	NA
0.25			NA	NA	NA	NA	NA	NA	NA	NA	NA	NA	NA	NA	NA	NA	NA	NA
0.50	KB	Feb-86	1.6	1.4	5.3	3.6	Tr	0.45	0.70	5.3	3.5	2.7	0.69	1.04	0.42	Tr	1.48	Tr
1.00	KB	Feb-86	4.7	4.8	11.5	12.4	0.87	1.51	2.23	16.7	10.0	8.0	2.20	2.69	1.04	0.48	3.08	0.67
2.00			NA	NA	NA	NA	NA	NA	NA	NA	NA	NA	NA	NA	NA	NA	NA	NA
4.00	KB	Feb-86	Tr	0.0	Tr	12.5	1.08	0.00	1.53	0.0	0.8	6.1	2.04	3.39	1.11	0.72	Tr	Tr
8.50	KB	Feb-86	5.4	2.7	Tr	20.8	2.37	1.24	4.96	0.0	1.7	16.1	4.67	6.55	2.08	0.77	Tr	Tr
12.00	KB	Feb-86	11.6	9.7	1.4	34.6	3.73	3.89	7.45	0.9	4.8	22.1	5.63	7.48	2.40	0.88	0.84	Tr
15.25	KB	Feb-86	7.0	5.6	Tr	20.8	1.81	2.06	3.82	0.9	3.4	16.5	3.80	5.47	1.69	0.80	28.07	Tr
24.00	KB	Feb-86	9.2	11.6	1.4	38.9	2.72	3.72	6.01	1.5	11.4	25.8	6.22	7.77	2.61	1.00	1.82	0.92
48.00	KB	Feb-86	5.8	8.7	14.3	30.9	2.09	3.22	5.73	23.5	24.2	21.9	4.23	5.82	1.81	0.85	1.41	Tr
73.50	KB	Feb-86	5.3	6.3	22.8	24.7	1.62	2.41	4.50	27.1	18.8	17.0	3.78	4.30	1.35	Tr	Tr	0.00

12 Day Weathered Prudhoe Bay Crude Oil and Jakolof Bay Sediments

Time from start (hrs)	FID-GC Run:		Dissolved Phase Hydrocarbon Concentrations (ug/l of sea water)										Dissolved Phase Hydrocarbon Concentrations (ug/l of sea water)					
	Place	Time	Toluene	Ethylbenz	p-Xylene	o-Xylene	Camene	n-Propylbenz	Mesitylene	Naph	2-MeNa	1-MeNa	2,6-diMeNa	1,3-diMeNa	1,2-diMeNa	2,3,6-triMeNa	Fluorene	Phenanth
0.00	KB	Feb-86	Tr	Tr	Tr	Tr	0.000	0.000	Tr	1.51	2.3	1.7	0.74	1.06	0.44	Tr	0.59	Tr
0.25	KB	Feb-86	Tr	Tr	Tr	Tr	0.000	0.000	Tr	4.32	4.1	3.2	0.97	1.42	0.49	Tr	0.89	Tr
0.50	KB	Feb-86	Tr	Tr	Tr	Tr	0.000	Tr	Tr	9.75	8.0	6.3	1.41	2.32	0.85	0.42	Tr	0.44
1.00	KB	Feb-86	Tr	Tr	Tr	Tr	0.000	Tr	0.57	16.06	12.5	10.1	2.51	3.28	1.19	0.55	Tr	0.68
2.00	KB	Feb-86	Tr	Tr	Tr	0.699	Tr	Tr	1.17	7.86	24.1	21.2	4.96	6.64	2.54	0.83	1.94	1.25
4.00	KB	Feb-86	Tr	Tr	0.000	0.513	Tr	Tr	1.30	0.51	21.2	23.9	5.82	7.67	2.99	0.96	2.17	1.46
8.00	KB	Feb-86	Tr	0.000	Tr	0.000	Tr	Tr	1.57	Tr	24.4	31.1	7.76	10.46	3.98	1.31	2.41	1.62
12.00	KB	Feb-86	Tr	Tr	0.000	Tr	0.000	0.000	Tr	Tr	1.4	2.2	Tr	1.16	0.63	0.29	0.41	Tr
18.00	KB	Feb-86	Tr	Tr	0.000	Tr	0.000	0.000	0.00	Tr	1.4	0.9	Tr	0.46	0.49	Tr	Tr	Tr
36.00	KB	Feb-86	Tr	Tr	0.000	0.297	0.000	Tr	0.30	Tr	3.7	8.0	4.71	6.78	2.15	0.98	0.55	0.71
48.00	KB	Feb-86	Tr	Tr	0.373	0.000	0.000	Tr	Tr	Tr	3.7	8.1	3.25	5.65	1.60	0.55	0.00	0.40
72.00	KB	Feb-86	Tr	Tr	0.000	0.556	0.000	0.000	0.00	Tr	4.0	7.4	0.77	3.30	1.31	0.45	1.81	0.36
96.00	KB	Feb-86	Tr	Tr	Tr	0.620	0.000	0.000	0.30	Tr	18.8	21.0	4.32	6.64	2.52	0.92	4.29	1.31

HYDROCARBON CONCENTRATIONS FROM STIRRED CHAMBER EXPERIMENTS

RATIOS: Compound/nC19 for selected n-alkanes and aromatics

SURFACE OIL

Unweathered Prudhoe Bay Crude Oil and Jakolof Bay Sediments

Time from start (hrs)	Surface Oil											
	RATIOS: compound/nC19						Naph/nC19	2-MeNa/nC19	1,3-diMeNa/nC19	1,2-diMeNa/nC19	2,3,6-triMeNa/nC19	Phenanth/nC19
	nC10/nC19	nC12/nC19	nC16/nC19	nC19/nC19	nC22/nC19	nC25/nC19						
0.00	2.55	2.56	1.71	1.00	0.82	0.54	0.20	0.94	0.24	—	—	—
0.25												
0.50												
1.00												
2.00												
4.00												
8.00												
12.00												
18.00												
24.00												
48.00												
72.00	2.11	2.45	2.00	1.00	0.96	0.66	0.15	0.89	0.21	—	—	—
96.00												
120.00												
168.00	1.35	1.96	1.43	1.00	0.75	0.55	—	0.75	0.37	0.18	0.15	0.16
216.00	1.28	2.13	1.54	1.00	0.68	0.44	0.28	0.77	0.38	0.17	0.12	0.18

2 Day Weathered Prudhoe Bay Crude Oil and Jakolof Bay Sediments

Time from start (hrs)	Surface Oil											
	RATIOS: compound/nC19						Naph/nC19	2-MeNa/nC19	1,3-diMeNa/nC19	1,2-diMeNa/nC19	2,3,6-triMeNa/nC19	Phenanth/nC19
	nC10/nC19	nC12/nC19	nC16/nC19	nC19/nC19	nC22/nC19	nC25/nC19						
0.00	1.53	1.97	1.59	1.00	0.88	0.61	0.40	0.72	0.56	0.27	0.29	—
0.25												
0.50												
1.00												
2.00												
4.00												
8.50												
12.00												
15.25												
24.00												
48.00												
73.50	1.21	1.82	1.43	1.00	0.71	0.44	0.30	0.63	0.48	0.20	0.24	—

12 Day Weathered Prudhoe Bay Crude Oil and Jakolof Bay Sediments

Time from start (hrs)	Surface Oil											
	RATIOS: compound/nC19						Naph/nC19	2-MeNa/nC19	1,3-diMeNa/nC19	1,2-diMeNa/nC19	2,3,6-triMeNa/nC19	Phenanth/nC19
	nC10/nC19	nC12/nC19	nC16/nC19	nC19/nC19	nC22/nC19	nC25/nC19						
0.00	0.32	1.43	1.42	1.00	0.91	0.68	0.17	0.48	0.35	0.12	0.17	0.09
0.25												
0.50												
1.00												
2.00												
4.00												
8.00												
12.00												
18.00												
36.00												
48.00												
72.00												
96.00	0.13	1.52	1.72	1.00	0.94	0.75	0.04	0.43	0.41	0.13	0.19	0.08

HYDROCARBON CONCENTRATIONS FROM STIRRED CHAMBER EXPERIMENTS

RATIOS: Compound/nC19 for selected n-alkanes and aromatics

DISPERSED OIL PHASE

Unweathered Prudhoe Bay Crude Oil and Jakolof Bay Sediments

Time from start (hrs)	Dispersed Oil Phase											
	RATIOS: compound/nC19						Naph/nC19	2-MeNa/nC19	1,3-diMeNa/nC19	1,2-diMeNa/nC19	2,3,6-triMeNa/nC19	Phenanth/nC19
	nC10/nC19	nC12/nC19	nC16/nC19	nC19/nC19	nC22/nC19	nC25/nC19						
0.00	—	—	1.22	1.00	0.87	0.54	0.00	0.00	0.00	0.00	0.00	0.00
0.25	—	—	1.23	1.00	0.85	0.63	0.00	0.00	0.00	0.00	0.00	0.00
0.50	0.18	0.31	1.23	1.00	0.78	0.54	0.00	0.00	—	0.00	—	0.00
1.00	0.53	0.67	1.63	1.00	0.74	0.55	0.00	0.13	0.09	0.00	0.06	0.13
2.00	0.33	0.87	1.83	1.00	0.84	0.60	0.10	0.46	0.17	0.06	0.08	0.06
4.00	0.55	1.67	2.17	1.00	0.92	0.65	—	0.67	0.19	—	0.09	0.00
8.00	0.91	1.90	2.08	1.00	0.81	0.45	0.11	0.73	0.19	—	—	0.10
12.00	1.00	1.88	1.88	1.00	0.78	0.54	—	—	0.28	0.12	0.16	0.12
18.00	—	—	—	—	—	—	—	—	—	—	—	—
24.00	—	—	—	—	—	—	—	—	—	—	—	—
48.00	1.13	1.69	1.76	1.00	0.84	0.72	0.24	0.56	0.40	0.15	0.19	—
72.00	—	—	—	—	—	—	—	—	—	—	—	—
96.00	1.18	1.70	1.50	1.00	0.70	0.45	0.26	0.55	0.47	0.23	0.26	0.14
120.00	1.19	1.66	1.49	1.00	0.72	0.38	0.27	0.54	0.47	0.23	0.26	0.13
168.00	1.27	1.86	1.69	1.00	0.99	0.57	0.30	0.56	0.41	0.13	0.19	0.06
216.00	1.11	1.94	1.62	1.00	0.70	0.43	0.26	0.60	0.36	0.16	0.13	0.13

2 Day Weathered Prudhoe Bay Crude Oil and Jakolof Bay Sediments

Time from start (hrs)	Dispersed Oil Phase											
	RATIOS: compound/nC19						Naph/nC19	2-MeNa/nC19	1,3-diMeNa/nC19	1,2-diMeNa/nC19	2,3,6-triMeNa/nC19	Phenanth/nC19
	nC10/nC19	nC12/nC19	nC16/nC19	nC19/nC19	nC22/nC19	nC25/nC19						
0.00	—	—	—	—	—	—	—	—	—	—	—	—
0.25	—	—	—	—	—	—	—	—	—	—	—	—
0.50	0.51	1.02	1.27	1.00	0.74	0.56	—	0.21	0.20	0.06	0.17	—
1.00	0.57	1.20	1.68	1.00	0.81	0.57	0.05	0.25	0.23	0.08	0.16	—
2.00	0.59	1.26	1.77	1.00	0.80	0.54	—	0.14	0.30	0.10	0.23	0.05
4.00	0.84	1.54	1.51	1.00	0.85	0.60	0.07	0.43	0.37	0.14	0.20	0.08
8.50	1.38	2.13	1.68	1.00	0.90	0.67	0.15	0.61	0.43	0.15	0.22	0.08
12.00	1.10	1.70	1.54	1.00	0.85	0.74	0.11	0.52	0.38	0.14	0.19	0.09
15.25	1.06	1.69	1.60	1.00	0.90	0.73	0.13	0.53	0.40	0.14	0.20	0.11
24.00	1.16	1.91	1.78	1.00	0.78	0.42	0.22	0.64	0.47	0.15	0.23	0.08
48.00	1.08	1.79	1.61	1.00	0.89	0.73	0.18	0.57	0.40	0.14	0.20	0.10
73.50	0.90	1.65	1.63	1.00	0.89	0.75	0.21	0.54	0.40	0.14	0.20	0.07

12 Day Weathered Prudhoe Bay Crude Oil and Jakolof Bay Sediments

Time from start (hrs)	Dispersed Oil Phase											
	RATIOS: compound/nC19						Naph/nC19	2-MeNa/nC19	1,3-diMeNa/nC19	1,2-diMeNa/nC19	2,3,6-triMeNa/nC19	Phenanth/nC19
	nC10/nC19	nC12/nC19	nC16/nC19	nC19/nC19	nC22/nC19	nC25/nC19						
0.00	—	0.46	1.24	1.00	0.74	0.58	0.00	0.00	—	0.00	—	0.00
0.25	0.26	1.55	1.66	1.00	0.84	0.64	0.17	0.51	0.39	0.14	0.19	0.10
0.50	0.37	1.79	1.78	1.00	0.70	0.59	0.20	0.59	0.42	0.14	0.21	0.09
1.00	0.32	1.58	1.62	1.00	0.85	0.62	0.15	0.65	0.36	0.12	0.19	0.11
2.00	0.39	1.80	1.49	1.00	0.68	0.38	0.11	0.65	0.36	0.16	0.13	0.18
4.00	0.34	1.68	1.40	1.00	0.61	0.34	0.10	0.60	0.32	0.16	0.13	0.16
8.00	0.35	1.74	1.51	1.00	0.62	0.37	0.11	0.63	0.35	0.18	0.15	0.17
12.00	0.29	1.61	1.38	1.00	0.60	0.34	0.05	0.58	0.32	0.15	0.12	0.17
18.00	—	—	1.26	1.00	0.81	0.55	—	—	0.36	0.09	0.18	—
36.00	0.19	1.42	1.43	1.00	0.64	0.38	—	0.47	0.32	0.23	0.10	0.18
48.00	0.18	1.51	1.41	1.00	0.60	0.37	—	0.53	0.33	0.29	0.12	0.16
72.00	0.13	1.32	1.40	1.00	0.67	0.38	0.00	0.43	0.30	0.24	0.10	0.16
96.00	—	0.97	1.24	1.00	0.80	0.56	—	0.30	0.26	—	0.14	0.12

HYDROCARBON CONCENTRATIONS FROM STIRRED CHAMBER EXPERIMENTS

RATIOS: Compound/nC19 for selected n-alkanes and aromatics

SPM PHASE

Unweathered Prudhoe Bay Crude Oil and Jakolof Bay Sediments

Time from start (hrs)	SPM Phase											
	nC10/nC19	nC12/nC19	nC16/nC19	nC19/nC19	nC22/nC19	nC25/nC19	Naph/nC19	2-MeNa/nC19	1,3-diMeNa/nC19	1,2-diMeNa/nC19	2,3,6-triMeNa/nC19	Phenanth/nC19
0.00												
0.25												
0.50	0.51	0.32	1.03	1.00	0.79	0.48	—	0.14	—	0.00	—	—
1.00												
2.00	0.00	—	1.05	1.00	0.82	0.56	0.00	—	—	0.00	—	0.13
4.00	0.00	—	1.18	1.00	0.74	0.37	0.00	—	—	0.00	—	—
8.00	0.00	0.38	1.37	1.00	0.88	0.59	—	0.21	0.23	0.06	0.17	0.07
12.00	—	0.54	1.41	1.00	0.90	0.59	—	0.19	0.23	0.07	0.19	0.06
18.00	0.56	1.01	1.64	1.00	0.82	0.56	0.00	0.18	0.12	—	0.10	—
24.00	0.49	1.20	1.72	1.00	0.84	0.50	—	0.45	0.18	—	—	0.12
48.00	—	—	—	—	—	—	—	—	—	—	—	—
72.00	—	—	—	—	—	—	—	—	—	—	—	—
96.00	0.50	1.28	1.32	1.00	0.71	0.44	0.06	0.34	0.26	0.12	0.11	0.13
120.00	0.64	1.51	1.47	1.00	0.68	0.46	0.10	0.44	0.33	0.14	0.13	0.13
168.00	0.41	1.20	1.40	1.00	0.65	0.43	0.07	0.37	0.29	0.22	0.11	0.13
216.00	0.34	1.12	1.40	1.00	0.71	0.43	—	0.27	0.26	0.10	0.10	0.11

2 Day Weathered Prudhoe Bay Crude Oil and Jakolof Bay Sediments

Time from start (hrs)	SPM Phase											
	nC10/nC19	nC12/nC19	nC16/nC19	nC19/nC19	nC22/nC19	nC25/nC19	Naph/nC19	2-MeNa/nC19	1,3-diMeNa/nC19	1,2-diMeNa/nC19	2,3,6-triMeNa/nC19	Phenanth/nC19
0.00	1.14	0.43	1.58	1.00	0.62	0.51	—	—	—	0.00	0.00	0.00
0.25	0.83	0.23	0.86	1.00	0.75	0.60	—	—	—	0.00	0.00	—
0.50	0.69	—	0.99	1.00	—	—	—	—	—	0.00	0.00	—
1.00	0.48	0.25	0.90	1.00	0.72	0.43	—	—	—	0.00	—	—
2.00	0.61	0.24	0.96	1.00	0.79	0.71	—	—	—	0.00	—	—
4.00	0.31	0.22	0.85	1.00	0.84	0.74	0.00	—	—	0.00	—	0.00
8.50	0.48	0.58	0.96	1.00	0.89	0.65	0.00	—	0.20	—	—	—
12.00	0.28	0.22	1.16	1.00	0.81	0.60	0.00	—	0.11	—	—	—
15.25	0.26	0.43	1.22	1.00	0.87	0.67	0.00	—	0.16	—	0.10	—
24.00	0.13	0.66	1.43	1.00	0.85	0.54	0.00	0.15	0.23	0.08	0.17	—
48.00	0.52	0.13	0.73	1.00	0.71	0.29	0.16	0.35	0.16	—	0.09	—
73.50	0.67	0.20	0.80	1.00	0.87	0.71	0.25	0.37	0.17	—	0.08	—
Bot. Sd. (73.50)	0.94	1.80	1.62	1.00	0.89	0.69	0.18	0.54	0.44	0.13	0.19	0.04

12 Day Weathered Prudhoe Bay Crude Oil and Jakolof Bay Sediments

Time from start (hrs)	SPM Phase											
	nC10/nC19	nC12/nC19	nC16/nC19	nC19/nC19	nC22/nC19	nC25/nC19	Naph/nC19	2-MeNa/nC19	1,3-diMeNa/nC19	1,2-diMeNa/nC19	2,3,6-triMeNa/nC19	Phenanth/nC19
0.00	0.12	0.28	1.97	1.00	0.36	—	0.00	—	—	0.00	—	0.00
0.25	0.30	0.16	1.42	1.00	0.33	—	0.00	—	—	0.00	—	—
0.50	0.32	—	0.93	1.00	0.60	—	0.00	—	—	0.00	—	—
1.00	0.36	0.19	1.21	1.00	0.69	0.27	0.00	0.13	—	0.00	—	—
2.00	0.48	0.29	1.41	1.00	0.89	0.68	—	0.32	0.21	—	0.12	0.18
4.00	0.35	0.21	1.10	1.00	0.75	0.65	—	0.20	0.19	0.07	0.12	0.19
8.00	0.30	0.18	1.64	1.00	—	—	0.00	0.14	0.22	—	0.13	0.22
12.00	—	—	—	—	—	—	—	—	—	—	—	—
18.00	0.16	0.11	1.06	1.00	0.74	0.44	0.00	—	—	0.00	—	—
36.00	0.45	0.20	1.08	1.00	—	—	—	—	0.16	—	0.09	0.10
48.00	0.37	0.69	1.39	1.00	0.76	0.61	—	—	0.19	—	0.13	—
72.00	0.67	0.22	1.41	1.00	0.78	0.56	—	—	0.11	—	—	—
96.00	0.54	0.19	1.36	1.00	—	—	—	0.21	0.20	—	0.12	—
Bot. Sd. (96.00)	0.11	1.11	1.36	1.00	1.08	0.80	—	—	0.11	0.03	0.08	—

APPENDIX B
TABLE OF MATHEMATICAL
EXPRESSIONS

APPENDIX B

Table of Mathematical Expressions

<u>SYMBOL</u>	<u>DEFINITION</u>
k_p	partition coefficient
C_p	concentration of oil on SPM
C_w	concentration of oil in water
$\tau_{yz}, (\tau_{zx}, \tau_{xz})$	shear stress exerted in the z-direction on a fluid surface of constant y by the region of lesser y
μ	viscosity
ϵ	energy dissipation rate
C_i	concentration of species i
$v_x, (v_y, v_z)$	velocity component in the x- (or y- or z-) direction
$k_x, (k_y, k_z)$	dispersion component in the x- (or y- or z-) direction
R_i	reaction term for species i
R_{op}	reaction rate for oiled particles
k_{op}	oil-SPM interaction rate constant
C_o	concentration of oil droplets
C_p	concentration of SPM
w_z	rise velocity
u_z	particle settling velocity
u	fluid velocity in the x-direction
G	turbulent shear
n_i	number density of particles of species i

APPENDIX B

Table of Mathematical
Expressions

<u>SYMBOL</u>	<u>DEFINITION</u>
a	radius of a "collision" sphere
r_i	radius of particles of species i
α	stability constant or "sticking" factor
ν	kinematic viscosity
k_a	lumped parameter for "sticking" and including the effects of particle radius
t	time
P	power
mgh	change in potential energy in a gravity field
k_s	rate of SPM - SPM interaction